Structure, metamorphism, geochronology and deformation history of Mesozoic formations in the central Rudabánya Hills

Deák-Kövér Szilvia

Dissertation submitted to the Ph.D. program for Geology and Geophysics at the Ph.D. School of Earth Sciences, Eötvös Loránd University, Budapest
in partial fulfilment of the requirements for the degree of
Philosophiae Doctor

Supervisor:
Dr. László I. Fodor, scientific advisor
MTA-ELTE Geological, Geophysical and Space Science Research Group

Head of the Ph.D. School: **Prof. Gyula Gábris**
Chair of the Ph.D. Program: **Prof. Andrea Mindszenty**

2012
Eötvös Loránd University
MTA-ELTE Geological, Geophysical and Space Science Research Group
Budapest, Hungary

Table of contents

1. Introduction

The present study deals with the structural evolution of the central part of the Rudabánya Hills. The combined structural, metamorphic petrological, geochronological and sedimentological investigations resulted in a better understanding of this small segment of the Inner Western Carpathians. On the other hand, the results can contribute to the geodynamic evolution of the Eastern-Alpine–Western-Carpathian orogenic belt.

The main goal of my work was suggesting a new structural model and evolution for the central part of the Rudabánya Hills. I worked on the next topics in details: (I) sedimentary features and age of the Jurassic slope and basinal, subduction-related formations in the Rudabánya Hills, (II) new definition or redefinition of the tectonic units of the Rudabánya Hills, (III) polydeformational tectonic evolution of the different nappes based on structural mapping and micro-tectonic studies, (IV) p-T conditions of the very low- to low-grade metamorphic event in different tectonic units, (V) dating of the deformation phases derived from K-Ar white mica analyses (VI) p-T conditions of the nappe movements.

The main direction of my research was the geological mapping, tectonic and metamorphic petrologic studies. During this work several problems emerged on the depositional conditions, age and sedimentological characteristics of the different Mesozoic sequences. To have a better view on the examined series new sedimentological and micropaleontological studies were needed. To hit these targets several lithofacies units were defined, depositional environments were characterized and valuable microfossil data were revised and new data were provided with the indispensable help of microfossil specialist.

The wide spectrum of new data set suggest notable revisions of the lithostratigraphic content, boundaries, and mutual relationships of formerly defined tectonic units and contribute to the knowledge on deformation history of the Eastern Alpine–Western Carpathian orogenic belt.

My study was related to and mainly supported by the Hungarian National Research Foundation projects (OTKA) T048824 entitled: Structural geological research of the Rudabánya and Aggtelek Mts. (L.I. Fodor) and T061872 titled: Importance of Triassic and Jurassic slope facies in the geodynamic reconstruction of the NW termination of the Neotethys (J. Haas). Among many others, aims of these research projects were obtaining new stratigraphical, sedimentological, paleontological, structural, metamorphic petrological and geochronological data to better characterise the different structural units of the Aggtelek and Rudabánya Hills (Inner Western Carpathians). This work was also connected to 3 international bilateral projects: a) Comparison of Triassic and Jurassic pelagic and slope successions of the Northern Calcareous Alps (Austria) and of the Aggtelek-Rudabánya and Bükk Mts. (NE Hungary) (Austrian-Hungarian bilateral project) b) Comparison of Triassic–Cretaceous Sedimentary Successions in the Eastern Alps, the tectonic Terranes in the surroundings of the Pannonian Basin, the Western Carpathians and the Dinarides: Palaeogeographic origin and geodynamics evolution (Austrian-Hungarian bilateral project) c) Fault-controlled diagenetic stages at the base of Silice, Martonyi and Telekesoldal Nappes, Inner Western Carpathians (Slovak-Hungarian bilateral project).

2. Geological background

2.1. Geographic position, morphologic and outcropping conditions

The examined Mesozoic sequences of the Rudabánya Hills are situated in NE Hungary, north of the Bükk Mountains and south from the SE part of the Slovakian Republic (Fig. 1). It is a hilly area with a maximum elevation of 500-550 m forming low hills with gentle morphology. The surface is usually covered by thick forests and grasslands in the Bódva Valley and plough-lands on some very gentle rolling hills of the Aggtelek area. Geographically the study area involves the central and northern part of the Rudabánya Hills and the south-eastern rim of the Aggtelek Hills. The two hilly regions are separated in their northern segments by the ~NNE-SSW oriented valley of the Bódva River. As the river reaches the central part of the Rudabánya Hills it turns sharply to the ESE and forms the quite narrow Bódva Gorge between Perkupa and Szalonna villages. This gorge separates the northern Dunnatető-Szár Hill area and the southern Nagy-Telekes Hill area.

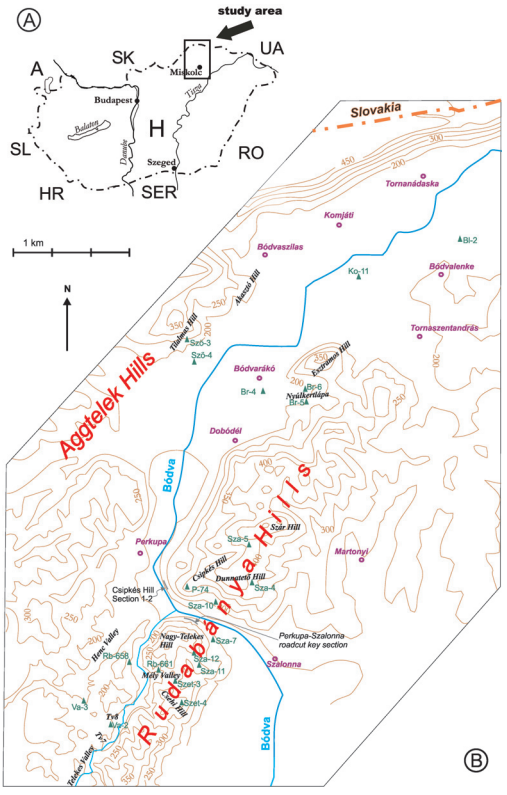

Figure 1. Geographic position of the investigated area. The main geographic names (e.g. hills, valleys, villages) and the location of the most commonly used boreholes (green triangles) are indicated.

The outcropping conditions of this hilly area are quite bad due to the usually gentle topography and in case of the Lower Triassic and Jurassic formations to the clayey, marly and shaley lithologies. This is why I focused my examinations mainly on narrow creek valleys (e.g. Telekes Valley and its side valleys, Bódva Gorge), on steeper slopes of the hills (e.g. SE slope of the Aggtelek Hills, NE slope of Nagy-Telekes Hill, southern to south-western slope of Csipkés and Dunnatető Hills, SE slope of Esztramos Hill), on abandoned quarries (e.g. Esztramos Hill, small quarries along the NW margin of the Rudabánya Hills) and on old geological trenches (e.g. Dunnatető Hill, Telekes Valley Tributary Valleys 6, 7, 8). The area was penetrated by several boreholes, with depths ranging from one hundred to seven hundred meters, drilled during geological mapping and ore research projects in the late 1970's and 1980's.

Examination of the stored cores issued important data supplementing the surface observations and provided several fresh samples fit for metamorphic petrological measurements and K-white mica geothermobarometry.

2.2. Geological settings

The Aggtelek-Rudabánya Hills are parts of the Inner Western Carpathians (Fig 2a), and contain a nappe stack of Late Permian–Jurassic sediments (Balogh & Pantó 1949, 1952, Less et al. 1988). The Aggtelek and Rudabánya Hills are considered to be separated by the western boundary fault of the Cretaceous–Cenozoic Darnó Fault Zone while the other margin of the fault zone is located at the eastern side of the Rudabánya Hills (Fig. 2b). The Darnó Zone is an important NNE-SSW structural element, located in NE Hungary reaching the southernmost part of the Slovak Republic. Earlier works considered both boundary faults as a Miocene sinistral structure (Zelenka et al. 1983, Szentpétery 1997, Szentpétery & Less 2006), but the newest review of Fodor et al. (2005) – on the basis of fault slip data – argued for the presence of a pre-middle Miocene thrusting event, too.

Detailed geological mapping and related extensive academic research of the 1980's defined several tectono-stratigraphical units in the Aggtelek-Rudabánya Hills (Grill et al. 1984, Less et al. 1988, Kovács et al. 1989, Szentpétery & Less 2006). The basis of the tectonic subdivision was the variable late Permian to Jurassic stratigraphy (Kovács et al. 1989, Less 2000) which was combined with limited field observations on deformation (Grill 1989) and with preliminary laboratory data on very low to low-grade metamorphism (Árkai & Kovács 1986, Kovács & Árkai 1989). Tectonic superposition was occasionally encountered in boreholes and seen on the surface, but the interpretation of tectonic data were not unequivocal. In the following these traditional tectonic units will be introduced, focusing on the supposed structural position and main lithological content.

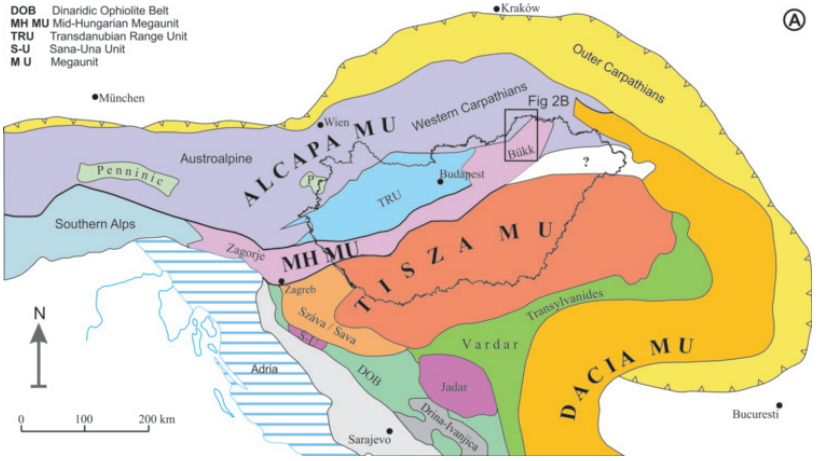

Figure 2. a) Structural units of the Pannonian basin and related areas after Haas et al 2010. Location of Fig. 2b is indicated.

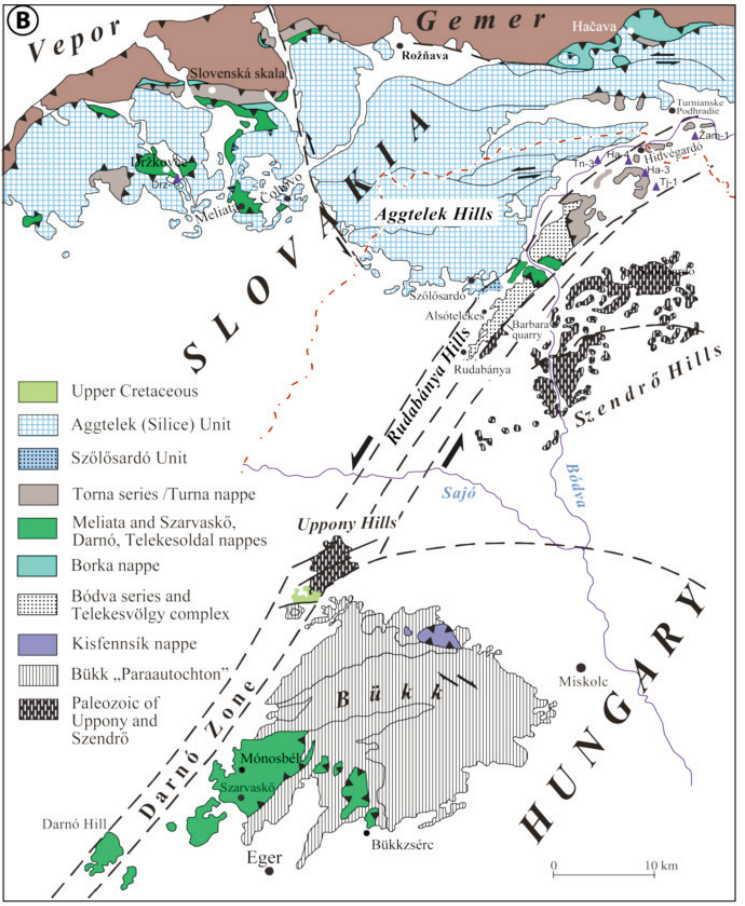

Figure 2b. Simplified tectonic map of NE Hungary (modified after Kovács 1989 and Koroknai 2004)

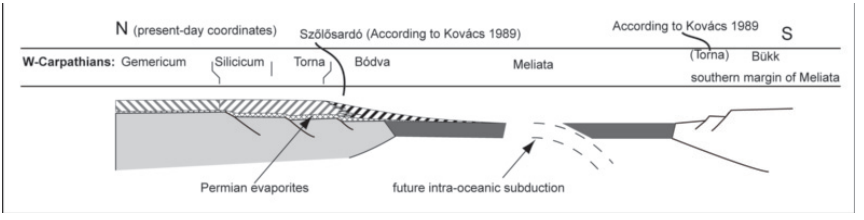

Figure 3. Supposed paleogeographic relationships of the different series in the Aggtelek-Rudabánya Hills (after Schmid et al. 2008). Differences in comparison with the model of Kovács (1984, 1989) is indicated.

2.2.1. Silice nappe system

The Silice (Szilice) nappe system contains non-metamorphosed Upper Permian–Jurassic sequences (Fig. 3), deposited on partly thinned continental crust (passive margin) of the Neotethys Ocean (Mello 1974, 1975, Mello et al 1996, Less et al. 1988, Kovács et al. 1989, Szentpétery & Less 2006). This nappe system contains several different developments which were interpreted as different facies units (Kovács et al. 1989, Less et al. 1988, 1998, Szentpétery & Less 2006). In Slovakia different nappe outliers of this nappe system (Silice s.s., Stratená, Muráň, Vernár and Drienok nappes Fig 4) thrust over different tectonic units (Hók et al. 1995, Mello et al. 1996, Vojtko 2000). What is widely accepted, that the Silice nappe system is always occupy the uppermost tectonic position.

While the inner classification of the different units of the Silice nappe system is different in Slovakia and in Hungary, they will be discussed separately. All of the different facies units and nappe outliers start with Permian evaporite and associated siliciclastic sediments (Perkupa Anhydrite Fm.), along which the Silice nappes were detached from their pre-Permian basements (Fig 4). The evaporite-bearing association is followed by Lower Triassic sandstone (Bódvaszilas Sandstone), marl (Szin Marl) and limestone (Szinpetri Limestone) sequence and Anisian ramp carbonates (Gutenstein and Steinalm Formations) (Bystrický 1964, Mello 1974, Less et al. 1988, Kovács et al. 1989, Hips 2001, Szentpétery & Less 2006). The characteristic and distinctive lithological units are Middle to Late Triassic rocks presumably reflecting diverse paleogeographic and tectonic positions deposited on variably thinned continental crust (Fig. 3). They are platform carbonates with reefs in all the Slovakian nappe outliers (Kovács et al. 2011) and in the ***Aggtelek nappe*** (Wetterstein Formation) which can be interrupted (or locally completely replaced) by intraplatform basinal sediments (Szádvárborsa and Derenk Limestone) (Kovács et al. 1989, Piros 2002, Hagdorn & Velledits 2006) (Fig 4). Both platforms and intraplatform basins persisted up to the early Late Triassic (Fig. 4) (Kovács et al. 1989, Nádor 1990) while the later part of the Triassic is built up by different lithologies in the different nappe outliers. In the Vernár nappe along with the major part of the s.s. Silice, Muráň and Stratena nappes the Dachstein-type platform survived till Late Norian times. While on the area of the Aggtelek nappe and the rest of the above mentioned nappe outliers pink and grey slope to basin facies carbonates and variegated to grey marls deposited (e.g. Hallstatt Limestone, Zlambach Marl; Fig. 4). Jurassic is represented by reduced pelagic sediments in the Silice nappe (Mello et al. 1997).

Meanwhile, no shallow water carbonates formed after the Middle Anisian in the other facies units. The most characteristic stratigraphic unit of the ***Bódva series*** is the late Anisian–Late Triassic red (Bódvalenke Fm.), grey (Reifling Fm.) and black (Bódvarákó Fm.) cherty limestone and occasionally radiolarite (Szárhegy Radiolarite) (Grill et al. 1984, Kovács et al. 1989) (Fig 4). These rocks represent deep-sea sediments widely occurring in the Tethys region (Bernoulli et al. 1990, Dimitrijević et al. 2003).

As a distinction, the slope sediments are predominant from the second half of the Middle Triassic till the early Late Triassic in the ***Szőlősardó series*** (Fig. 3, 4). The predominantly slope carbonate sedimentation (Nádaska and Reifling Limestone) was interrupted by the Carnian siliciclastic event resulted in the deposition of the Szőlősardó Marl horizons. From the late Carnian the slope sedimentation was taken over by the formation of the basin facies cherty limestone (Pötschen Fm.). No ages younger than middle Norian are known (Fig. 4).

In the concept of Grill et al. (1984), Árkai & Kovács (1986), Less et al. (1988), Kovács et al. (1989), Less (2000), Less & Mello (2004) the Silice nappe system (included the Bódva and Szőlősardó series, too) represented the highest tectonic unit of the Aggtelek-Rudabánya Hills. The

Aggtelek nappe of the Silice nappe system occurs only in the Aggtelek Hills, while the Bódva series is present only in the Rudabánya Hills. The Szőlősardó unit is located in the vicinity of the tectonic contact of the two hills, in the wide Darnó Zone (Fig. 5). However, the primary tectonic contact of the Aggtelek, Bódva and Szőlősardó series was obliterated.

All these facies units occur in different structural units and one structural unit contains only one facies unit; transitional developments between different facies units are scarce within the same tectonic unit. So in a first approximation, one can speak about tectonic units, which are marked by a single specific facies unit, e.g. a specific stratigraphy. On the other hand, the past and my recent works delineated more numerous tectonic units than facies development; different tectonic units can consist of the same facies development. This is the case for the Bódva series which builds up two structural units due to a relatively late thrusting event (see Chapter 7.5) reworking the original nappe contacts. In the result of these later tectonic phases tectonic units containing sedimentary rocks of the Bódva series are present in the lowermost and in much higher tectonic position (Chapter 7.5).

Another problem is the hierarchy of tectonic units: are they large scale, widespread first-order nappes or just relatively small imbrications within one nappe, which are synchronous or postdate original nappe stackes? I will return to this question and discuss it in my thesis on the basis of observations, petrological and structural data.

2.2.2. Meliata nappe system

The next clearly distinguishable tectonic unit is the Meliata nappe system, which contains diverse rock series, with interpretations and contents varying with authors. The Meliata nappe system s.l. in Slovakia is considered to be an accretionary wedge by most of the authors. It is built up by the remnants of the oceanic crust and connecting sediments formed in the Triassic–Jurassic Neotethys Ocean (Mock et al. 1998). However, due to the differences in metamorphism, age and protoliths, there is a confusion in the usage of the Meliata name in tectonic and in paleogeographic sense. Basically, there are two different approaches: Mello et al (1997) subdivided the unit on basis of metamorphism: the HP/LT metamorphosed blueschist facies part was classified to the Bôrka nappe, while the low-grade part to the Meliata nappe s.s.

The other type of classification is based on the supposed paleogeographical position; however the degree and age of the metamorphism were also taken into account. This scheme subdivided only the Bôrka nappe into two groups: one with lithologies derived from the Meliata Ocean, and one with other (continental crust) protoliths (Faryad 1995, Faryad & Henjes-Kunst 1997). This type of classification usually

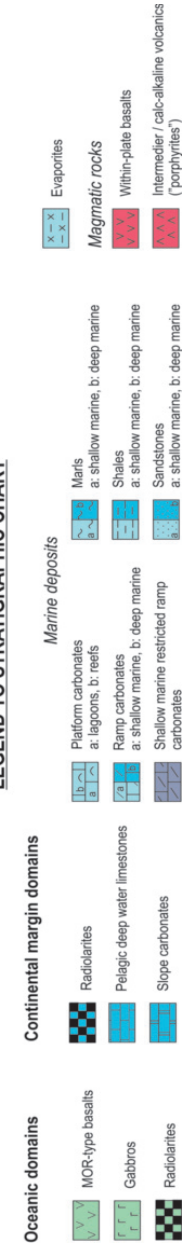

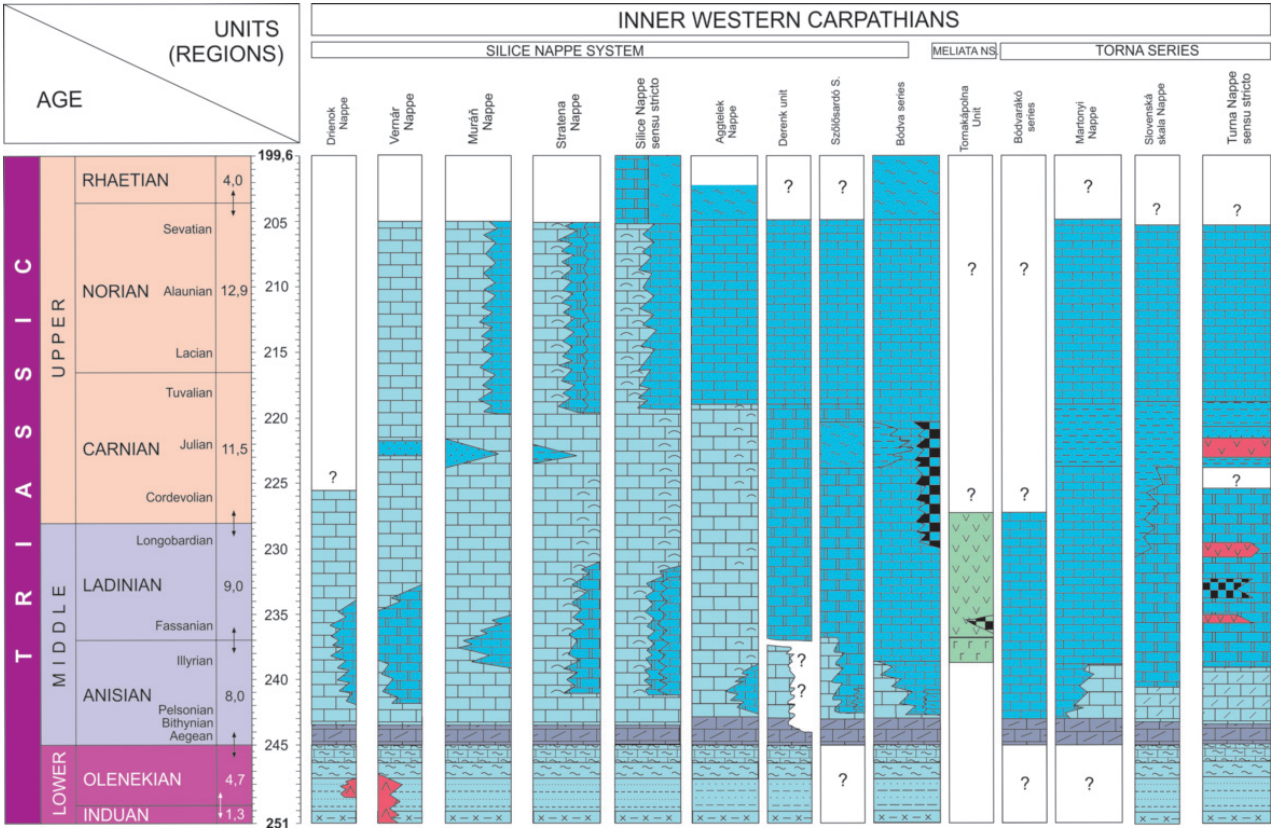

Figure 4. Triassic stratigraphic columns of the different nappes and facies zones in the Inner Western Carpathians (Kovács et al. 2011).

counts by a lower unit formed by a sequence of thrust sheets derived from thinned continental margin. The main lithologies are Permian clastics, Triassic limestones – supposedly forming the southern slope of the European continental margin – and blueschist facies basalts. The upper unit is built up by a subduction-related mélange complex, containing the deep-water sediments of the Meliata Ocean with relics of the oceanic crust.

The ***Meliata nappe s.s.***, (in the sense of Mello et al (1997) and Mock et al. 1998) contains diverse olistoliths, including Triassic limestone, oceanic crust fragments and radiolarite in a slaty matrix and is considered as a Jurassic tectono-sedimentary mélange accreted to the overlying units during subduction. This mélange-like complex is supposed to lack in the Aggtelek-Rudabánya Hills (Fig. 4) (Less 2000), although a similar unit is present further to the SW near the Bükk Mts. (Haas et al. 2006, Kovács et al. 2008). The Meliata nappe s.s. underwent anchi- to epizonal metamorphism (Árkai et al. 2003).

Additionally, in the literature of the last decades the Meliata name refers not only to this structural unit (Meliata nappe/nappe system) but also to an ocean, the Meliata-Hallstatt Ocean (Kozur 1991, Channel & Kozur 1997), or a back-arc basin of the Neotethys Ocean (Stampfli & Borel 2002). In my work I will use the Meliata name in a structural sense, referring to the previously described nappe system of the Inner Western Carpathians.

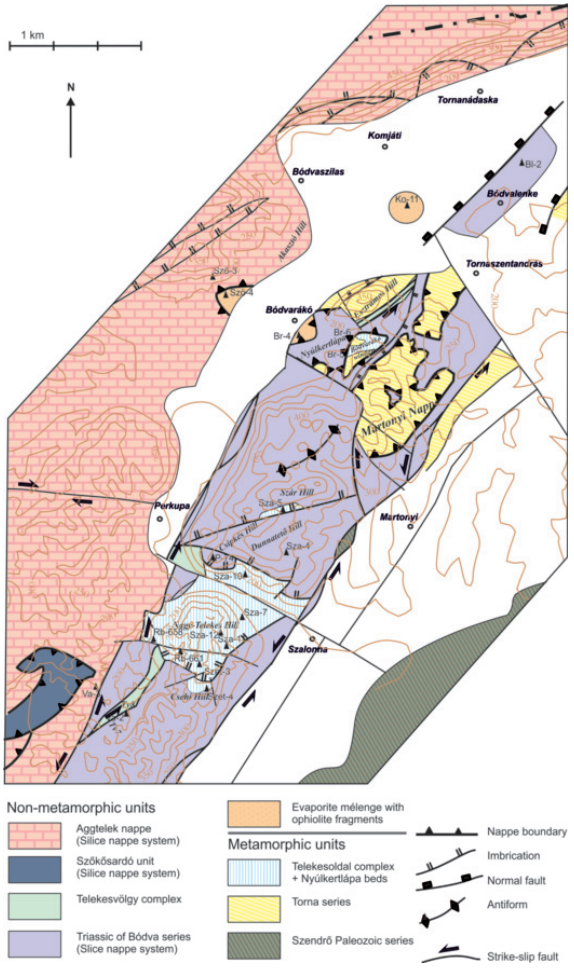

Figure 5. Concept of the previous authors about the structural position of the different nappes and units in the central part of the Rudabánya Hills (Less et al. 1986, Less & Mello 2004).

The ***Tornakápolna series*** (***Bódva Valley Ophiolite complex***) – which is considered to be part of the Meliata nappe s.l. (Kovács et al. 1989) – consists of dismembered serpentinite, gabbro, basalt and radiolarite (Fig. 4), representing real MORB-type ophiolite and cover sediments of Ladinian age (Réti 1985, Dosztály & Józsa 1992, Józsa et al. 1996), embedded in evaporitic tectonic mélange. The tectonic lenses were considered not having suffered metamorphism, although later studies indicate higher pressure mineral assemblage (Horváth 1997, 2000).

The ***Bódvarákó series*** is a reduced, tectonically truncated Middle Triassic series, whose particularity is that it shows the earliest sign of subsidence, while middle Anisian is represented by deep-water instead of shallow-water carbonates (Fig. 4) (Kovács et al. 1989). This series occurs in the core of an antiform (Bódvarákó Window), below the evaporite mélange and the Bódva series (Less et al. 1988, Less 2000) (Fig. 5). Paleogeographically this series was placed between the Bódva and Meliata series (Less 2000) but its metamorphosed nature and similar stratigraphy permit its classification to the Torna unit (Fodor & Koroknai 2000) (Fig. 4).

2.2.3. Torna (Turňa) series

The next unit distinguished by the previous authors is the ***Torna (Turňa) series***, which contains anchi- to epimetamorphic Triassic rocks, deposited on thinned continental crust (Fig. 4) (Mello & Mock 1977, Less 1981, Less et al. 1988, Kovács et al. 1989, Árkai & Kovács 1986). In Slovakia, the anchi- to epimetamorphosed Turňa series is classified into two nappes (Turňa Nappe and Slovenská skala Nappe), and thought to be thrust over the Meliata nappe, while the Silice nappe system forms the uppermost nappe (Mello et al. 1996, Kovács et al. 2011). According to Mello et al. (1996) the Turňa series is represented by rocks of Middle Carboniferous to Late Triassic and/or Jurassic. The Mesozoic part of the succession starts with Werfen-type Lower Triassic siliciclastic formations (Mello & Mock 1977, Mello 1979, Mello et al. 1996). This lithology lacks from the Hungarian part (Fig 4). The Torna series sensu Less (1981, 2000) generally contains early to middle Anisian shallow water (ramp) carbonates, upper Anisian-Ladinian slope or basinal facies limestone, Carnian slate, upper Carnian-Norian cherty limestone. However, this "general" stratigraphy shows several notable variations in the different sections, so the realistic definition of the Torna tectonostratigraphic unit incorporates diverse Triassic series, which were formed on different paleogeographic positions on the attenuated continental crust (Fodor & Koroknai 2000) (Fig. 4). The diverse Triassic sequences occur in separate geographic positions, and form different nappes (Chapter 7) due to the reworking of the original nappe system.

One of these nappes occurs in the study area as tectonic klippe (eroded remnant of a higher nappe): the ***Martonyi nappe*** (Grill 1989, Less 1998, Fodor & Koroknai 2000) (Fig. 5). According to previous concepts the Torna series originally formed the lowermost known allochton tectonic member of the Aggtelek-Rudabánya Hills (Less et al. 1988, Less 2000) and was considered as the subducted continental margin of the Meliata Ocean (Less 2000). In fact, the Torna tectonostratigraphic unit is clearly below the Silice nappe system (and its evaporitic sole) in several sites in Slovakia (Mello 1979, Kozur & Mock 1973, Kozur 1991) and possibly at one place (Esztramos Hill) in the NE Rudabánya Hills (Less et al. 1988, Szentpétery & Less 2006) (Fig. 5). However, the mutual position of the Meliata nappe system and the different klippes of the Torna series is not unequivocal; most Hungarian authors intended to put the Torna below the Meliata nappe (Csontos & Vörös 2004), while opinion was opposite looking from Slovakian sites (Rakús et al 1998). In addition, in most of the occurrences the metamorphic Torna series lies on non-metamorphic units like the Martonyi nappe (Torna) is over the Bódva series (Fig. 5) (Fodor & Koroknai

2000). All these complexities are attributed to later nappe emplacement after the first nappe stacking event and metamorphism (Grill et al. 1984, Less 2000), thus the original nappe order is difficult to reconstruct.

2.2.4. Hidvégardó series

The Hidvégardó series was thought to be an autochtonous series below the overturned Martonyi nappe (Torna series) (Less et al. 1988, Szentpétery and Less 2006). It consists of black shale, evaporite with grey and green shale, dark grey and black marls with variable carbonate content. The shaly and evaporite-bearing part of the succession was correlated with the similar lighologies of core Zsarnó (Žarnov) Žam-1 in Slovakia. From that locality, Permian-Early Triassic(?) sporomorphs was reported by Planderová (Szentpétery and Less 2006). On basis of its evaporite content the whole series was classified into the Permian-Lower Triassic (Mello 1979, Szentpétery and Less 2006).

The Hidvégardó series was penetrated by the lower part of the Hidvégardó Ha-3 borehole (Fig 6). The core starts with an overturned Torna-type succession (0-112 m) which thought to be thrust over this autochtonous unit (Szentpétery & Less 2006). The Hidvégardó series contains grey laminated marl, claymarl, limestone and shale between 112 and 158 m. It is followed by the evaporite-bearing succession, in which green and grey shale alternates with gypsum, dolomite and anhydrite layers. From ca. 170 m till 717 m partly silicified dark grey and black shale alternates with sandstone. These sandstones were interpreted as nodules.

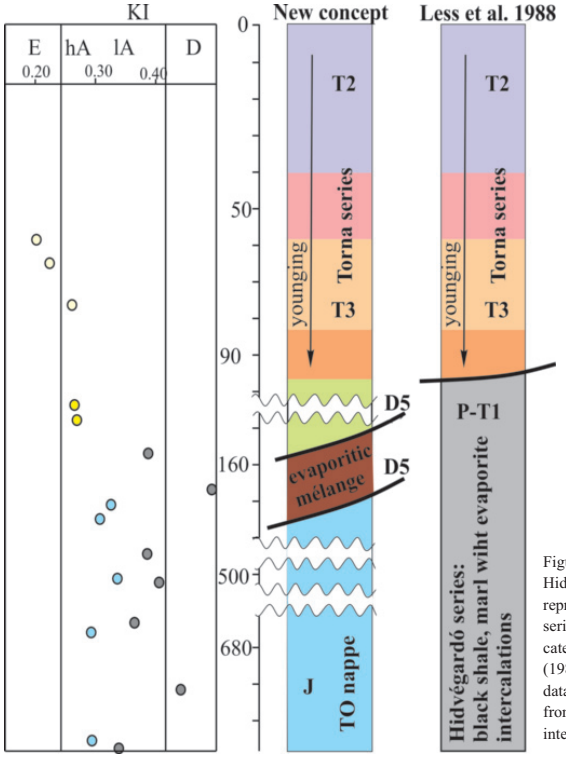

Figure 6. Earlier and new interpretation of the Hidvégardó Ha-3 borehole. Pinkish colours represents different T2-T3 formations of Torna series. Illite "crystallinity" data are also indicated. White and grey circles are data of Árkai (1983, 1985). Yellow circles represents new data from the Torna series, while bule ones from the lower part of the borehole. For more interpretation see chapter 5.4.2, 7.4)

2.2.5. Jurassic sediments with uncertain attribution

2.2.5.1. Telekesvölgy complex (TV)

Based on lithological and paleontological data the Jurassic rocks were subdivided into two lithostratigraphic units: the Telekesvölgy (TV) and Telekesoldal (TO) complexes (Grill & Kozur 1986, Grill 1988, Dosztály 1994, Dosztály et al. 2002). Both Jurassic complexes were placed over the Bódva Triassic series, although the stratigraphical continuity remained doubtful (Fig. 7) (Chapter 5.2.4).

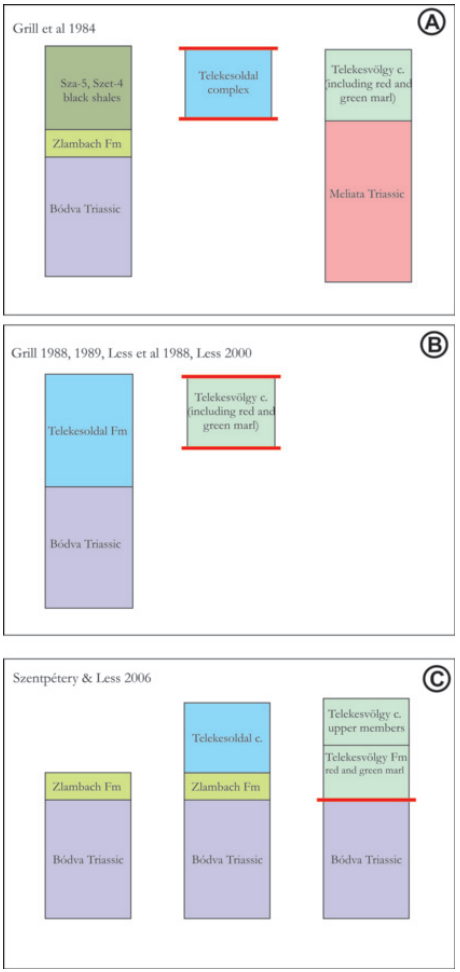

Figure 7. The relationship of the uppermost Triassic-Jurassic sequences and deeper Triassic series according to the previous investigations. Black lines indicate continuous or sedimentary contacts (including unconformity), whereas the red ones indicate tectonic boundaries (For details, see chapter 5.2.4)

The lowermost part of the TV complex consists of variegated marl and claymarl ("red and green claymarl member" of Grill 1988). This member gradually progresses into grey calcareous marl and claymarl, containing significant amount of redeposited crinoid fragments ("crinoideal limestone member" of Grill 1988). The uppermost part of the formation contains Mn-bearing black shale, representing typical deep pelagic basinal sediment. The locally silicified shale contains large amount of radiolarians and sponge spicules. Based on radiolarians the black shale was looked as Aalenian–Bathonian age (Dosztály 1994).

2.2.5.2. Telekesoldal complex (TO)

It is a Middle–Late Jurassic complex, consisting of black shale, sandstone olistoliths ("sandstone olistholitic member" of Grill 1988) and olistostromes ("conglomerate olistholitic member" of Grill (1988) and Kovács (1988)). However, their stratigraphic relations are poorly constrained due to the scarcity of age-diagnostic fossils and continuous successions. The supposed lowermost part of the complex consists of dark grey, partly silicified marlstone, claymarl and calcareous slate. Based on a single radiolarian specimen (core Rudabánya Rb-661, 59.0–59.1 m) only the Jurassic age of this interval could be determined (Dosztály 1994). Dark grey shale with fine to medium-grained

sandstone bodies – interpreted as olistoliths (Grill 1988) – made up the middle member of the TO complex. The most characteristic lithofacies type is the olistostrome unit, where different types of carbonate clasts are predominant (Grill 1988) while highly altered rhyolite fragments are also present. In the dark grey slate and marlstone occasionally ten to hundred meters sized rhyolite bodies occur. According to Grill (1988), Szakmány et al. (1989) and Máthé & Szakmány (1990) they can be subvolcanic rhyolite bodies. The volcanic activity was supposed to be more or less coeval with the sedimentation of the shale. Uncertainty of the sedimentary age and lack of exact radiometric age for the volcanism (Rb/Sr 154±38 Ma) (Kovács 1988) was made impossible to decide the order of the events on bases of the ages. However, investigations aiming the boundary of the rhyolite and the surrounding shale were carried out, with an interpretation of having thermal contact between the igneous and sedimentary rocks (Szakmány et al. 1989). Belemnites from the upper part of the complex may indicate Upper Jurassic age (Galácz in Grill 1988), while radiolarian investigations of Dosztály et al. (1998) resulted in Aalenian-Bath interval for the upper part of the complex.

2.2.5.3. Nyúltkertlápa beds (NL)

The Nyúltkertlápa beds (NL) consist of greenish grey slate, siltstone, slaty marlstone with limestone olistoliths and microolistostrome horizons. Although no stratigraphic age is known, these beds are considered as Upper Triassic(?)-Jurassic(?) (Kovács & Árkai 1989, Szentpétery & Less 2006) or Lower Triassic (Pelikán pers. com.). The rocks suffered anchizonal metamorphism (Árkai 1981, 1985, 1989). The suite occurs in the Bódvarákó tectonic window, above the middle Triassic Bódvarákó Fm. (Fig. 5), and despite the considerable stratigraphic gap and/or tectonic truncation, they were considered as part of a unique sequence (Bódvarákó series) (Fig. 4).

2.2.5.4. Szö-3 borehole (Akasztó unit)

Black to grey slate and calcareous shale was encountered in the Szögliget Szö-3 borehole and similar rocks occur on surface in the surroundings. Former classification (Less et al. 1988) attributed this series to the Lower Triassic of the non-metamorphic Aggtelek series (Fig. 5). In contrast, new investigations treated it as part of a separate tectonic scale – the so-called Akasztó unit (Chapter 5.4.3).

2.3. Structural evolution, concepts

The structural and paleogeographic relationships between the different nappes (Silice, Meliata, and Torna) and their relations to the more external structural units of the Western Carpathians (Gemer, Vepor) are still enigmatic in the light of the literature. The main uncontroversial periods in the Mesozoic evolution of the region are the next ones: 1) platform stage in Early to Middle or Late Triassic, 2) continental to oceanic rifting processes leading to the thinning of the crust (Middle Triassic to Middle Jurassic), 3) subduction and obduction of the oceanic crust, resulted in thickening of the crust (Middle Jurassic to Early Cretaceous), and finally post-metamorphic nappe-stacking from the mid-Cretaceous (Plašienka et al. 1997, Less 2000, Szentpétery & Less 2006). The main differences are in the supposed original paleogeographic position of the structural units, timing and direction of subduction, obduction and nappe movements (Grill et al. 1984, Lexa et al. 2003, Schmid et al. 2008).

Part of the authors consider the Meliata nappe system as a suture zone (Rožnava suture), placing the Silice nappe system and the slightly metamorphosed Torna series to an upper plate position over the Meliata nappe sys-

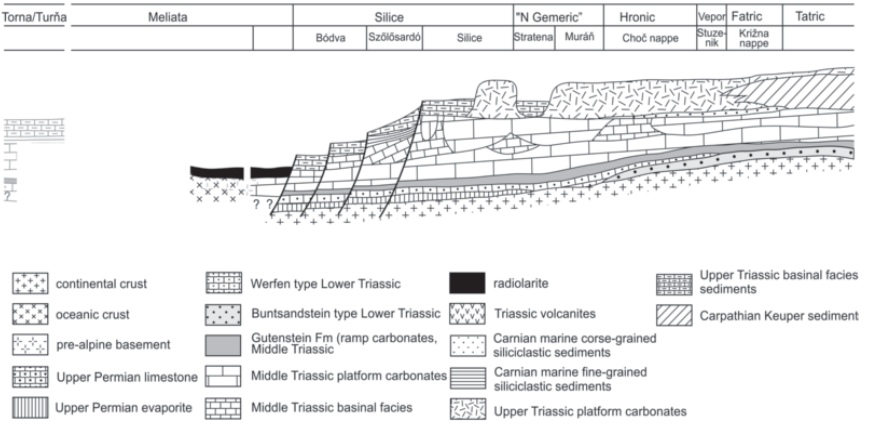

Figure 8. Paleogeographic reconstruction of the Western Carpathians (Haas 2006 ed.). Note Torna series on the other side of the ocean.

tem (Mello et al. 1996, Plašienka et al. 1997). In this model the southern units of the Western Carpathians formed the active margin of the Meliata branch of the Neotethys Ocean, while the oceanic crust subducted beneath the Torna series and Silice nappe system as a passive margin (Plašienka et al. 1997, Plašienka 1998).

According to another concept, the Silice nappe system was derived from the northern passive margin of the Meliata branch of the Neotethys Ocean (Fig. 3, 8), with the Szőlősardó series forming a transitional zone, and Bódva facies unit representing the southernmost and most distal margin (Kovács et al. 1989, Kovács 1992). The low-grade metamorphism of the Torna series was attributed to its location at the southern, active margin (and thus lower plate position) with respect to northward subduction (Grill et al. 1984, Less 2000). This latter paleogeographic reconstruction was recently modified (Schmid et al. 2008) placing all the Western Carpathian-derived tectonic units (including Torna series) to the northern, passive margin (according to present-day coordinates) of the Meliata-Neotethys Ocean, while the southern, active margin is represented by the Dinaridic-related units of Bükk (Fig. 8).

Csontos and Vörös (2004) presented a new palinspastic reconstruction suggesting new interpretation for the Silice nappe system. It was supposed, that the Silice nappe system (together with other exotic units e.g. Juvavic nappe, Upper Codru nappe, Persani nappe) correlates with an enigmatic micro-continent that lay to the NE of the southern, Dinaric margin, across the Meliata – Vardar ocean. Northern (European) origin of the micro-continent was proposed.

The vergency of the Cretaceous collision event varies between the different authors, too. South-verging nappe movement was assumed by Less (Less 2000) in the Cretaceous. In contrast with it, shear direction from blueschists indicated northward transport (Faryad & Henjes-Kunst 1997). North-verging collision of a southern continent with the northerly lying West Carpathian domain (European plate) was described by (Lexa et al. 2003), too. In this model the southern continent behaved as a rigid indenter controlling the deformation of all northern foreland crustal units, and was moving toward the north (in recent coordinate system). The rheological assumptions between the Variscan Vepor basement complexes composed of gneisses and granites and the low-grade slates of Gemer Unit led to the formation of complex, polyphase deformation, including a cleavage fan (Lexa et al. 2003).

3. Questions and aims

The basic aim of my research was establishing a new model on the Mesozoic tectonic evolution of the central part of the Rudabánya Hills and integrates it into the existing models about the evolution of the Western Carpathians. To achieve this aim the main tasks were

Defining nappes: How many nappes are present in the research area? What is their present-day position? What is the geometry of the nappe boundaries? What were the relative and absolute ages of the nappe stacking phases? Can I find some shear criteria to characterize the direction of the nappe movements? What is the present-day structural order of the nappes? How many nappe stacking phases can be distinguished?

Characterizing their lithostratigraphic content: What is the relationship between the different Triassic and Jurassic series? Is it possible to find Jurassic stratigraphic continuations of the Triassic sequences? Did all Jurassic sequences have/used to have a Triassic basement? How to distinguish the Jurassic series on field and in laboratory? What was the depositional environment for the poorly constrained Jurassic series? What is the source area of the clasts of the Jurassic olistostromes? Is it possible to find proofs on the relationship of the rhyolite and the shale in the TO complex? Is there any other method to get the sedimentary age of the poorly constrained black shale?

Describing the inner deformation (partly ductile) of the nappes: How many ductile deformation events were present in the investigated rocks? Are they present in all of the nappes or diagnostic for some of them? What is the order of the events? Is it possible suggesting any age constrain for the deformation phases? How the micro-texture look like? What are the main micro-scale deformational features? What were the main mechanisms of deformation?

Characterizing the P, T and t conditions of the metamorphism: What minimum temperature can be suggested by the above mentioned deformation mechanisms? What kind of tectonometamorphic evolution can be suggested in the investigated nappes? What was the age of the metamorphic event(s)? Is it possible to use the previously measured metamorphic petrological data, and compare them with the new results? Is it possible to distinguish nappes on basis of their metamorphic degree/history?

Characterizing the P, T and t conditions of the nappe movements: What kind of information can be squeezed out from nappe-base (nappe-sole) rauhwackes? Is it possible to find suitable syn-deformational minerals for fluid inclusion studies?

Comparison: Do my observations/results suite in any of the existing models about the Mesozoic evolution of the Inner Western Carpathians? Do they suggest any changes? Do I add some new data to better understanding the Mesozoic evolution of the Neotethys Ocean?

4. Methods

Structural observations and measurements were carried out in the majority of Triassic and Jurassic outcrops in the central part of the Rudabánya Hills. Measurements included bedding, foliation and occasionally fold axes. Representative cross sections were constructed from outcrop-scale observations and reinterpretation of borehole data. A detailed, but not complete geological mapping of the key areas completed the structural observations. The main goals were to check formation boundaries, measuring dip values and to determine the bedding-foliation relationship.

Several boreholes and core sections (Szet-3, -4, Sza-4, -5, -7, -10, -12, Va-1, -2, -3, -4, P-74, Szö-3, Ha-3, -4, Rb-658, -661, Tsz-16) were reinvestigated to examine the penetrated structural/ sedimentological boundaries, and take new samples for **thermometamorphic and microtectonic studies**. The relationship of the Upper Triassic and Jurassic series was the target of special interest, because it has crucial importance in the evaluation of stratigraphic and tectonic problems.

For microstructural investigations oriented thin sections were prepared from rock slabs cut perpendicular to the foliation planes. The usual lack of lineation prevented the preparation of thin sections along X-Z fabric planes.

More than one hundred-twenty rock samples from the Triassic–Jurassic of the Rudabánya Hills and the Triassic Bódva and Torna series were selected for new metamorphic petrologic studies. Almost two hundred illite Kübler index (KI), chlorite "crystallinity" (ChC) and K-white mica b cell dimension data were elucidated in order to separate the different nappes and characterize the temperature and pressure conditions of the metamorphic event(s). Part of the data was measured more than 20 years ago by the same laboratory and team (Árkai & Kovács 1986, Kovács & Árkai 1989, Árkai 1981, 1985, 1989). Thus it became possible to compile a comparable database of the earlier and recent data in this study.

To constrain the timing of the detected very low to low-grade metamorphism **K-Ar age data** were measured on <2μm grain size fractions from 10 samples on which metamorphic petrological samples investigations had been carried out.

Samples were collected from rhyolite bodies of the TO complex to carry out **U/Pb dating**. The specimens had different position in compare with the Jurassic shale matrix: 100 m size body, few cm-sized olistoliths from the olistostrome horizons, volcanoclastic material from the matrix of the olistostrome.

Paleostress reconstructions from the measured fault-slip data were carried out by the software of Angelier (1984, 1990). Stress axes were calculated by the Tensor modul of the software. Automatic phase separation was carried out for sites, where multiple faulting phases were suspected. Automatic separation was sometimes complemented by manual separation. In this case conjugate pairs of fractures (faults and joints) were separated and stress axes were estimated using the theory of Anderson (1951). The software of Angelier (modul Diagra) was also used for visualisation of ductile structural data, like foliation, shear bands, lineation. Fold axes for kinks, and other type folds were estimated visually on the stereograms. In this case, the shortening direction for folds was also estimated. Symbols were adapted from the detailed work of Fodor (2010). For each site a detailed, evaluation procedure was executed, registered on Corel Draw sheets, but only the stereograms classified to tectonic phases are presented, mainly in chapter 7.

Basal tectonic breccias (rauhwacke) were collected from 5 different contact zones to characterize the temperature and pressure conditions of the nappe enplacements. Synkinematic minerals from these samples were separated for **fluid inclusion studies**. These inclusions provided valueable information about the composition and the temperature of the fluids which lubricated the bases of the nappes during the tectonic processes. Pressure conditions could also be estimated. These data had a great importance during tectonic reconstructions and interpretation of the metamorphic petrological data.

5. Lithological and sedimentological investigations of the Jurassic series

5.1. Introduction

The Jurassic sequences of the Aggtelek-Rudabánya Hills have been studied since the middle of the 19th century (Foetterle 1869). Until the 1980-ies the whole Mesozoic succession was assigned to the Triassic. As a result of the works of Grill & Kozur (1986), Grill (1988) and (Dosztály 1994) Jurassic age of these formations became generally accepted. These uppermost Triassic(?)—Middle Jurassic formations have a great importance for understanding the Jurassic evolution of the Neotethys Ocean. However, no detailed report on the sedimentological characteristics and component analysis of the redeposited clasts has been published so far except from the Szalonna-Perkupa road cut key-section of Telekesoldal Formation by Kovács (1988). The aim of this part of the work was defining lithofacies units, summarizing the facies characteristics of the defined units, providing interpretation for the provenance of the redeposited clasts and depositional environments, and last but not at least revising the existing radiolarian data, and providing new age data (if possible) by foraminifera and palynomorph investigations.

Beside the well known occurrences of Telekesoldal and Telekesvölgy complexes (Grill & Kozur 1986, Less et al. 1986, Grill 1988, Dosztály 1994), geological mapping revealed some other occurrences, which easily can be uppermost Triassic or Jurassic on the bases of their stratigraphic and/or structural position. These are the olistostrome outcrops at Hidvégardó and Csipkés Hill. The former one was considered to be the lowermost part of the Telekesvölgy complex (Less et al. 2006) while the latter was not differentiated within the Telekesoldal complex.

5.2. Telekesvölgy complex (TV)

On the basis of macroscopic observations and microfacies studies performed on cores Rudabánya Rb-658, Szalonna Sza-5, Szendrő Szet-4, Varbóc Va-2 cores (Fig. 1), trenches in the Telekes Valley (Tributary Valley 7 and 8) and outcrops on Csipkés Hill (Appendix 2, 3) Fig. 1) various lithofacies units could be distinguished. However, continuous sections exposing the whole formation are not available, the relevant biostratigraphic data are very limited and the stratigraphic superposition of the lithofacies units is ambiguous. Figure 9 shows the most probable lithofacies succession referring to the relevant cores and surface exposures and the discussion below follows this pattern.

5.2.1. Microfacies studies

5.2.1.1. Variegated and grey marl; crinoideal limestone

In the lowermost part of the **Perkupa P-74** core (Fig. 10) brown to grey marl occurs above the Norian Hallstatt Formation with slightly disturbed contact (~210 m). The marl is tectonically overlain by overturned Upper Triassic hemipelagic carbonates. The~30 m thick variegated and grey marl interval shows great similarities to the Zlambach Formation. Texture of these rocks is rather unspecific; mudstone—wackestone containing small bioclasts, silt-sized quartz and in one thin section

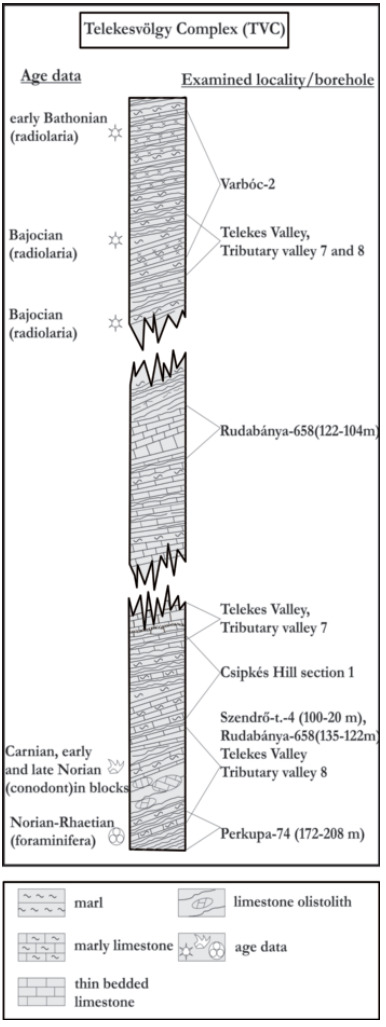

Figure 9. Simplified reconstructed stratigraphic column of the Telekesvölgy complex. The positions of the age data, the studied boreholes and outcrops are approximately indicated.

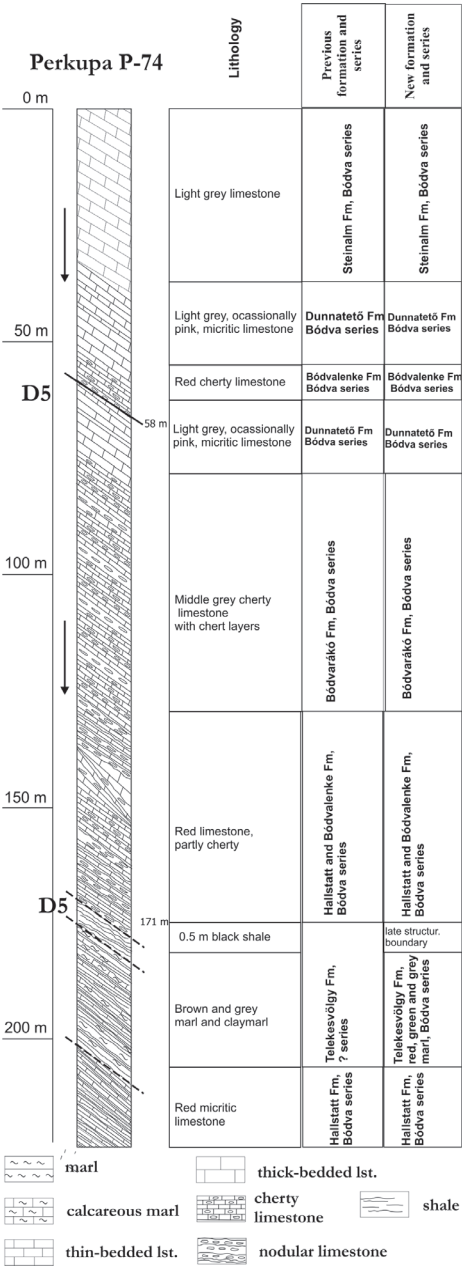

Figure 10. Lithologic and stratigraphic features of Perkupa P-74 borehol with old and new interpretations. For the structural interpretation see chapter

poorly preserved foraminifers (see chapter 5.2.2.3.), ostracodes, fragments of bivalves, echinoderms and radiolarian moulds (Fig. 11.1).

In the **Rudabánya Rb-658** core (Fig. 12), red and green claystone alternating with grey marl and calcareous marl was encountered (~80-130 m) above Hallstatt-type red, locally cherty limestone (Kovács in Szentpétery & Less 2006). The lowermost, about 13 m thick part of this succession is made up of red and green claystone intercalating with grey marl. The texture of the samples studied is strongly sheared, and altered. However, the original radiolarian wackestone texture could be recognized (Fig. 11.2). Calcite moulds of radiolarians are usually deformed showing lenticular shape. Sponge spicules and other bioclasts can also be recognized in a few cases. The rocks were commonly affected by dolomitization and subsequent selective silicification. Under microscope the texture is seemingly silty shale containing dis-

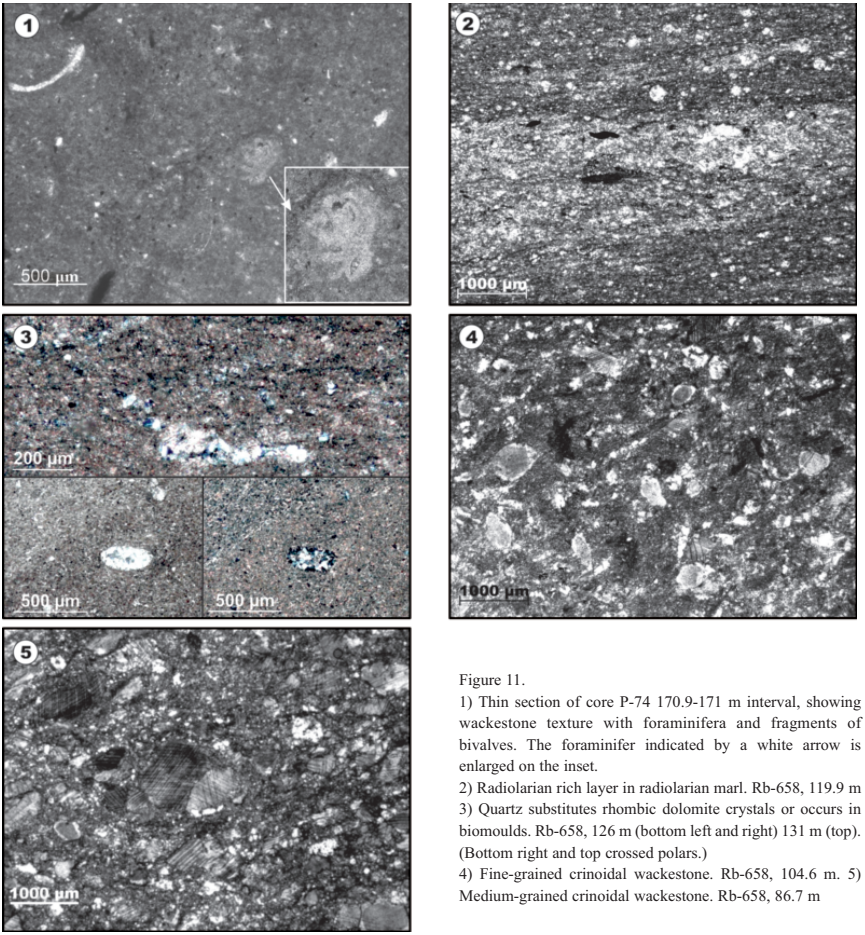

Figure 11.
1) Thin section of core P-74 170.9-171 m interval, showing wackestone texture with foraminifera and fragments of bivalves. The foraminifer indicated by a white arrow is enlarged on the inset.
2) Radiolarian rich layer in radiolarian marl. Rb-658, 119.9 m
3) Quartz substitutes rhombic dolomite crystals or occurs in biomoulds. Rb-658, 126 m (bottom left and right) 131 m (top). (Bottom right and top crossed polars.)
4) Fine-grained crinoidal wackestone. Rb-658, 104.6 m. 5) Medium-grained crinoidal wackestone. Rb-658, 86.7 m

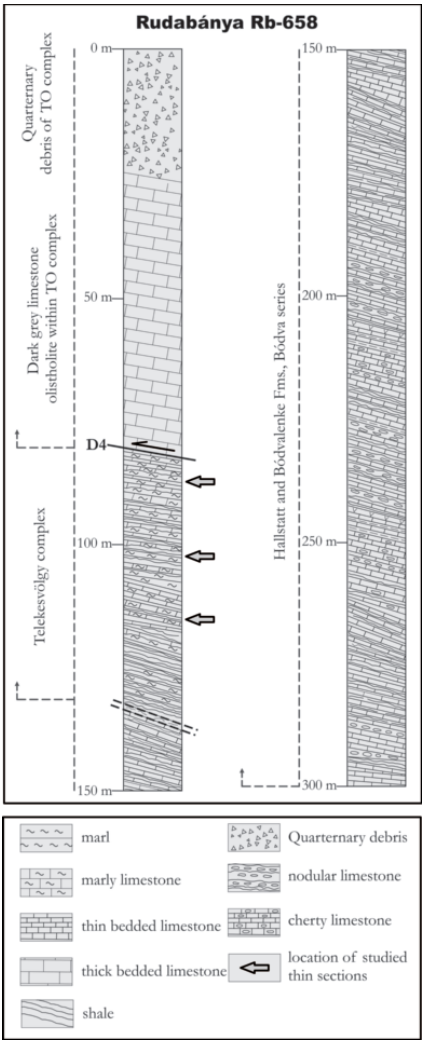

Figure 12. Lithologic and stratigraphic features of the Rudabánya Rb-658 borehole with new interpretations. For structural interpretation see chapter 7.4.

seminated silt-sized quartz. However, in a lot of cases quartz occurs in biomoulds (Fig. 11.3) or substitutes rhombic dolomite crystals. Accordingly, the majority of the quartz particles are probably not terrigenous grains, but they formed by diagenetic alteration and structural deformation processes.

In the middle part of the section (~100-120 m) the proportion of the grey marl and calcareous marl continuously increases, while the ratio of red and green claystone interlayers decreases. In this ~20 m thick interval fine to medium sand-sized crinoid ossicles are common in a micritic—microsparitic matrix and thin crinoidal packstone to grainstone interlayers also occur (Fig. 11.4, 11.5). The matrix is often, crinoids are rarely silicified. Grey siliceous crinoidal marls and limestones akin to those in Rb-658 core (104—122 m) were reported by Grill (1988) from the Telekes Valley Tributary Valley 7 section and Csipkés Hill section 1 (Fig. 1).

The next ~20 m thick segment (100-80m) is made up of green and pink marl, calcareous marl and thin limestone layers progressing upward into grey marl. The marls and the calcareous marl have uniformly barren mudstone texture. It is tectonically overlain by dark grey limestone, showing microsparitic texture with no sign of any diagnostic microstructure or fossil, which can refer either to the depositional environment or to the age of sedimentation. On basis of its macroscopic features, this limestone was assigned to the Gutenstein Formation (Less et al. 1988). Its stratigraphic and tectonic interpretation will be discussed in chapter 7.4.2.2.

In **Szalonna Sza-5** core (Fig. 13) Upper Triassic red, locally cherty limestone (Hallstatt Limestone) is concordantly overlain by red, green and grey marl in 23 m thickness that was assigned to the Upper Triassic Zlambach Formation (Nádor 1990, Szentpétery & Less 2006). It is followed by grey marl with slump structures in a thickness of 30 m. As this variegated marl is highly resembles to the previously investigated marls, I agree with this classification.

Brownish grey, green and red claymarl, alternating with red or yellow limestone and cher-

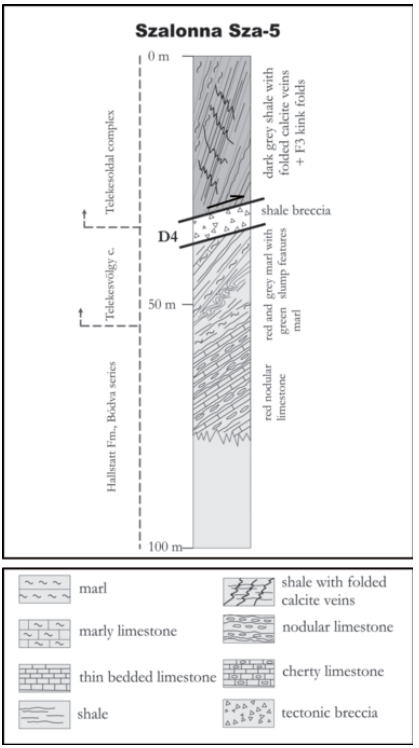

Figure 13. Lithologic and stratigraphic features of the Szalonna Sza-5 borehole with new interpretations. For structural interpretation see chapter 7.5.

ty limestone exposed in the Telekes Valley, Tributary Valley 8 section may also belong to this lithofacies unit but it is poorly constrained (Grill 1988). It contains pink limestone olistoliths with Carnian age and yellow limestone which yielded Late Norian conodonts (Balogh & Kovács 1977). This latter limestone was interpreted as an intercalated layer, being the same age as the marl beds. Thus the fossils probably indicate real depositional age of late Triassic.

In the sample taken from the Csipkés Hill section 1, alternating red and yellow laminas are visible. The yellow layers consist of fine sand to silt-sized clasts that might be silicified carbonate particles while the red layers are radiolarian wackestone.

5.2.1.2. Black siliceous shale

In **Varbóc Va-2** borehole the Norian Hallstatt Limestone is tectonically overlain by black shale about 80 m thick. The locally silicified shale contains large amounts of radiolarians (see chapter 5.2.2.1.) and sponge spicules.

In the western part of the section exposed on the higher valley side of **Telekes Valley, Tributary Valley 8**, beside the mentioned steeply dipping Upper Triassic claymarl succession, black shale and siliceous shale were found. Radiolarian wackestone, radiolarian-sponge spicule wackestone and packstone (Fig. 14.1, 14.3), sponge spicule packstone (Fig. 14.4), and radiolarite are typical textures of this lithofacies unit. In some samples sharp, erosional boundaries are visible between the radiolarian shale and the crinoidal calcarenite layer (Fig. 14.5, 14.6); the latter is formed via redeposition. The same texture types were found in the samples taken from black shale in the Telekes Valley Tributary Valley 7 section (Grill 1988).

5.2.2. Revision of the radiolarian and foraminifer fauna in the Telekesvölgy Complex

The first studies of radiolarians of the Rudabánya Hills were conducted by Grill & Kozur (1986). Their samples were collected from the Varbóc-2 borehole and from several different outcrops in the Rudabánya Hills (i.e. Csehi Hill, Telekes Valley Tributary Valley 7 and 8). Radiolarians were always found in the sequence of monotonous black to dark grey shales, mudstones, siliceous shales, manganese shales (Grill & Kozur 1986). Previous biostratigraphic data of radiolarian investigation presumed **Aalenian to middle Bajocian** ages in different sequences. According to the re-assessment of the Varbóc-2 borehole (Dosztály 1994), the biostratigraphic age assigned the lower part to the

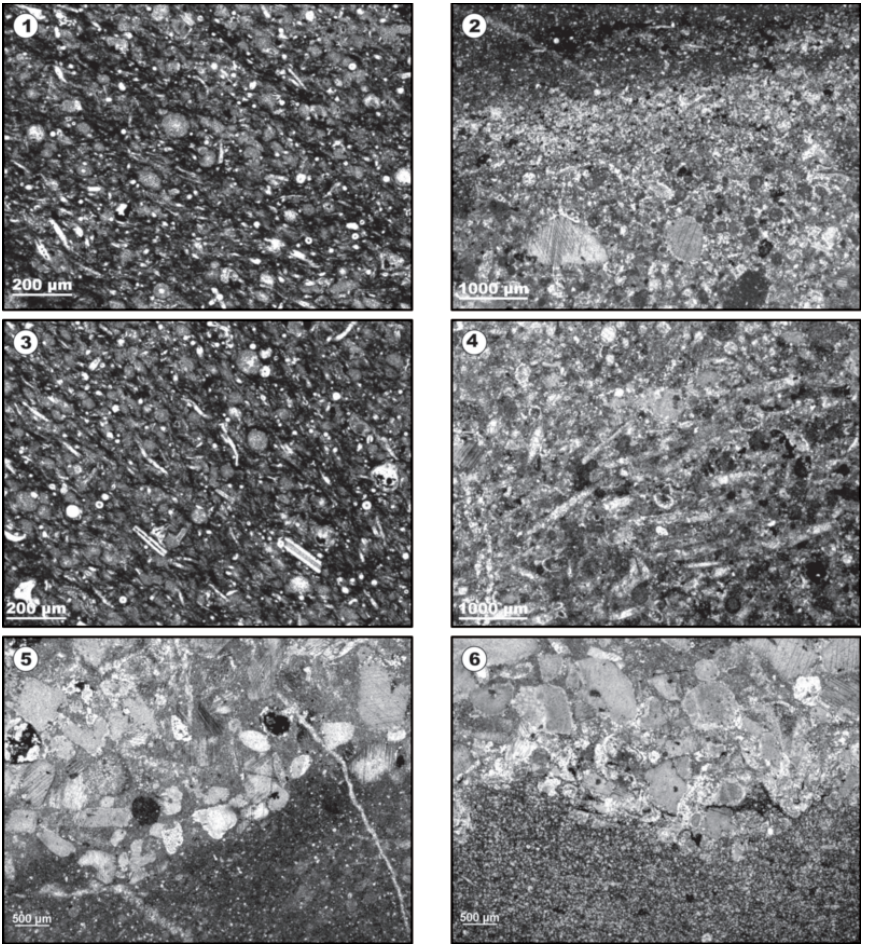

Figure 14. 1, 3: Radiolarian- sponge spicule packstone, Telekes Valley Tributary Valley 8.
2, 4, 5, 6: Detailes of a calciturbidite layer, Telekes Valley: above an uneven erosion surface a mudstone layer is overlained by coarse-grained crinoidal packstone that is the basal part of a carbonate turbidite (5,6). Sponge spicula and crinoid packstone in the higher part of the turbidite layer (4). The topmost part of the turbidite layer showing gradual transition to wackestone-mudstone texture (2)

Aalenian, and the upper part to the **Bajocian or Bathonian**.

In the study of Kövér et al. (2009b), the re-assessment of the radiolarian biozonation is based on the Unitary Association Zones (UAZ95) proposed by Baumgartner et al. (1995). The occurrence and the stratigraphical distribution of the radiolarians in the examined samples are shown in Appendix Table 1.

Varbóc-2 borehole

The Varbóc-2 borehole penetrated the 87 m thick Jurassic monotonous black to dark grey shales, with thin siliceous shales and cherts, and crinoidal limestones intercalated with grey marl and mudstone. 16 samples – collected and prepared by L. Dosztály – yielded abundant and moderately well preserved radiolarian assemblages. The following stratigraphically important radiolarian taxa were identified from the samples **80.9 m, 79.1 m, 77.6 m, 73.9 m, 73.0 m and 69.7 m** (Fig 15, 16) (Kövér et al. 2009b): *Hsuum mirabundum* Pessagno & Whalen, *H. belliatulum* Pessagno & Whalen, *H. matsuokai* (Isozaki & Matsuda), *Transhsuum maxwelli* (Pessagno), *Parahsuum officerense* Pessagno & Whalen, *P. snowshoense* (Pessagno & Whalen), *Semihsuum inexploratum* (Blome), *Pseudodictyomitrella spinosa* Grill & Kozur, *Archaeodictyomitra rigida* Pessagno, *Laxtorum(?) hichisoense* (Isozaki & Matsuda), *Canoptum hungaricum* Grill & Kozur, *Tetratrabs zealis* (Ožvoldová).

The co-occurrence of *H. mirabundum* Pessagno & Whalen (UAZ 3—6), *L.(?) hichisoense* Isozaki & Matsuda (UAZ 1—4) and *T. zealis* (Ožvoldová) (UAZ 4—13) indicates the UAZ 4 (Late Bajocian). However, presence of *H. belliatulum* Pessagno & Whalen and *H. snowshoense* (Pessagno & Whalen) makes the lower - middle **Bajocian** age probable for this sequence as well, because these taxa co-occur in that close range in North America (Pessagno & Whalen 1982).

Samples from **64.1 m to 3.4 m** yielded the following stratigraphically important radiolarian taxa (Fig. 15, 16) (Kövér et al. 2009b): *Hsuum mirabundum* Pessagno & Whalen, *H. rosebudense* Pessagno & Whalen, *H. matsuokai* Isozaki & Matsuda, *Parahsuum stanleyense* (Pessagno), *Transhsuum hisuikyoense* (Isozaki & Matsuda), *T. maxwelli* (Pessagno), *Semihsuum inexploratum* (Blome), *Pseudocyrtis buekkensis* Grill & Kozur, *Eucyrtidiellum nodosum* Wakita, *Eucyrtidellum* cf. *E. unumaense* (Yao), *Stichocapsa robusta* Matsuoka, *Stichocapsa* sp. E. Baumgartner, *Archaeodictyomitra rigida* Pessagno, *A. exigua* Blome, *A. cellulata* O'Dogherty, Goričan & Dumitrica, *A. prisca* Kozur & Mostler, *Pseudodictyomitrella hexagonata* (Heitzer), *Protunuma turbo* Matsuoka, *Canoptum hungaricum* Grill & Kozur, *Dictyomitrella (?) kamoensis* Mizutani & Kido.

The co-occurrence of *H. mirabundum* Pessagno & Whalen (UAZ 3—6) and *Stichocapsa robusta* Matsuoka (UAZ 5—7) indicates the UAZ 5—6 (latest Bajocian to Early Bathonian), furthermore the presence of *Stichocapsa* sp. E. Baumgartner (UAZ 5) presumably narrows the range to the UAZ 5 (**latest Bajocian to Early Bathonian**).

Telekes Valley — Tributary Valley 8

In this section seven samples collected from the black and siliceous shale are re-assessed. The samples yielded the following, relatively well preserved and stratigraphically important radiolarian taxa (Fig. 15, 16) (Kövér et al 2009b): *Pseudodictyomitrella spinosa* (Grill & Kozur), *Canoptum hungaricum* (Grill & Kozur), *Unuma cf. U. typicus* (Yao), *Parahsuum izeense* (Pessagno & Whalen), *Transhsuum hisuikyoense* (Isozaki & Matsuda), *T. maxwelli* (Pessagno), *T. brevicostatum* (Ožvoldová), *Eucyrtidiellum nodosum* Wakita, *E. (?) quinatum* (Takemura).

The co-occurrence of *P. izeense* (Pessagno & Whalen) (UAZ 1—3) and *T. maxwelli* (Pessagno) (UAZ 3—10) idicates the UAZ 3 (**early-middle Bajocian**). Contrary to Dosztály's previous data (1994) no difference in biostratigraphic age between the lower and upper part of the investigated sequence could be recognized.

Perkupa-74 172-208 m foraminifer fauna

Sample was collected from the lowest, normal younging structural scale from borehole Perkupa

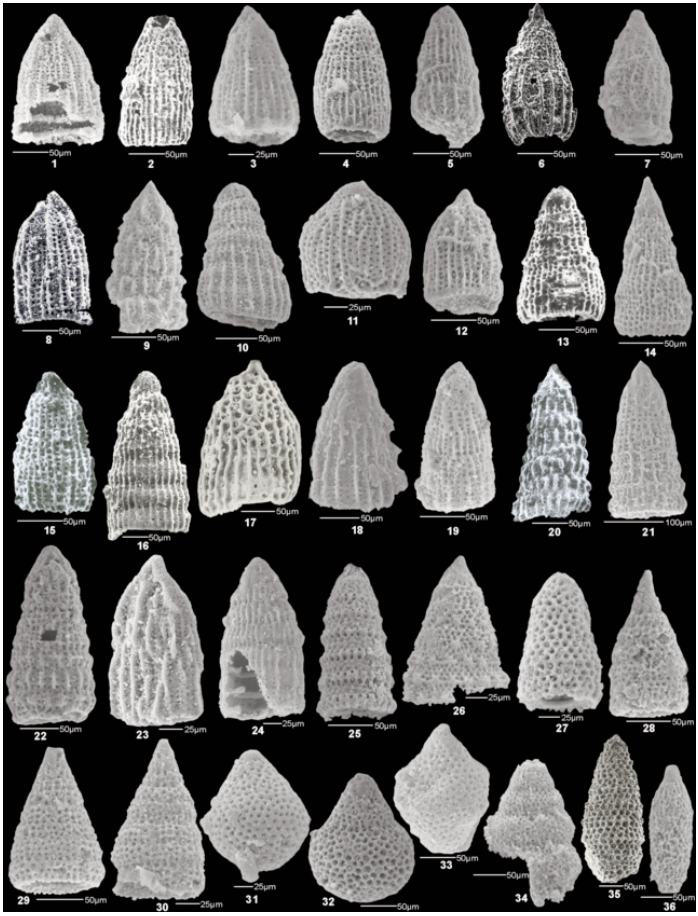

Figure 15. Determined radiolaria fauna from the Telekesvölgy complex (Kövér et al. 2009b).
1 Archaeodictyomitra cellulata O'Dogherty, Goričan and Dumitricã; Va-2 borehole: 49.3 m 2 Archaeodictyomitra exigua Blome; Telekes Valley - Tributary valley 8: 8-43a 3 Archaeodictyomitra patricki Kocher, Va-2 borehole: 3.4 m 4 Archaeodictyomitra rigida Pessagno, Va-2 borehole: 64.1 m 5 Hsuum baloghi Grill and Kozur, Va-2 borehole: 48.5 m 6 Hsuum matsuokai Isozaki and Matsuda, Va-2 borehole: 73.0 m
7 Hsuum mirabundum Pessagno and Whalen, Va-2 borehole: 3.4 m 8 Hsuum rosebudense Pessagno and Whalen, Va-2 borehole: 49.3 m 9 Hsuum sp. E in Hull, Va-2 borehole: 58.5 m 10 Hsuum cf. cuestaense Pessagno, Telekes Valley - Tributary valley 8: 8-47a 11 Hsuum cf. sp. 1 sensu O'Dogherty et al., Telekes Valley, Tributary valley 8: 8-43a 12 Parahsuum carpathicum Widz and De Wever, Va-2 borehole: 30.2 m 13 Parahsuum indornitum (Pessagno and Whalen), Telekes Valley, Tributary valley 8: 8-55a 14 Parahsuum officerense (Pessagno and Whalen), Va-2 borehole: 79.1 m 15 Parahsuum izeense (Pessagno and Whalen), Telekes Valley, Tributary valley 8: 8-47 16 Parahsuum snowshoense (Pessagno and Whalen), Va-2 borehole: 64.1 m 17 Parahsuum stanleyense (Pessagno), Va-2 borehole: 3.4 m 18 Semishuum inexploratum (Blome), Va-2 borehole: 3.4 m 19 Semishuum sp., Va-2 borehole: 30.2 m 20 Transhsuum brevicostatum (Ožvoldová), Telekes Valley, Tributary valley 8: 8-47a 21 Transhsuum hisuikyoense (Isozaki and Matsuda), Va-2 borehole: 69.7 m 22 Transhsuum maxwelli (Pessagno), Va-2 borehole: 64.1 m 23 Transhsuum sp. 1, Va-2 borehole: 48.5 m 24 Transhsuum sp. 2, Va-2 borehole: 49.3 m 25 Dictyomitrella (?) kamoensis Mizutani and Kido, Va-2 borehole: 45.4 m 26 Parvicingula sp., Va-2 borehole: 49.3 m 27 Pseudodictyomitrella hexagonata Grill and Kozur, Va-2 borehole: 64.1 m 28 Pseudodictyomitrella spinosa Grill and Kozur, Va-2 borehole: 77.6 m 29 Pseudodictyomitrella cf. spinosa Grill and Kozur, Va-2 borehole: 77.6 m 30 Pseudodictyomitrella wallacheri Grill and Kozur, Va-2 borehole: 77.6 m 31 Stichocapsa robusta Matsuoka, Va-2 borehole: 13.1 m 32 Stichocapsa sp., Va-2 borehole: 64.1 m 33 Stichocapsa sp. E in Baumgartner, Va-2 borehole: 3.4 m 34 Stichomitra sp., Va-2 borehole: 49.3 m 35 Pseudoeucyrtis elongata Grill and Kozur, Va-2 borehole: 30.2 m 36 Pseudoeucyrtis sp., Va-2 borehole: 69.7 m

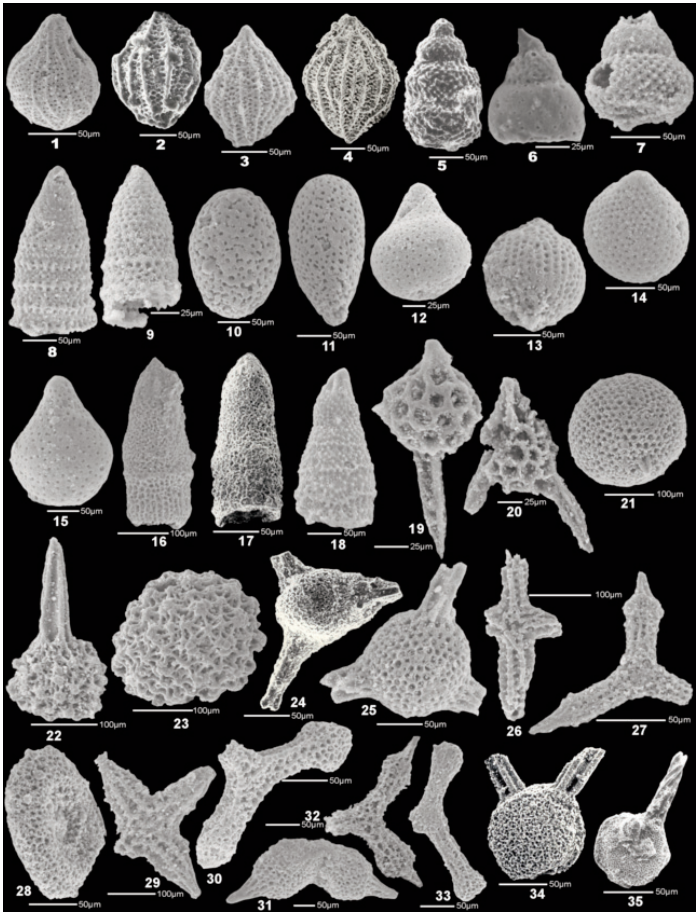

Figure 16 Determined radiolaria fauna from the Telekesvölgy complex

1 Protunuma turbo Matsuoka, Va-2 borehole: 64.1 m 2 Unuma ochiensis (Matsuoka), Va-2 borehole: 3.4 m 3 Unuma typicus Yao, Va-2 borehole: 64.1 m 4 Unuma cf. typicus Yao, Telekes Valley - Tributary valley 8: 8-43 5 Eucyrtidiellum (?) quinatum Takemura, Telekes Valley - Tributary valley 8: 8-53 6 Eucyrtidiellum cf. unumaense (Yao), Va-2 borehole: 64.1 m 7 Eucyrtidiellum sp. 1, Va-2 borehole: 51.5 m 8 Canoptum hungaricum Grill and Kozur, Va-2 borehole: 69.7 m 9 Canoptum rudabanyaense Grill and Kozur, Va-2 borehole: 48.5 m 10 Archicapsa sp. 1, Va-2 borehole: 64.1 m 11 Archicapsa sp. 2, Telekes Valley - Tributary valley 8: 8-47 12 Williriedellum sp., Va-2 borehole: 13.1 m 13 Striatojaponocapsa synconexa O'Dogherty, Goričan and Dumitrică, Va-2 borehole: 13.1 m 14 Praewilliriedellum convexum (Yao), Va-2 borehole: 30.2 m 15 Praewilliriedellum sp., Va-2 borehole: 58.5 m 16 Laxtorum (?) hichisoense Isozaki and Matsuda, Va-2 borehole: 73.0 m 17 Laxtorum (?) jurassicum Isozaki and Matsuda, Va-2 borehole: 80.9 m 18 Spongocapsula palmerae Pessagno, Va-2 borehole: 58.5 m 19 Pantanellium sp. 1, Szet-3: 52.0 m – 53.0 m 20 Gorgansium sp., Szet-3: 52.0 m – 53.0 m 21 Cenosphaera sp. X Yao, Szet-3: 69.8 m – 70.6 m 22 Acaeniotylopsis (?) sp., Szet-3: 69.8 m – 70.6 m 23 Praeconocaryomma sp., Va-2 borehole: 69.7 m 24 Triactoma cf. jonesi (Pessagno), Szet-3: 52.0 m – 53.0 m 25 Triactoma sp. 1, Szet-3: 69.8 m – 70.6 m 26 Tetratrabs zealis (Ožvoldová), Va-2 borehole: 73.9 m 27 Tritrabs simplex Kito and De Wever, Szet-3: 52.0 m – 53.0 m 28 Orbiculiforma sp. X in Baumgartner, Szet-3: 69.8 m – 70.6 m 29 Emiluvia lombardensis Baumgartner, Szet-3: 69.8 m – 70.6 m 30 Angulobracchia sp., Va-2 borehole: 69.7 m 31 Paronaella sp., Va-2 borehole: 69.7 m 32 Homoeoparonaella elegans (Pessagno), Szet-3: 52.0 m – 53.0 m 33 Homoeoparonaella argolidensis Baumgartner, Szet-3: 52.0 m – 53.0 m 34 Bernoullius rectispinus Kito et al., Va-2 borehole: 48.5 m 35 Bernoullius sp., Telekes Valley - Tributary valley 8: 8-52

P-74 (structural details in Chapter 7.5.2). This 172-208 m interval is represented by variegated to grey marl (Chapter 5.2.1.1). From this interval the following foraminifera taxa could be determined (Kövér et al. 2009b): *Aulotortus friedli* (Kristan-Tollmann), *A. parallelus* (Kristan-Tollmann), *Semiinvoluta clari* (Kristan), *Turrispirillina minima* Pantić, *Lamelliconus* sp., *Meandrospira* sp., *Frondicularia* sp., *Lingulina* sp.

The dominance of the Involutinidae (*Aulotortus, Semiinvoluta, Lamelliconus*) and Spirillinidae (*Turrispirillina*) indicate a warm, well-ventilated, shallow-water environment like the habitat for these forms.

The co-occurrence of these genera is characteristic in the Late Triassic. Except *A. friedli* (Kristan-Tollmann) – which appeared already in the lowermost Carnian – all species determined only in the Norian—Rhaetian (Kristan 1957; Kristan- Tollmann 1962, 1964, Zaninetti 1976, Salaj et al. 1983, 1988, Trifonova 1993). According to Salaj et al. (1983), the age range of the species *T. minima* Pantić is **Norian-Rhaetian**, although it was mostly reported from the Norian (e.g. Oravecz- Scheffer 1987). This new findings strengthen our conclusion that the lower part of the TV complex has the same age as the lithologically also similar Norian-Rhaetian Zlambach Marl.

5.2.3. Interpretation of the lithofacies units of the Telekesvölgy Complex

Based on data discussed above the observations on the TV complex as follows:

The red and green **variegated marl** develops continuously from the underlying Norian Hallstatt Limestone. This gradual transition was also reported by J. Mello from Bohúnovo and Silická Brezová localities (Slovakia) of the Silice nappe-system, where Upper Norian age of the Zlambach Marl was evidenced, and its continuous sedimentation was supposed into the Liassic (Mello 1974).

Middle to Late Triassic pelagic limestone olistoliths – slided blocks, which are lithologically similar to the underlying strata – occur locally in the variegated marl unit. The presence of redeposited, coeval shallow-water foraminifers (Perkupa-74 core) and older Triassic limestone blocks in this environment most probably refers to gravitational mass movements, transporting platform-derived material into the basin. The presence of slump folds (Telekesvölgy, Tributary Valley 7, core Szalonna Sza-5) also indicate base-of-slope environment. The age of the variegated marl is most probably upper **Norian** possibly extending to the **Rhaetian**. This age interval is supported by its stratigraphic position (continuous development from the Norian Hallstatt Fm.), conodonts (Telekes Valley, Tributary valley 8) and foraminifera fauna encountered from core Perkupa P-74 (previous chapter).

The upper Norian(-Rhaetian?) variegated marl gradually progresses into **grey marl** and calcareous marl, containing significant amount of redeposited crinoid fragments. Accordingly it may be interpreted as a hemipelagic facies, relatively close to submarine highs (or to the slope of the platform itself), from where the crinoid fragments can be originated (Kövér et al. 2009b). The age of this lithofacies unit is unknown, maybe Rhaetian–Early Jurassic.

Although this basal part of the TV complex has the same age and lithology as the Zlambach Formation, I suggest keeping the TV complex as defined above, and not classify the basal part to the Zlambach Formation. The main reason is that the lower and middle parts of the TV complex can hardly be separated without very detailed lithological and paleontological research. Thus, a Zlambach Fm. and a reduced TV complex could hardly be mappable units.

The **black shale**, rich in radiolarians and sponge spicules is a typical deep pelagic basin facies, Bajocian to Early Bathonian in age. The stratigraphic relationship of this lithofacies unit with the previously described one is not proven due to the lack of continuous outcrops or borehole material.

5.2.4. The contact of the Bódva series and the TV complex

The most important question concerning the structural position of the Jurassic formations is their relationship to the Triassic basements. This problem remained quite enigmatic in the light of earlier publications (Grill 1988, Less et al. 1988, Less 2000, Szentpétery & Less 2006). According to the most accepted former conception the Jurassic TO complex is the original sedimentary cover of the Triassic Bódva series (Fig. 7b,c), and they have a continuous sedimentary contact (core Szalonna Sza-5 Fig. 13) or their boundary is an erosional discordance surface (Szendrő Szet-4, Fig. 17, 7). In case of the TV complex it was considered to have an unknown Triassic basement (Fig. 7b) or do not have any (Less et al. 1988, Grill 1989, Grill 1988, Less 2000, Dosztály et al. 2002).

There are some other variations of the previously mentioned generally accepted conception (Fig. 7a). The Zlambach beds and the black shales of Szendrő Szet-4 (Fig. 17) and Szalonna Sza-5 (Fig. 13) were considered to be part of the Bódva series by Grill et al (1984). Besides these formations two other Jurassic series were mentioned in the Rudabánya Hills: the black Telekesoldal and the variegated Telekesvölgy. In this concept the TV was the original sedimentary cover of a Meliata-type Triassic series (it was before the verification of Jurassic age of the Meliata series), while the Triassic basement of TO thought to be unknown (Fig. 7).

Illite "crystallinity", Conodont Colour Alteration Index and vitrinite reflectance measurements were carried out on Mesozoic samples from the Rudabánya Hills by Árkai and Kovács (1986). There were samples both from TO and TV among the investigated samples. The tectonic position of the two Jurassic series was not discussed in details, but both of them were classified into the so called Bódva nappe (Fig. 7).

The structural position of the TO and TV complexes stayed controversial in the latest publication, too (Fig. 7c) (Szentpétery & Less 2006). The light brown and grey shale of Szendrő Szet-4 (Fig. 17) and the red and green and grey marls of Szalonna Sza-5 (Fig. 13) were separated (like in the version of Grill 1984) and thought to be part of the Zlambach Formation, developing continuously from the underlying Triassic beds of the Bódva series (Fig. 7a, c). The "Red and green Claymarl Member" of the TV complex was classified temporarily into the Bódva series, however tectonic contacts were supposed at every location (e.g. tributary valleys of the Telekes creek, Csipkés Hill, Szentpétery & Less 2006). Since the remaining part of the series was considered to be in sedimentary contact with the red and green marl, thus they suggested that although the boundaries between the lithologies were more or less tectonised in every location, the TV complex was the original cover of the Triassic of Bódva series (Fig. 7c). This claim is in contradiction with their other opinion, considering the TO complex as the Jurassic continuation of the Bódva series (Szentpétery & Less 2006), namely suggesting two different Jurassic cover for the same Triassic series.

To eliminate this contradiction several cores which seemed to be interesting from a structural point of view were reinvestigated.

The contact between the Late Triassic of Bódva series and the red, green and grey marl of the TV complex can be investigated in the following cores: Rudabánya Rb–658, Szendrő Szet–4, Perkupa P–74, and Szalonna Sza–5. It is common among these cores that Bódva-type Triassic sequence (Steinalm Limestone, ± Dunnatető Limestone, ± Bódvarákó Formation, Bódvalenke Formation, and Hallstatt Limestone) is followed by variegated or grey marl. The

stratigraphic and tectonic interpretation of the latter formation is equivocal.

The following observations were made on the relationship of the Hallstatt Limestone and the variegated marl. In the core **Szalonna Sza-5** (Fig. 13) a Bódva-typer Triassic succession is overlain by Jurassic rocks. The lower part of the borehole is built up by the Bódva series. From 53 m a sequence containing variegated marl, calcareous marl, claymarl and light brown limestone is developing continuously from the underlying red Hallstatt Limestone. The colour of the alternating marly beds is turning more greyish upwards. The upper, grey marl part contains slump folds. This marl is most probably equivalent with the Zlambach Marl, and I suggest classification into the lowermost part of the Telekesvölgy complex. The boundary of the two formations (Hallstatt Fm. and TV complex) is a sharp plane dipping in the same angle and direction as the bedding. It can be observed in one coherent piece of core. The boundary can be interpreted as a discordant surface, but notable structural contact is rather unlikely.

The situation is a little bit different in borehole **Rudabánya Rb-658** (Fig. 12). The lower 135.5 m of this core is represented by the uppermost part of a Bódva-type Triassic sequence of Upper Triassic red, occasionally cherty limestone (Bódvalenke and Hallstatt Formations). A rock association containing alternating beds of red, green and grey claystone, claymarl, marl, calcareous marl and limestone appears between 135.4 and 80.3 meters. The proportion of the different lithologies is changing. The sediments are well bedded; signs of bioturbation are not present. This marly succession shows great similarities to the marl beds of the previously mentioned Szalonna Sza-5. Similarly to the previous authors (Grill 1988, Less et al. 1988), I suggest classification of these marls into the Telekesvölgy complex. At the boundary of the red limestone and the variegated marl group 0.4 meters of black shale can be seen showing continuous transition in colour or lithology neither from the underlying, nor to the overlying strata.

In the base of borehole **Perkupa P-74** (Fig. 10) the Hallstatt Limestone seems to change continuously to the the variegated marl. In the upper part of the borehole, the overturned Triassic sequence is truncated by thrust, so the stratigraphic relationship can not be judged.

In the case of the borehole **Szendrő Szet-4** (Fig. 17) the lowermost 100 meters of the core is built up by an Anisian-Norian carbonatic sequence: Steinalm Limestone, Bódvarákó Fm., Bódvalenke Limestone, and Hallstatt Limestone. As closing to the overlying beds, the red Hallstatt Limestone is turning into light brown marl, which infiltrates into the fissures of the limestone, too. The marl, after a short 0.3 meters section, suddenly changes into tectonically mashed black claymarl (0.5 m) then turns again into brownish-greyish marl. This greyish occasionally silicified marl, calcareous marl section last up to 20 meters depth. Flattened clay intraclasts are common in the marl. Locally flaser clayey limestone intercalations appear.

According to the previous concepts (Grill 1988, Grill 1989, Less et al 1988, Less 1998, 2000) this core Szendrő Szet-4 was one of the main proofs on having sedimentary contact in-between the Triassic of Bódva series and the TO complex, and these two formations are the original stratigraphic continuation of each other. In this case not the TV complex, but the Zlambach Fm. and the lowermost part of the TO complex developed from the Hallstatt Limestone. This is this classification what we contested in the light of other data (Kövér et al. 2008).

For distinction of the two formations (TV and TO) characterised by similar lithologies, the presence or absence of ductile deformation features, and the degree of metamorphism turned out to be the best methods (see chapter 6, 7). Since the marl appearing in core Szendrő Szet-4 has not participated in any remarkable ductile deformation event, it is suggested to be classified into

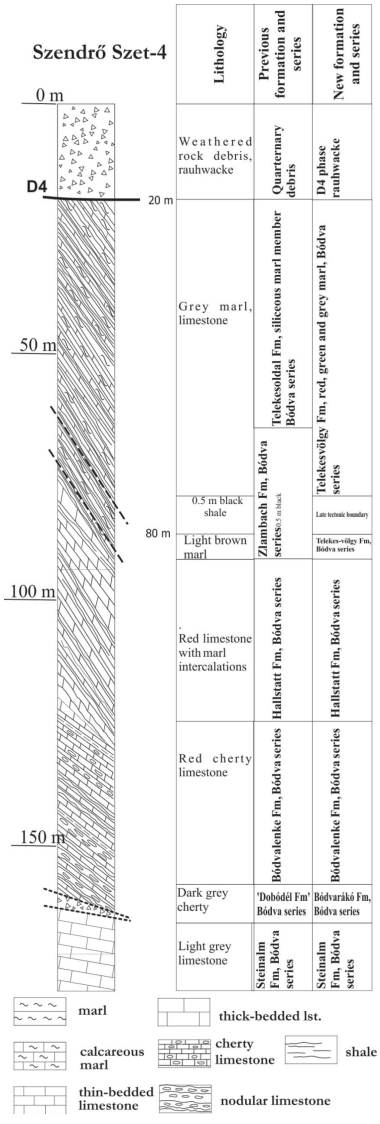

Figure 17. Lithologic and stratigraphic features of the Szendrő Szet-4 borehole with previous and new interpretations. For structural interpretation and the details of the rauhwacke see chapter 7.4.3 and 8.

the TV complex independently from the fact that the characteristic red and green coloured version of the marl is absent (Kövér et al. 2008). According to my opinion the position of the light brown marl which infiltrates into the fissures of the Hallstatt Limestone, and continuously developing from it, is a sufficient proof on being in sedimentary contact with the underlying limestone. The marl which used to be classified into the Zlambach Formation could be equivalent with the variegated marl of the TV complex. This latter has similar sedimentation age as the Zlambach F. as pointed out by new biostratigraphic data.

The 0.5 meters thick black shale indicates a tectonic boundary, as it was already mentioned by Gy. Less, the original descriptor of the borehole Szet-4. Since above this shale the next formation is light grey marl which is lithologically identical with the underlying one, the contact is suggested to be of tectonic origin, but the tectonic movements did not modified the original stratigraphic order.

Since in core Szalonna Sza-5 (Fig. 13) the boundary between the Hallstatt Limestone and the variegated marl of TV complex is most probably of sedimentary origin, it is presumed, that the 0.3-0.5 meters tectonic zones appearing in the lower part of the marly formation in several other cores are not remarkable structural elements, but tectonic boundaries in between one structural unit.

Accordingly, the variegated marl of TV complex is suggested to be the original sedimentary cover of the Triassic Bódva-type series. The transition into the younger lithofacies unit, the crinoideal grey marl and calcareous marl is thought to be sedimentary on the basis of microsedimentological studies performed on thin sections from Csipkés Hill section 1. If the continuous transition into the radiolarian black shale lithofacies could be provable, the whole TV complex would be the part of the Bódva series, in contrast with the previous conceptions (Grill 1988, 1989; Less et al. 1988, Less 1998, 2000; Szentpétery & Less 2006).

5.3. Telekesoldal complex

The classical model of Grill (1988) subdivided the TO complex into shale and marl, sandstone olistolith, limestone olistolith and rhyolite members. These members were supposed to built up an upward coarsening sequence, with the shale and silicified marl in lowermost, while the olistoliths in uppermost position. The rhyolite bodies were described as subvolcanic intrusions, intruded into the lowermost, shale and marl member (Grill 1988, Chapter 2.2.5). However, according to my field observations and microfacies studies, these lithofacies units cannot be separated in time. Sandstone, siltstone and micro-olistostrome layers occurs in the dark shale and marl in almost every locality. Coarser-grained, polymict olistostrome layers are also widespread in every stratigraphic level. In the next chapter the characteristic lithofacies types will be described (Fig. 18), but in contrast with the previous view (Grill 1988), they are not considered representing different stratigraphic and age intervals.

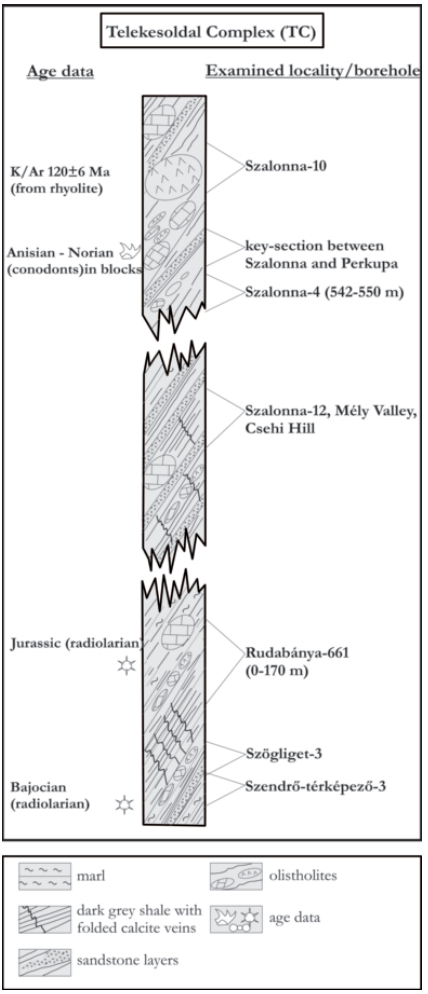

Figure 18. Simplified reconstructed stratigraphic column of the Telekesoldal complex. The stratigraphic positions of the age data, the studied boreholes and outcrops are approximately indicated.

5.3.1. Microfacies studies

Szalonna Sza-4, -7, -10, -11, -12, Szendrő Szet-3 and Rudabánya Rb-661 cores and outcrops on Csehi Hill and the road cut key-section between Szalonna and Perkupa villages provided important data on lithological character of the complex.

5.3.1.1. Black shale and clay marl with sandstone layers

One of the typical lithofacies units of the TO complex is made up of dark grey to black shale and sandstone. Outcrops of this unit occur S of the Nagy-Telekes Hill, in the Mély Valley, Csehi Hill (Fig. 1b) and it was also exposed by the Szalonna Sza-12 core.

The dark shale is actually claymarl and slate, which contain quartz silt or fine-grained sand scattered in the clay or forming thin laminae. Several microstructural phenomena connected to ductile deformation are present in the formation (see chapter 7.). However, there are samples, where the effects of ductile deformation are

not so strong, and the original sedimentary structures are preserved. In these intervals erosional bases of the sandstone layers are common (Fig. 19.2). Graded bedding (Fig 19.1, 19.2) and cross-lamination can also be observed within some of the sandstone beds (Perk-161, Fig. 19.3). Alternation of fine- to medium-sized sandstone and sandy siltstone laminae (Fig 19.2) were also observed in thin sections. In some samples taken from the **Mély Valley** alternation of mm-thick sandstone laminae and thicker silty claystone layers were found. The sandstones consist predominantly of quartz, but the amount of feldspars (plagioclases) is usually significant and muscovites also occur in varying

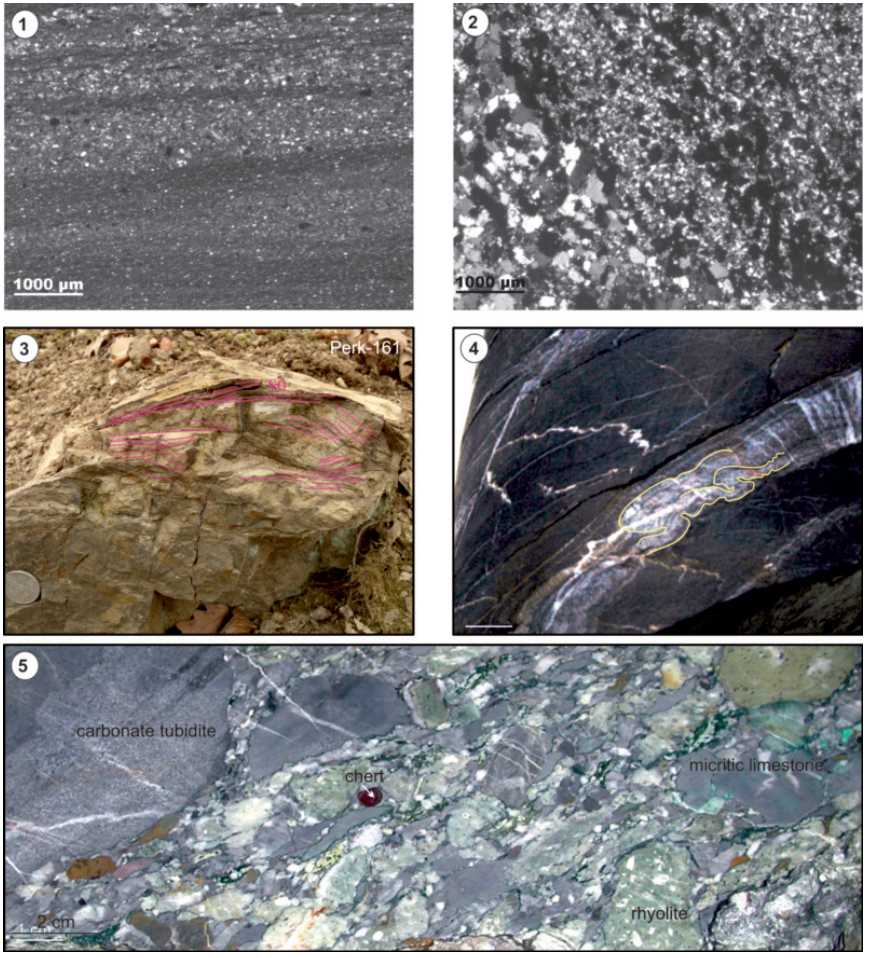

Figure 19. Lithologic characteristics of the TO complex. 1) radiolaria turbidites 2) Erosional base and normal gradation of the sandstone and siltstone beds from core Szalonna Sza-12 3) cross lamination in sandstone layers of the Telekesoldal complex in outcrop Perk-161 on Nagy-Telekes Hill 4) Fine grained sandstone intercalation in claymarl. The slump folds of the sandstone refer to gravitational mass flow origin. Core Szet-3, 32.2 m, Telekesoldal complex 5) Olistostrome of TO complex from the type-locality at the Szalonna-Perkupa roadcut keysection. Note the different types of clasts, the grain-supported texture and the stylolitic grain boundaries.

quantity. The size of the grains varies from silt to medium-sized sand. The contacts of the grains are mostly pressure solution surfaces.

Slump folds are visible occasionally in the sandstone-bearing successions (Fig. 19.4). Lens shaped sandstone bodies in the shale are also common (for details, see Chapter 7.1.1). They may have formed either by early post-diagenetic disintegration of sandstone beds and gravitational redeposition of the sandstone blocks with later flattening during ductile deformation or by subsequent tectonic deformation processes leading to boudin formation (see Chapter 7.1.1).

The **Szalonna Sza-12** core exposed dark grey shale and marl with varying amounts of radiolarian moulds (calcite and quartz) in its lower part. It is overlain by a few meter thick interval containing 0.3—20 mm sized grey clasts with subordinate shale matrix or without any matrix but microstylolitic grain contacts (olistostrome beds). The typical components are as follows: "filament" wackestone, "filament" packstone (coquina), crinoidal wackstone, crinoidal packstone, dolosparite, siltstone, sandy shale, and highly altered volcanoclasts with quartz and feldspar phenocrystals. The boundaries between the matrix and the clasts are usually pressure solution surfaces; dark solution seams of insoluble material commonly occur around the clasts. The upper segment of the core section is made up of alternation of fine-grained siliciclastic sandstone to siltstone and dark grey shale.

5.3.1.2. Dark grey shale and marl with olistostrome layers

The **road cut key-section** along the road between Szalonna and Perkupa is the best type exposure of the olistotrome lithofacies (Kovács 1988). In the exposed succession 1—5 m thick dark greenish-grey bioturbated marl beds alternate with 0.1—5 m thick olistostrome beds. Centimeter- to meter sized clasts (mostly grey limestone and green rhyolite clasts) occur in the olistostrome beds (Fig. 19.5). The original shapes of the limestone and rhyolite clasts are rarely visible due to pressure solutional grain contacts and tectonic deformation. Angular brownish shale clasts, 0.5—2 cm in size, also commonly occur. The thickest beds contain the coarsest grains where size of rhyolite clasts may reach 0.5 m in diameter. Grain-supported texture is typical but mud-supported debris flow deposits are also present, rarely. In the grain-supported beds the matrix is usually missing or subordinate; the microstylolitic grain contacts are typical. The other characteristic feature for pressure solution is the displacement of layering or caclcite veins along certain planes (Fig. 20.1). In the matrix supported olistostromes the matrix is dark shale, marl with organic material and pyrite or fine siliciclastics with altered volcanogenic components.

In the olistostrome beds the **carbonate clasts** are predominant, their typical texture types are as follows: thin-shelled bivalve ("filament") wackestone, radiolarian and "filament" wackestone, bioclastic (crinoidal), peloidal wackestone, peloidal grainstone, crinoidal wackestone, radiolarian wackestone, micritic mudstone (partially dolomitized or silicified in some cases), oolitic crinoidal packstone, dolomicrosparite and dolosparite, sparry calcite, and pervasively silicified rock. Some platform derived carbonate clasts were also detected. Early Ladinian to Late Norian conodonts were found in some grey limestone clasts by S. Kovács (Balogh & Kovács 1977). The predominant part of the carbonate clasts is probably Triassic in age, and represents hemipelagic facies.

The sample presented on Figure 20.2 to 20.4 is a succession, starting with greenish grey silty claystone basin facies. Above an uneven erosional surface, it is overlain by a 2 cm thick lithoclastic, bioclastic packstone layer with subordinate microsparitic matrix (Fig. 20.2). The typical grain size is between 1—5 mm, no grading is visible. The bioclasts are coarse sand-sized crinoid ossicles. The types of lithoclasts are as follows: bioclastic wackestone, peloidal wackestone, peloidal microsparite with a

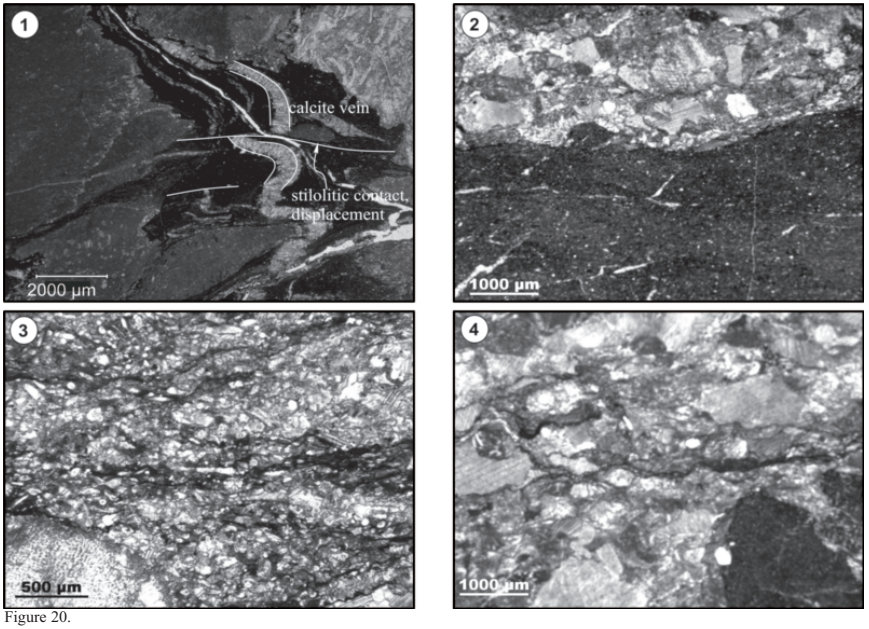

Figure 20.

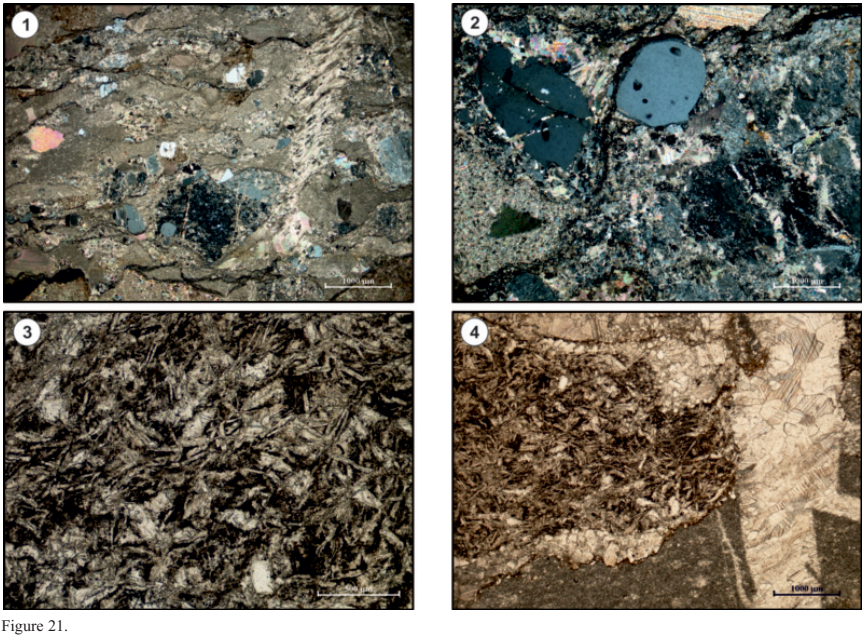

Figure 21.

few “filaments”, dolosparite and silty claystone (yellow). This layer is overlain by a 1 cm thick sponge spicule packstone (partially silicified) (Fig. 20.3) that is followed by a turbidite layer with an erosional contact. The ~1 cm thick allodapic layer is lithoclastic crinoidal packstone showing definite grading (Fig. 20.4).

Along with carbonate clasts highly altered **volcanoclasts** are usually common. Holocrystalline, locally spherulitic, porphyritic rhyolites are typical (Fig. 21.1). They contain perthitic orthoclase, quartz of undularory extinction and idiomorhic resorbed quartz (Fig. 21.2), commonly surrounded by a siliceous ring. Strongly altered intersertal-intergranular basalt-dolerite clasts with slightly bent plagioclase lathes were also encountered rarely (Fig. 21.3, 21.4). Individual idiomorphic resorbed quartz grains, mosaic like quartz crystals or crystal stacks, sericitic orthoclase and rarely plagioclase (oligoclase) derived from volcanites, together with coarse sand-sized crinoid ossicles also occur in some samples.

In the Telekes Valley, opposite of the **Hunter House** the contact of a 100 m sized rhyolite body and the shale is cropping out (Fig. 22.1-2). The volcanite is a light green rhyolite with vitroporphiric texture. In the green glassy matrix 4-5 mm-scale feldspar phenocrystalls are present (Fig. 22.2). The S0-1 foliation of the shale goes around the rhyolite body, late shearing at the contact can be observed.

300 m E from the Hunter House outcrop, the the **Rudabánya Rb-661** borehole (Fig. 23) penetrated

Figure 20. 1) A caracteristic feature for pressure solution: displacement of calcite vein on certain planes in TO olistostrome. 2-4) Greenish grey silty claystone is erosionally overlain by a 2 cm thick lithoclastic, bioclastic packstone layer (2). It is overlain by a 1 cm thick sponge spicule packstone (partially silicified) layer (3), which is followed by a turbidite layer, lithoclastic crinoideal packstone (4)

Figure 21. 1) Rhyolite fragment with holocrystalline partly spherolitic matrix, rounded quartz and large K-feldspar crystals. Crossed polars, Telekesoldal key section. 2) Resorbed quartz and large K-feldspar crystals in a strongly carbonatised fragment, in a carbonate rich olistostrome. Crossed polars, Telekesoldal key section. 3) Strongly altered opacitised and carbonatised intersertal basalt fragment with skeletal structured laths of plagioclase and some parallel shearing zones. 1 polar, Telekesoldal key section. 4) Strongly altered opacitised and carbonatised intersertal basalt fragment with skeletal structured laths of plagioclase, calcite and limonitised magnetite aggregates. 1 polar, Telekesoldal key section.

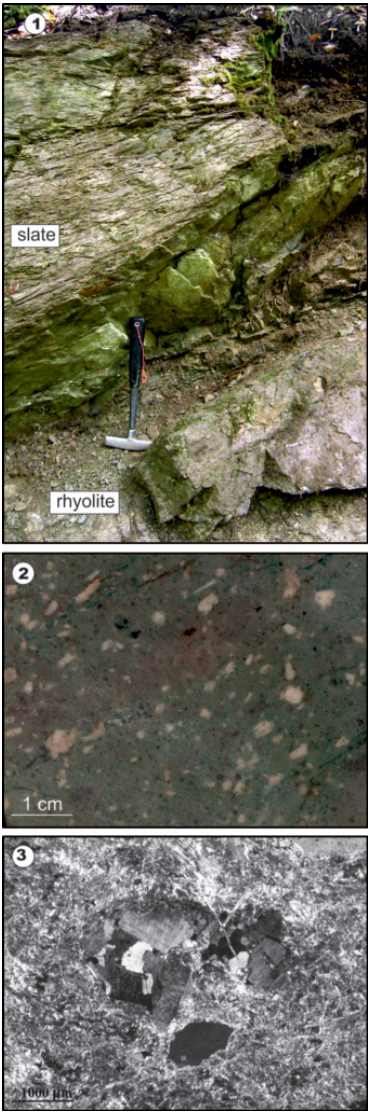

Figure 22. 1) The contact of the slate and rhyolite at the Hunter's house locality in Telekes Valley. IC and AI of the slate were investigated (see chapter x). 2) Green rhyolite with plagioclase porphyroclasts of the same locality. 3) Slightly melted plagioclase free granite cataclasite within the rhyolite of TO from the neighbourhood of the Hounter House in the Telekes valley

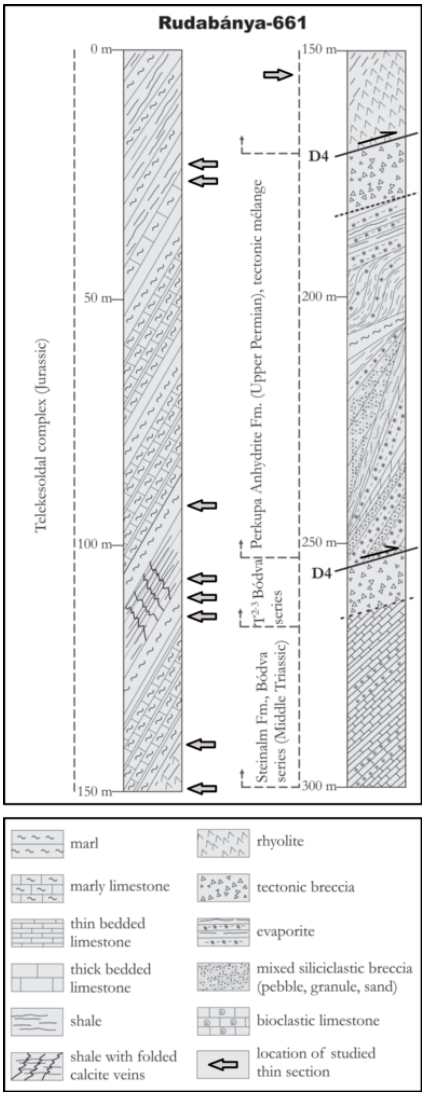

Figure 23. Reconstructed lithologic and stratigraphic features of the Rudabánya Rb-661 borehole. Note tectonically reduced pelagic Bódva Triassic below the evaporite, underlain by Bódva platform carbonate. For tectonic interpretation see chapter 7.4. For details of the evaporitic mélange see chapter 8.

similar **rhyolite body** at its bottom part, just above the tectonic contact with the Upper Permian Perkupa Evaporite Formation and a more than 10 m thick tectonic breccia. In this core the boundary of the large rhyolite-ignimbrite body (19 m apparent thickness) is sharp. Altered vitrophyric rhyolite, rhyolite tuff and ignimbrite are the main rock types. Under the microscope fragments of volcanic glass and pumiceous texture – the characteristic features of ignimbrite – are clearly visible (Fig. 24.1, 4, 6). Thin laminae of sericite-chlorite are predominant in the matrix (Fig. 24.1). The porphyritic components are pertitic orthoclase, idiomorphic quartz with resorbed margin, fractured quartz with undulatory extinction, commonly partly melted, and few large sericitic plagioclases or plagioclase-orthoclase composite grains, and few biotites (Fig. 24).

Small (mm to 1 cm-sized) **rhyolite clasts** (Fig. 24.2, 24.3, 24.5) were encountered in "spotty" shale (usually silty claymarl, marl, calcareous marl) in several horizons in a 40 m thick interval above the large rhyolite body. There are clasts consisting of large quartz and feldspar crystals in a calcified matrix. Composite grains also occur together with resorbed quartz and orthoclase crystal fragments. There are lithoclasts consisting of resorbed quartz and sheared, fractured perthitic orthoclase in a squeezed chloritic, calcitized and silicified matrix.

Along with the rhyolite clasts a few **carbonate clasts** of similar size were also found. In the sample taken from 101.7 m, radiolarian wackestone (3 cm) (Fig. 25.1), "filament" wackestone (2 cm) clasts and an altered rhyolite clast (2 mm) were observed (Fig. 25.2). The typical texture types of the clastsin this interval is bioclastic wackestone containing large number of radiolarians recrystallized to calcite, probably also sponge spicules and small fragments of thin-shalled bivalves ("filaments") locally. Darker bioturbation patches rich in organic matter and pyrite are common.

Only slightly squeezed and deformed shale also occur in several horizons, rarely. In the upper part of

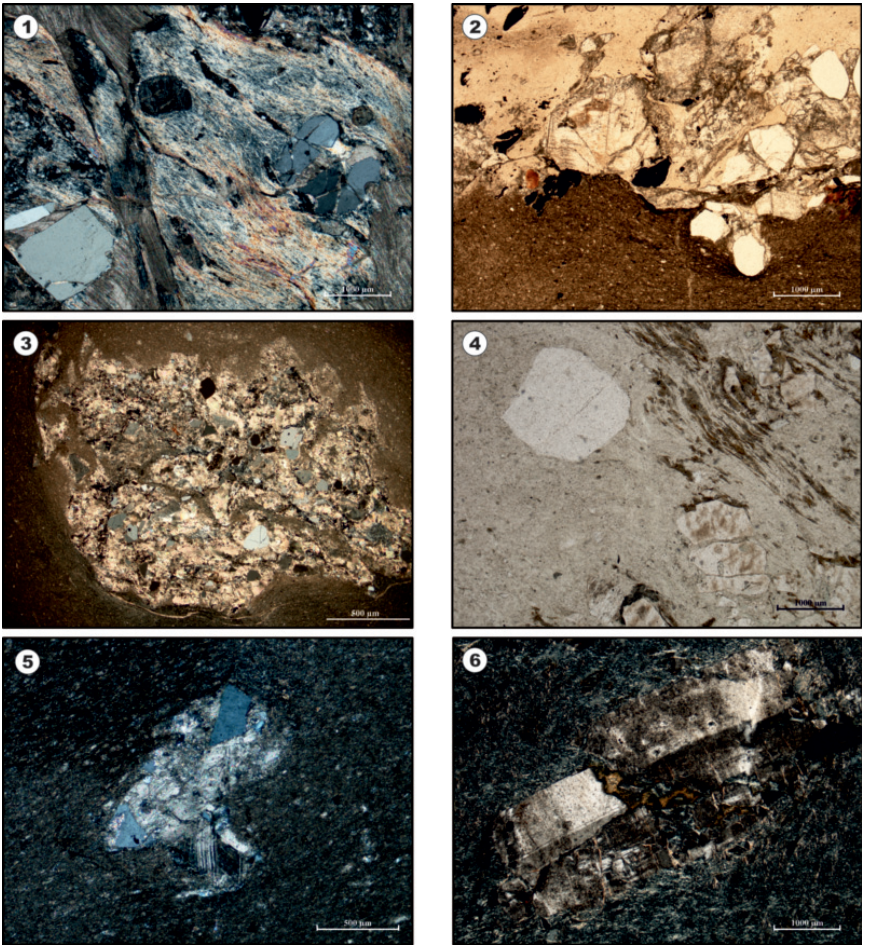

Figure 24. 1) Rock fragment surrounded by fibrous calcite cement and containing large, fragmented quartz and smaller K-feldspar crystals in a sheared fine-grained, mostly sericitized matrix. Crossed polars, Rb-661, 116.1 m. 2) Boundary of siltstone and sheared carbonatized rock fragment (rhyolite), in which large quartz, K-feldspar opaque minerals and few biotite crystals are surrounded by totally chloritized, sericitized glassy matrix. 1 polar, Rb-661, 149.0-149.1 m. 3) Sheared, carbonatized rock fragment containing large quartz and K-feldspar crystals with diffuse boundary in siltstone. Crossed polars, Rb-661, 132.6 m. 4) K-feldspar, quartz and biotite in glassy groundmass with characteristic texture of pumice bearing rhyolite tuff (ignimbrite). 1 polar, Rb-661, 153.3 m 5.) Irregular shaped rock fragment with angular quartz crystals and sparitic matrix in siltstone. Crossed polar, Rb-661, 108.8 m 6) Large, slightly deformed and altered plagioclase (most probably albite) crystal in glassy groundmass, + polar, Rb-661, 153.3 m

the borehol (above 100 m) spotty shale (marl, silty marl) lithology and radiolarian wackestone texture continues, but the clasts are missing. In the uppermost ~40 m of the core section the barren mudstone texture is prevailing. In a single sample at 25.0 m, probably representing a larger clast, well preserved thin-shalled bivalve fragments (Fig. 25.3) were found in silicified marl matrix (“filament” wackestone).

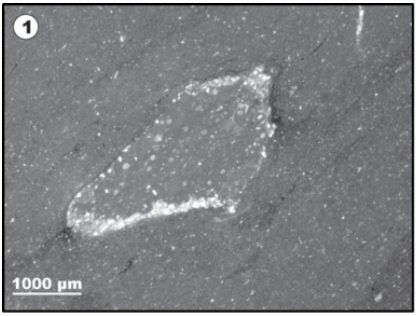

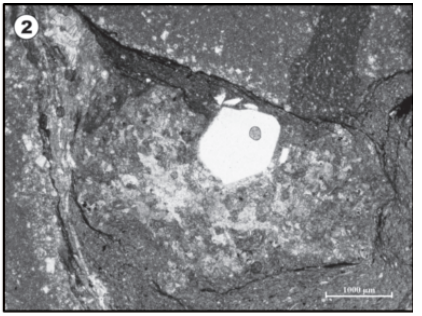

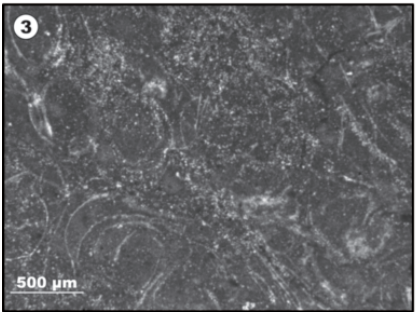

Figure 25.
1) Radiolarian wackestone intraclast in radiolarian wackestone matrix containing much less radiolarian moulds than the clast. Note the microstylolitic grain boundaries. Rb-661, 113.0 m
2) Rhyolite fragment consisting of holocrystalline mosaic like carbonatised quartz matrix and resorbed idiomorphic porphyric quartz crystal embedded in fine grained silty matrix, 1 polar, Rb-661, 101.7 m
3) Thin-shelled bivalvs in partially silicified micritic matrix - "filament" wackestone. Most probably it is a large lithoclast in the shale that was found below and above this interval. Rb-661, 25.0 m.

Rhyolites within marl and claystone succession were also encountered in the **Szalonna Sza-10** core. An olistostrome layer containing predominantly radiolarian wackestone (Fig. 26.1), radiolarian—"filament" wackestone, rhyolite and a single, probably platform-derived clast (Fig. 26.2, 26.4) was found in the 95.4—95.5 m interval. These platform facies carbonate clasts are very rare in the olistostrome of the TO complex. Except for this finding, the only platform-derived clast was found in core **Szalonna Sza-11**, where at 36.5—57.26 m along with the radiolarian "filament" wackstone, coarsely crystalline dolosparite and shale lithoclasts, an oolitic-crinoidal packstone clast was found in shale matrix (Fig. 26.3, 26.5).

Partially silicified carbonates containing carbonate lithoclasts were found in some samples taken from outcrops on the **range between the Telekes and Henc Valleys**. The texture is lithoclastic grainstone. Along with the 1—2 mm sized, medium to well-rounded lithoclasts coarse sand-size bioclasts (bivalve and echinoderm fragments) also occur, rarely. The composition of the lithoclasts is as follows: micritic and microsparitic mudstone, "filament" wackestone, radiolarian wackestone and totally silicified clasts.

As a summary, the detected clast composition of the olistostrome horizons in the TO complex is as follows. Most of the lithoclasts are carbonates, but rhyolite, shale and basalt clasts also occur in variable quantity. Among the carbonates the grey pelagic limestones are predominant, dolomite is frequent, and uniqually, shallow-water limestone clasts were also detected. Among the volacanoclasts the rhyolite is predominant, while basalt clasts are rare. The size of the rhyolite clasts and bodies can vary from mm to 100 m. Shale and marl lithoclasts were also encountered.

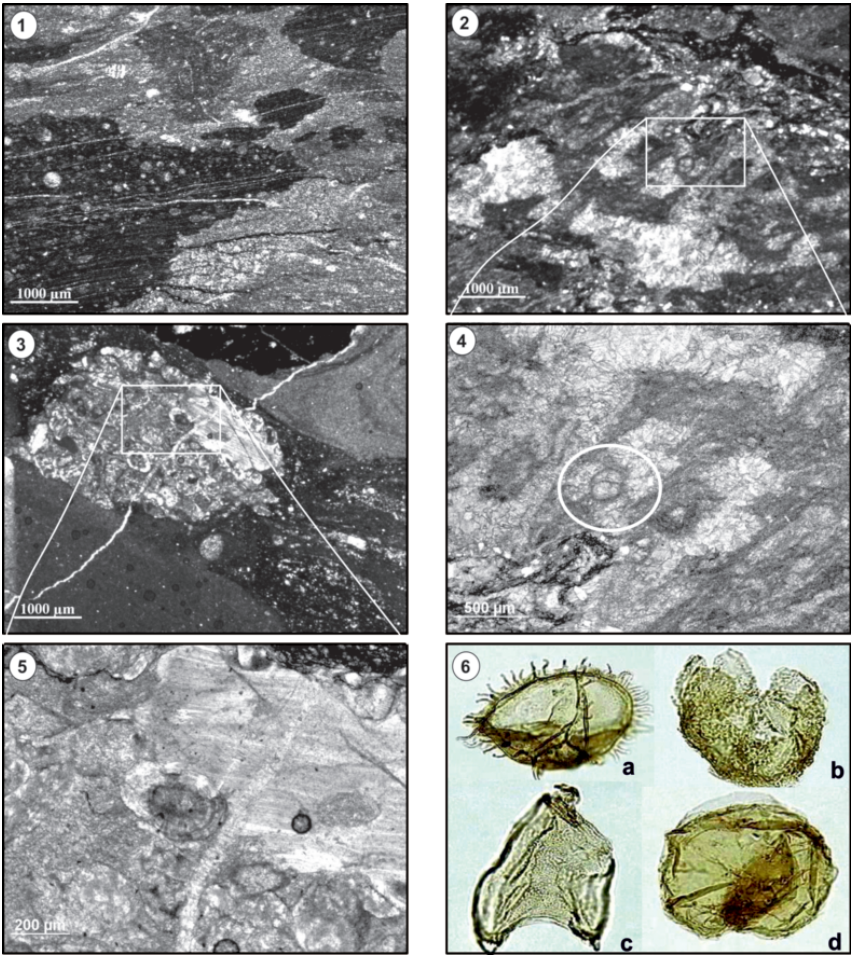

Figure 26. 1) Radiolarian wackestone and radiolarian "filament" wackestone components of the TO olistostrome. Sza-10, 95.4m. 2,4) A rare platform-derived clast containging a foraminifera (in the white circle) and molds, filled with coarse crystalline sparite. Sza-10, 95.4m. 3,5) A unique ooidal-crinoideal packstone texture clast from the TO olistostrome. Sza-11, 36.5m. The white boxes on 2 and 3 indicates the enlarged areas 4) and 5) 6) Age diagnostic dinoflagellata cysts from the Telekesoldal Complex. a - Ctenidodinium sp.: Callovian, core Sza-12, 50.3 m b - Lithodinia sp.c - Nannoceratopsis gracilis: Bajocian, core Szö-3 76.0 m d - Wanaea sp.: Callovian, core Sza-12 50.3 m

5.3.2. Revision of the radiolarian fauna in Telekesoldal complex

Several new samples were collected from cores and outcrops to refine or define the age of the Telekesoldal complex. Previously it was supposed without any biostratigraphical data, that the succession involves the whole Liassic with shorter gaps (Grill 1988). Dogger was evidenced by radiolarians (Grill & Kozur 1986, Dosztály 1994), while the youngest part of the complex was considered to be

early Late Jurassic on basis of "field data" (Grill 1988). Unfortunatelly, the radiolarians of the new samples were calcified or so badly preserved that it made further investigations impossible. Revision of the samples collected and prepared by Dosztály (1994) is discussed in the next chapter.

Two samples (sample at 52.0 m—53.0 m and sample at 69.8 m—70.6 m) from the borehole yielded moderately well preserved and relatively abundant radiolarian assemblages, mainly characterized by spumellarians. The following stratigraphically important radiolarians were identified from the sample at **69.8 m—70.6 m** (Kövér et al. 2009b): *Emiluvia lombardensis* Baumgartner, *Emiluvia* spp., *Unuma* cf. *typicus* Ichikawa & Yao, *Laxtorum* (?) *jurassicum* Isozaki & Matsuda, *Triactoma* spp., *Pseudoeucyrtis* sp., *Orbiculiforma* sp. X sensu Baumgartner et al. The biostratigraphic range of *E. lombardensis* Baumgartner indicates UAZ 1—4 and *L.* (?) *jurassicum* Isozaki & Matsuda indicates UAZ 2—3.

Co-occurrence of these species and the presence *Unuma* cf. *typicus* Ichikawa & Yao (UAZ 3—4) indicates that this sample can be assigned to UAZ 3 (**early-middle Bajocian**).

The sample from **52.0 m—53.0 m** yielded moderately well preserved and diversified radiolarian fauna (Fig. 16) (Kövér et al. 2009b) including *Pseudodictyomitrella spinosa* Grill & Kozur, *Transhsuum* cf. *maxwelli* (Pessago), *Homoeoparonaella argolidensis* Baumgartner, *Homoeoparonaella elegans* (Pessagno), *Homoeoparonaella* cf. *elegans* (Pessagno), *Unuma* sp. F sensu Yao, *Gorgansium* sp., *Pantanellium* sp., *Tritrabs simplex* Kito & De Wever, *Tritrabs* cf. *ewingi* (Pessagno), *Emiluvia lombardensis* Baumgartner*, Triactoma cf. jakobse* Carter*, Pseudocrucella?* sp., *Paronaella cf. corpulenta* De Wever*, Angulobracchia digitata* Baumgartner, *Hsuum fuchsi* Kozur.

The biostratigraphic range of *E. lombardensis* Baumgartner indicates UAZ 1—4, while *H. argolidensis* Baumgartner*, H. elegans* (Pessagno) indicate UAZ 4—11. It follows that co-occurrence of them indicate the UAZ 4 (**Late Bajocian**).

In summary, these findigs indicate a depositional age probably spanning from **early to late Bajocian**.

5.3.3. Palynological age determination from the Telekesoldal complex and Akasztó unit

Three wells (Sza-10, Sza-12, Szö-3) (Fig. 1) were sampled to analyse the sedimentary organic matter content. Two of them are located in the central Rudabánya Hills (Fig. 1), while the Szö-3 borehole is located at the eastern margin of the Aggtelek Hills. The surrounding of this latter was considered as Early Triassic (Less et al. 1988) and will be refered to as the Akasztó unit, defined in chapter 2.2.5.4.

Age-diagnostic dinoflagellate cysts (*Wanaea* sp., *Ctenidodinium* sp.) were detected (Fig 26.6) in sample 50.3 m from well **Szalonna Sza-12**, indicating **Callovian age** (Kövér et al. 2009b). Sample 74.0 m from well Sza-10 is characterized by opaque phytoclasts only; no palynomorphs are preserved.

Sample 76.0 m of well **Szögliget Szö-3** penetrates black to dark grey shales of Akasztó unit. The sample yielded poorly to moderately preserved sedimentary organic particles. Poorly preserved specimens of the dinoflagellate cyst *Nannoceratopsis gracilis* Alberti were identified, which refers to **Bajocian** age (Kövér et al. 2009b).

In summary, revision of the radiolarian specimens and the first findings of marine palynomorphs in the TO complex was resulted in refinement of the supposed depositional age interval. The examined samples indicate **Bajocian-Callovian** age.

5.3.4. Radiometric age of the rhyolite occurrences

Radiometric age determinations were carried out on zircon grain separates from different sized rhyolite pebbles and bodies of the TO Complex. Samples from different locations and positions were treated separately during the measurements. However, some of them were contracted by right of their cathodluminescence (CL) images and isotope ratios in the course of age calculations. Grain separation and morphological investigations were made at the Department of the Mineralogy and Petrology, University of Miskolc (Majoros, 2008). Back-scattered electron (BSE) and CL imaging with a Tescan Vega 2 instrument was performed at the Geological Survey of Austria (Geologische Bundesanstalt). The main parameters of the measurements were 10 kV acceleration, 0.5 nA amperage and 17 mm sample distance. The in-situ high-precision U-Th-Pb dating was performed at Department of Lithospheric Research, University of Vienna (by the guidance of U. Klötzli) with a NewWave 193SS laser-ablation system which was in connection with a Nu PLASMA HR MC-ICP mass spectrometer. Spot-selection was guided by internal structures (zonation) as seen in CL images of mounted and polished zircon grains. Data processing was made by Isoplot.

5.3.4.1. Results from zircon morphological investigations

As a result of the zircon morphological investigations the zircon grains are classified into two main groups, which may refers to difference in their original chemical composition (Majoros 2008). The first group contains zircon grains from the matrix of the olistostrome from the roadcut key-section between Szalonna and Perkupa, from the big rhyolite body at the Hunters House locality, and from upper stratigraphic levels of cores Rudabánya Rb-661, Varbóc Va-4 and Szalonna Sza-10. While the other group is consists of mineral grains from pebbles of the olistostrome from the same roadcut key-section, and from lower stratigraphic levels of the previous cores. The interpretation of Majoros (2008) was that the rhyolite is the result of a longer volcanic activity. During this rather long period, the previously solidified rocks redeposited as different sized pebbles, blocks (cores) and fine-grained material (matrix of olistostrome).

5.3.4.2. CL imaging

<u>Sample No 1 Olistolith from the TO olistostrome (Perkupa-Szalonna road cut key-section)</u>

Number of measured grains: 7

Number of analyses: 10

Grains (Fig. 27, 28, 29) frequently display bright luminescent, prismatic cores with close growth bands (1-a-4, 1-b-1, 1-c-3, 1-c-6). The oscillatory zoning is often blurred and widened, or fully replaced by CL-homogeneous domains (1-c-6, 1-e-6). These cores usually have resolved rims, and are enclosed by variably wide CL-bright domains with well-developed oscillatory zoning typical of magmatic growth (1-a-4, 1-b-1, 1-c-3, 1-c-6, 1-e-6). One crystal contains CL-dark core (1-b-2), with CL-bright overgrowth similar to the previous rims. The most elongated crystal shows CL-bright close zoning (1-a-9) with no clearly distinguishable core.

<u>Sample No 2 Matrix of the olistostrome (Perkupa-Szalonna roadcut key-section)</u>

Number of measured grains: 3

Number of analyses: 4

Two of the grains display bright luminescent: one with seemingly CL-homogeneous core with

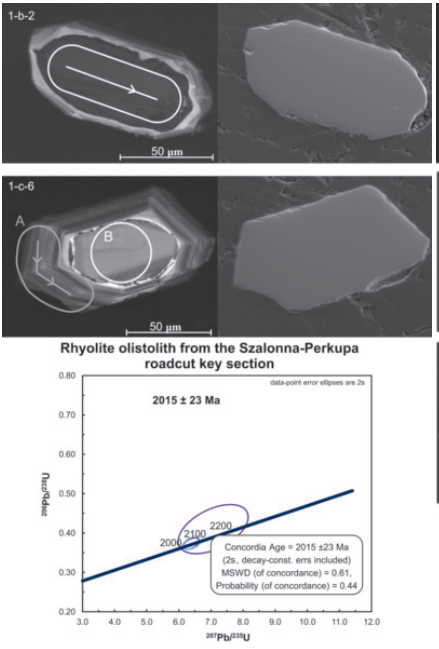

Figure 27. CL and BS images of the investigated zircon crystals from a rhyolite olistolith of the TO complex, Szalonna-Perkupa roadcut keysection. Place of the LA-ICP-MS measurements are indicated. White line shows the measurement included in this age group, while grey indicates those fit in another age group. Calculated ages and the related Concordia diagram are also indicated

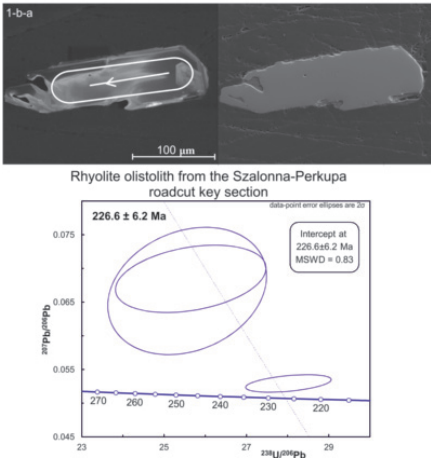

Figure 28. CL and BS images of the investigated zircon crystals from a rhyolite olistolith of the TO complex, Szalonna-Perkupa roadcut keysection. Calculated ages and the related Terra-Wasserburg diagram are also indicated.

wide rim of bright growth bands (2-a-4) and one with CL-bright close zoning in all the crystal (Fig. 30). The core of the third grain is mostly CL-dark, and is enclosed by brighter growth bands.

Sample No 3 Layer from the olistostrome (Perkupa-Szalonna roadcut key-section)

Number of measured grains: 3

Number of analyses: 3

Two grains display dark luminescent, prismatic cores with some CL-bright, narrow growth band (3-c-8, 3-d-10). The rim of zircon 3-d-10 is CL-bright. The third sample was cut not exactly in the middle during sample preparation, so the growth bands seen on the image refer to the rim of the crystal (Fig. 30).

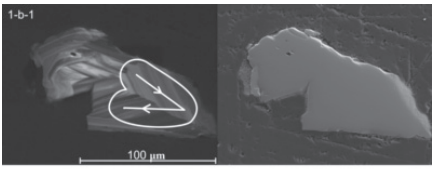

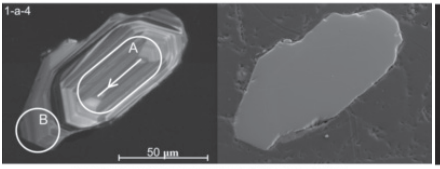

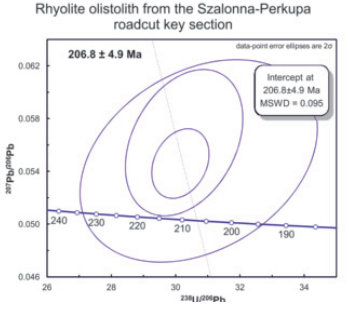

Figure 29. CL and BS images of the investigated zircon crystals from a rhyolite olistolith of the TO complex, Szalonna-Perkupa roadcut keysection.Calculated ages and the related Terra-Wasserburg diagram are also indicated.

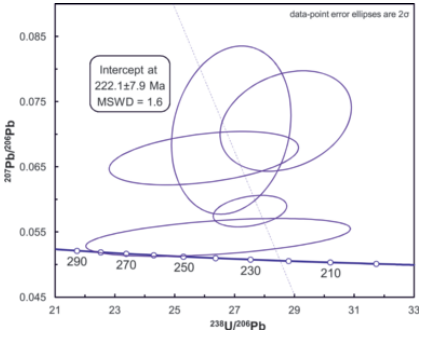

Figure 31. Calculated age and the related Terra-Wasserburg diagram of the samples 2 and 3 (Fig. 30).

Zircon grains from the matrix (2) and from a layer (3) of the TO olisthostrome from the Szalonna-Perkupa roadcut key section
222.1 ± 7.9 Ma

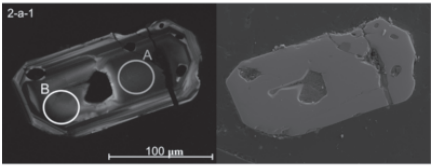

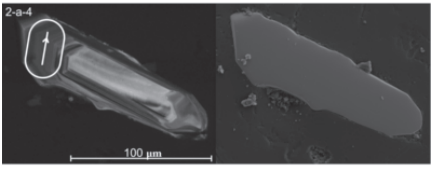

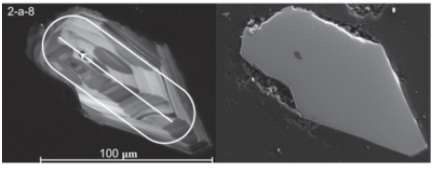

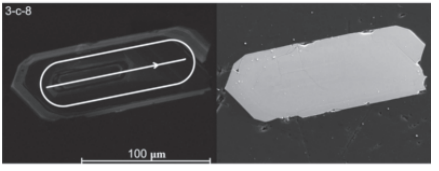

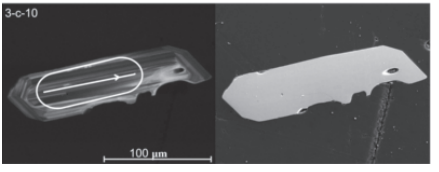

Figure 30. CL and BS images of the investigated zircon crystals from a layer and the matrix of the TO olistostrome, Szalonna-Perkupa roadcut keysection.

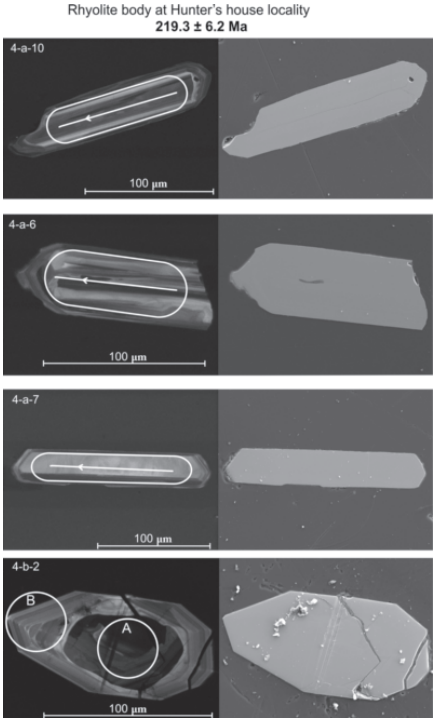

Figure 32. CL and BS images of the investigated zircon crystals from the rhyolite body at Hunter House locality.

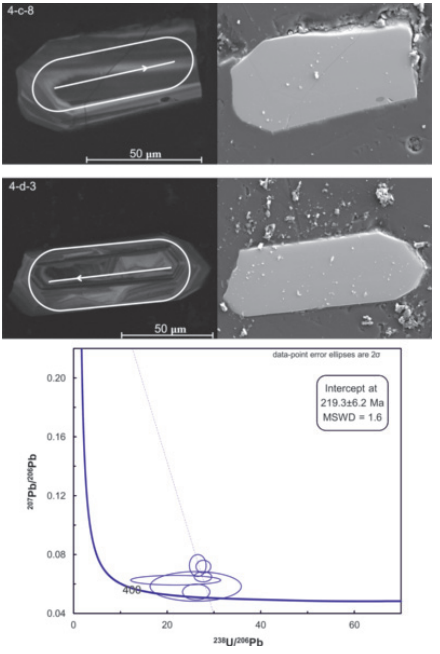

Figure 33. CL and BS images of the investigated zircon crystals from the rhyolite body at Hunter House locality. Calculated ages and the related Terra-Wasserburg diagram are also indicated.

Sample No 4 Rhyolite body at Hunter's House locality

Number of measured grains: 9

Number of analyses: 10

Grains frequently display middle-bright or dark luminescent, rounded cores with complicated inner structure (Fig. 32, 33). These cores are enclosed by variably wide CL-bright domains with well-developed oscillatory zoning (4-a-6, 4-b-2, 4-c-8, 4-d-3, 4-e-1). The more elongated grains show no different shaped or bright cores (4-a-10, 4-a-7, 4-b-5, 4-c-4), but built up by close, CL-bright growth bands, too.

Sample No 7 Core Szalonna Sza-10 125 m

Number of measured grains: 5

Number of analyses: 5

Grains frequently have CL-dark, usually homogenous cores (7-a-5, 7-b-5, 7-d-7). These cores are enclosed by very thin, CL-dark domains with well-developed oscillatory zoning. In these cases the dark overgrowths form less than 10 µm wide rims around the relatively large cores (Fig. 34). Two grains containing CL-dark core with homogenous inner structure have wide rim with CL-dark to middle bright growth bands (7-b-6, 7-d-4).

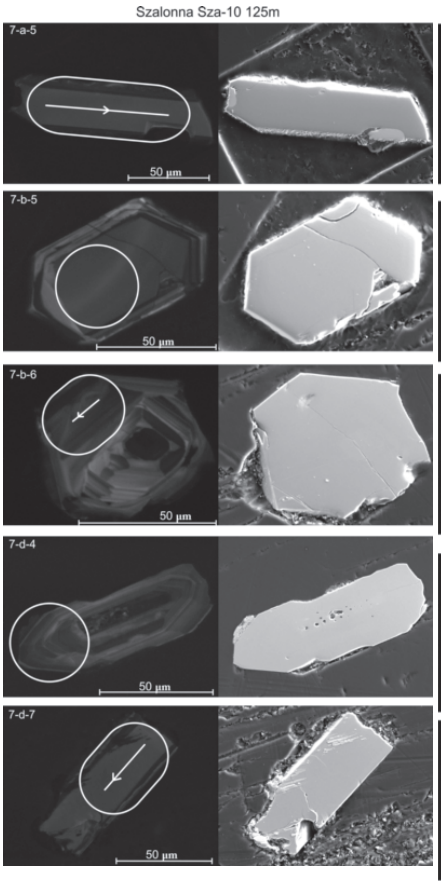

Figure 34. CL and BS images of the investigated zircon crystals from the rhyolite body in core Szalonna Sza-10 125m. Place of the LA-ICP-MS measurements are indicated.

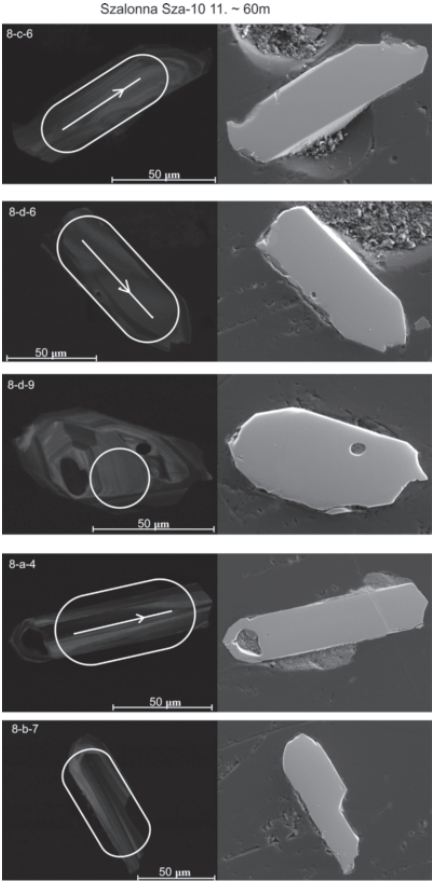

Figure 35. CL and BS images of the investigated zircon crystals from the rhyolite body in core Szalonna Sza-10 ~app. 60 m. Place of the LA-ICP-MS measurements are indicated.

Sample No 8 Core Szalonna Sza-10 ~ 60 m

Number of measured grains: 4

Number of analyses: 4

The more elongated grains are CL-dark, usually homogenous domains with signs of very pale CL-brighter growth bands (8-c-6, 8-d-6, 8-a-4). The fourth grain has a more complex inner structure. It displays medium-bright luminescent, prismatic core with close oscillatory zoning (Fig. 35). This core is enclosed by a differently oriented domain with variably wide growth bands displaying medium-bright luminescent (8-d-9).

Sample No 9 Core Varbóc Va-4 49 m

Number of measured grains: 5

Number of analyses: 5

The grains can be divided into two groups (Fig. 36, 37). The first contains grains 9-b-2 and 9-c-9 having CL-dark, CL-homogeneous, prismatic cores. The rims of these cores are rounded, slightly dissolved. These cores are overgrown by medium-bright luminescent domains showing some not pronounced chaotic inner structure. The other three crystals are characterized by CL-bright oscillatory zoning from cores to rims (9-c-2, 9-e-10, 9-e-3). These growth bands are close spaced. Grain 9-e-10 may have a CL-darker, very thin core. The others are cut not exactly in the middle, that's why only the brighter rims are visible.

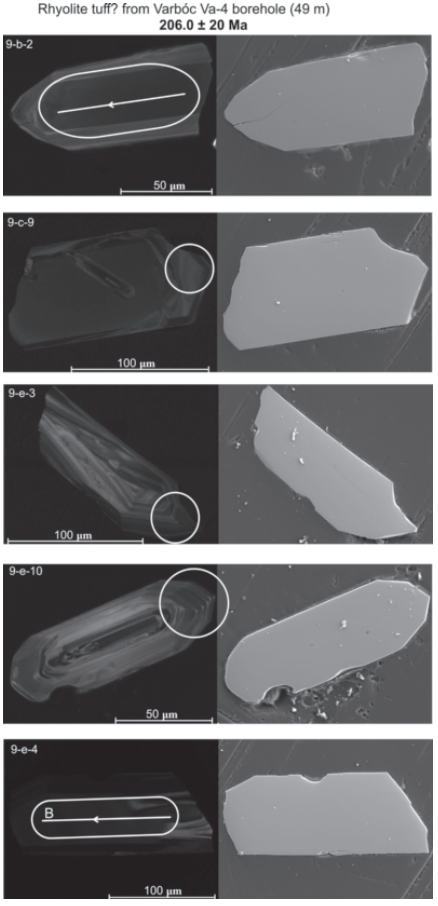

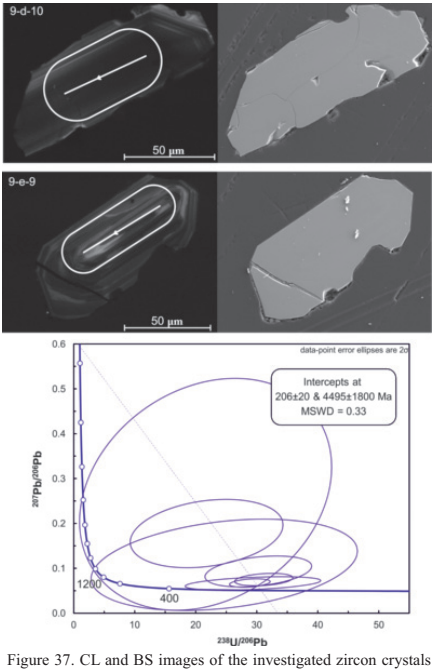

Figure 37. CL and BS images of the investigated zircon crystals from the rhyolite in core Varbóc Va-4 49 m. Place of the LA-ICP-MS measurements are indicated. Calculated ages and the related Terra-Wasserburg diagram are also indicated.

Figure 36. CL and BS images of the investigated zircon crystals from the rhyolite tuff in core Varbóc Va-4 49 m. Place of the LA-ICP-MS measurements are indicated

5.3.4.3. U/Pb ages

Forty-one U-Pb isotope analyses were performed on core and mantle of 36 prismatic zircon crystalls.The raw Pb/U and Pb/Pb ratios measured by LA-ICP-MS was corrected using the local instrumental parameters. After isotope ration and age calculations the results were visualized by Isoplot and MsExcel.

Sample No 1 Olistolith from the TO olistostrome (Perkupa-Szalonna road cut key-section)

Within this sample, three age groups can be distinguished. The oldest ages are calculated from two spot measurements on cores with resolved margins but different CL brightness (1-b-2, 1-c-6) with an age of **2015 ± 23Ma** (2σ) (Fig. 27). The next, **226 ± 6.2 Ma** (2σ) old group was measured on the core of an elongated prismatic grain (1-b-a) and two zoned rims (Fig. 28). In case of the 1-c-3 crystal, the 2 billion aged core partly solved during a later event, then it was overgrown by this younger zoned rim. There is no sign of dissolution or change in crystallographic orientation between the core and rim of the other grain (1-e-6). The youngest**, 206.8 ± 4.5 Ma** (2σ) age was detected on crystals 1-b-1 and 1-a-4. In the latter case there is no age difference within the core and rim of the grain in spite of the visible solution surface separating the two parts (Fig. 29).

Sample No 2 and 3 Matrix and layer of the olistostrome (Perkupa-Szalonna roadcut key-section)

During the examination of the thin sections (Chapter 5.3.1.2.) the volcanic material was interpreted as redeposited debris in contrast with the previous interpretations describing these layers as coeval tuff horizons. Thus supposingly there is no difference in the origin of zircons separated from the matrix of the olistostrome and from a nearby layer, thus they were counted together during the age calculations. The **222.1 ± 7.9 Ma** (2σ) age was measured on the core of two CL-dark crystals (2-a-1 B spot, 3-c-8), on one zoned core (3-c-10) and on two highly zoned owergrow of the equally oriented cores (2-a-4, 2-a-8) (Fig. 30, 31).

Sample No 4 Rhyolite body at Hunter's House locality

6 crystals with different morphological (elongated or tabular) and CL character were measured with the same **219.3 ± 6.2 Ma** (2σ) age group result (Fig. 32, 33). In case of grain 4-b-2 there was no detectable difference between the CL dark core and the CL light rim in spite of a well-visible solution event between the growth of the two, chemically different parts.

Sample No 9 Core Varbóc Va-4 49 m

The zircon crystals of this sample were the largest and most promising ones on basis of their BS images (rare cracks or fissures, no visible inclusions Fig. 36, 37). Unfortunatelly, the U content of these crystals were very low (CL dark), that is why the error of the measured isotope ratios became very large. It resulted in equally large deviation of the age data (**206± 20 Ma** (2σ)).

The results of the U/Pb age determinations can be summarized in the next way. The measurements were carried out on 33 zircon crystals of 7 sample groups. Unfortunatelly, some of the samples had very low U content or extremely variable isotope ratios, which not allowed reliable age calculations. However, we have new radiometric age data from every different position of the rhyolite occurrences (e.g. fine-grained volcanite interpreted as matrix or a layer of the olistostrome, cm-dm-sized clast of the same olistostrome, 100 m-sized big body from the Hunter House location, and tuff intercalation in pelagic limestone from Va-4 borehole). Except from some very old cores (**2015 ± 23Ma**) the results are culminating around two ages: 220 Ma and 206 Ma. Both of them indicate volcanic activity in the

Late Triassic. Without more information on the magmatism, it can indicate either an elongated magmatic event in time, or two distinct episods within a long magmatic event. These age data evidenced, that the Late Triassic rhyolites – even the 100 m-sized big bodies – must be olistoliths in the Middle Jurassic slate matrix. They are definitely not coeval subvolcanic bodies (as supposed by Szakmány & Máthé 1989), and cannot have thermal contact towards the much younger shale.

5.3.5. Depositional conditions of the Telekesoldal complex

The sedimentological characteristics of the sandstone layers such as alternation of shale and sandstone layers, erosional base and normal gradation of the coarser-grained layers, slump folds, and cross-lamination of the fine-grained sandstone refers to turbiditic origin. The sandstone-bearing shale lithofacies is suggested to form in a relatively deep pelagic basin that was reached by proximal to distal siliciclastic turbidity currents. The sand to silt-size siliciclastic material can be derived from a distal provenance. The coarse-grained gravity deposits (debrites, coarse grain turbidites) may have been accumulated closer to the slope. The carbonate components (extraclasts) of the gravity flow deposits (olistostromes) are predominantly Middle to Late Triassic (Kovács 1988) pelagic limestones showing features of the grey Hallstatt (Pötschen) facies.

Rhyolite volcanoclasts and related quartz and feldspar grains of the olistostrome derive both from lava rocks and ignimbrites. However, locally intrusive rock fragments are present as inclusions. The large rhyolite-ignimbrite bodies in core Rudabánya Rb-661, Szalonna Sza-10 and in the surface outcrop at Hunter House were already investigated in details by Szakmány et al (1989) and Máthé & Szakmány (1990). They described thermal contact between the shale and the volcanite, thus they interpreted the rhyolite as subvolcanic body. The age of the rhyolite was considered to be the same Middle Jurassic as the sediments, or a little bit younger (Szakmány et al 1989). However, I interpret the big rhyolites – similarly to the previously mentioned mm to cm-sized ones – as olistoliths in the shale and marl matrix. The contact to the shale is pressure solution contact. Often local shearing occurred along these surfaces during formation of S1 foliation due to competence contrast between the different lithologies. Kübler index measurements do not indicated higher T values in the shale close to the rhyolite body (Chapter 6.4.1). These measurements do not supply the theory of a thermal contact zone. Finally, zircon U/Pb age determinations (Chapter 5.3.4) proved the Upper Triassic age of the rhyolite. This fact excludes thermal contact towards the Middle – Upper Jurassic shale. The only interpretation can be the olistholitic origin of these large rhyolite blocks, too. The existence of small rhyolite clasts also supports this idea. For depositional environment of these 100 m-sized blocks a close source area and base-of-slope depositional setting can be suggested.

In summary, the lithological features described above imply a relatively deep marine basin in the proximity of a submarine slope as the depositional environment of TO complex. The typical components of the olistostromes indicate that the Triassic and probably Jurassic carbonates formed on an attenuated continental crust (grey Hallstatt facies zone) and volcanic rocks (Upper Triassic) must have been present in the source area of the gravity flows. Compressional tectonics due to the subduction and coeval formation of the accretionary wedge lead to nappe stacking of the ocean margin may have created suitable conditions for this sedimentation pattern. The source of the occasionally present basalt clasts probably indicate involvement of the oceanic crust in the nappe stacking. Nappe stacking brought superposition of Triassic pelagic carbonates and volcanic formations. These movements led to formation of steep slopes and intense tectonics caused fragmentation of hard rocks and triggered gravity mass movements. The coarse gravity deposits formed slope apron along the fore-

land of the thrust belt in this subduction-related basin.

Revision of the radiolarian fauna from Szendrő Szet-3 borehole resulted in Bajocian-Bathonian age for this succession of the TO complex. Depositional age can be extended to Bajocian-Callovian by first findings of marine palynomorphs in core Szalonna Sza-12 and Szögliget Szö-3. Thus revision of the radiolarian fauna and new palynomorph determinations evidenced only Middle Jurassic ages. Liassic and Malm ages supposed by previous authors (Chapter 2.2.5) was not evidenced. However, they can not be excluded for other parts of the complex.

In summary, the depositional area must have been in the vicinity of the ongoing nappe stacking of the thinned continental margin and the oceanic lithosphere in connection with the Middle—Late Jurassic subduction and accretionary wedge forming processes of the Neotethys Ocean (Schmid et al. 2008).

5.4. Other series similar to Telekesoldal complex

5.4.1. Nyúlkertlápa beds

Lithologically the NL beds are built up by grey, greenish grey and black slate and marl. Sometimes it contains mm to cm sized grey limestone and marl olistoliths. Metamorphic petrological data indicate that the metamorphic alteration of NL series reached the boundary of anchizone and epizone (Chapter 6.4.1). Field structural observations demonstrate the presence of ductile structures, namely $S0-_1$ foliation (Chapter 7.1.1) and D5b extensional shear zones (Chapter 7.6). All these features strengthen earlier views that this series is part of a metamorphic unit (Less 2000, Less et al. 1988). While KI indices, the lithological characteristics and the ductile deformational features are quite similar to the TO complex, I consider these units as equivalents. This idea has been already suggested by Csontos (1988), too.

5.4.2. Hidvégardó series

Formations cropping out only in form of scant debris in the vicinity of Hidvégardó and Tornaszentjakab villages and penetrated by the boreholes Hidvégardó Ha-3, Tornaszentandrás Tsz-16, Tornaszentjakab Tj-1 were classified into the Hidvégardó Formation or Series. In the core Ha-3 (Fig. 6) it is tectonically overlain by an overturned Torna series (Kovács & Árkai 1989). The series were divided into 4 main lithofacies units:

a., lowermost black shale rock association, partly silicified with siderite and siltstone nodules containing radiolarian molds,

b., middle evaporite-bearing member: light green and grey shale, siltstone, anhydrite, gypsum and dolomite

c., upper part: thin-bedded limestone with crinoid and echinoid fragments, marl and shale

d., the uppermost part is the so called Tornaszentjakab beds which are built up by the alternation of 0.1-0.3 m thick grey (near the surface light brown) limestone and silty limestone beds.

Since all the conodont and sporomorph probes were negative the age of the formation/series was not proven. On the basis of the lithological similarities the formation was thought to be equal with the rock association penetrated by the borehole **Zsarnó (Žarnov) Žam-1** (Fig. 38.) in the Slovak Republic. From the evaporitic succession of Zsarnó Žam-1 (46.2 m and 13.2 m) lowermost Triassic sporomorph assemblage was identified by Planderová (Szentpétery & Less 2006). By right of these

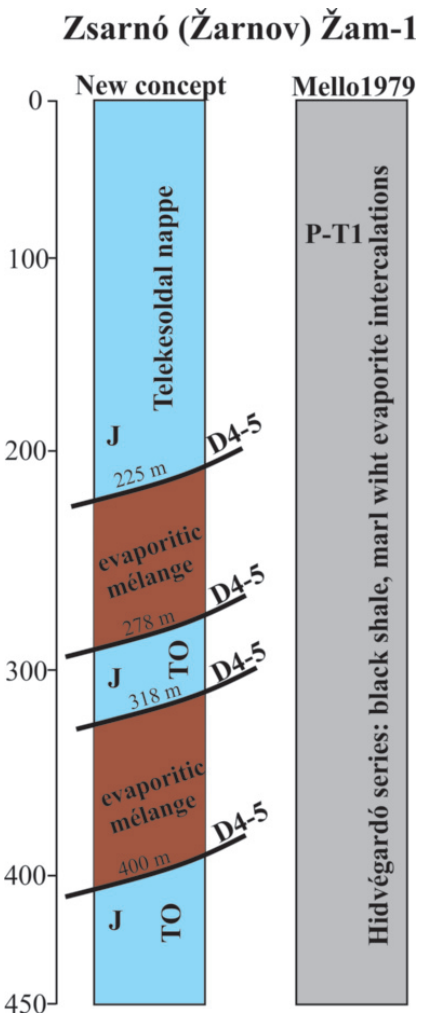

Figure 38. Structural interpretation of borehole Zsarnó (Žarnov) Žam-1. Previous concept interpret the whole core as a continuous section containing grey limestone, graphitic shale, green and grey clay, dolomit and anhydrite intercalations.

findings the whole Hidvégardó series was considered to be most likely Upper Permian-Lower Triassic, which was in agreement with the general opinion about the age of the evaporites in the Aggtelek-Rudabánya Hills (Grill et al. 1984, Kovács 1989, Less et al. 1988). For the black nodular shale a deep sea depositional environment was suggested in contrast with the shallow water hypersaline lagoon of the evaporitic part of the succession. Further discussion about the sedimentary contact of the deep sea originated shale and the lagoonal evaporite was not carried out.

However, some observations were controversial with the suggested Upper Permian-Lower Triassic age of the whole sequence. Mello (1979) brought on that the microfacies of some limestones from core Zsarnó (Žarnov) Žam-1 are highly reminiscent of the Upper Triassic and Liassic ones near Csoltó (Coltovo).

I made new observations on the available cores of the Zsarnó (Žarnov) Žam-1 borehole. Unfortunatelly, only short sections of the core is preserved in the core depository in Bratislava. The uppermost 225 m of the core consists of dark grey to black slate and marl. Corser grained intercalations of silt and fine-grained sandstone are also present. At 72-73 m an olistostrome horizon is visible (Fig. 39.1). It is a grain-supported, polymict sedimentary breccia with mm to cm sized clasts. The clasts are mainly different types of light grey to dark grey limestones and dolomites. The contacts of the grains are pressure solution surfaces. In thin sections most of the clasts are carbonates, but individual, large-scale (up to 0.5 cm in diameter) quartz crystals are also present (Fig. 39.3-7). Large crinoideal frag-

Figure 39. Sedimentary features of the samples from core Zsarnó (Žarnov) Žam-1. 1) macroscopic view of the sedimentary breccias horizon at 73.1 m 2) dolomite clasts incorporated into evaporite at 381.6 m 3-7) microscopic view of the olistostrome horizon at 73.1 m. It is characterized by grain-supported texture with the following components: 3) quartz, dolomite, crinoid fragments and biomicrite clasts 4) dolomite with pseudomorphs after gypsum, quartz, crinoid fragment, micritic limestone 5) quartz, biomicrite, crinoid fragment, coarse-grained dolomite 6) shale clast is also present 7) large radiolarian packstone with filament and sponge spicules 8) fine-grained sandstone intercalation in the slate of Hidvégardó series in Hidvégardó Ha-3 core (282.4 m).

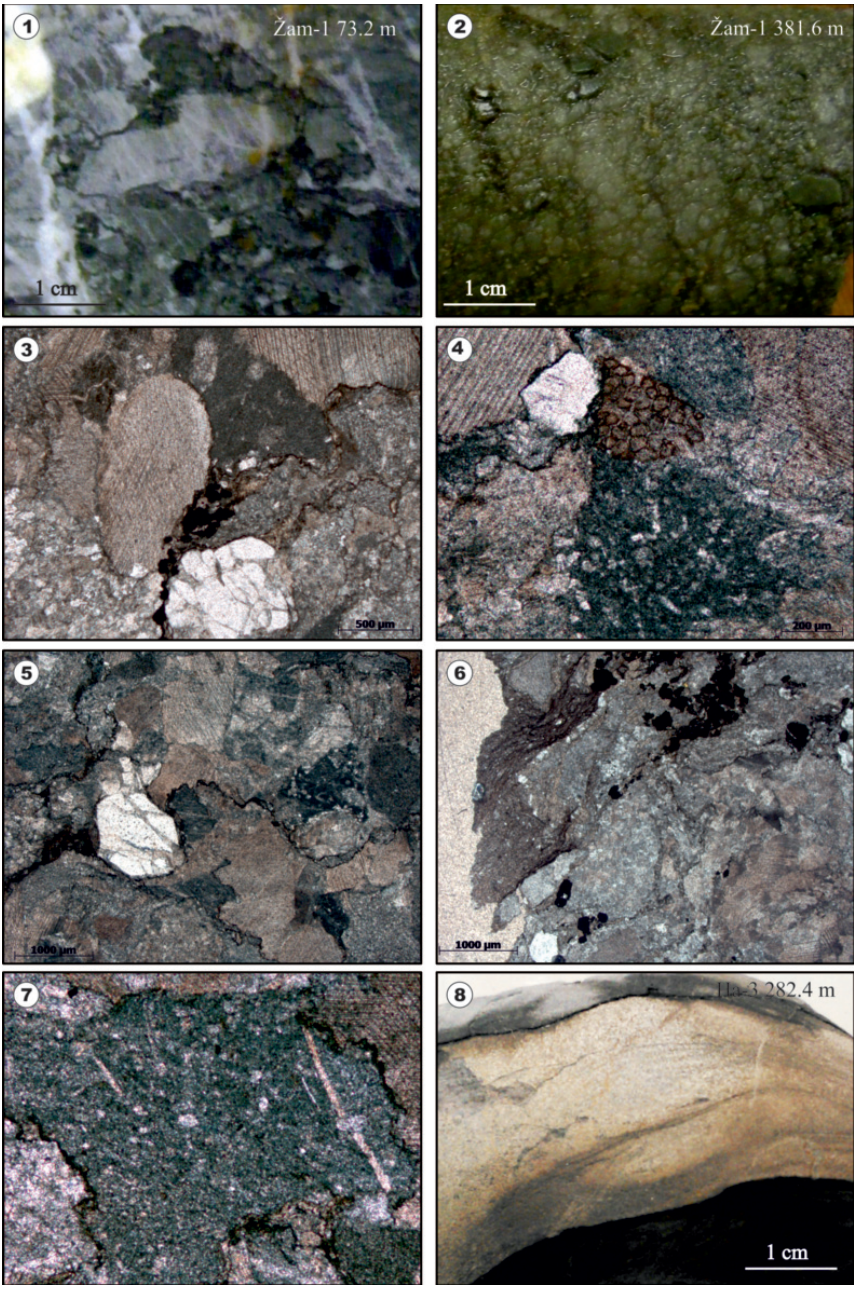
1
Žam-1 73.2 m
1 cm
2
Žam-1 381.6 m
1 cm
3
500 µm
4
200 µm
5
1000 µm
6
1000 µm
7
8
Ila-3 282.4 m
1 cm

ments are also frequent (Fig. 39.3, 4, 7). The carbonate texture of the clasts is mainly bioclastic micrit (Fig. 39.3, 7). The main biogene components are forams (Fig. 39.3), sponge spicles (Fig. 39.7) and radiolarian molds (Fig. 39.7). All the bioclasts are recristallised. Radiolarian-filamental packstone (Fig. 39.7), corse-grained dolomite and shale (Fig. 39.6) are also present among the clasts. Dolomite clasts with rectangular shapes filled with silicious material are characteristic components (Fig. 39.4). These are pseudomorphs after gypsum crystals which were originally present in the dolomite clasts.

Between 213 and 225 m the originally dark slate is altered into light brown slate. At 225 m a 5 cm thick calcite+quartz vein is visible, which separates the slate from an evaporitic breccia below. The evaporite lasts till 278 m depth, and contains dolomite clasts (Fig. 39.2). Another calcite+quartz vein indicates the lower boundary of the evaporitic breccia. Between 278 and 318 m dark grey slate and marl occurs with allodapic limestone layers. This part of the core shows great similarity to the upper part. Between 318 and 400 m a second evaporitic slice occurs. Below it the dark grey slate and marl is continuing.

In my interpretation, the olistostrome layers of the dark slate represent gravitationally redeposited sediments. The clasts highly resemble those of the Telekesoldal complex (for details see chapter 5.3.1) and they are most probably of Triassic age. The radiolarian, filamental packstones with sponge spicles resembles to the Upper Triassic deep-water limestones. The dolomite clasts containing pseudomorphs after qypsum crystals are probably derive from the Middle Triassic Gutenstein Dolomite. The observed deformational features, namely S0-1 foliation, F2 folds, extensional shear zones which may correlate with my D5b phase are also very similar to the ductile deformational features of the Telekesoldal complex (Chapter 7.4). Because of these similarities in the sedimentologic and deformational features, I suggest, that the 0-225 m, 278-318 m and from 400 m sections of the core corresponds to the Telekesoldal complex. I interpret the contact of the slate and the evaporite not as a sedimentary, but as a tectonic contact. In my opinion it represents the basal evaporitic breccia of the Telekesoldal complex, similarly to borehole Rudabánya Rb-661 (Chapter 7.4.2, 8, Fig. 23). The two evaporitic horizons separate three slices of the Telekesoldal complex.

I came to the same interpretation in case of the Hidvégardó series, too. Although, no Jurassic age is available from the slate, I suggest, that the slate, sandstone (Fig. 39.8), marl and limestone of the Hidvégardó series (a, b and d member of Szentpétery and Less 2006; see the beginning of this chapter) is the part of the Telekesoldal complex. Similarly, I suggest, that the evaporite (c member of Szentpétery and Less 2006) of Hidvégardó Ha-3 core is not a sedimentary intercalation, but the evaporite-bearing tectonic breccias separating different slices of the same Telekesoldal complex (Fig. 6). The evaporite and the adjacent shale, sandstone and dolomite have diagenetic or very low-grade IC values, while the higher metamorphic grade correletes well with the Telekesoldal complex (Chapter 6.4.3.).

5.4.3 Akasztó unit

Black and grey shale, calcareous shale and marl crops out on the eastern slope of Akasztó Hill (BOSZ-001). Same lithologies were observed in core Szögliget Szö-3, too. The shale shows a penetrative, closely spaced foliation (S0-1) dipping steeply to the NW. Small-scale kink-folds with steep axes are frequent. Micropaleontologic investigations evidenced Middle Jurassic age for this series (Chapter 5.3.3) which is in contrast with its classical Lower Triassic classification (Less et al. 1988). On basis of its similar lithology, age, deformational features (Chapter 7.1, 7.3, 7.5), metamorphic degree (Chapter 6.3.5) and structural position (Chapter 7.4.1.4) I suggest, that the Akasztó unit is the part of the Telekesoldal complex.

5.5. Csipkés Hill olistostrome

5.5.1. Lithological characteristics

A small, previously unmentioned sequence was recently encountered on the south-eastern slope of **Csipkés Hill** (Fig. 1) (Kövér 2005). It contains alternating beds of carbonate turbidites and silicified marls (Fig. 40.1, 2) that are overlain by fine-grained (Fig. 40.2), and followed by coarse-grained olistostrome beds (Fig. 40.3, 4).

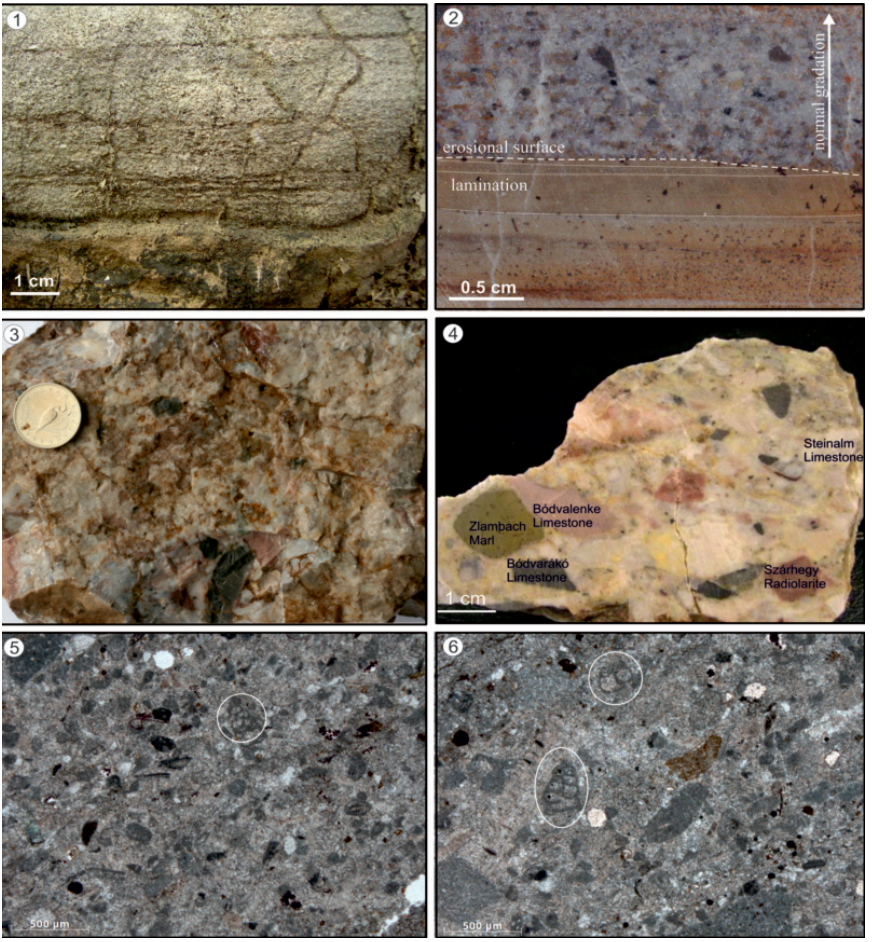

Figure 40. 1-2) Calciturbidite layers from Csipkés Hill olistostrome 3) Polymict breccia containing light grey, dark grey, red limestones and red radiolarite clasts, Csipkés Hill 4) Coarse-grained, polymict sedimentary conglomerate (olistostrome) from the Csipkés Hill. 5-6) Micrograph of sample taken from calciturbidite layer of the Csipkés Hill olistostrome. Bioclastic, peloidal, intraclastic wackestone. Note the single foraminifer grains (circles).

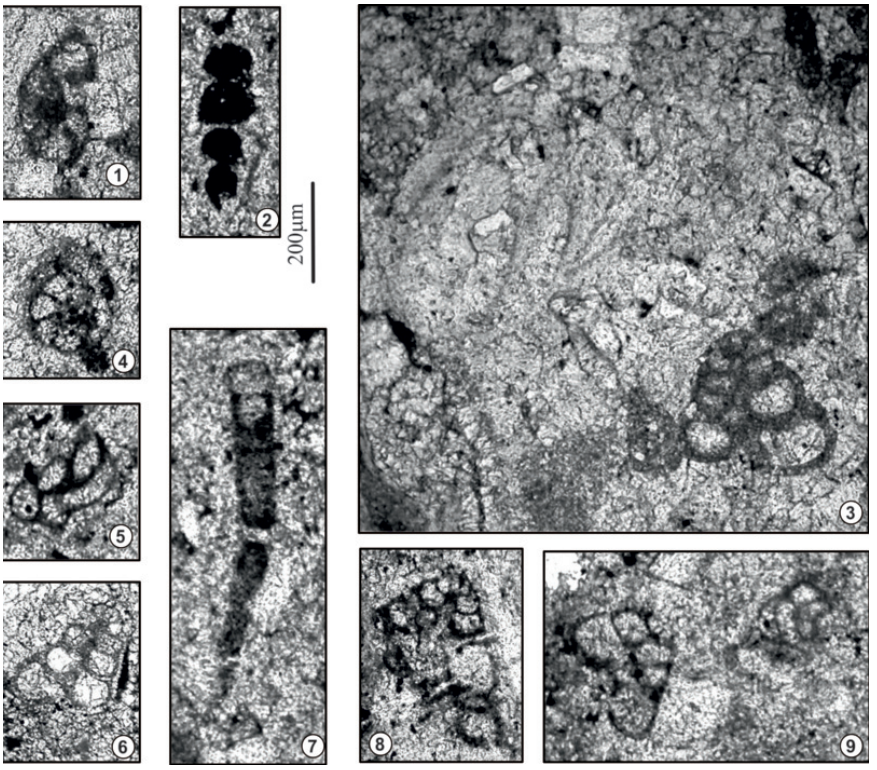

Figure 41. The encountered foraminifera assemblage from the matrix of the calciturbidites in Csipkés Hill. 1 *Callorbis minor?* Wernli & Metzger, 2 *Nodosaria* sp., 3 *Eoguttulina* sp. and *Trochammina* sp., 4 *Protopeneroplis striata*? Weynschenk, 5 *Planiinvoluta* sp., 6 *Siphovalvulina*? sp., 7 *Tubinella*? sp., 8 *Valvulina* sp., 9 *Trochammina* sp.

Macroscopically the calcarenite beds show normal gradation (Fig. 40.2). The contacts between the marl and carbonate sandstone layers are usually undulate erosional surfaces (Fig. 40.2). The olistostromes are grain-supported, containing clasts from 1—2 mm to 4—5 cm in size (Fig. 40.3, 40.4). They are poorly sorted; the size of the clasts may vary in the same layer between a few mm-s and a few cm-s. The visible clasts are usually well-rounded. The following components could be distinguished by the naked eye: pink, red, light grey and black limestones, grey and green marl, red and light grey cherts.

In microscopic view the graded carbonate turbidites are made up of mm-thick microlayers. Lithoclastic, bioclastic packstone of medium arenite grain size alternates with fine-grained lithoclastic peloidal grainstone. “Filament” wackestone and packstone, radiolarian wackestone and dark brown limonitic sparites are the typical lithoclast types. Crinoid ossicles and foraminifers occur in the interparticle micritic or microsparitic to fine sparitic matrix (Fig. 40.5, 6)). The following foraminifer assemblage was encountered (Kövér et al. 2009b): *Planiinvoluta* sp., *Trochammina* sp., *Siphovalvulina* sp., *Valvulina* sp., *Tubinella*? sp., *Eoguttulina* sp., *Nodosaria* sp., *Callorbis minor*

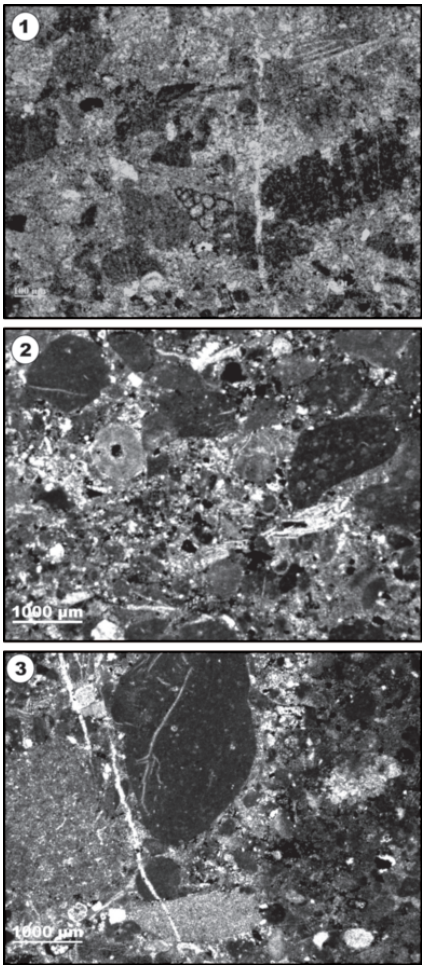

Figure 42. Details of calciturbidite layers from Csipkés Hill olistostrome. Lithoclastic, bioclastic packstone of medium arenite grain size (1) alternates with fine grained lithoclastic peloidal grainstone (2). "Filament" wackestone and packstone, radiolarian wackestone and dark brown limonitic sparites are the typical lithoclast types (3).

Wernli & Metzger, *Protopeneroplis striata* Weynschenk (Fig. 41). In case of the latter two species due to strong recrystallization and partial dissolution of the calcite walls the sections do not show the characteristic features. *Callorbis minor* has been known exclusively from the Bajocian but it was reported only from a few places (Wernli & Metzger 1990; Bassoullet 1997; Piuz 2004). It was also encountered in the Bükkzsérc Limestone in core Bükkzsérc Bzs-5 (Haas et al. 2006). The stratigraphic range of the *Protopeneroplis striata* is Late Aalenian—Late Tithonian (Schlagintweit & Ebli 1999; Schlagintweit et al. 2008). The range of *Siphovalvulina* is Hettangian to Early Cretaceous (Kaminski 2004). Consequently Jurassic depositional age of the beds is proven and **Middle Jurassic (Bajocian?)** age for the exposed beds is highly probable.

In microscopic view the investigated olistostrome sample contains a large amount of lithoclasts, 1—3 cm in size (Fig. 42). The following lithoclasts could be recognized: thin-shelled bivalve ("filament") coquina, radiolarian—"filament" wackestone, calcitized radiolarite, silicified "filament" wackestone, peloidal wackestone—packstone, clotted micrite with shrinkage pores that contains foraminifers and, brown carbonate grains with limonite staining. Lithoclastic, crinoidal packstone with fine arenite-sized grains that is either a layer or larger lithoclast was also observed (Fig. 42).

Lithoclastic packstone containing 1—3 mm sized lithoclasts in a microsparitic matrix (microolistostrome) is another typical texture of the exposed succession. The lithoclasts are slightly rounded to well-rounded. "Filament" wackestone and packstone, radiolarian wackestone, micritic mudstone, silicified "filament" packstone and chert are the typical components (Fig. 42).

5.5.2. The depositional environment of the Csipkés Hill olistostrome

On basis of their microfacies pattern, the above mentioned components are derived most probably from the formations of the Middle to Upper Triassic Hallstatt facies. However, the light grey limestone clasts of peloidal wackestone—packstone texture and clotted micrite with shrinkage pores

texture, may have originated from platform limestone, likely from the Anisian Steinalm Limestone. The red cherts (the calcitized radiolarites found in thin sections, too) and pink limestones with thin-shelled bivalve ("filament") coquina are possibly equivalent to the Ladinian to Carnian Bódvalenke Limestone (red cherty limestone). The dark grey or black cherty limestones (radiolarian wackestone, micritic mudstone in thin sections) may have been derived from the Bódvarákó Formation (dark grey cherty limestone and marl). These coarse-grained gravity deposits must have been accumulated close to a slope. The typical components of the olistostromes indicate that Middle to Upper Triassic carbonates formed in the Hallstatt facies zone must have been present in the source area of the gravity flows. Taking into account that a shallow-marine carbonate platform was the habitat of Siphovalvulina and Protopeneroplis, and platform foreslope to deeper shelf of *Callorbis minor* these fossils must have been derived from a contemporaneous active platform just like in the case of the similar genera found in the Bükkzsérc Limestone in the Mónosbél Complex in the Bükk Mts (Haas et al. 2006).

Middle to Upper Jurassic nappe stacking of the partly thinned continental margin may have created suitable conditions for this sedimentation pattern. Nappe-stacking brought superposition of Triassic pelagic carbonates from different localities. The platform-derived elements most probably originated from the coeval Adriatic carbonate platform (Haas et al. 2011) – being the only active platform in the area in the Middle Jurassic – or from a smaller-scale patch or island platform.

Both the stratigraphic and the tectonic position of the Csipkés Hill olistostrome are quite uncertain. It is definitely not the part of the TO complex, because the clast composition is very different, the clasts kept their original shape; they are neither flattened nor have stilolitic contacts. The whole series does not show any other signs of ductile deformation. According to its deformational degree it can easily be part of the TV complex. However, the TV complex is built up by black shales in the Bajocian-Bathonian age range (Chapter 5.2.2), which was supposed as the most probable depositional age for the Csipkés Hill olistostrome, too. While the latter has completely different lithology and depositional environment, it is not likely that they are the same. However, inaccuracy of biostratigraphic data (only Middle Jurassic age is sure for this series) does not exclude its younger age (maybe Callovian), thus it could be the continuation of the TV complex. Further investigations are needed to make the depositional age of the Csipkés Hill olistostrome more precise.

5.6. Comparison of the Jurassic sequences of Rudabánya Hills with similar units in the Alp-Carpathian-Dinaridic system on the basis of lithological similarities

The formation of the Jurassic complexes exposed in the Rudabánya Hills can be related to the evolution and mostly to the closure of the westernmost sector of the Neotethys Ocean. Complexes showing more or less similar features and evolution occur north of our study area near to Meliata and Jaklovce villages, Slovakia (Meliata nappe system) (Kozur et al. 1996, Mock et al. 1998) and also south of the Rudabánya Hills, in the Darnó-Bükk area, NE Hungary (Haas & Kovács 2001; Haas et al. 2006). Both areas are close to the Rudabánya Hills; however the relationship with some other localities such as the "Hallstatt Mélange" in the Northern Calcareous Alps (Kozur & Mostler 1992; Gawlick et al. 1999, 2002; Frisch & Gawlick 2003; Gawlick & Frisch 2003), and the ophiolite-bearing mélanges of the Dinarides (Vardar Zone and Dinaridic Ophiolite Belt) (Karamata et al. 2000; Pamić et al. 2002; Dimitrijević et al. 2003; Karamata 2006) should also be considered.

5.6.1. Inner Western Carpathians – Meliata series

There are two important occurrences of the Meliata series in SE Slovakia. Near to Meliata village, where dark shale with radiolarite, sandstone and olistostrome intercalations crop out. Based on radiolarians, the age of the radiolarite interbeds is Middle Bathonian to Early Oxfordian (Kozur & Mock 1985; Kozur et al. 1996). Large blocks (olistoliths) of Triassic rocks and Triassic and Jurassic radiolarites commonly occur in the shaley matrix. The olistostromes contain mostly carbonates of a different composition (Table 1). The lowermost olistostrome bed contains 10—30 cm sized subangular clasts of Carnian grey cherty limestone and 10—20 cm sized angular clasts of red radiolarian chert. It is followed by calcareous shale containing an upward decreasing amount of Carnian and Norian limestone blocks (Mock et al. 1998). It is overlain by spotty shale with radiolarite interlayers and greyish green shales with sandstone to microbreccia intercalations. In the coarse-grained breccia limestone clasts are predominant, oomicrite and oosparite texture also occur along with individual ooids and oncoid grains and crinoid ossicles. In the fine-grained breccia the volcanic components (various kinds of submarine basalts showing glass to "dolerite" texture – Mock et al. 1998) are dominant, butcarbonates and rarely oosparit are also present. Mn-bearing beds are visible in the topmost part of the exposed section (Mock et al. 1998).

	Clast composition									
	Grey pelagic lst./chert	Red pelagic lst./chert	Triassic platform	Jurassic platform	Marl	Shale	Phyllite	Rhyolite	Basalt/UB	Other
TO complex	***		*		*	*		**	*	
Csipkés Hill olistostrome		***	**	**	*					
Meliata series	***	*	*		*	*		*	**	
Lammer basin	***		**							T1
Mónosbél unit	*	**		***	*		*	*	*	andesite

Table 1. Clast compostion of the different Jurassic olistostromes. *** major component ** main component * minor component

The other important occurrence of the Meliata Unit is located near to Jaklovce village. Here the mélange is made up mostly by olistoliths of various sizes, whereas the sandstone to microbreccia intercalations are less common in this Middle Jurassic dark shale matrix (Kozur & Mock 1995). The blocks consist of light, probably shallow marine, slightly metamorphosed limestone (Honce Limestone of unknown age), siliciclastic rocks, pelagic cherty limestone, dolomite, radiolarite, rhyolite, basalt, serpentinite (Table 1).

In summary, the Meliata Unit in Slovakia is made up of black and spotty shales with sandstone and olistostrome intercalations. The main components of the olistostrome beds are as follows: Anisian to Norian grey limestones, metamorphosed limestone, ooilitic limestone, red chert, basalt of backarc basin origin, rhyolite and serpentinite.

The stratigraphic age, the sedimentological features and the predominance of the Middle to Upper Triassic basin facies in the carbonate components show a great similarity to characteristics of the olistostrome beds of the TO in the Rudabánya Hills. However, there are differences in the composition and particularly in the proportion of the olistostrome components (Table 1). In the TO metamorphosed limestone clasts are absent, the serpentinite clasts are missing and among the volcanic com-

ponents the rhyolite is predominant, while the basalt is rare. In spite of the differences, the major similarities in the sedimentation pattern and the later structural evolution (Chapter 9.3) may indicate a common basin for the depositional area of these units, in the vicinity of the ongoing nappe-stacking of the attenuated continental margin and oceanic crust of the Neotethys Ocean. The differences in the rate of clast composition can be explained by deposition in other parts of the same basin, with variable distances from the distinct source areas.

5.6.2. Northern Calcareous Alps – Tirolic Nappe Group, Lammer Basin and Hallstatt Mélange

In the Northern Calcareous Alps various gravity mass flow deposits occur in the Middle to Late Jurassic deep marine sequences reflecting closure of the Neotethys Ocean (Gawlick et al. 1999, 2002). Among them, the "Hallstatt Mélange" was defined as a complex that is made up of reworked fragments of deposits formed on the Late Triassic to Early Jurassic attenuated Neotethys margin, and small remnants of the oceanic basement (Meliata Zone) (Frisch & Gawlick 2003). It contains elements of the Zlambach/ Pötschen and Hallstatt facies zones, respectively. According to Gawlick and his co-workers (Gawlick et al. 1999, 2002, Frisch & Gawlick 2003) the "Hallstatt Mélange" was formed in the late Early to early Late Jurassic interval as a result of a progressive shortening of the basin (Hallstatt Zone). During this process trenches developed in the foreland of the advancing nappes and filled up by various deposits, subsequently incorporated into the accretionary prism. Parts of the accretionary prism were resedimented in the Lammer Basin or occur as overthrust remnants (e.g. the Florianikogel Formation in the eastern Northern Calcareous Alps – Mandl & Ondrejičková 1991, 1993, Kozur & Mostler 1992).

The Lammer Basin was roughly coeval with the formation of the complexes studied in the Rudabánya Hills, and it also contains a large selection of different clasts.

The Lammer Basin received mass-flow deposits and large slides derived from the grey Hallstatt facies zone ("Hallstatt Mélange"). The thickness of the basin fill may reach 2000 m (Gawlick 1996; Gawlick & Suzuki 1999). Olistostromes and large olistoliths originated from the Pötschen Limestone occur in the Callovian to Lower Oxfordian. The Middle Oxfordian is made up mostly by olistolithes of the Lower Triassic Werfen Formation, Upper Triassic Pötschen and Hallstatt Limestone intercalated in marl and radiolarian chert layers. The upper part of the succession is composed of Middle and Upper Triassic platform carbonate mega-slides (Gawlick 2000).

The roughly coeval lower part of the Lammer Basin fill shows some similarity in lithology (pelagic limestone and radiolarite), sedimentary features and supposed geodynamic position to that of the TO in the Rudabánya Hills. However, there are remarkable differences in the clast composition of the olistostromes (Table 1). Those of the Lammer Basin consist only of Middle to Upper Triassic pelagic limestone clasts, clasts from the Lower Triassic Werfen beds, and no volcanic material is present among the redeposited clasts.

5.6.3. Bükk–Darnó area – the Mónosbél Unit

In the Bükk—Darnó area the Middle to Upper Jurassic Mónosbél Complex – containing great amounts of gravity mass flow deposits in shale and radiolarite matrix – is comparable to the contemporaneous formations in the Rudabánya Hills.

In the western part of the Bükk Mts, the Mónosbél Unit is made up of Bajocian to Kimmeridgian deep marine siliciclastics, carbonates and siliceous sediments with intercalations of olistostrome

beds, containing very heterogeneous clasts transported into the basin via gravity mass movements. In the olistostrome beds along with fragments of acidic, intermediate and basic magmatites, phyllites, metasiltstones, metasandstones, pelagic carbonates and radiolarites, and lithoclasts of redeposited carbonates are common (Table 1). The latter carbonate clasts consist of ooids, oncoids, and skeletal fragments of shallow-marine biota. This type is also present in the form of large blocks (olistoliths). These platform derived ("Bükkzsérc-type") limestones of Bajocian to Bathonian age are particularly common and typical in the Mónosbél Unit (Haas et al. 2006).

Gravity deposits of the Mónosbél Unit are also exposed in the Darnó area and in ore exploratory wells more to the west, in the eastern Mátra Mts. at Recsk Fig. 2b). Olistoliths of marine Upper Permian and Upper Triassic Hallstatt Limestone were encountered within Bajocian to Callovian shale and radiolarite (Haas et al. 2006). The thickness of the olistostrome-rich intervals may exceed 100 m. The usually matrix supported breccia is typically oligomict, consisting mostly of carbonate clasts of various colours and compositions (Haas et al. 2006). Detailed component analysis of the olistostromes is under way.

In a borehole drilled near the central Mátra Mts (Recsk Rm-109), Bajocian platform derived redeposited carbonates, more proximal than those in the Bükk Mts, were encountered in a remarkable thickness (Haas et al. 2006).

In summary, the most characteristic features of this Mónosbél Unit are the presence of coeval platform-derived foraminifers, ooids, oncoids, peloids – redeposited as individual clasts – and large amounts of Middle Jurassic shallow-water limestones of mm to hundred m in size. The individual clasts indicate that the source area of the platform material must be a coeval, active carbonate platform, most probably the Adriatic Carbonate Platform, which was the only known Middle Jurassic active platform in the whole region (Tišljar et al. 2002, Vlahović et al. 2005). The presence of rhyolite, andesite and basalt clasts are also common in some horizons indicating the complexity of the provenance.

Among the examined Jurassic series of the **Rudabánya Hills**, the only one, which has Middle Jurassic platform derived material, as a characteristic feature, is the Csipkés Hill olistostrome (Table 1). Like the Mónosbél Unit, it contains carbonate turbidite beds with platform-derived foraminifers (following the previous reasoning: it probably originated from the Adriatic Carbonate Platform) and olistostrome horizons, but in contrast to that, volcanites and roughly coeval lithoclasts are missing among the clasts.

There is a common feature in the composition of the olistostromes of the Mónosbél Unit and the TO, as well (Table 1). The TO contains few rhyolites and basalts, but the volcanic clasts from the Mónosbél Unit are more varied. However, the 201.9±6.4 Ma from the rhyolite clasts in the Mónosbél Unit (Kövér unbulished data) is similar to the clasts of TO complex (206.8 ± 4.5 Ma).

Summarized, there are a lot of common sedimentological features in the Middle to Upper Jurassic complexes discussed above that can be attributed to the processes of the Neotethys closure (Table 1). However, due to their different palaeo-positions, the composition of the redeposited clasts shows significant differences depending on geological features of the source area. Fragments originating from the Hallstatt facies zone occur in all of the compared units. Grey Hallstatt-type limestone clasts are typical components of the Telekesoldal complex; they are also characteristic elements of the lowermost olistostrome of the Meliata-type section. Both grey and red Hallstatt-type pelagic carbonates prevail in the Lammer Basin fill, and they are present as olistoliths in the Mónosbél Complex of the Darnó area. The clasts derived from the red Hallstatt-type area are predominant in the olistostrome of Csipkés Hill.

6. Metamorphic petrological and geochronological studies

6.1. Introduction

Low-temperature metamorphism is usually present in subduction and obduction-related mélanges, where high-pressure metamorphic blocks and slices – ranging from several decimetres to several kilometres in size – are tectonically emplaced in unmetamorphosed or only slightly metamorphosed, usually clastic sedimentary matrix (Árkai et al. 2003, Willner et al. 2004, Crouzet et al. 2007, Liu et al. 2008, Bousquet et al. 2008). Metamorphic features of the various constituents of these mélanges may elucidate the physical conditions (pressure–temperature paths) of subduction, collision and subsequent cooling (exhumation) of the upper oceanic crust and related rocks of the accretionary prism.

However, diagenetic sedimentary rocks and metasediments at an incipient stage of metamorphism usually do not contain facies- or zone-indicating mineral assemblages. Since only local equilibrium may be achieved in these systems, most of the methods used in the higher grades, i.e. geothermobarometers (equilibrium mineral phases) and trace element patterns are useless because of the lack of diagnostic minerals.

Fortunately, the interest in the thermal history of sedimentary rocks has rapidly been growing for the last 40 years due to the oil industry, where predicting hydrocarbon generation is one of the most important questions (Foscolos et al. 1976, Abu et al. 1991, MacCulloh & Naeser 1989, Suchý et al. 2002). This interest resulted in the development of several methods, which can approach the transition between diagenesis and low-grade metamorphism. In the very low-grade metamorphic zone empirical parameters are used in order to characterize the reaction progress of the predominant phyllosilicates. One of the most widely adopted parameter is the XRPD (X-ray powder diffraction)-based illite "crystallinity" introduced by Kübler (1966, 1968), and abbreviated as KI (Kübler index) (Guggenheim et al. 2001). Árkai (1991) suggested using chlorite "crystallinity" indices as complementary tools to determine the diagenetic/metamorphic grade of various lithotypes. This latter index was suggested to be called Árkai index by the AIPEA Nomenclature Committee (Guggenheim et al. 2001).

The most widely used method for the estimation of pressure conditions in case of these very low-grade metamorphosed sedimentary rocks was developed by Guidotti and co-workers from the late seventies on the basis of the b cell dimension data of K-white mica (Guidotti 1984, Guidotti & Sassi 1986, Guidotti et al. 1989). The combined usage of the methods mentioned above give the possibility to determine temperature and pressure conditions in the very low-grade metamorphic realm.

Tectonic units of the southern Inner Western Carpathians (Slovak Republic, Hungary) were derived from the Jurassic subduction of the Meliata branch of the Neotethys Ocean (Kovács et al. 1997, Plašienka et al. 1997, Less 2000), and subsequently underwent post-collisional mid- to late Cretaceous deformation phases. Although blueschist facies metasedimentary and metavolcanic rocks are present in the (tectonosedimentary) subduction mélange, and dismembered ophiolite suite is known in an evaporitic mélange, the internal structure of this orogen, the number and contents of nappes, stacking order, direction of subduction, still remain under discussion (Plašienka et al. 1997, Less 2000, Mello 1997, Lexa et al. 2003). In addition to poor outcrop conditions and the lack of paleontological data from some stratigraphic units, the debate is fuelled by the lack of metamorphic petrological, structural and geochronological data from different low-grade metasediments which represent considerable part of the area.

Based on complex methodology, Árkai et al. (2003) recently reconstructed the p-T-t paths for the

former accretionary wedge, the Meliata nappe system which underwent very low-grade to blueschist facies metamorphism during the subduction and exhumation processes (Faryad 1995, Faryad & Henjes-Kunst 1997, Lexa et al. 2003). However, the knowledge is incomplete on the metamorphic conditions of similar tectonic units found in Hungary, in the Rudabánya Hills.

This is why a systhematic sampling and metamorphic petrological research was carried out on the rocks of the central and northern Rudabánya Hills and the eastern margin of the Aggtelek Hills. The methods for this part of the research were the following.

The X-ray powder diffractometric (XRPD) measurements were carried out in the Institute for Geochemical Research of the Hungarian Academy of Sciences. XRPD patterns were obtained using a Philips PW-1730 diffractometer (with computerized APD system) with the following instrumental and measuring conditions: CuKα radiation, 45 kV/35 mA, proportional counter, graphite monochromator, divergence and detector slit of 1°, and collection of data with 0.01 and 0.02° 2Θ steps, using time intervals of 1 and 5 s, respectively. Diffraction patterns were performed from non-orientated and highly orientated powder mounts of whole rock and <2μm spherical equivalent diameter (SED) size fraction samples in order to determine bulk-rock mineral assemblages, b cell dimension of K-white mica, and illite Kübler and chlorite "crystallinity" indices.

The <2μm grain-size fraction samples were obtained using the following procedure. Rock samples were disaggregated under standard conditions using a jaw crusher followed by crushing in a mortar mill (type Pulverisette 2, Fritsch) for 3 minutes. Further disaggregation was achieved by repeated shaking in deionised water. The <2 μm grain size fraction was separated from aqueous suspension based on the differential settling of grains of different diameters in order to eliminate or at least reduce in the future the possibility of misleading age data induced by the contribution of various amounts of old, detrital K-white mica, usually occurring more frequently in the larger grain size fractions than in the fine ones. Following the technique of Kübler (1975), aqueous suspensions of the given fraction were pipetted onto glass slides with a material amount of 3 mg/cm2. Portions of air-dried <2μm grain-size fraction were saturated with ethylene glycol (60 C/overnight) in order to identify the possible swelling phase(s) (smectite and/or vermiculite) of the samples. Calibration procedure of phyllosilicate "crystallinity" index measurements was carried out against that of Kübler's laboratory using 0.25 and 0.42 Δ°2Θ as anchizone boundary values (for details see Árkai et al. 1996). The illite "crystallinity" (KI=Kübler index) boundaries of the anchizone correspond to 0.25 and 0.42 Δ°2Θ in the present work. On the basis of this calibration, using also the linear regression equations between KI and chlorite "crystallinity" (ChC) indices (Árkai et al. 1995b), the actual ranges of the anchizone are 0.26–0.38 Δ°2Θ for ChC (001), and 0.24–0.30 Δ°2Θ for ChC (002). These entire boundary values refer to air dried (AD) mounts.

It is generally accepted that the temperature is the main physical factor that affects "crystallinity" (Frey 1987). However, phyllosilicate "crystallinity" indices, as indicators of diagenetic or metamorphic grades, ought to be used cautiously because many other factors may affect the XRPD profiles of the phyllosilicate basal reflections.

B cell dimension of the illite–K-white mica was measured on whole rock samples.

The K-Ar dating was carried out on representative <2 μm grain size fraction samples carefully selected from samples used earlier for metamorphic petrologic studies. The mineral separation did not allow the production of pure monomineralic K-white mica fractions in a strict sense (review by Hunziker (1987) and found also by Judik et al. (2004)). Instead, polyphase fractions were obtained, that might have introduced additional uncertainties in the geological interpretation of the K-Ar age

data. However, since the illite–K-white mica phase proved to be always dominant, and illite–K-white mica was the only K-bearing phase in the fractions, the K-Ar age values obtained on these fractions could reliably be used for estimating the time of the metamorphism (Steiger 1977, Hunziker 1987). K-Ar dating was carried out in the Institute of Nuclear Research (Hungarian Academy of Sciences) using the following procedure. Illite–K-white mica-rich fraction samples were degassed by high frequency induction heating; the released argon was cleaned applying furnaces with Ti sponge and St707 getter materials. 38Ar was introduced from a gas pipette. For Ar isotopic ratio measurements a magnetic mass spectrometer of 150 mm radius and 90° deflection was used in the static mode. Before the determination of K the samples were digested by a mixture of HF+H2SO4+HClO4 and dissolved in HCl. K content of the samples was measured with a flame emission photometer. Results of the inter-laboratory standardization were published by Odin et al. (1982). K-Ar ages were calculated using the constants proposed by the IUGS Subcommission on Geochronology (Steiger & Jäger 1977).

6.2. Inferences from literature

Previously published palaeo-temperature estimations have been deduced mainly from KI and Conodont Colour Alteration Indices (CAI) (Árkai & Kovács 1986, Kovács & Árkai 1987), however, only summarized and the mean statistical parameters were published. The samples were taken from different tectonic units, following the concept of Grill et al. (1984) and Less et al. (1988).

The Szilice (Silice) nappe system and the Szőlősardó unit which were supposed to be in uppermost position were shown to get only medium or deep diagenetic alteration, so the maximum temperature did not reach 200-250ºC (Árkai & Kovács 1986).

In case of the Komjáti Unit which was thought to be constitute the tectonic unit below the Aggtelek nappe and Bódva series (cores Szögliget Szö-3 and Hidvégardó Ha-3) the KI-averages indicated regional metamorphism corresponding to the boundary of the diagenetic zone and anchizone. However, I will propose a different formation classification for both the Szö-3 and main part of the Ha-3. This will suggest discrediting an average KI value of the entire data set of these boreholes.

The samples from the underlying Bódva series (in sense of Grill et al. 1984 and Less et al. 1988, Less et al. 2004) showed mainly diagenetic alteration; however, in few locations low anchizonal values were measured (Dunnatető Hill), which were interpreted as the result of local tectonic movements (Árkai & Kovács 1986). In the subsequent chapters I will discuss the structural concept, which can explain this anomalous data.

The lowermost Torna tectonic unit (built up by the Torna series), was subjected to anchi- to epizonal metamorphism (Árkai & Kovács 1986). The estimation for pressure on basis of the K-white mica b cell dimension data suggested medium/high pressure system (Árkai & Kovács 1986). This data set was used as a basis to establish a first-order nappe stack, where Torna (Turna) unit was originally at the lowermost strucutural position (Grill et al. 1984, Less et al 1988).

Both the Telekesoldal and Telekesvölgy complexes were affected by only deep diagenetic alteration on basis of the measured KI values (Árkai & Kovács 1986) thus the palaeo-temperature might be close to the low temperature boundary of the anchizone, i.e. about 200-250°C. However, in case of the Telekesoldal complex the whole rock samples gave lower KI-averages, which were explained by mica inheritance. The vitrinite reflectance values were characteristic for the anchizone, being in contradic-

tion to the averaged KI values and textural features. This phenomenon was considered to be the result of either the allochtonous character of vitrinite or a short static thermal effect (Árkai & Kovács 1986).

The metamorphic grade of the Meliata nappe s.s. in the Slovak Karst was pointed out to vary, corresponding to the low-temperature part of the anchizone at the type locality and to the glaucophanitic greenschist facies around the Rozsnyó (Rožnava) zone. Both the temperature and pressure conditions (low/medium pressure range) of the locus typicus were recognized to be rather similar to those of the Komjáti Nappe (core Szögliget Szö-3).

6.3. Petrography

Besides the intensity of the physical and chemical weathering, the lithology, the chemistries of fluids and bulk rock, the abundance of the detrital K-white mica and its degradation state may also affect the peak shape of illite–K-white mica intensively (Judik et al. 2004). That is why the knowledge of the mineral composition – especially the quality and quantity of the clay minerals – is a pre-requisite of the usage of KI measurements. Appendix Table 2 contains the mineral phases (and their relative abundance) of the investigated whole rock samples, while Appendix Table 3 shows the similar data of the separated <2μm size fraction samples of the studied units determined by petrographic microscopy and XRPD.

The paragonite and the swelling phyllosilicate (smectite and/or vermiculite) content either as a discrete phase or as a mixed-layered component of the K-white mica affects the peak shape intensively. Thus samples containing paragonite or swelling phyllosilicates do not provide reliable data for KI measurements. In these cases, when chlorite is also present in the samples chlorite "crystallinity" indices can be used as substitute parameters (Árkai et al. 1995b). If chlorite "crystallinity" data are not available, the metamorphic degree can only be estimated, because paragonite is often present in anchi- to epizonal metamorphic pelitic rocks (Frey 1987). The swelling phases may affect the chlorite (001) reflexions that are why the chlorite (002) reflexions were used in the interpretation of the chlorite "crystallinity" data.

6.3.1. Uppermost Triassic–Jurassic Telekesvölgy Complex

Claystone, claymarl, marl, siltstone, calcareous limestone and limestone were studied from this complex. The whole rock samples usually contain quartz, illite–K-white mica, chlorite, calcite and/or dolomite, and small amount of plagioclase (albite). All of the samples from borehole Sza-5 and one from Szet-4 borehole contain subordinate rutile. Some samples collected typically from surface outcrops (marked with TV=Telekes Valley) include subordinate swelling phase(s) (smectite and/or vermiculite) among the clay minerals.

6.3.2. Bódva series, Lower-Upper Triassic

Calcareous marl, marl, claystone, siltstone, dolomite and limestone were investigated from the Triassic series. The formations with considerable clay mineral content are the Lower Triassic siltstone and claystone and the Upper Triassic pelagic limestone, which occasionally have clay-bearing horizons intercalating with limestone layers. The thickest claystone/marl beds are in the Carnian part of the series. They usually contain quartz, illite–K-white mica, chlorite, calcite, with or without

dolomite, and small amount of plagioclase (albite) in the whole rock samples. All of the samples taken from borehole Rb-658, Va-3, P-74 and Ha-4 contain subordinate rutile. Some samples collected typically from surface outcrops (marked with TV=Telekes Valley and E=Esztramos Hill) include subordinate swelling phase(s) (smectite and/or vermiculite) among the clay minerals.

6.3.3. Telekesoldal Complex

Slate, meta-siltstone, claymarl, and marl are the most common rock types among the examined samples. The most common minerals in the samples are as follows: quartz, illite–K-white mica, chlorite, calcite and dolomite, small amount of rutile. The lowermost sample from borehole Rb-661 contains considerable amount of gypsum.

In comparison with the samples of Bódva series, these samples usually contains considerable amount of plagioclase (albite) both in the whole rock samples and in the <2μm phase.

6.3.4. Nyúlkertlápa beds (NL beds)

These slate samples basically contain illite–K-white mica and chlorite, and occasionally small amount of albite and rutile. Smectite and illite/smectite is also present in the sample T-26. Since this sample was taken from a surface outcrop, it is likely to be a secondary phase, formed during weathering processes.

6.3.5. Szögliget-3 borehole

Dark-grey slate and dolomite-bearing slate with mm thick calcite veins and lenses are the main investigated lithotypes. The main minerals are quartz, illite–K-white mica and chlorite. All of the samples contained plagioclase (albite). Besides the previously mentioned mineral phases a smaller amount of calcite and dolomite is present in samples Szö-3 32 m and 76.1 m. All of the samples contain paragonite. The smectite, illite/smectite – present only in the sample taken from the uppermost part of the borehole – are very likely to be the results of sub-surface weathering processes, or induced by migration of low-temperature fluids, because the swelling phases are completely missing from the lower part of the succession.

Summing up the results of the mineral composition investigations, a considerable part of the samples provided reliable KI data, although all the samples taken from borehole Szö-3 contains paragonite thus the KI data could not be evaluated.

6.3.6. Torna series

Grey Carnian marl from the Esztramos Hill, Dunnatató Hill (small Martonyi nappe outlier) and Tornaszentandrás (Martonyi nappe) were collected for KI studies. Different marly and limestone lithologies from the upper part of Hidvégardó Ha-3 borehole and the Bódvarákó window were also investigated among the new samples. In the marl samples the main mineral phases are illite-K-white mica, plagioclase and quartz. These samples do not contain chlorite. The samples from core Ha-3 contain large amount of calcite (30-75%). The clay minerals are chlorite and illite-K-white mica. All the samples were suitable for KI investiations.

6.4. Metamorphic grade and temperature: Illite Kübler index (KI), chlorite "crystallinity" (ChC) and vitrinite reflectance (VR)

Several attempts have been made in order to constrain the temperature conditions of very low-grade metamorphism (Árkai 1991, Árkai et al. 1995b, Frey 1987, Kisch 1983, Merriman & Frey 1999). On the basis of these comprehensive works, it is widely accepted that the lower and upper boundaries of the anchizone are at around 200 and 300 ºC–350 ºC, respectively. For my compilation, the comprehensive and comparative chart of Árkai (Árkai 1991) was used as a base, suggesting ~200 ºC for the lower, while ~300–350 ºC for the upper boundary of anchizone.

6.4.1. Telekesoldal complex, borehole Szögliget Szö-3 (Akasztó unit), Nyúlkertlápa beds

Illite KI, chlorite "crystallinity" and vitrinite reflectance measurements were carried out on samples from the Jurassic TO complex, the borehole Szö-3 and the Nyúlkertlápa beds in order to characterize the temperature conditions of the very low to low-grade metamorphism. In case of the **TO complex** the KI values (Table 3, Fig. 43) fall into the high-temperature part of the anchizone (KI=0.25–0.30 Δ°2Θ) giving an average of 0.265±0.067 (SD) Δ°2Θ, while some of them reaching the anchizone-epizone boundary (0.25 Δ°2Θ). Samples from boreholes Sza-10 and Sza-12 are in the epizone. Only a few KI values are in the low-temperature part of the anchizone (0.30–0.42 Δ°2Θ) (Appendix Table 4, Fig. 43). However, the samples taken from borehole Szet-3 shows significantly higher KI values. This southerly located borehole and the other data may suggest that the Kübler indices of the samples vary from N to S, showing a little bit lower values in the northern and higher in the southern part of the series (Fig. 44).

Similarly to the relationships found by Árkai (1991) the ChC (001) and ChC (002) values show positive correlation with the KI data (Appendix Table 4). Most of the ChC (002) data fall into the anchizone (0.24–0.30 Δ°2Θ) with an average of 0.252±0.018 Δ°2Θ. Almost the same amount of samples reaches the anchizone-epizone boundary (0.24 Δ°2Θ) (Appendix Table 4). The samples from the core Szet-3 – where the KI values were a

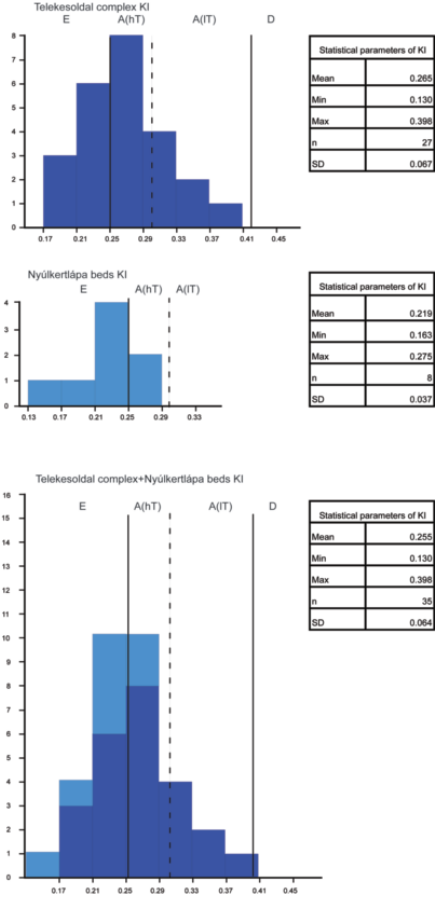

Figure 43. Statistical parameters and distribution diagrams of the measured illite Kübler indices from TO complex, borehole Szö-3 and NL beds. E: epizone, A(hT): (high-temperature) anchizone, A(lT): (low-temperature) anchizone, D: diagenetic zone.

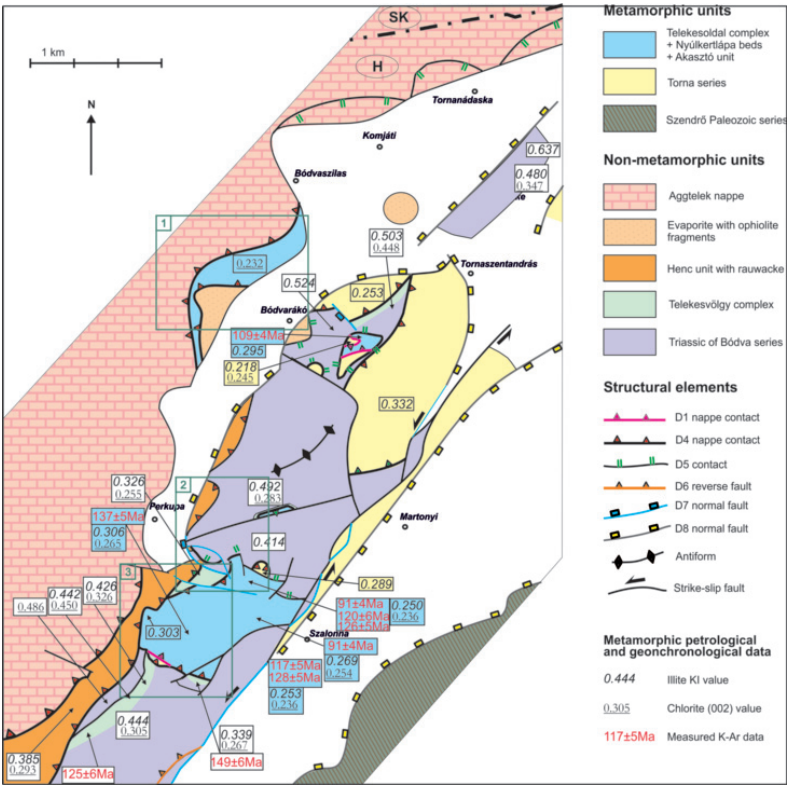

Figure 44. K-Ar data, illite Kübler indices and chlorite "crystallinity" indices from the central Rudabánya Hills, after unpublished data of Árkai (1981, 1985, 1989), Árkai & Kovács (1986) and recent measurements represented on the simplified structural map of the area (for detailed map see Appendix 1-3). In case of more data from one locality of the same lithology and structural unit (e.g. boreholes) the average value of the measured data is represented. Grey letters indicate K-Ar data of Árva-Sós et al (1987). White boxes indicate data from non-metamorphosed units. Compare with the original concept of Less et al. 1988, Fig. 5.

little bit higher – do not show significant differences from the rest of the group on basis of the chlorite "crystallinity" values. In case of the ca. 14 Å reflection of the chlorite, half of the ChC (001) data reach the anchizone-epizone boundary (0.26 Δ°2Θ); while the other measured values correspond to the anchizone.

KI and ChC data falling into the high-temperature part of the anchizone and reaching the boundary of anchizone and epizone indicate a palaeo-temperatures of 300–350°C (Árkai 1991).

The maximum VR (R_{max}) values are 4.8–5.6% (50). From the several approaches, that developed to convert VR data to peak palaeo-temperatures, the equation of Barker (1988) was chosen, because the random vitrinite reflectance (%Rr) is the only input parameter of this regression equation (T(°C) = 104 (lnRr) + 148). It follows that it neglects the effect of heating time. Using the equation on the average Rr=4.86% of the TO complex estimated peak temperature of metamorphism is of ca. 310 °C.

The result of this method correlates well with the palaeo-temperature estimated by the KI and chlorite "crys-

tallinity" data. Accordingly, the peak temperature of the metamorphism of TO complex was 300–350°C.

All the samples taken from borehole **Szögliget Szö-3 (Akasztó unit)** contain paragonite, indicating anchi- to epizonal alteration. The chlorite "crystallinity" values show good correlation with the previous data, all the measured values exceed the boundary of the anchi- and epizone (0.24 Δ°2Θ) (Appendix Table 4), with an average of 0.232±0.006 Δ°2Θ.

In case of the **NL beds**, the average of the KI indices (0.219±0.037 Δ°2Θ) fall into the epizone (Appendix Table 4, Fig. 43), while some of the measured values correspond to the high-temperature (high-T) part of the anchizone. The ChC (002) data show good correlation with the Kübler indices, indicating partly high-T anchizonal, partly epizonal metamorphic alteration, with an average value of 0.245±0.020 Δ°2Θ.

6.4.2 Uppermost Triassic–Jurassic Telekesvölgy complex

KI results (Appendix Table 4, Fig. 45) provide scattered values between 0.227 and 0.702 Δ°2Θ for the uppermost Triassic–Jurassic TV complex. On the distribution diagrams (Fig. 45) two maximums are visible: one in the low-temperature anchizone and another, higher one in the field of diagenetic alteration. Most of the samples refer to anchizonal values contained swelling phases (smectite), indicating weathering processes or alteration of clay minerals due to late low-temperature fluid movements. In these cases the measured KI values are not reliable for temperature estimation.

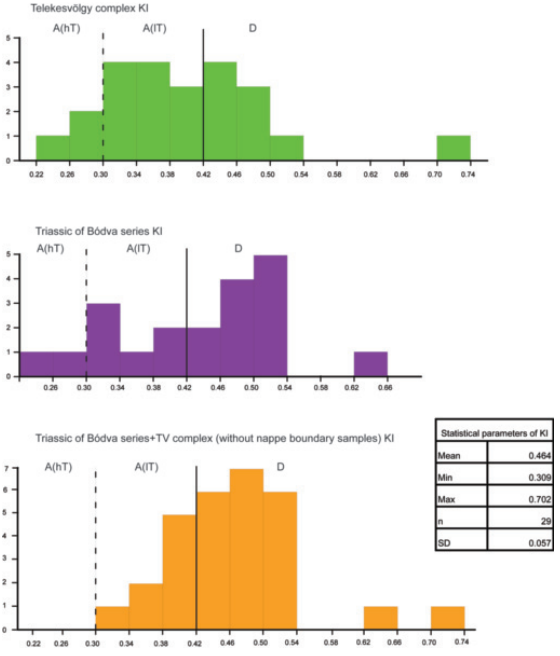

Figure 45. Statistical parameters and distribution diagrams of the measured illite Kübler indices from TV complex and Bódva series. A(hT): high-temperature anchizone, A(IT): low-temperature anchizone, D: diagenetic zone.

The range of the ChC (002) data is also wide (Fig. 46), containing values in the interval of 0.240-0.421 Δ°2Θ. Part of the data for samples that do not contain clay swelling phases indicates diagenetic alteration (Appendix Table 4). However, the standard deviation of both the KI and chlorite "crystallinity" data is high, values range from the anchi-epizonal boundary to the diagenetic zone. Some samples show significant differences in the metamorphic degree on the basis of the KI and the chlorite "crystallinity" data. Among this, the rocks from the borehole Szet-4 suffered only low-temperature anchizonal alteration by right of illite KI data, while their chlorite "crystallinity" indices reach the boundary of the anchi-and epizone. Most of these samples – refer to anchizonal

"crystallinity" values – contained swelling phases (smectite) (Appendix Table 3), indicating weathering processes or alteration of clay minerals due to low-temperature fluid flow. Similarly to the illite method, these altered samples are not reliable for temperature estimation.

6.4.3. Triassic Bódva series

Both KI results (Table 4, Fig. 45 – with a range of 0.245-0.637 Δ°2Θ – and chlorite "crystallinity" data (Table 4, Fig. 46) – 0.274-0.382 Δ°2Θ – indicates a wide range for the alteration of the Triassic part of the Bódva series. Similarly to the TV complex, the standard deviation of both the KI and chlorite "crystallinity" data is quite high, having values from the high T anchizone deep into the diagenetic zone, while the distribution diagrams (Fig. 45, 46) show two maximums: one in the low-temperature anchizone and another, higher one in the field of diagenetic alteration.

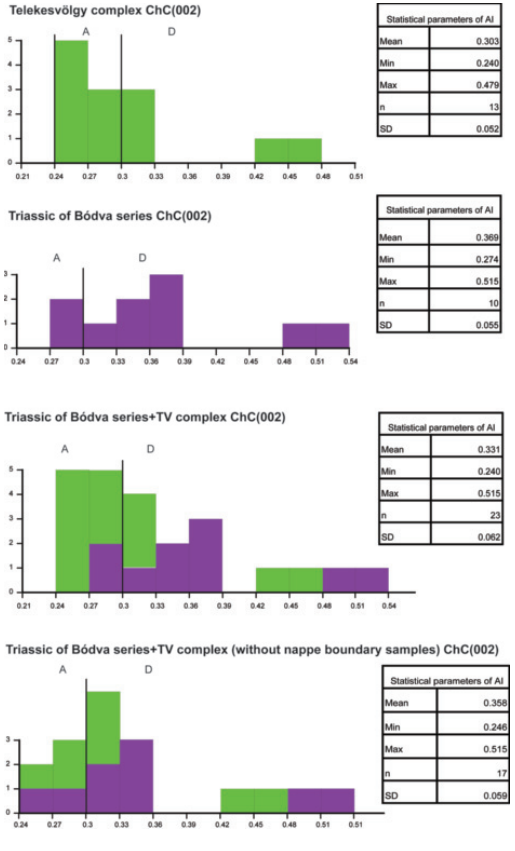

Figure 46. Statistical parameters and distribution diagrams of the measured chlorite Árkai indices from TV complex and Bódva series. A: low-temperature anchizone, D: diagenetic zone.

The areal distribution of the samples from TV complex and the Triassic of Bódva series (Appendix Table 4, Fig. 44, 45, 46) shows that the KI values and the chlorite "crystallinity" indices are significantly modified in the vicinity of major tectonic boundaries (boreholes Szet-4, P-74, Rb-658, Sza-4); this may indicate late alteration of these rocks. These tectonic zones could concentrate low-temperature fluid movements during or just after late-stage nappe emplacement (for details, see chapter 8). If the samples which were taken from the vicinity of nappe boundaries were removed from the sample group, the distribution diagrams of the KI values change significantly (Fig. 45). The peak of the diagram is in the field of diagenetic alteration (with an average of 0.464 ±0.057 Δ°2Θ), and only a few samples show low-temperature anchizonal values. The KI values vary from N to S within the samples, showing a little bit lower values in the southern, and higher in the northern part of the series. On basis of these data, both the TV complex and the Triassic of Bódva series correspond to the medium to deep diagenetic stages, so the palaeo-temperatures reached maximum ca. 200 to 250°C (Árkai 1991, Árkai et al. 1995a, Frey 1987, Kisch 1983, Merriman & Frey 1999).

6.4.4. Torna series

Samples from different structural positions e.g. Bódvarákó window, Esztramos Hill, Hidvégardó and 2 localities of the Martonyi nappe were investigated. There is no significant distribution of the KI values among the samples taken from different locations or structural position (Fig. 47). KI values (Appendix Table 4, Fig. 47) mainly fall into the epizone, partly to the high-temperature part of the anchizone (KI=0.25–0.30 Δ°2Θ) giving an average of 0.266±0.051 (SD) Δ°2Θ. Only some samples show low-tem-

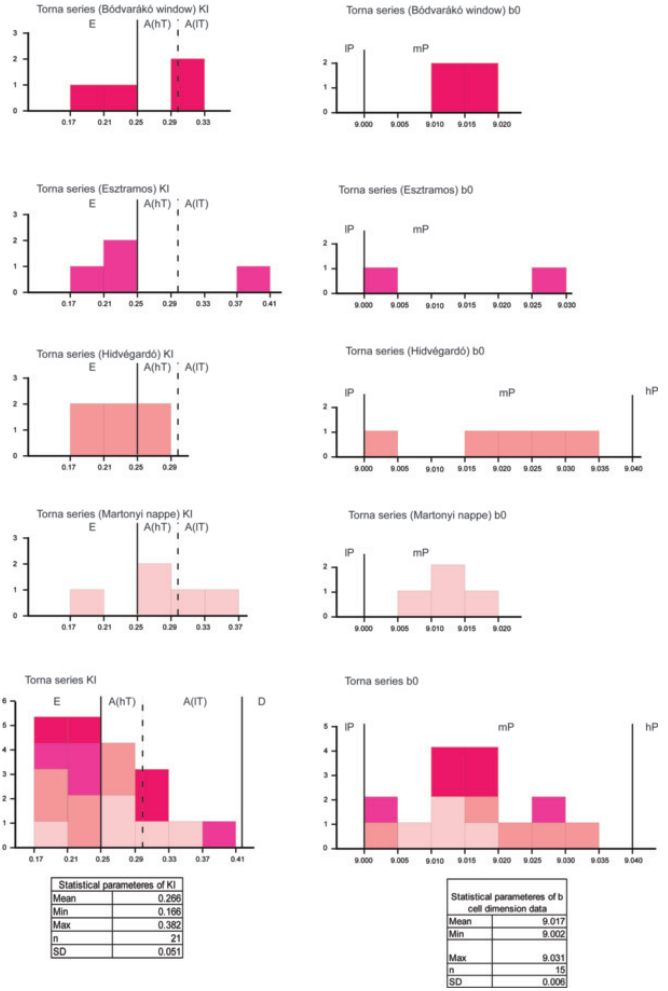

Statistical parameteres of KI	
Mean	0.266
Min	0.166
Max	0.362
n	21
SD	0.051

Statistical parameteres of b cell dimension data	
Mean	9.017
Min	9.002
Max	9.031
n	15
SD	0.006

Figure 47. Statistical parameters and distribution diagrams of the measured K-white mica b cell dimension data from the different tectonic units of the Torna series (new measurements + unpublished data of Árkai (1981, 1985). E: epizone, A(hT): (high-temperature) anchizone, A(lT): (low-temperature) anchizone, D: diagenetic zone, lP: low-pressure zone, mP: medium-pressure zone, hP: high-pressure zone.

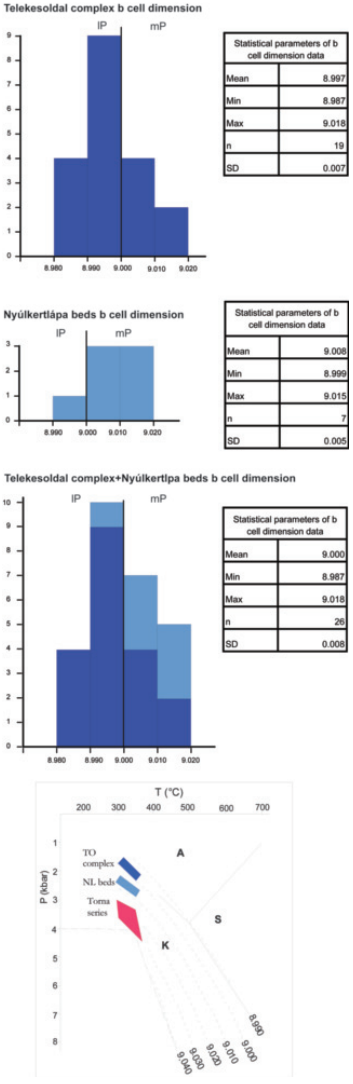

Figure 48. Statistical parameters and distribution diagrams of the measured Kübler indices and K-white mica b cell dimension data from TO complex NL beds and Torna series (new measurements + unpublished data of Árkai (1981, 1985). lP: low-pressure zone, mP: medium-pressure zone, hP: high-pressure zone. Bottom: The estimated temperature and pressure conditions for the metamorphism of TO complex and NL beds (diagram of Paddan et al. 1982)

preture anchizonal alteration. The measured values a little bit higher in average then those of the TO complex. But they are still at the upper boundary of anchi- and epizones, referring to 300–350°C. There is no possibility to make more precise T estimation with this method.

6.5. Pressure estimations: K-white mica b cell dimension data

K-white mica b cell dimension measurements were carried out on samples from the Torna series, from the Jurassic TO complex and the NL beds in order to characterize the pressure conditions of the very low- to low-grade metamorphosed rocks.

Samples taken from the Torna series are situated in the medium-pressure zone giving an average of 9.017±0.006 Å (Fig. 47). Some samples are even close to the lower boundary towards the high-pressure zone. Accepting the temperature estimates of ~300–350°C for the Torna series (KI data) minimal pressure of 3–4.5 kbar can be estimated on basis of Guidotti & Sassi (1986) (Fig. 48).

The data from the TO complex and the NL beds were measured on paragonite-free whole rock samples that were characterized by appropriate mineral composition described by Guidotti & Sassi (1976, 1986), Guidotti et al. (1989). The measured data and the statistical parameters of b cell dimension values are listed on Appendix Table 5 and also displayed on Fig. 48. The samples of the TO complex – measured partly by Árkai in 1985 – fall into the transition zone of low- and medium-pressure zones (9Å), giving an average of 8.997±0.007 Å (Fig. 48). The NL beds of the Bódvarákó window show scattered b cell dimension data, ranging from the uppermost part of low-pressure zone to the medium pressure zone. The average of the measured values is 9.008±0.005 Å. Based on the findings of Padan et al. (1982), Fig. 48 (bottom) shows the linear extrapolation of isolines of b0 values given by Guidotti & Sassi (1986) for the p–T field of greenschist facies towards the anchizone (subgreenschist facies). Accepting the temperature estimates of ~300–350°C for the TO complex and NL beds deduced from the illite Kübler-index, chlorite „crystallinity" and vitrinite reflectance data, the following approximate minimal pressures can be estimated: TO complex: ~1.5-2.5 kbar, NL beds ~2.5-3 kbar. This represents significantly lower b0 values than the Torna series (Fig. 48).

6.6. Geochronology

To constrain the timing of very low to low-grade metamorphism K-Ar age data were measured on <2μm grain size fractions from 10 samples on which metamorphic petrological samples investigations had been carried out (Fig. 44, 49). Interpretation of K-Ar ages measured on illite–K-white mica rich separates is a difficult task, since illite–K-white mica can be formed below and also above the closure temperature of K-Ar system, which is estimated as 260 ± 30ºC for the <2 μm grain size fraction of illite (Hunziker 1987). Because the estimated temperature range of metamorphism in the TO complex exceeds the closure temperature, the interpretation of the K-Ar data is either formation ages of illite or marks the time of cooling below the closure temperature. However, the formation of white micas can be a very long lasting process, which can be strongly influenced by the chemical composition of fluids present in the rock (Robertson & Lahann 1981). Moreover, isotopically non-equilibrated detrital micas can be present in metasedimentary rocks, which complicate the interpretation. During the age interpratations all these complications were tried to take into account.

The mineral parameters (Fig. 49) for samples Sza-12 (50.3 m) and Sza-10 (74.0 m) are very similar and their K-Ar ages also agree (**125.8±4.8 and 127.9±5 Ma**). The previously measured 120 ± 6 Ma K-Ar feldspar age of biotite-free rhyolite from Sza-10 (56.7 m) (Árva-Sós et al 1987) shows good correlation with the newly measured K-Ar ages obtained on illite–K-white mica rich separates from closely located sample. Age data achieved from 21.3 m sample of Rudabánya Rb-661 is a little bit older (**136.6±5.2 Ma**) but locates in the same age group within error range.

Younger ages of **91.1±3.7 Ma, 90.5±3.6 and 108.6±4.1 Ma** were measured in the Sza-7, Sza- 10 boreholes and T-26 outcrop. They can be interpreted as the results of another low temperature event, which reopened the K-Ar system by circulating fluids, since temperature difference between the two samples of Sza-10 borehole with different ages is very unlikely. The concept of closure temperature can be usually applied when Ar release is only governed by the temperature. But the system may be released again above closure temperature by several processes, e. g. when circulating hot fluids induce the change of mineral structure.

K-Ar ages from the **TV** (149 ± 6 Ma, 125.2±5.6) are most probably mixed ages, resulted by the contribution of detrital K-white mica in the separated <2 μm size fraction samples, which was dis-

Structural unit	Sample number	Depth/locality	KI (Δ °2Θ)	ChC(002) (Δ °2Θ)	K %	40Ar(rad) 10^{-5} cm^3 STP/g	40Ar(rad)%	<2 μm size fraction, K/Ar age in Ma (±1σ)
Telekesoldal complex	Rb 661/1	21.3 m	0,251	0,222	2.410	1.330	81,3	136.6±5.2
	Sza-12	50.3 m	0,269	0,235	4,506	2,322	69,1	127.9±5
	Sza-10	74.0 m	0,288	0,234	4,564	2,311	81,8	125.8±4.8
	Sza-10	*56.7 m*			*1.99*	*0.956*	*66.0*	*120±6*
	Sza-12	71 m	0,246	0,235	4,105	1,923	82,4	116.7±4.5
	Sza-7	50.3-51.0 m	0,278	0,276	3,182	1,155	57.0	91.1±3.7
	Sza-10	91.4 m	0,275	0,232	3,476	1,254	66,5	90.5±3.6
NL beds	T-26	Esztramos	0,211	0,265	5.410	2,354	87,5	108.6±4.1
TV complex	Va-2/1-Tk	71.0 m	0,454	0,315	3.220	1,623	44,2	125.2±5.6
	Szet-4	78 m	0,397	0,240	4,177	2,515	79,4	148.6±5.7

Figure 49. The measured K-Ar ages for the TO complex, NL beds and TV complex. Grey italics indicate the samples measured by Árva-Sós et al (1987). For locations of the boreholes see Fig. 44, Appendix 1-3.

turbed (or partly reset) during a later, low-temperature event. The presence of swelling clay mineral phases in the <2 μm grain size fraction of these samples also agrees with the possibility of a late low-temperature alteration. In these samples detrital K-white mica flakes are also recognized by petrographical microscopy. The age of 149 ± 6 Ma is not much younger than the sedimentation age and can hardly be connected to metamorphism.

In conclusion, the obtained data do not provide information only about the age of the metamorphic event, but also about some later, fluid migration-related event. So the next ages can be interpreted as the very-low to low-grade metamorphism of the **Telekesoldal complex: 125.8±4.8 Ma, 127.9±5.0 Ma, 136.6±5.2 Ma** (Fig. 44, 49). The pre-existing 120 ± 6 Ma feldspar data and the new 116.7±4.5 Ma (Sza-12) can be interpreted in two ways. It can be still the reflection of the metamorphic event or may reflect partial resetting of the K/Ar system due to the later, hot-fluid related event.

Ages **91.1±3.7 Ma and 90.5±3.6 Ma** mark late alteration due to fluid migration, which can be connected to a late-stage overthrusting event. Newly obtained temperature values from these nappe contacts highly support this suggestion (see chapter 8).

The 108.6±4.1 Ma data from the Nyúlkertlápa beds may indicate post-metamorphic fluid migration during nappe emplacement, too. It may reflect only partial reset of the metamorphic age, or a structurally meaningful age between low-grade metamorphism and late-stage overthrusting, e.g. an older nappe contact. This latter suggestion is in good correlation with the structural interpretation of D1 phase contact between the Nyúlkertlápa beds and the Bódvarákó series (Chapter 7.1).

The oldest datum from the TV is very likely a mixed age from detrital source and later partial reopening of the K/ar system, while the diagenetic or low-temperature anchimetamorphic conditions (with max. temperatures of ca. 200–250 °C) were most probably not sufficient to reset the K-Ar system.

7. Structural observations

7.1. D1 deformation phase

7.1.1. F1 foliation of the Telekesoldal complex and related series

6 locality groups of the Telekesoldal nappe were studied in details to reconstruct the deformation history of the Jurassic sequence. The best outcrops were in the Mély Valley (Perk-164-166) and the roadcut keysection of the Perkupa-Szalonna road on the northern slope of Nagy Telekes Hill (Perk-167-171, Perk-057). Valuable data were measured along a forest road on the southeastern slope of Nagy-Telekes Hill (Perk-158-161) on the way to the Mély Valley. Outcrops in the Telekes Valley (Perk-186-187 and Perk-192) also revealed a complex deformation history. The secondary contact zone of the Telekesoldal complex and the Bódva series was investigated on the southern slope of Dunnatető Hill (P-22, BP-FL-02-13). For detailed microstructural investigations oriented samples were collected from the outcrop-scale structural domains displaying different intensity of deformation. Oriented thin sections were prepared from rock slabs cut parallel to the X-Z fabric plane.

At outcrop-scale a closely-spaced (millimetre-scale), penetrative foliation (S1) is the most characteristic structural feature of the Telekesoldal complex. This foliation is equally present in the slate, siltstone, sandstone and olistostrome horizons. However, the development and spacing of the foliation varies depending on the lithology and the structural position of the sample. This schistosity was already identified by Grill & Kozur (1986), Grill (1988, 1989) and Seres-Hartai (1980).

In map view, the general moderate NW (in average: 320/40) dipping of the S_1 foliation can locally change into steep, almost vertical position, or alternate with steep, SE dipping segments (Dunnatető Hill, Szalonna-Perkupa roadcut section), indicating later (D4, D5) folding phases. The intensity of the foliation varies with different lithologies. The closely-spaced (millimetre-scale), penetrative foliation is well developed in the slate. The foliation planes are rich in flakes of white mica. When the sample contains a considerable amount of carbonate or being silicified the foliation is less developed. In some samples, especially in thin sections the original sedimentary alteration of marl, siltstone and shale is visible (Fig. 19.2). The bedding or sedimentary lamination is parallel with the well developed foliation, thus this schistosity refers to S_{0-1}.

The previously described sandstone (Chapter 5.3) within the shale can be present as individual layers or lens-shaped bodies. These bodies were interpreted to be individual olistoliths in a shaley matrix (Grill 1988). However, in some surface outcrops (Telekes Valley, Perk-186-187) these lens-shaped sandstone bodies are situated along foliation planes, and segmented by extensional fabrics; thus they could represent boudins and not sedimentary olistoliths (Fig. 50).

The fabric of the olistostrome is also characterized by layer-perpendicular flattening (Fig. 51.1-3). In the grain-supported olistostromes stylolitic contact and oriented position of the clasts are also well visible (Fig. 51.2-4). In case of the matrix-supported type foliation planes are well recognisable in the matrix and these anastomosing surfaces wrap the flattened clasts (Fig. 51.5-6).

In microscopic view all samples from the slate display a well developed, domainal spaced foliation (Fig. 51.6). This F1 foliation is defined by the alternation of slightly anastomosing lenses of relatively intact shale and pressure solution seams - rich in opaque solution residual material (Fig. 51.6). The contact between the

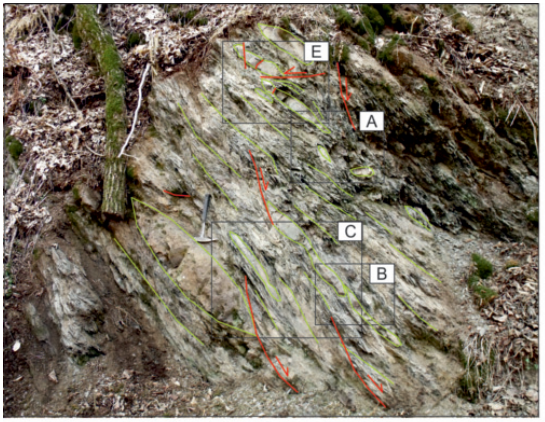

Figure 50. Lens-shaped sandstone bodies along S0-1 foliation planes (light green) in the Telekesoldal complex in Telekes Valley (Perk-187). They are segmented by D5b extensional fabrics (red); thus they could represent boudins. White coin is 2cm in diameter.

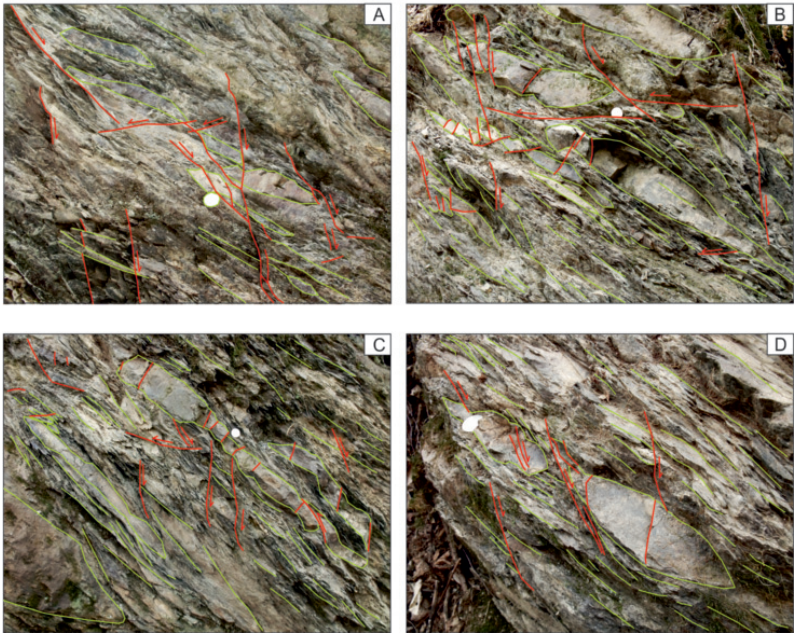

Figure 51. S0-1 foliation of the Telekesoldal complex. 1) extremly flattened clasts of the grain-supported olistostrome in outcrop Perk-166 on Nagy-Telekes Hill. Note the outsized clast. 2) Anastomosing foliation caused by the mm to cm sized clasts of the micro-olistostrome of outcrop P-22 on the southern slope of Dunnatető Hill. 3) Anastomosing foliation caused by the cm sized carbonate clasts of the olistostrome of outcrop P-101 on the southern slope of Dunnatető Hill 4) pressure solution contact of the clasts in the olistostrome. Szalonna-Perkupa roadcut keysection. Note the quartz grain squeezed into the carbonate clast. 5) Lithoclast within slate matrix. At the rim of the clast dark seams consist of insoluable material concentrated during dissolution are visible . 6) Domainal spaced foliation in coarse grained turbiditic layers (with crinoid fragment) of Rudabánya Rb-661. Pressure solution seams separate the more intact domains. 7) Indicator of the strong layer-perpendicular shortening by means of the originally subrounded bioclast (radiolarians, r) and flattened bioturbation traces radiolarias from core Rudabánya Rb-661 8) Signs of intracrystalline deformation: undulose extinction of the quartz grains, subgrain boundaries separate the neighbouring crystal fragments. Nagy-Telekes Hill.


1
Perk-166
5 cm

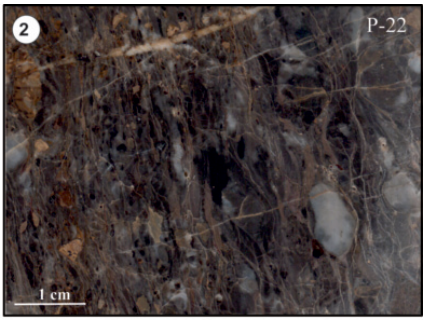
2
P-22
1 cm

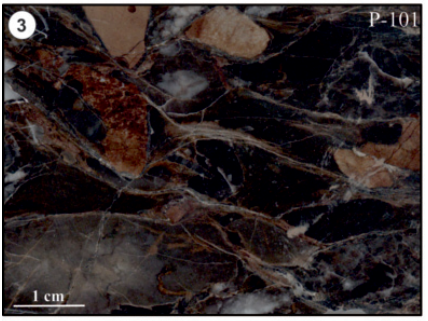
3
P-101
1 cm

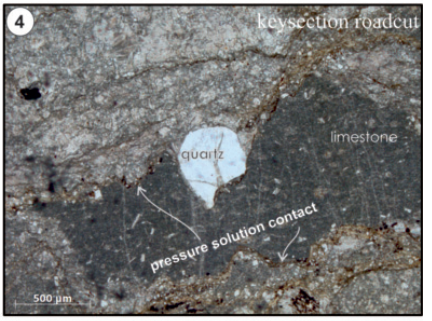
4
keysection roadcut
quartz
limestone
pressure solution contact
500 µm

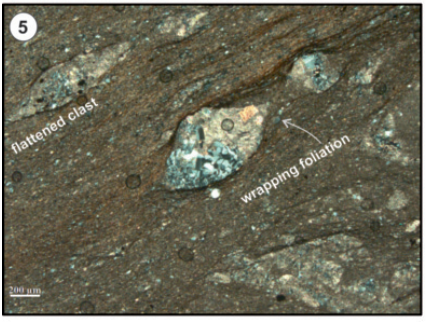
5
flattened clast
wrapping foliation
200 µm

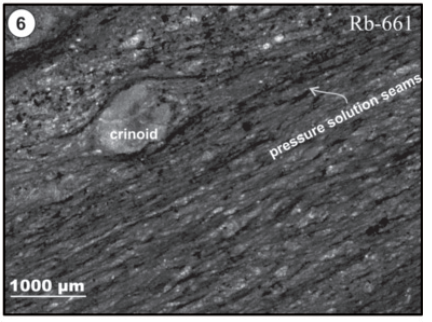
6
Rb-661
crinoid
pressure solution seams
1000 µm

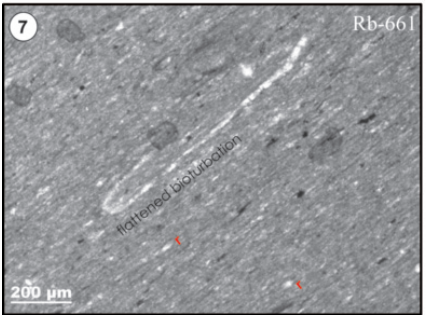
7
Rb-661
flattened bioturbation
200 µm

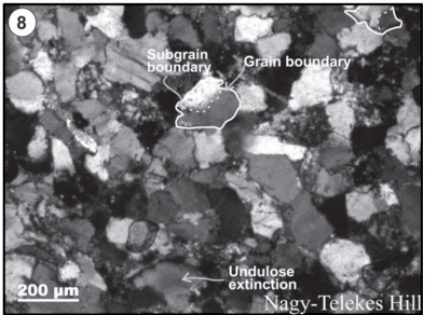
8
Subgrain boundary
Grain boundary
Undulose extinction
200 µm
Nagy-Telekes Hill

shaley matrix and the occasionally present clasts are usually pressure solution surfaces, too (Fig. 51.5-6). In the slate bedding-parallel nature of foliation can sometimes be demonstrated by sandstone and siltsone intercalations (Fig. 19.2). The layer-perpendicular shortening is clearly visible when originally subrounded bioclasts (e.g. radiolarians) are present (Fig. 51.7). In spite of the later deformation the original sedimentary texture can be recognized in some cases. For example in core Rudabánya Rb-661 the original radiolarian wackestone texture is recognizable, but calcite moulds are more or less deformed, the globular moulds became lens shaped, and the bioturbation patches also got flattened (Fig. 51.7).

An equivalent, closely-spaced foliation can be observed in the Zsarnó (Žarnov) Žam-1 borehole in Slovakia, where dark grey to black slate and marl alternates with silt and fine-grained sandstone. The slate has a penetrative foliation, which is parallel with the original sedimentary alteration. This S0-1 foliation is subvertical.

The sandstone layers consist predominantly of quartz, but the amount of feldspars (plagioclases) is usually significant and K-white mica also occurs in varying quantity. Some evidences for intracrystalline deformation are present. Undulate extinction of the quartz grains is common. In some grains the recovery has achieved the last phase: subgrain boundaries separate the neighbour crystal fragments, which are slightly disoriented with respect to each other (Fig. 51.8).

No macroscopic or microscopic folding was observed to be associated with S_{0-1} foliation. In all units, S_{0-1} foliation represents the only structural feature of D_1 deformation phase.

7.1.2 Contact of the Telekesoldal complex and the Torna series

The previously described penetrative bedding-parallel foliation is present in the rocks of the Torna (Turna) series, too (Fodor & Koroknai 2000). F2 tight folds and F3 kink-like folds bending the S0-1 foliation were also described from the Martonyi nappe (Fodor & Koroknai 2000). Very similar, F2 ductile folds and F3 kink-folds were observed in the outcrops and thin sections of the Telekesoldal nappe (see next chapters). As the result of the metamorphic petrologic studies (Árkai & Kovács 1986, chapter 6.4) both nappes turned to be metamorphosed under 300–350°C, although Torna series significantly have lower IC values (Fig. 43, 47, 48). The main difference in their metamorphism is the pressure values. The b0 values suggest transitional medium/high pressure conditions (3-4.5 kbar) for the Torna series, while a lower, 1.5-3 kbar for the Telekesoldal nappe (Fig. 47, 48, 52).

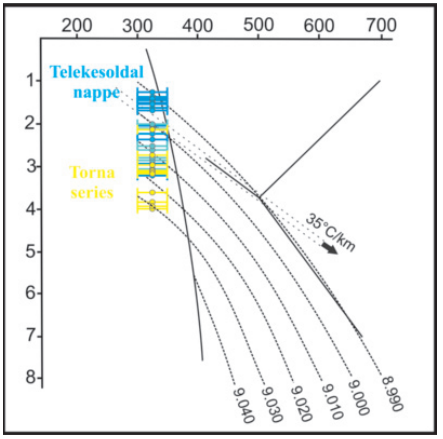

Figure 52. p-T datapairs from the TO nappe and the Torna series. Note the continuous transition from TO (lower) to Torna (higher) pressure values.

Because of their very similar early deformational history (D1-D3) and metamorphic degree, I suppose, that their tectonic contact is a very early, pre-metamorphic nappe contact. S0-1 foliation was most probably formed due to deep tectonic burial, which was caused by overthrusting of higher nappes. In this early D1 phase the Telekesoldal nappe (with other, higher nappes) thrust over the Torna series. It means that during the metamorphism the Telekesoldal

nappe was at higher crustal level than the Torna series. Higher pressure values of the Torna series strengthen this hypothesis. Since the D1 deformational phase these two structural units were connected and participated in the younger events together (see chapter 7.2-7.6).

The result of this new concept can be applied in the Bódvarákó window and in a small, but structurally important outcrop in the Telekesvalley Tributary Valley 8 (Appendix 3). In the first case anchi- to epimetamorphic (Chapter 6.4.4., Fig. 43, 47) Bódvarákó series occurs in two tectonic windows (Fig. 44, Appendix 1). The windows contain Gutenstein Dolomite and black, cherty limestone (Bódvarákó Formation). Its age is middle Anisian-upper Ladinian (Kovács et al., 1989). This deep water limestone is overlain by the Nyúltkertlápa beds, which is considered to be part of the Telekesoldal series (Chapter 5.3). These rocks also suffered high temperature anchizonal metamorphism (Chapter 6.4.4., Fig. 43, 47, 48). The contact of the two structural units is suggested to be an early, pre-metamorpic nappe contact.

In the outcrop of the Telekes Valley tributary valley 8 (Appendix 3) topographically above the steeply dipping marl of the TV complex well foliated limestone crops out. It is a light grey limestone with well developed penetrative foliation. The foliation of the limestone is almost perpendicular to the bedding of the TV marl. Above the limestone the Telekesoldal nappe is the next structural unit. There are two reasonable interpretations for this setting. The limestone body can represent olistolith(s) within the TO series (similar to those cropping out elsewhere in the complex), so the TO nappe juxtaposes the TV complex as usually (see D4 phase). The other option is demonstrated on the geological map (Appendix 3), interpreting this well-foliated limestone body as the remnant of the Torna series on the base of the TO nappe. In this case the upper contact of this tectonic slice towards the TO nappe is a D1 contact, while the lower one towards the TV series is a later, D4.

7.2. F2 tight folds, S2 inicipient foliation in the Telekesoldal nappe

In the outcrops of the Mély Valley and in boreholes Rudabánya Rb-661, Szalonna Sza-7 and -12 small scale, relatively close folds are present (Fig. 53, 54). They bend the S0-1 foliation planes, thus they represent a later, D2 folding event with F2 folds. The geometry of these F2 folds are few mm to few cm-scale close to tight folds. Their hinges are rounded and the limbs are straight (Fig. 53, 54). Most of the F2 folds are similar folds with thickened hinges (Fig. 53, 54). The limbs can be extremely thinned, sometimes the hinges are completely sheard off from their limbs, forming routless folds (Fig. 53.3, 5, 6).

Similar folds bending the subvertical S0-1 foliation were developed in the slate of Zsarnó (Žarnov) Žam-1 borehole (Fig. 38). The slate contains several generations of calcite veins. Part of them crosscuts the S0-1 foliation planes, but others are folded. At 202.8 m a few cm-sized tight fold is visible (Fig. 53.6). The fold has rounded, thickened hinge. It bends the S0-1 folitaion, thus locally it is an F2 fold.

Inicipient, or in infrequent cases more developed axial plane cleavage is visible (Fig. 53.3, 4, 5, 8, 54.2). The fold-related S_2 foliation is spaced, and defined by anastomosing opaque and clay-mineral-rich planes. Micro-scale transposition of the S0-1 surfaces along the S2 folitaion planes is well visible in sample Szalonna Sza-12 37.5 m (Fig. 53.8). In some thin sections (Fig. 54.1) only two different foliations are present, intersecting each other at a small angle. The original sedimentary alternation of silty, sandy or marly layers defines the S0-1 foliation (Fig. 53.2, 7-8, 54.1). The crosscutting foliation is the S_2 one (Fig. 53.7-8, 54.1).

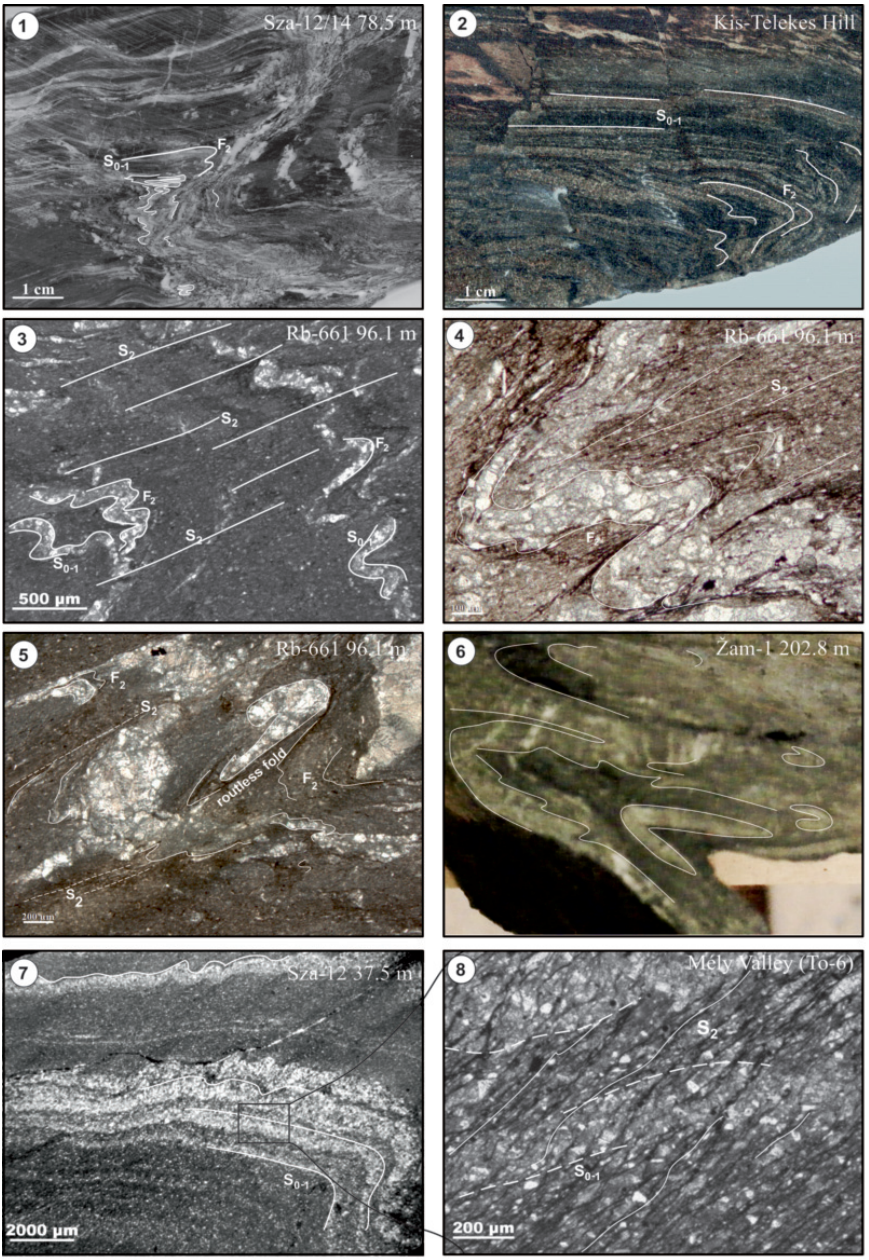

Figure 53. S0-1 foliation of the TO series folded into close to tight F2 folds. Incipient S2 foliation is visible.

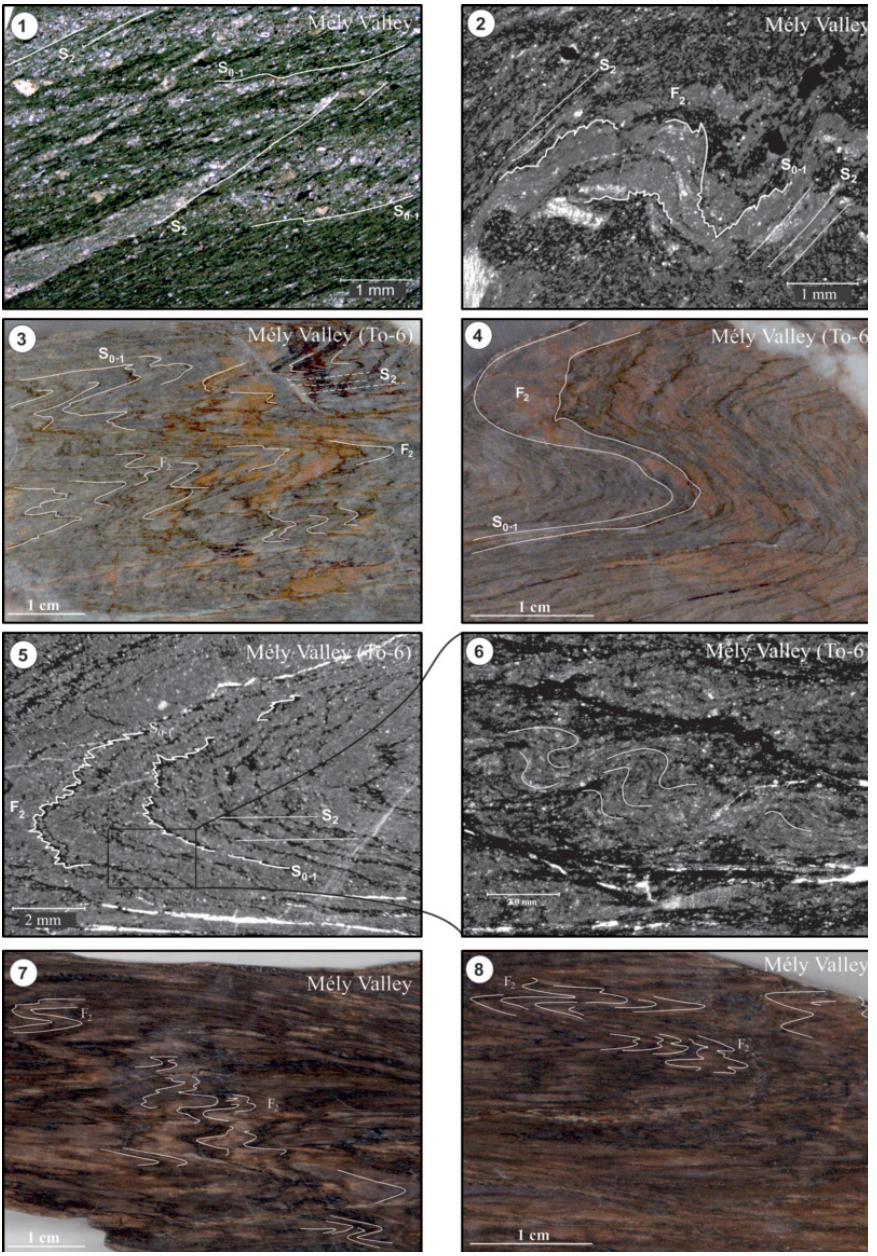

Figure 54. S0-1 foliation of the TO series folded into close to tight F2 folds. Incipient S2 foliation is visible.

7.3. F3 kink folds in the Telekesoldal nappe

Locally, the penetrative foliation is slightly folded into small-scale (maximum dm), open to close, usually kink-like F3 folds with ca. NW-SE trending fold axes (Fig. 57). These folds are the best developed in the Mély Valley (Perk-164-166) (Fig. 55, 56.2, 4) and in cores Rudabánya Rb-661 (19.5 m, Fig. 56.6), Szalonna Sza-7 (15 m) and -12 (37.5 m, 49.3 m, 71.0 m Fig. 56.1, 3, 7). These kink folds have linear limbs and angular hinges. Tension joints syndeformationally filled with calcite are frequent in the hinge zone (Fig. 56.2, 4, 6), while the S0-1 foliation planes worked as sliding surfaces. In sample Szal-14 (Fig. 56.4) from the Telekes Valley joint drags with triangular calcite filled spaces arising from rotation of the kinked sector are well visible. The kink axes dip gently to the NW or SE indicating NE-SW compression (Fig. 57).

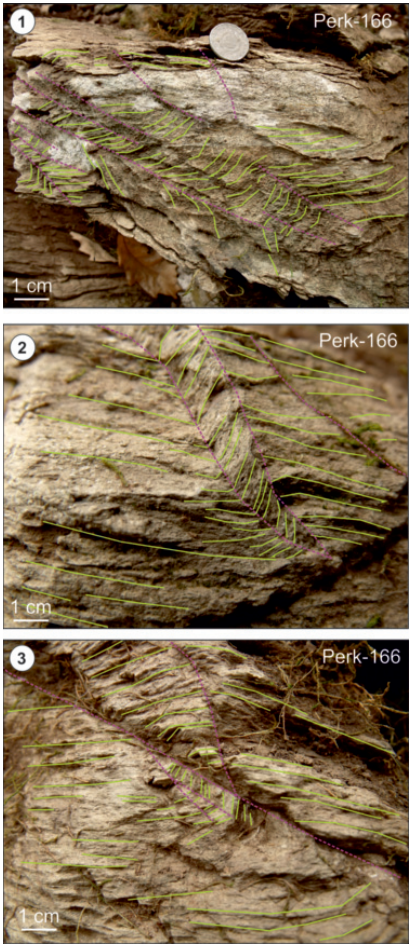

Figure 55. F3 kink-type folds in the shale of TO complex from the Mély Valley (Perk-166). S0-1 folitaion planes (light green) are bended by the kink-bands (purple).

The kink-type F3 folds are also present in the BOSZ-001outcrop of the **Akasztó unit** (Fig. 58). In this locality the penetrative S0-1 foliation was often bent by several dm-scale folds. These F3 folds are open to close folds with linear limbs and angular hinges (Fig. 58). Thrust connected fold-propagation-folds are also present (Fig. 58). In present-day position they indicate top-to-NW normal movement. In present-day position the axial planes are subhorizontal, referring to subvertical compression. The S0-1 planes are also in subvertical position, dipping to SE and NW. The fold axes plunge moderatelly to NE (Fig. 57). Field observations (e.g. subvertical axial planes, steeply dipping of the S0-1 folitation) referred to pre-tilt position of these small-scale kink-folds. To obtain the presumably original position of the folds, tilt tests were carried out. On Figure 57 all the structural elements on these stereograms are tilted back to their original position. This pre-folding position makes much more sense from a structural point of view. The majority of the fold axes became subhorizontal, dipping moderately to the NW or to the SE. They indicate NE-SW compression. Measured thrust planes and fold-propagation-folds in this backtilted position also refer to NE-SW compressional stress field.

These F_3 kink-like folds bend the S_{0-1} foliation, giving a good reason to connect them with a younger event. The superposition of D_2 and D_3 events cannot be analysed directly, because no sample has been found with the fabrics of both deformation phases. However, the two phases have

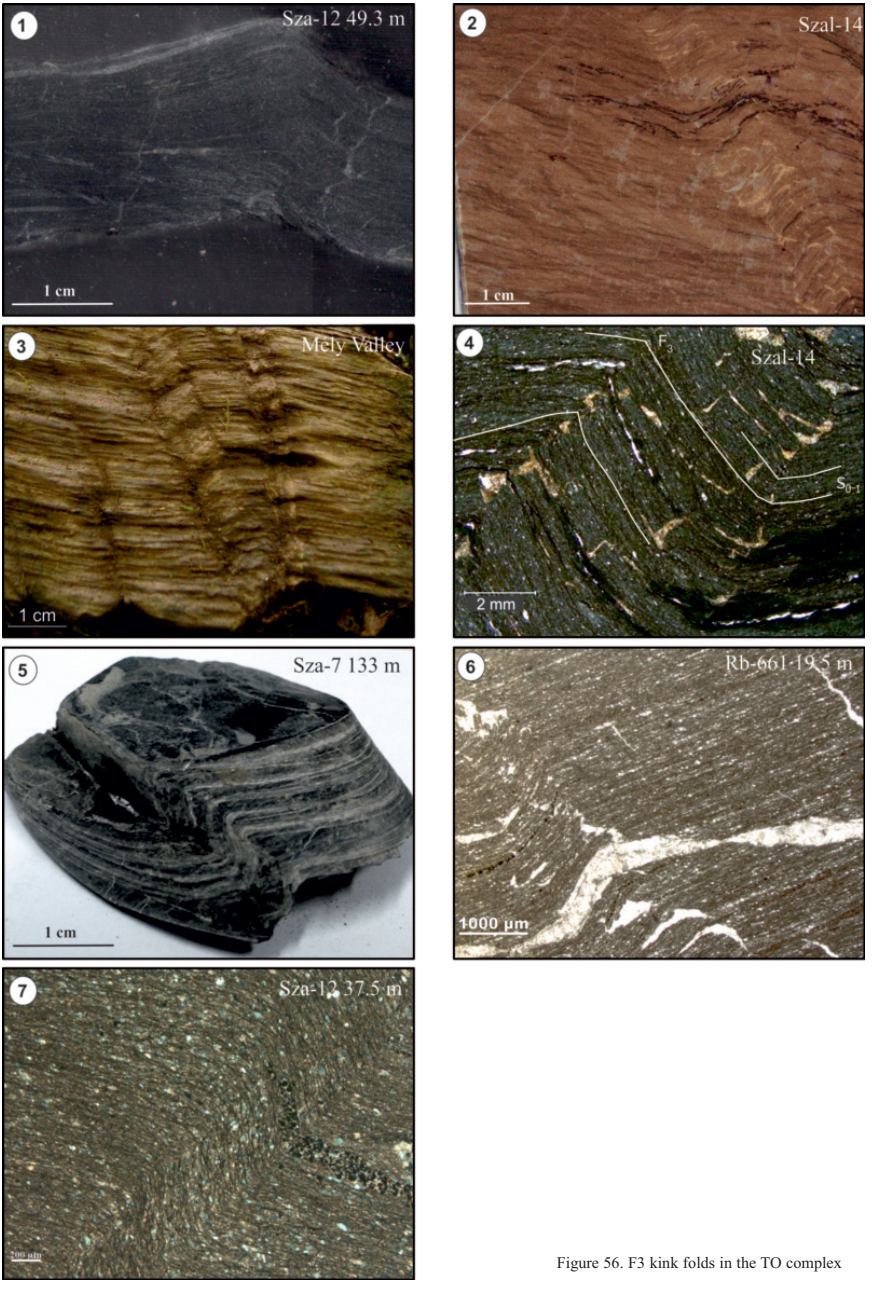

Figure 56. F3 kink folds in the TO complex

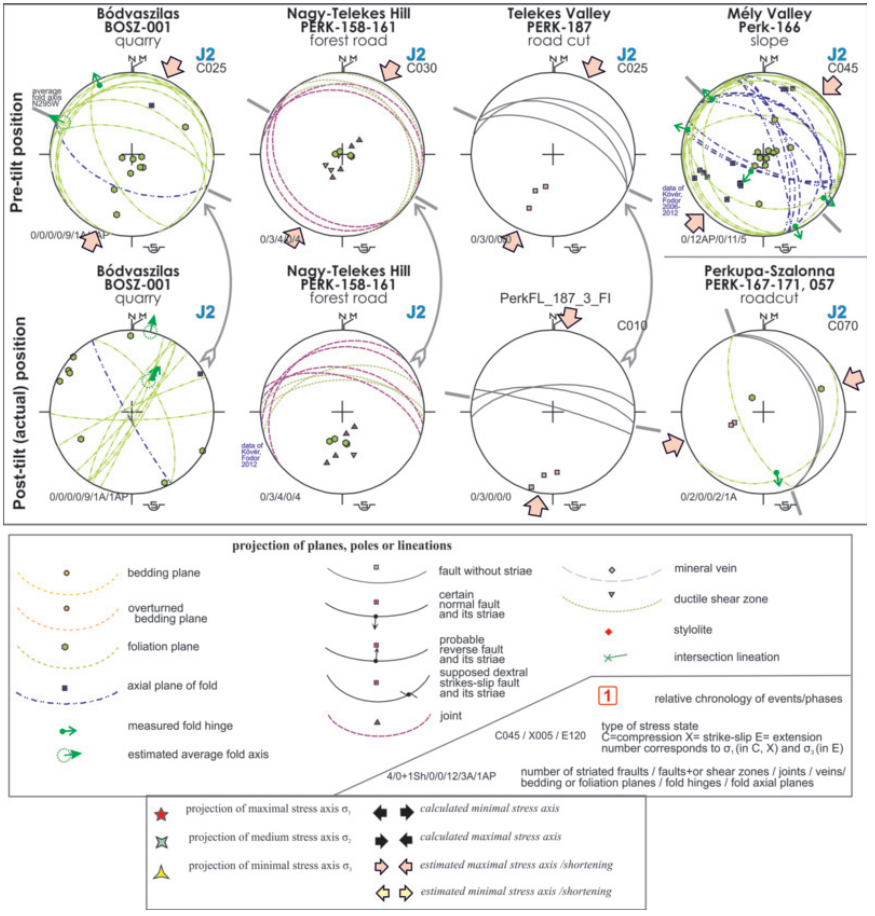

Figure 57 . Summarized stereograms of the D3 tectonic phase containing NW-SE trending F3 fold axes, NE and SW-verging thrusts. NE-SW compression. Tilt test is shown for three data sets with original (pre-tilt) and recent (post-tilt) position.

been separated, because the close to tight style of F_2 folds with ductile deformation indicates development under higher temperature and pressure conditions, while kink folds have joints or calcite-filled veins in the axial planes. They indicate deformation at least partly under brittle conditions.

Figure 58. a) map view drawing of the BOSZ-001 outcrop on the Akasztó Hill, near Bódvaszilas village. 10 cm-scale kink-folds bend the S0-1 foliation. Note the very steep axial planes and axes. b) F3 folds in Jurassic marl. Pre-tilt position of the kinks can be observed. It is demonstrated via pre- and post-tilt stereograms. Post-tilt normal fault was also observed.

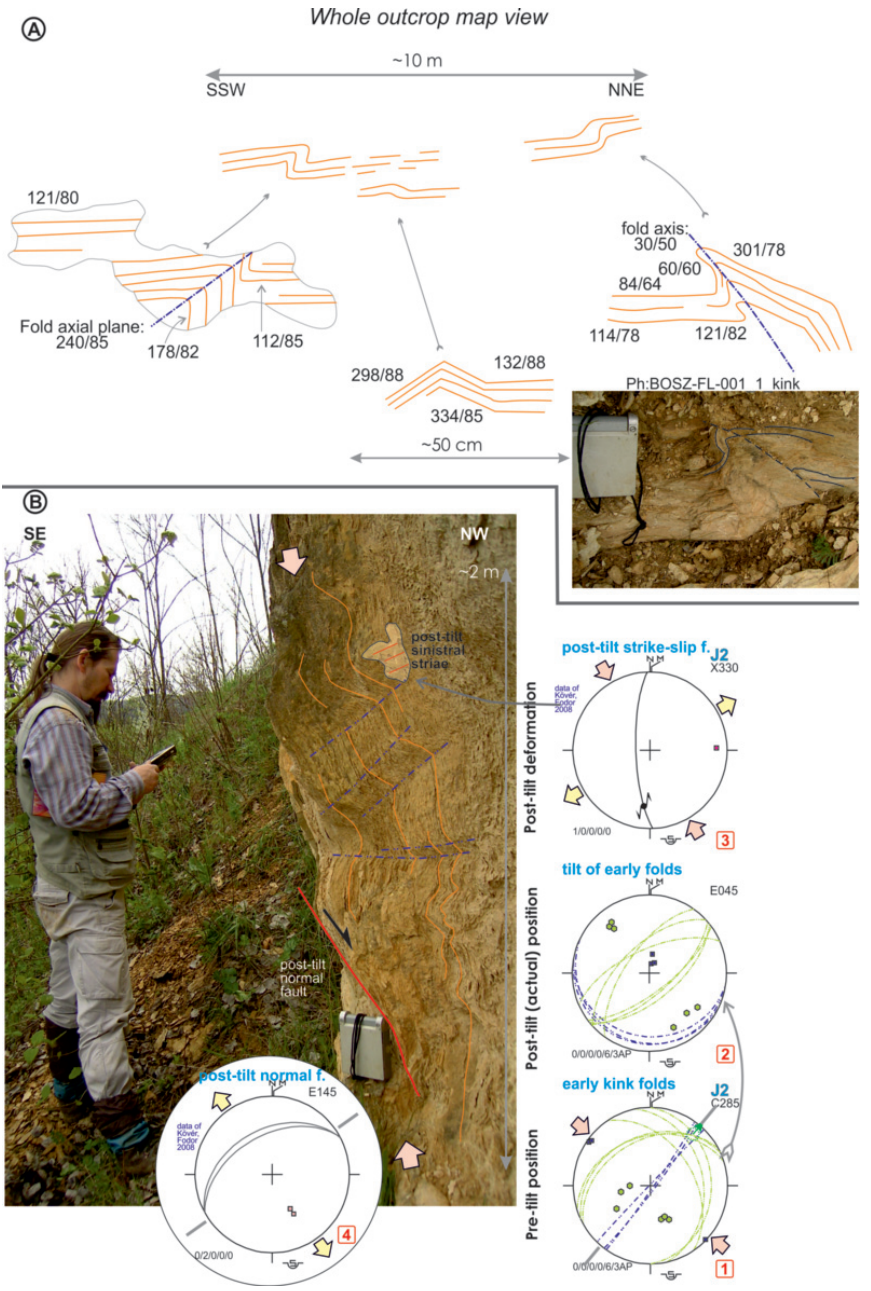
A
Whole outcrop map view
~10 m
SSW
NNE
121/80
Fold axial plane:
240/85
178/82
112/85
fold axis:
30/50
60/60
84/64
301/78
114/78
121/82
298/88
132/88
334/85
~50 cm
Ph:BOSZ-FL-001_1_kink
B
SE
NW
~2 m
post-tilt
sinistral
striae
post-tilt
normal
fault
post-tilt strike-slip f.
J2
X330
data of Kövér, Fodor 2008
1/0/0/0/0
3
Post-tilt deformation
tilt of early folds
E045
0/0/0/0/6/3AP
2
Post-tilt (actual) position
post-tilt normal f.
E145
data of Kövér, Fodor 2008
0/2/0/0/0
4
early kink folds
J2
C285
0/0/0/0/6/3AP
1
Pre-tilt position

7.4. D4 nappe stacking, NW-SE compression

The effects of the previous 3 deformational phases are recognisable only in the metamporphosed Torna series and the Telekesoldal nappe. However, all the investigated tectonic units were involved in the later events (Appendix 1-3). According to this observation the juxtaposition of the Aggtelek nappe, Telekesoldal nappe (locally Torna series on its base) and the Bódva series should have happened prior to or during D4 phase. In the next chapters I will follow these nappe contacts from top to bottom. Simple sketches aim to help understanding of structural relationships between the different tectonic units and age relationship of the contacts (59. ábra).

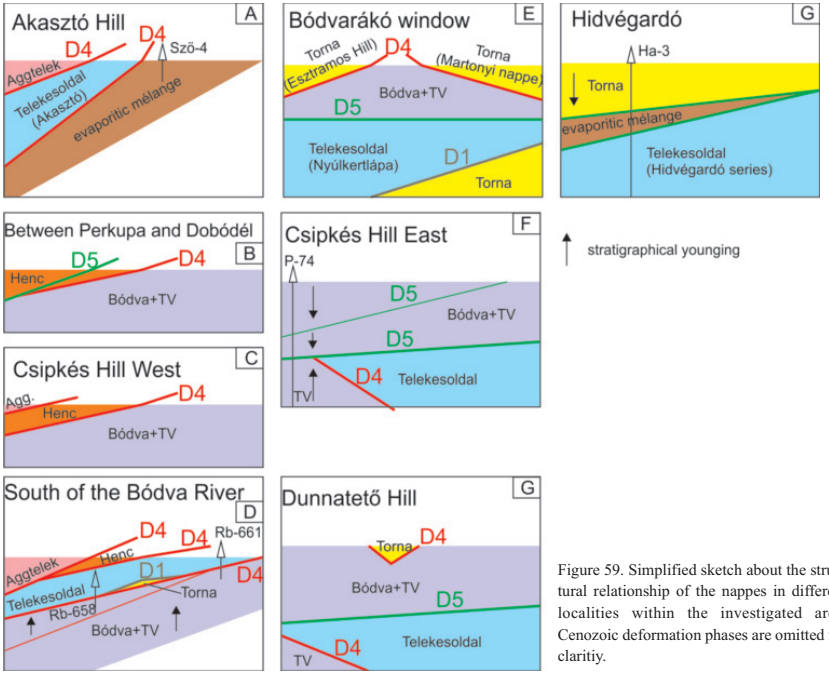

Figure 59. Simplified sketch about the structural relationship of the nappes in different localities within the investigated area. Cenozoic deformation phases are omitted for claritiy.

7.4.1. The base of the Aggelek nappe

The base of the Aggtelek nappe can be investigated in several points all along the eastern boundary of the Aggtelek Hills. It is a complex tectonic contact zone, with Aggtelek nappe in uppermost structural position, while the underlying unit varies along the roughly N-S striking contact zone (Appendix 1-3). In general, the Aggtelek nappe juxtaposes the Telekesoldal nappe (south of the Bódva river, Fig. 59d), or the equivalent Akasztó unit in the north (Fig. 59a), or with different scales or duplexes incorporated into the basal tectonic breccia (rauhwacke) in between the two main structural units (Fig. 59d). The thickness and lithological composition of these tectonic slices varies along the strike of the nappe boundary.

7.4.1.1. Henc Valley

The southern segment of the investigated tectonic contact is located along the road from Perkupa to Szőlősardó in the Henc Valley, and on the small range between the Telekes Valley and the Henc Valley (Appendix 3, Fig. 59d). The tectonic contact zone is characterized by tens to hundreds of meters of basal tectonic breccia, namely rauhwacke (Chapter 8). It contains relatively intact tectonic slices, few to hundreds of meters in size which are also in contact with the host rauhwacke or directly with the overlying or underlying nappes (Appendix 3, Fig. 60). These slices are usually built up by Lower Triassic Bódvaszilas Sandstone (PERK-172), Szin Marl (HB-105, -106) or most commonly Middle Triassic Gutenstein Dolomite (HB-99), or rarely Steinalm Limestone (PERK-173). A good example observed in site P172 (Fig. 61), where the red, mica and quartz rich sandstone of the Lower Triassic Bódvaszilas Fm is in direct tectonic contact with rauhwacke bodies. The recognizable intact rock types served as base for classification of the outcrops on earlier maps (Less et al. 1988), but their disrupted nature and incorporation to a wide belt of rauhwacke were not recognised. The rauhwacke lenses were usually classified into the Gutenstein Formation.

I suppose that a narrow evaporite belt occurs within the tectonic contact zone near the Henc valley jaws, extending from the Perkupa evaporite mining area (Fig. 60). Near the jaws of the Telekes Valley, a southward extension of the Telekesvölgy Formation can be supposed (Fig. 60).

These tectonic slices built up by different lithologies are sheared off from their original basement and younger cover during the nappe emplacement. The Early and early Middle Triassic succession is very similar, or equivalent in all the structural units of the

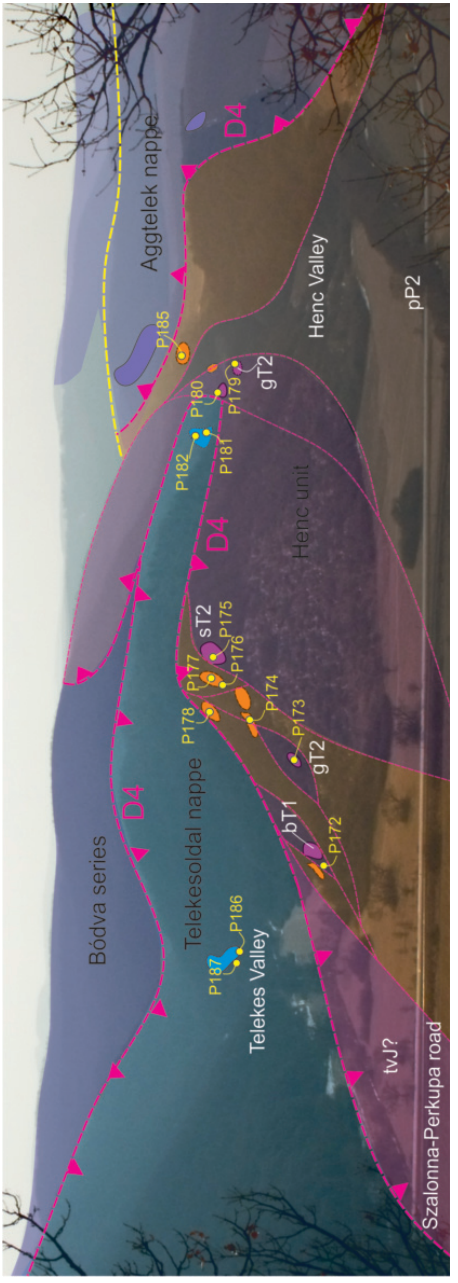

Figure 60. Panorama photo of the Nagy-Telekes Hill, Telekes Valley and Henc Valley from the Csipkés Hill (looking to the S). The structural units and the main investigated outcrops are approximately indicated.

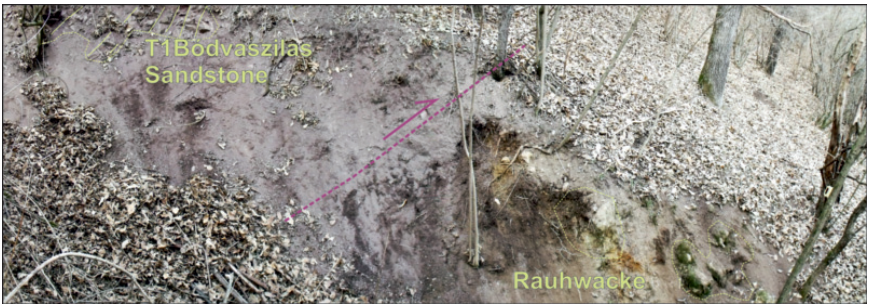

Figure 61. D4 contact of the Lower Triassic Bódvaszilas Sandstone of Henc unit and rauhwacke within the basal tectonic zone of the Aggtelek nappe.

Aggtelek-Rudabánya Hills (Kovács 1989, Fig. 4). Thus, the original paleogeographical position of these tectonic slices and thus the classification into paleogeographic units is uncertain. On basis of their present-day locality, the Henc unit name is used throughout the text for these Lower to Middle Triassic slices in between the Aggtelek nappe and Telekesoldal complex.

These tectonic slices of Henc unit along the Henc Valley (Appendix 2-3) show NE-SW elongated geometry. This refers to NW-SE compression similarly to the outcrop-scale measurements. So it is most probable, that the juxtaposition of the Henc unit and the underlying nappe (Telekesoldal) took place in this D4 tectonic phase.

7.4.1.2. Western side of the Csipkés Hill

These N to NE striking tectonic slices can be followed north from the Bódva River along the western side of the Rudabánya Hills. The main outcrops are on the western slope of Csipkés Hill (Appendix 2), in some abandoned quarries (PERK-007 between Perkupa and Dobódél villages, and along N-S striking forest roads (PERK-005, -006, -008) parallel with the road between Perkupa and Dobódél. In these locations the northward continuation of the tectonic contact zone can be followed with variable Lower to Upper Triassic tectonic slices in between the Aggtelek nappe in upper, and the Telekesvölgy complex or Bódva series in lower position (Appendix 2, Fig. 62). Toward Dobódél village this tectonic belt becomes narrower, containing thinner and smaller number of relatively intact tectonic slices, while the amount of rauhwacke is also reduced.

On the westernmost part of the contact zone Permian evaporite underlies the Aggtelek nappe. This evaporite was penetrated by several boreholes and was the target of mining activities for decades (Havas 1980). The continuation of this evaporite slice can be seen on Fig. 62.

The most complex part of the investigated area is the western slope of the Csipkés Hill and its continuation to the east (for details see Less et al 1988, Appendix 2, Fig. 59c, 62). The lowermost structural unit (Fig. 59, 62) is represented by the Telekesvölgy Formation (Csipkés Hill key-sections, sites P-91, -92) including the olistostrome of Csipkés Hill (P-90, -44). This Jurassic sequence is interpreted to be the same sequence as the one south of Bódva River (e.g. Telekes Valley Tributary Valley No 6, 7, 8, Varbóc Va-2 borehole) overlying the Triassic of Bódva series. Structurally above it small slices of Middle Triassic carbonates are mappable (P-135, Perk-16, Fig. 59c). On the SW corner of the hill one of these slices is visible (P-135, Fig. 59, 62, Appendix 2). There were more interpretations for this Steinalm Limestone body in the last decades: a) Less et al. (1988) surround-

ed this ambiguous block with faults between the Telekesoldal and Telekesvölgy Formations. b) it was interpreted as a slided block in Kövér (2005). The other small slice consists of partially altered Gutenstein Dolomite (P126, P130).The contact of these slices and the underlying rocks are usually marked by altered tectonic zone (rauhwacke). Following the presented new concept, the Steinalm Limestone body, and the Gutenstein Dolomite at the western part of the hill is considered to be the part of the Henc unit, and situated within the first order nappe contact zone (D4) incorporated into the base of the overriding Aggtelek nappe (Fig. 59c, 62, Appendix 2).

The deformation history within these slices and underlying outcrops of the Bódva and Teleksvölgy series can be reconstructed from the measured micro-scale structural elements and is quite complex. It could start with the formation of joints and faults before the main tilting and large-scale folding event (Fig. 63). These early pretilt joints can be measured in outcrops Perk-12 and 13. However, this fracturation can also be linked to the tilting and folding event (D4), because the extension is perpendicular to fold axis. In this scenario, fractures are fold-hinge-parallel set of joints. At the first step of folding few sinistral strike-slip faults could form in outcrops Perk-12-13 (Fig. 63). It was followed by the folding itself, then few post-tilt faults, probably in the same stress field. These deformation events were characterised by a NW-SE compression and the three events could be coaxial. This first folding phase can be seen equally in the outcrops of the Bódva series (Perk-12, -13) and the small scale overlying tectonic slices of the Henc unit (Perk 14-18). Thus during this phase they deformed together, indicating syn-D4 or pre-D4 nappe emplacement.

7.4.1.3. Between Perkupa and Dobódél

Following the Henc-Bódva contact zone more to the north, there are outcrops of Lower Triassic rocks, Gutenstein Dolomite and Upper Triassic cherty limestones along some N-S striking forest roads (Perk-008, -005, -006, -003) parallel with the road between Perkupa and Dobódél. These formations are in tectonic contact with Gutenstein Dolomite of the Bódva series

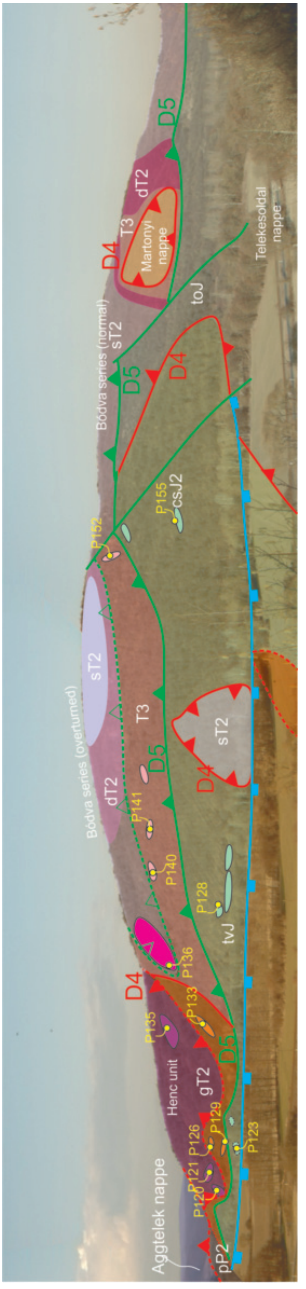

Figure 62. Panorama photo of the Csipkés Hill and Dunnatető Hill from the range between the Telekes and Henc Valleys (looking to the N). The structural units and the main investigated outcrops are approximately indicated.

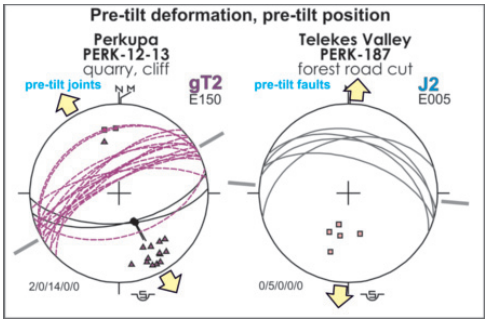

Figure 63. Stereographic projections of pre-tilt joints and normal faults. For legend, see Fig. 57.

(Fig. 59b, Appendix 2), and were interpreted as strike-slip duplexes (Less et al. 1988, Fig. 5). These duplexes were thought to be the result of Cenozoic sinistral movement along the Darnó zone. However, following my previous model, I suggest that these formations are part of the Henc unit, and primarily they formed relatively intact tectonic slices on top of the Bódva series.

7.4.1.4. Szögliget-3, Akasztó Hill

New attribution of the Akasztó unit into the metamorphosed Telekesoldal complex (Chapter 2.2.5, 5.3.3) changes considerably the local structural geometry (Appendix 1, Fig. 44, 59a). Topographically above the Szögliget Szö-3 borehole, the Aggtelek nappe occurs, whose Lower Triassic sequence is truncated. At its lower contact, poor occurrences of rauhwacke can be delineated a brittle thrust plane (for details see chapter 8). On the other side of the Akasztó unit, the Szögliget- Szö-4 borehole and a small outcrop expose gabbros and dolomite tectonically incorporated into an evaporitic mélange. This rock association of basic and ultrabasic rocks were classified into the Tornakápolna series (Pantó et al. 1950, Józsa et al. 1996, Dosztály et al. 2002). Thus the Akasztó unit is sandwiched between a non-metamorphosed nappe and the evaporitic mélange. The emplacement of the Aggtelek nappe post-date metamorphism (and D3 phase as well) and most probably occured during the D_4 phase. The result of the D4 tilting phase is well documented by outcrop Bosz-001 on the Akasztó Hill (Fig. 64). The penetrative S0-1 foliation of the Jurassic marly shale steeply dips both to the SE and NW (Fig. 58, 64). NE dipping fold axes were also measured related to this NW-SE compressional phase.

On the other hand, the nappe contacts were deformed later (during D_5 phase?) and resulted in the steep position of the tectonic boundaries of the units, and also its internal structures (foliation, bedding). As an alternative option, it is probable, that the uprising evaporite deform the pre-existing structures including bedding planes, foliation, nappe boundaries (Appendix 1).

7.4.2. Base of the Telekesoldal nappe

Structural boundary between the metamorphosed, deformed and exhumed TO complex and the underlying units can be directly studied only in a few key localities. The evaporitic sole was already involved in the overthrusting of TO nappe, which is proved by borehole Rudabánya Rb-661 (Fig. 23).

7.4.2.1. Rudabánya Rb-661

In this core between the TO nappe and the Bódva series in ~80 m thickness an alternation of anhydrite, siliciclastic sediments and dolomite, arranged in a tectonic breccia/mélange was penetrated (Fig. 23). The 0-151 m interval of the core is built up by dark grey, black claymarl, marl, calcareous marl and shale (Chapter 5.3, Fig. 24-25). The slate is characterised by ductile deformation features: e.g. kink folds, isoclinally folded calcite veins (see chapter 7.1.1, 7.2). Between 151 and 170 meters

altered and brecciated greyish green rhyolite occurs (Fig. 23). This volcanite is part of the TO complex as already mentioned by the previous authors (Grill 1988, Szentpétery & Less 2006). In chapter 5.3 I demonstrated, that this rhyolite is an olistolith. Below the rhyolite a wide tectonic breccia zone can be recognized containing black shale reminiscent of TO complex, rhyolite, evaporite, green anhydrite, rauhwacke (for details see chapter 8). Till the next structural boundary (225 m) variegated siliciclastic rock association appears mixed with dolomites and evaporites. In the uppermost part of this association black claystone alternates with thin laminas of gypsum followed by purple clay-

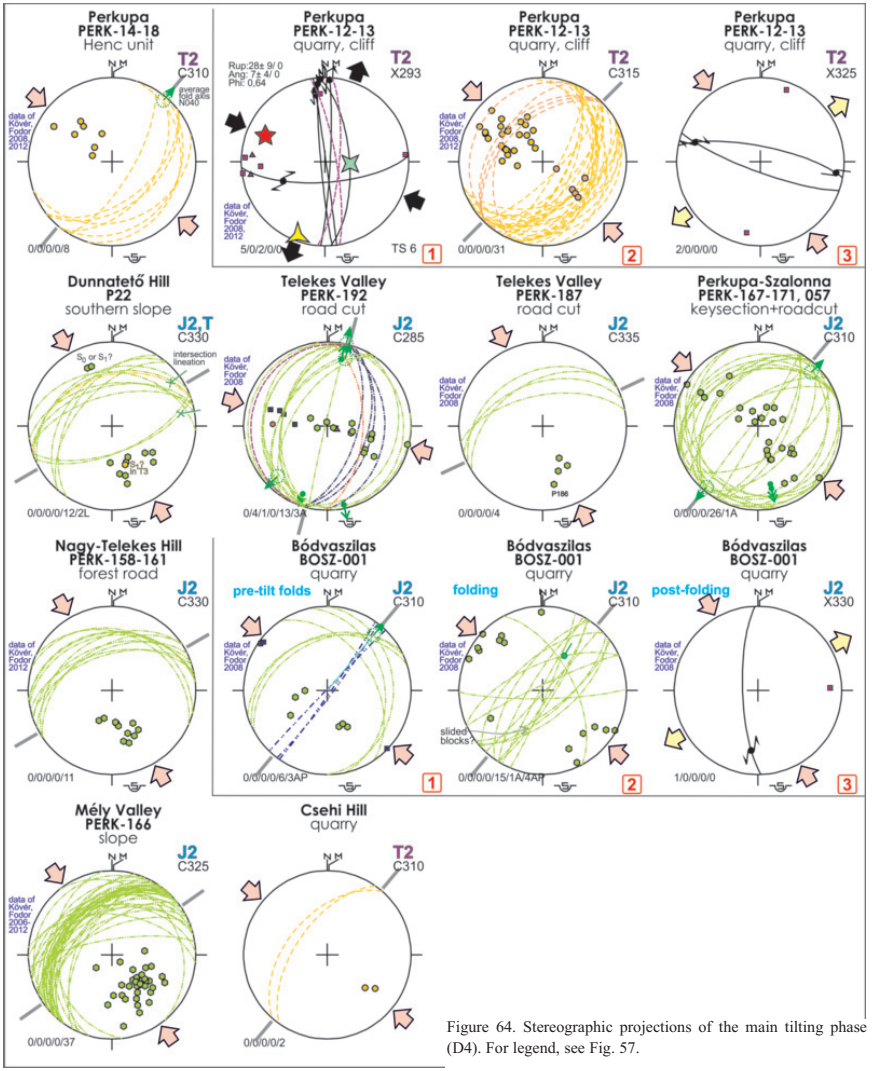

Figure 64. Stereographic projections of the main tilting phase (D4). For legend, see Fig. 57.

stone with anhydrite. The next meters are built up by the alternation of dolomite, anhydrite, purple and green claystone. At the lowermost part of this tectonic mélange coarse-grained siliciclastic beds and anhydrite laminas vary. This whole mixed rock association is suggested to be an evaporitic mélange, built up by clasts of the TO complex tectonically sheared into the Upper Permian Perkupa Evaporite Fm.

A 10 m thick tectonic breccia (255-265 m) is situated below the evaporitic-siliciclastic zone. There are red silicified claystone and red cherty limestone among the clasts of the breccia. The last 35 meters of the borehole is represented by light grey limestone occasionally containing coarse-grains of bioclasts. The previous descriptions about this core mentioned neither this tectonic breccia nor the limestone. However, they are very important from a tectonic point of view. The red silicified claystone and the red cherty limestone clasts of the tectonic breccia can be identified the best with the Middle-Upper Triassic Bódvalenke Limestone of the Bódva series among the known formations (Fig. 23). The light grey limestone from the bottom of the borehole is supposed to be equal with the Middle Triassic shallow-water carbonate of the Bódva series (Steinalm Limestone). Accordingly, the structural relationships penetrated by this borehole as follows (Fig. 23, 59d). In uppermost position the TO nappe can be found, below it a tectonic slice of the evaporitic series appears. It juxtaposes the tectonically truncated and smashed remnants of the basin facies Bódva-type Middle-Upper Triassic rock association. Finally in lowermost position the Middle Triassic Steinalm Limestone of the Bódva series is penetrated. In summary, core Rudabánya Rb-661 penetrated the nappe boundary between Telekesoldal and Bódva series.

7.4.2.2. Rudabánya Rb-658

The lower tectonic contact of the TO complex was penetrated by another borehole in the Telekes Valley, the **Rudabánya Rb-658** (Fig. 12). In this core above the grey marl of TV complex – developing continuously from the underlying Triassic beds of Bódva series – dark grey micritic limestone occurs. The transition between the limestone and the underlying TV complex is a sharp boundary, indicated by the different lithologies. On the basis of its macroscopic features, this limestone was previously assigned to the Gutenstein Formation (Less et al. 1988, Fig. 5).

In microscopic view the limestone has microsparitic texture with no sign of any diagnostic microstructure or fossil, which can refer either to the depositional environment or to the age of sedimentation. The most eye-catching phenomena are the two, almost perpendicular stylolitic planes. Accordingly, at least one of these directions is a poorly developed foliation controlled by tectonic processes. Rhombohedra shaped minerals secondarily replaced by calcite crystals are present sporadically in the microsparitic matrix. The original minerals have been resolved. The rhombohedra shapes of the cavities filled with secondary calcite are flattened perpendicularly to one of the stylolitic directions. Originally they could have been square shaped.

Above the dark grey limestone weathered shale debris can be found up to the surface. The uppermost part is represented by a 0.3 m long piece of core consisting of limestone olistostrome. The olistostrome is built up by flattened grey limestone clasts. All rocks above the dark grey limestone (supposedly Middle Triassic Gutenstein Formation) was classified into the TO complex (Grill 1988). In my opinion it is possible that both of the previous classifications are correct, but the upper boundary of the dark limestone is not of tectonic origin, but it represents an olistolith in the black shale matrix. The olistostrome horizon in the uppermost part of the core, and surface outcrops containing huge, foliated carbonate bodies strengthen this hypothesis. As an alternative option, the foliated

limestone can be the remnant of the Torna series, occasionally present at the base of the TO nappe (see chapter 7.1.2, Fig. 65).

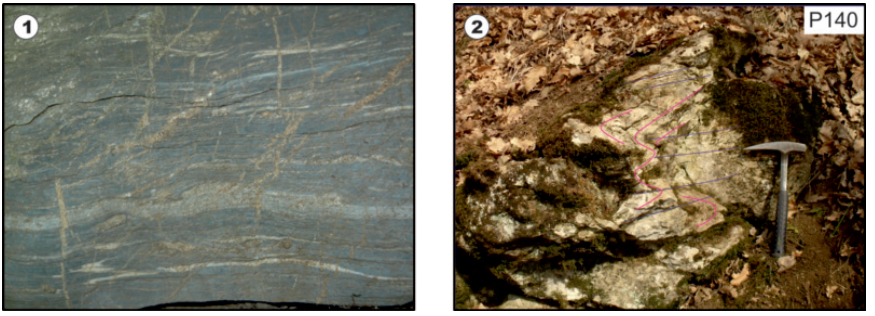

Figure 65. 1) Dark grey limestone olistostrome of the Telekesoldal complex. Note the well developed, penetrative foliation. The llimestone is similar to that in Rudabánya Rb-658, where the new interpretation is similarly olistolith. 2) New folitation developed in cherty limestone on the southern slope of Csipkés Hill. Folds and incipient folitaion planes (axial plane foliation) are connected to F5 phase.

This description shows that irrespectively of the classification of the dark grey limestone this borehole proves that the TO nappe juxtaposes the Bódva series (including the TV complex). Similarly to the previous ones, I suppose that this is a D4 phase nappe contact (Fig. 59d).

7.4.2.3. Other occurrences

The same structural situation can be seen on the very complicated, eastern segment of the Csipkés Hill, where the same TV complex is juxtaposed by the TO complex (Appendix 2, Fig. 59e, 62).

Similarly to core Rudabánya Rb-661, evaporitic mélange is present below the Akasztó unit (borehole Szö-4, Appendix 1, Fig. 59a). The co-occurrence of evaporite and slates similar to the TO complex helped the reinterpretation of the Hidvégardó Ha-3 and Zsarnó (Žarnov) Žam-1 boreholes (Chapter 5.3, Fig. 6, 38). In my view, these boreholes expose Jurassic shales, marls, sandstones and olistostrome horizons of TO complex and evaporite mélange. Originally this evaporite was incorporated into the basal tectonic breccias, developed during D4 nappe enplacement of the TO complex. Alternation of the evaporite breccias and the TO complex signs multiple thrusts in D4 phase, or alternatively, parts of thrusting occurred during the later D5 phase.

7.4.2.4. Outcrop-scale D4 deformation of the Telekesoldal complex

Outcrop-scale elements of the D4 structural phase characterised by NW-SE compression is widespread in the localities of the TO complex. The main fabric is the general NW dipping of the S0-1 foliation planes (Fig. 64). However, in some outcrops (e.g. Szalonna-Perkupa roadcut keysection) opposite, SE directions are present, too (Perk-167, -171, -057, Fig. 64). This indicates large-scale folding of the foliation. This tilting event is clearly postdates D3 kink-folding (see Chapter 7.1.3).

In outcrop Perk-192 in Telekes Valley cm to dm–scale open folds were observed (Fig. 66, 64). The folds have brittle, sharp hinges and straight limbs. The fold axes moderately plunge to the SW or NE (Fig. 64, 66). The measured data indicate NW-SE compression, which can be related to the D4 nappe-stacking phase.

Figure 66. Field observations and related stereograms in outcrop Perk-187/2 in Telekes Valley. The S0-1 foliation of the TO marl is bended by D4 open folds. Measured fold axes and foliation planes indicate NW-SE compression (D4).

However, in outcrop Perk-187 in the Telekes Valley (Appendix 3, Fig. 50) pre-tilt extensional faults were measuered, indicating N-S extension (Fig. 64). According to field observations and tilt tests, they predate the tilting phase. Similarly to outcrops Perk-12-13, these extensional features could form at the incipient stage of folding, indicating extension on the hinge zone, perpendicular to fold axis.

7.4.3. Base of the Martonyi nappe (Torna unit)

According to new macroscopic, microscopic and conodont age investigations (Kövér 2005), there are two Triassic sequences on the slope of Dunnatető Hill. One of them is a normal younging Bódva-type sequence (Appendix 2, Fig. 62, 67) with an age of Early Anisian to Middle Carnian based on conodont investigations. The other one is an Upper Ladinian to Upper Norian Torna-type s. s. sequence (Martonyi tectonic unit). This latter one probably occurs as a small nappe outlier (D4) on top of the Bódva series (Kövér 2005, Appendix 2, Fig. 62). The base of the nappe is folded by F5 large-scale folds (next chapter).

At the area of the metamorphosed s.s. Martonyi nappe the northwestern contact toward the Bódva series is represented by a well-constrained, moderately steep fault dipping to the southeast, beneath the metamorphic unit; this contact is marked by rauhwacke (for details see chapter 8). Because metamorphic rocks are at higher topographic position (Fig. 59e), they probably thrust onto the Bódva series (Less, 1998, Fodor & Koroknai 2000). While along this contact the situation is the same as on Dunnatető Hill, I suggest D4 phase for the overthrusting of the Martonyi nappe.

7.4.4. Effect of the D4 phase in the present-day structural geometry

On the basis of the previous observations and metamorphic petrological studies, the **Telekesoldal nappe** can be defined in the next way: it is an individual structural unit, a nappe, below which the tectonically truncated lenses of the Torna series (D1 contact), otherwise the Bódva series (D4 contact) can be found (Appendix 1-3, Fig. 59, 60, 62, 67). The geometry of the nappe boundary is mostly the same as the boundary of the TO complex on the geological map of Less et al. (1988) (Fig. 5). The main differences are as follows. A) in the borehole Szendrő Szet-4 (Chapter 5.2.4, Appendix 3, Fig. 17) I classify the uppermost, shale and marl part of the core to the TV complex, against the original classification into the TO complex (Less et al 1988) (Fig. 5, 7). B) in the surrounding of the borehole Szalonna Sza-5 according to my opinion the non-metamorphosed marls of the TV complex crops out (Chapter 5.2) which is in contradiction with the previous concepts (Less et al 1988, Fig. 5, 7). The basal D4 thrust surfaces of the TO nappe may have been reactivated or deformed several times (e.g. in phase D5) after the main nappe emplacement, so they certainly do not reflect the original structural geometry.

Accordingly, in the central part of the Rudabánya Hills the present-day structural order of the nappes is as follows. South from the Bódva River in the lowermost known tectonic position a Lower Triassic–Middle Jurassic Bódva series is present including the TV complex (Appendix 3, Fig. 59d, 60). Above it in the vicinity of the valley head of the Telekes Valley number 7 Tributary Valley an upper scale of Bódva series appears. On the top of these imbrications the TO nappe is emplaced during the D4 phase (maybe with some questionable slices of Torna series between the two main units). The Aggtelek nappe is in uppermost structural position. Between the Aggtelek and TO nappes, a few hundred m thick tectonic breccia zone, the Henc unit occurs, whith the relatively intact slices of Lower and Middle Triassic rocks (Fig. 59d).

North from the Bódva River (Appendix 2, Fig. 59b, c, 62, 67) this nappe pile is complicated by later movements along some younger structural elements, which belong to phase D5 (see next chapter). However, the effects of the D4 nappe stacking are preserved by the D4 contact of small slices of Henc unit on TV series. The Telekesoldal nappe does not appear in this segment, maybe it was tectonically truncated during nappe emplacement. The refolded nappe contact on Dunnatető Hill between the small Martonyi nappe outlier (Torna series) and the Bódva series in lower position also

belongs to this phase. Here the superposition of D5 folding is nicely wisible, because the upper Martonyi nappe is preserved in the core of an F5 syncline (see next chapter, Appendix 2, Fig. 62, 67)

7.5. D5 south-verging thrusts

The nappe order achieved during D4 phase is reworked by a N-S compressional event (D5) (see Fig. 68) resulted in south-verging thrusts concerning the whole Aggtelek-Henc-(Telekesoldal)-(Torna)-Bódva nappe pile. This compressional event is responsible for large scale folding, causing locally recumbent folding in the Bódva series.

7.5.1. Dunnatető Hill

On the southern slope of the Dunnatető Hill the structural order of the nappes is as follows (Appendix 2, Fig. 59g, 67). The TO nappe forms the lowermost structural unit on the surface. In the individual outcrops (P-22, roadcut keysection on the other side of the Bódva River) post-tilt, mod-

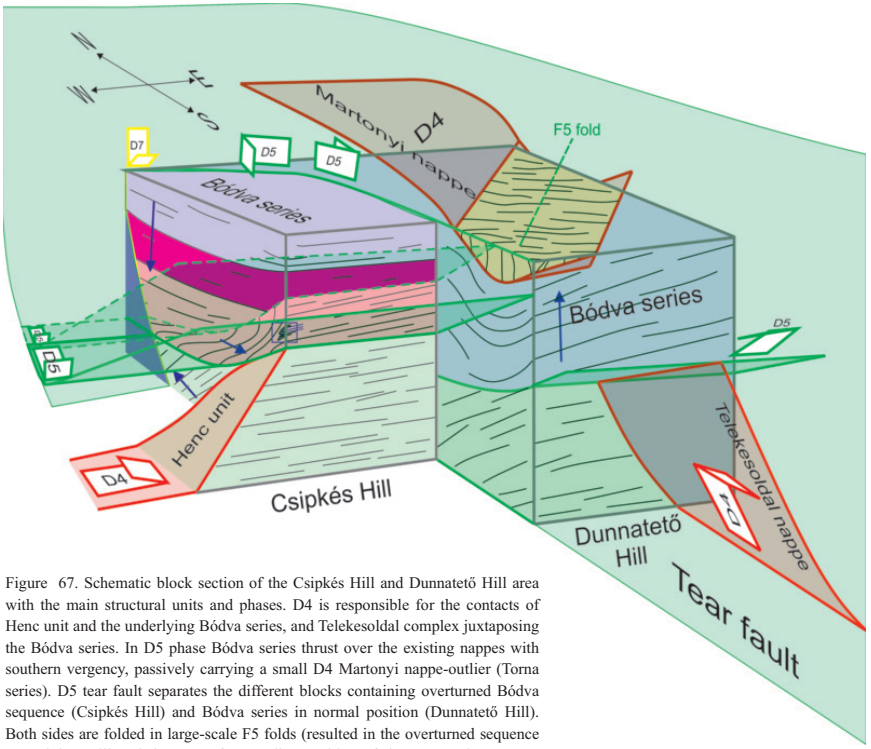

Figure 67. Schematic block section of the Csipkés Hill and Dunnatető Hill area with the main structural units and phases. D4 is responsible for the contacts of Henc unit and the underlying Bódva series, and Telekesoldal complex juxtaposing the Bódva series. In D5 phase Bódva series thrust over the existing nappes with southern vergency, passively carrying a small D4 Martonyi nappe-outlier (Torna series). D5 tear fault separates the different blocks containing overturned Bódva sequence (Csipkés Hill) and Bódva series in normal position (Dunnatető Hill). Both sides are folded in large-scale F5 folds (resulted in the overturned sequence on Csipkés Hill and the core of a syncline position of the Martonyi nappe on Dunnatető Hill). Purple arrows show younging directions.

erately northly and southly dipping joints can be measured. Field observations indicate reverse faulting along these planes, thus they refer to N-S compression (Fig. 68). The TO nappe is thrust over by a tectonic slice of the Bódva series (Fig. 59g, 62, 67). The contact between the two structural units is charaterised by a few m thick tectonic breccia zone (rauhwacke), which can be studied in outcrop P-22 (see Chapter 8). In map view, the contact dips moderately to the N, but it is cut perpendicularly by late structures. The north-directed thrust contact indicates top-to-S movements.

The Bódva series above the contact zone starts with highly altered Triassic carbonate with a great amount of dissolution cavities. The formations of the Bódva series are folded into large-scale folds. At outcrop P-22 a syncline is in contact with the underlying TO nappe. Due to the poor outcropping conditions, it is not clear, if the nappe boundary was involved in this folding phase. The axis of this map-scale syncline (Appendix 2, Fig. 67) plunges to the WSW (Fig. 68). Estimated fold axes are 265/20 and 250/20. In the core of the syncline a small nappe outlier of Torna series is preserved (Chapter 7.1.4). This D4 thrust contact is bended by this map-scale fold, thus it represent folding after the nappe enplacement. This syncline is bordered on the SE and NW by anticlines with similar axes, made up of Dunnatető and Steinalm Formations. Similar dip values, map-scale folds and fold axes were measured on the northern continuation of Dunnatető Hill at Szár Hill (Fig. 68) (Less et al. 1998, Péró et al. 2003). Fold axes estimations from alternating dip values refer to roughly N-S compression.

The next structural evolution can be reconstructed for the D5 phase from these observations and measurements. A scale of Bódva series thrust over the Telekesoldal nappe with southern vergency. It passively carries a small Martonyi nappe outlier (Torna series) on its top. During this N-S compressional phase, large-scale F5 folds developing in the Bódva series, bending also the pre-existing D4 boundary (Fig. 59g, 67).

7.5.2. Csipkés Hill

The situation is somewhat similar on the eastern Csipkés Hill. However, there are some more complications deriving from the more diverse D4 contacts and more intense F5 folding (Fig. 59f). Surface observations can be combined with borehole data of Perkupa P-74 (Fig. 10) drilled on top of the hill. The hilltop consists of and the borehole starts with Middle Triassic Steinalm Limestone of the Bódva series. Dunnatető Formation, then deep-water, Middle to Upper Triassic Bódvalenke Limestone develops continuosly from this shallow-water carbonate. It indicates overturned position for this scale (Appendix 2, Fig. 59, 62, 67). Below it, another overturned scale with similar formations occur (Fig. 10). The rocks consisting of these scales can be followed on hillslopes of the Csipkés Hill, where small-scale folds with gently north-dipping axial panes, and incipient axial plane cleavage were observed (P-140, Fig. 65). In the borehole, the lower, overturned Triassic sequence is bounded by a thrust toward the Jurassic black shale (Fig. 10). The lowermost part of the section contains TV complex and Hallstatt Limestone in normal position (Kövér et al. 2009b).

My summarized structural interpretation for the Csipkés Hill is as follows (Fig. 59, 62, 67). The Bódva series was affected by F5 large-scale folding, similarly to as described on Dunnatető Hill. The speciality of the Csipkés Hill is that this folding phase resulted in overturned folds and imbricates. The overturned limb of this map-scale fold thrust onto the Telekesvölgy complex and onto the Csipkés Hill olistostrome.

The present-day contact between these overturned tectonic slices and the rest of the Bódva nappe in normal position to the east and north (Fig. 62, 67, Appendix 2) is supposed to be a younger normal fault contact. However, some earlier movements are supposed along this NW-SE striking boundary fault of the

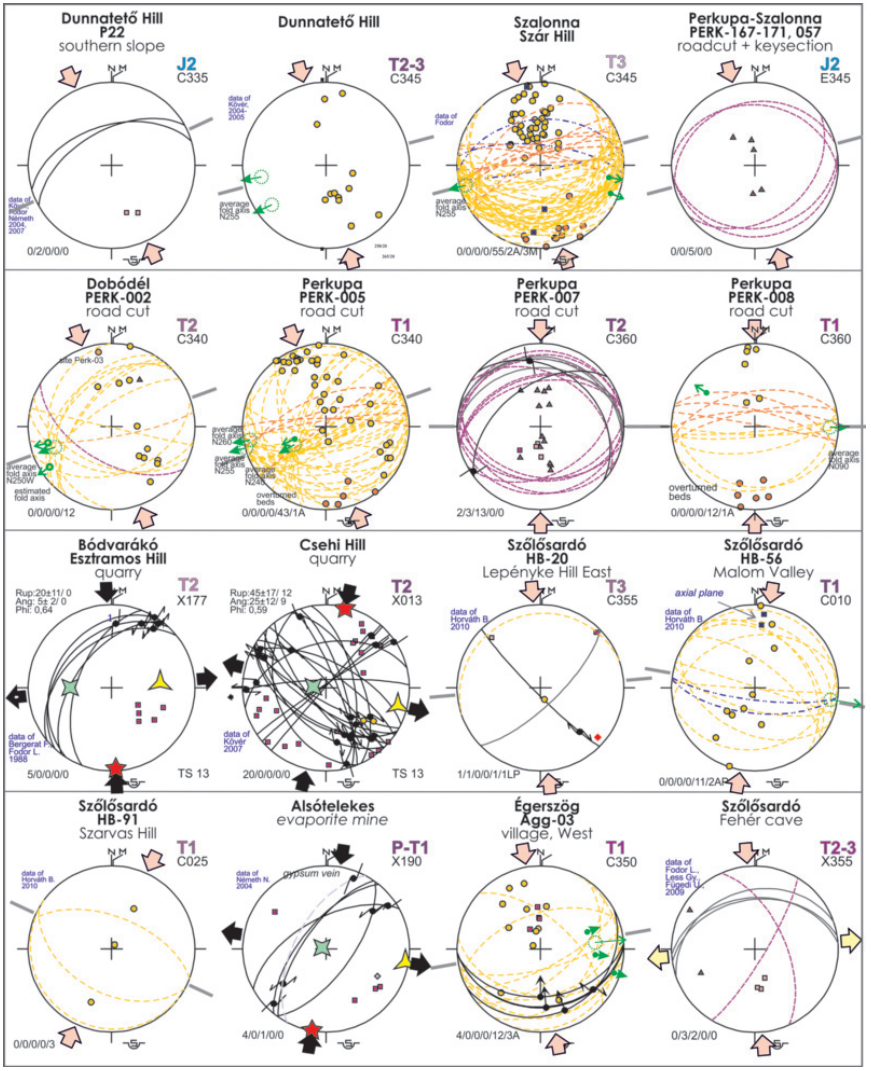

Figure 68. Stereographic projections of the D5 phase. The main structural elements are south-verging large-scale folds and thrust faults. For legend, see Fig. 57.

overturned imbrication. It is suggested to be a NW-SE striking tear fault during the S-verging thrusting event, separating areas of the Bódva nappe with different style and amplitude of F5 folding (Fig. 67). The main reason for this interpretation is that the overturned sequence seemingly has no continuation in strike to the east (towards the Dunnatető Hill), but the south-verging thrust and the large-scale F5 folds can be followed; all structures indicate roughly the same direction for compression (Fig. 59f, g, 67).

7.5.3 Between Perkupa and Dobódél

Micro-tectonic observations lead to similar results for D5 phase in case of Lower Triassic localities of the Henc unit (Perk-005, 008, Appendix 2, Fig. 68, 69, 70). The lithology in these outcrops is sandstone, siltstone and marl of Early Triassic age. In both outcrops the main structural phenomena is the dm-to m-scale folding of the beds. The folds have open to close geometry usually with rounded hinge. The axial planes are steep, and they dip to the N. Measured and estimated axes plunge moderately to the WSW in case of outcrop Perk-005. In Perk-008 almost horizontal, E dipping axis and moderately dipping WNW plunging axis were observed. The length of the fold limbs alternating in long-short-long geometry in outcrop Perk-008. Dipping of the axial planes, asym-

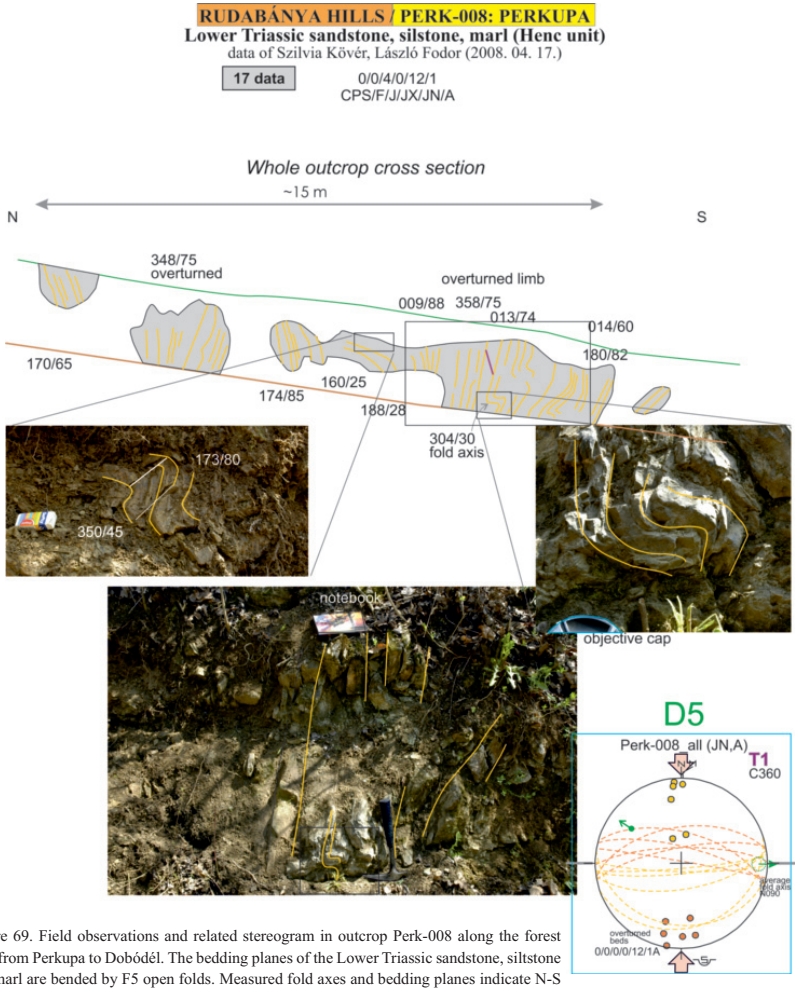

Figure 69. Field observations and related stereogram in outcrop Perk-008 along the forest road from Perkupa to Dobódél. The bedding planes of the Lower Triassic sandstone, siltstone and marl are bended by F5 open folds. Measured fold axes and bedding planes indicate N-S shortening (D5).

metry of the folds and fold axis geometry refers to N-S compression and southern vergency (Fig. 68, 69, 70,).

This S-verging thrusting event is responsible for local revorking of the structural units, resulted in northly dipping thrust planes separating different lithologies of the Henc unit. This later thrusting resulted in the juxtaposition of the younger Gutenstein Dolomite and the older Lower Triassic clastic formations. In other outcrops of this locality group (Perk-007 and -002) outcrop-scale reverse and thrust fault showing N-S compression were also measured (Fig. 68).

For regional correlation, the folding event fits to D5 phase with N-S compression, resulted in the south-verging folds and thrusts. Sinistral strike slip movements along some NNE-SSW striking steep faults connected to the D5 N-S compressional phase is probable and resulted in rework of the orig-

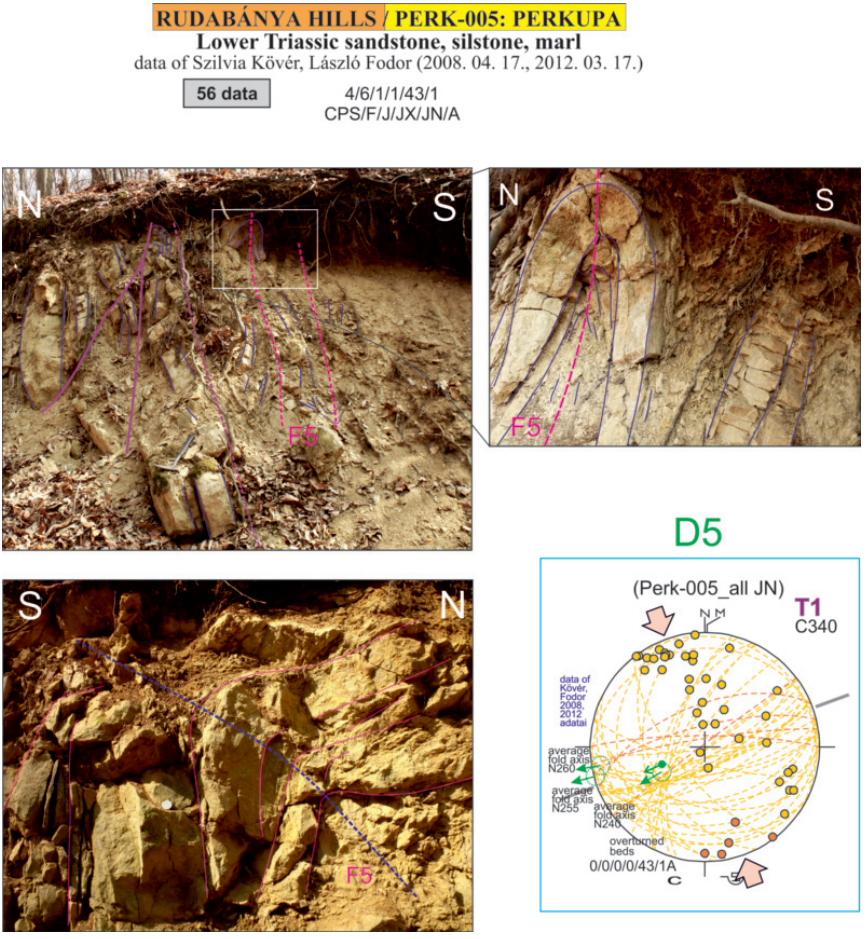

Figure 70. Field observations and related stereogram in outcrop Perk-005 along the forest road from Perkupa to Dobódél. The bedding planes of the Lower Triassic sandstone, siltstone and marl are bended by F5 open to close folds. Axial planes are subvertical. Part of the strata are in overturned position due to F5 folding. Measured fold axes and foliation planes indicate N-S compression (D5).

inal D4 nappe boundaries. This steep boundary is similar to the interpretation of Less et al (1988), (Fig. 5), the main difference is the assumption of an east-verging (D4) emplacement of the Henc unit onto the Bódva series prior to the strike-slip movements. Such strike-slip faults were measured on the Esztramos Hill quarry (Fig. 68).

7.5.4. Surrounding of the Bódvarákó window

The inner, D1 nappe contact of the Telekesoldal nappe and the Torna series in the core of the Bódvarákó window was described in Chapter 7.1.1. These two structural units in window position are cut by a detachment fault, which placed the evaporitic sole and non-metamorphosed Bódva series over the metasediments. This relationship is evident from the map, where Bódva series surrounds the window of metamorphosed rocks (Less et al. 1988) (Fig. 5, 44, 59e), and also from the Bódvarákó-4 borehole, which reached the Triassic of Bódvarákó series below the evaporitic unit. According to the KI values, a clear jump in the degree of metamorphism exists all along the window (Fig. 44, Appendix Table 4: samples for Bódva unit: E-6, 7, 10, 12; versus NL beds). Thus, motion along the upper contact of the Bódvarákó window postdates the very low to low-grade metamorphism. Micro-deformational investigations lead to the general conclusion, that nappe enplacement post-dates D3 phase (Chapter 7.3, 7.4). In chapter 7.4 D4 contact of the Torna and Bódva series was demonstrated, placing the metamorphic unit over the non-metamorphosed one. Thus the non-metamorphosed Bódva on metamorphosed Telekesoldal nappe (locally NL beds) is another, younger event. Similar contact was described from the Dunnatető Hill, which was classified into D5 phase. Although I have no direct measurement for S-verging tectonic transport above the Bódvarákó window, I suggest equally D5 phase contact for the top of the window (Bódva series juxtaposing TO nappe).

7.5.5. Correlation of D4 and D5 phases with the area near Szőlősardó village

To the south of the examined area, on the boreder of the Aggtelek and Rudabánya Hills a complicated nappe structure was recently reinterpreted by Horváth (2010) and Horváth et al. (2012). This work was carried out at the eastern margin of the Aggtelek nappe, near the village of Szőlősardó. It distinguished a total of five structural units as follows from top to bottom: Aggtelek nappe, Lászi, Henc, Szőlősardó and Bódva units. The northward continuation of Lászi and Szőlősardó units are not present in my area. They are small-sale structural units built up by slope-facies and pelagic limestones in the Upper Triassic. Outcrop-scale folds and minor reverse and thrust faults were measured, which indicate that the investigated units thrust onto each other first with southeasterly then with Sothern vergency. These two phases shows good correlation with the D4 and D5 phases of my recent study (Figure 64, 68). D5 deformation could also involve incipient salt tectonics near Alsótelekes, where Upper Permian gypsum and anhydrite form a dome (Zelenka et al. 2005) having rosen from below the Szőlősardó unit. The D5 phase was particularly marked by young-on-older (out-of-sequence) thrusts which formed a complex duplex system juxtaposing different tectonic slices of the Henc unit.

7.6. D5b E-W extension

Conjugate sets of N-S striking shear bands are very characteristic in several outcrops of the TO nappe (Perk-158-161, Perk-167-171, Perk-192, Perk-186-187, P-22). These shear bands indicate top-to-the-E shear along the E-dipping surfaces, while top-to-the-W shear along the oppositely directed planes (Fig. 71a, b). Some shear bands locally form an incipient extensional crenulation cleavage. In micro-scale the deformation is at least partly ductile. This phase was named D5b in the

Figure 71a. Stereographic projections of the D5b phase. The main structural elements are top-to-the-E shear along the E-dipping surfaces and top-to-the-W shear along the oppositely directed planes. For legend, see Fig. 57.

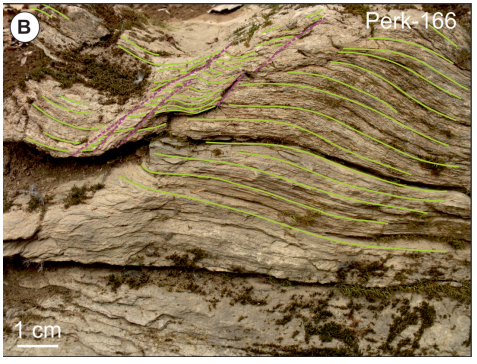

Figure 71b. Extensional shear zones in the Mély Valley. S0-1 foliation of the TO complex is dragged by the D5b extensional shear zones.

Figure 72. D5b extensional shear zones in outcrop-scale (1), in hand-specimen (3, 6, 7) and in micro-scale (2, 4, 5, 8). This feature can be observed in several outcrops of the To nappe (e.g. NL beds, Zam-1 borehole, the “classical” To complex. The shale and marl matrix behaved in a ductile way, while the clasts of the microolistostrome were deformed brittle.


1
P-22
D5b shear
S0-1
260/30

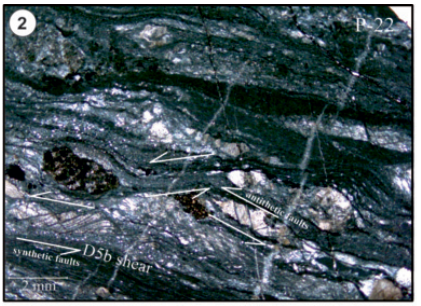
2
P-22
antithetic faults
synthetic faults
D5b shear
2 mm

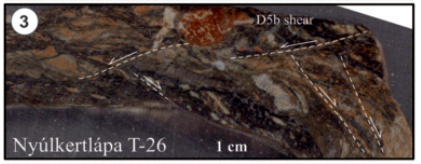
3
D5b shear
Nyúlkertlápa T-26
1 cm

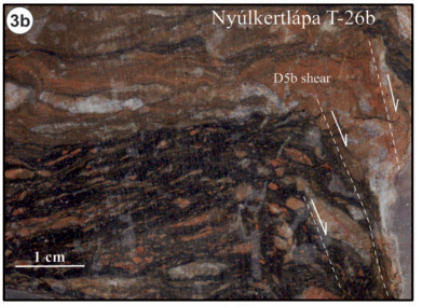
3b
Nyúlkertlápa T-26b
D5b shear
1 cm

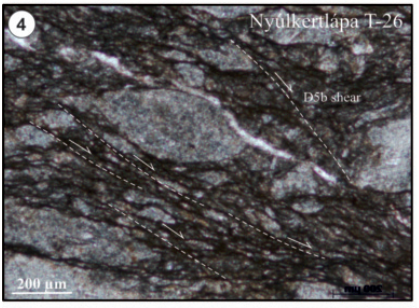
4
Nyúlkertlápa T-26
D5b shear
200 µm

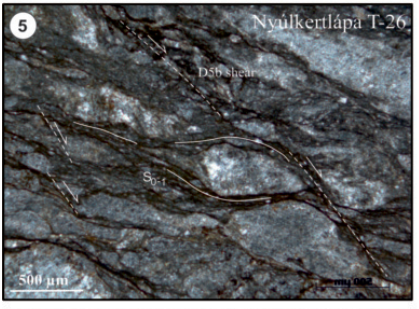
5
Nyúlkertlápa T-26
D5b shear
S0-1
500 µm

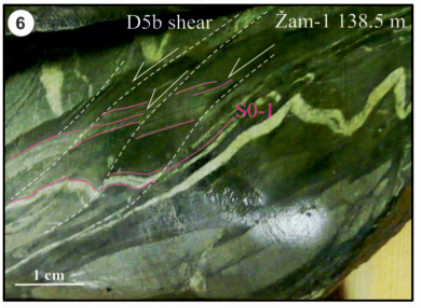
6
D5b shear
Žam-1 138.5 m
S0-1
1 cm

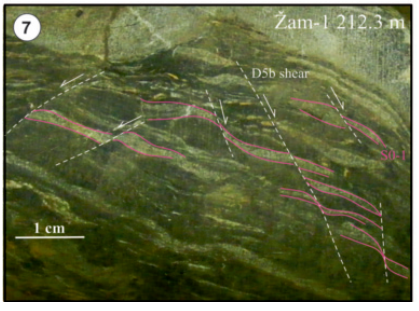
7
Žam-1 212.3 m
D5b shear
S0-1
1 cm

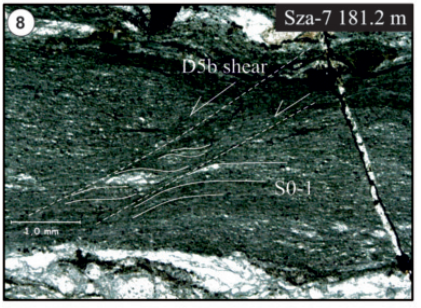
8
Sza-7 181.2 m
D5b shear
S0-1
1.0 mm

first approach, because it was clear even in field, that it postdates the D4 tilting event. Its relation to the D5 phase will be discussed in chapter 9.2.

In outcrop **P-22** near the tectonic contact between the TO nappe and the overriding Bódva series nice samples of these shear bands are visible both in outcrop and micro-scale (Fig. 72.1, 2). The lithology is olistostrome with calcareous shale as a matrix, and mm- to cm-scale carbonates are the clasts. During the shearing event the matrix behaved in a ductile way, why the more competent carbonate clasts in brittle way (Fig. 72.2). In the clasts domino-like structures developed during the shearing. These domains are separated by either synthetic or antithetic small-scale faults. These faults behaved in a brittle way only in the clasts, and they do not continue in the less competent marly matrix.

The same phenomena can be observed in the micro-olistostrome of the Nyúlkertlápa beds in the **Bódvarákó window.** The shearing bent the original S0-1 foliation planes of the olistostrome. In micro-scale the clasts behaved in rigid way, rotating within the ductilely deforming matrix (Fig. 72.3-5).

Conjugate extensional shear zones are also persent in samples 138.5 and 212.3 m of core **Zsarnó (Žarnov) Žam-1** (Fig. 72.7). During the shearing the slate and the siltstone intercalations behaved in a semi-ductile way, indicated by the dragged layers.

These D5b semi-ductile shear zones are responsible for the disintegration of the sandstone layers within the slate. These extensional shear zones separating the sandstone boudins are nicely visible in the Telekes Valley in locality **Perk-186-187** (Fig. 50) and in Mély Valley (Fig. 71b).

On the northern slope of Nagy-Telekes Hill, in outcrops **Perk-167-171** (near the Szalonna-Perkupa roadcut keysection) not only ductile – semi-ductile extensional features, but also brittle ones are present (Fig. 71b). These E and W directed fault planes dip quite steeply. The measured slickensides indicate normal movements. On WNW dipping planes sinistral movements were also observed. The presence of both ductile and brittle extensional structures separates this D5b phase into two events: an earlier ductile – semi-ductile phase followed by a later brittle one in the same E-W extensional regime.

7.7. D6 WNW-ESE compression and NNE-SSW extension

WNW-ESE compression and perpendicular tension was measuered in the small Gutenstein Dolomite quarry of Bódva series (Perk-12, -13) (Fig. 73). Joints and faults corresponding to this phase were also observed in Gutenstein Dolomite of Henc unit along the forest road between Perkupa and Dobódél villages. The corresponding structures are represented by conjugate strike-slip faults, N and S dipping normal faults and N-S striking reverse faults. Dextral strike slips are trending WSW-ENE, while sinistral ones are oriented NW-SE (Fig. 73). While all of the measurements were carried out in Mesozoic rocks, only relative timing of this phase can be made. One exception is the outcrop in the SE Rudabánya Hills (Barbara quarry on Fig. 73), where reverse faults and folds affected an Early Miocene (Eggenburgian) formation. According to field observations, this phase post-dates the tilting and thrusting events (D4 and D5), that is why it became D6. These tectonic directions and structures were also measuerd by Zelenka et al. (2005) and Fodor et al (2005). According to this latter work, this stress field was active from late Eocene till early Ottnangian (~34-18.5 Ma).

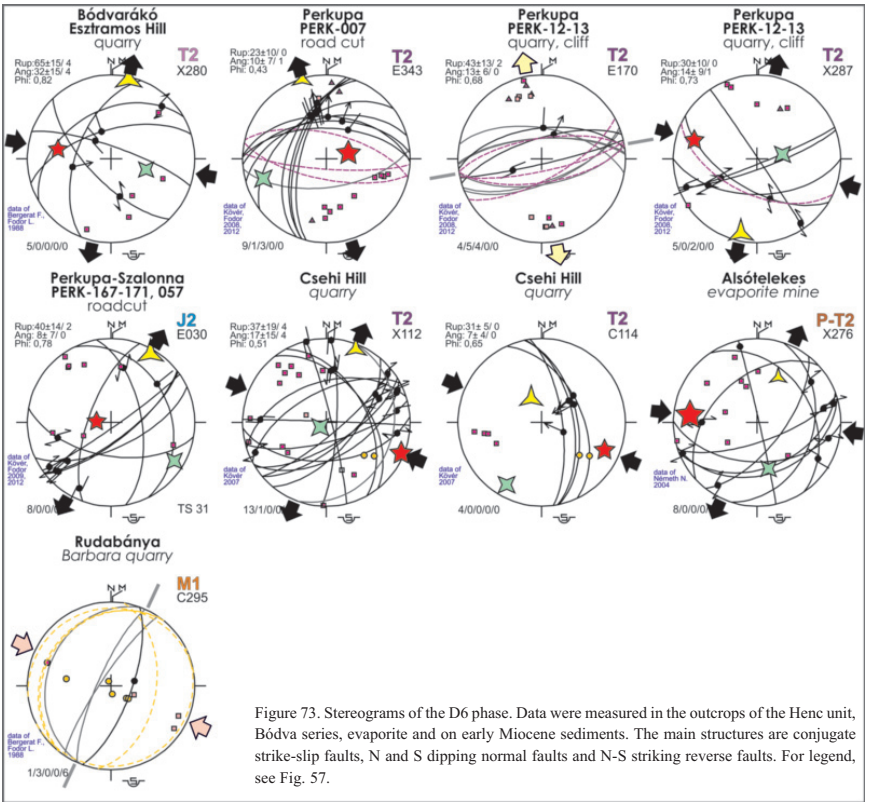

Figure 73. Stereograms of the D6 phase. Data were measured in the outcrops of the Henc unit, Bódva series, evaporite and on early Miocene sediments. The main structures are conjugate strike-slip faults, N and S dipping normal faults and N-S striking reverse faults. For legend, see Fig. 57.

7.8. D7 NE-SW extension

Signs of another post-tilt event can be observed in Lower and Middle Triassic rocks along the Perkupa-Dobódél forest road, in the quarry of Csehi Hill. The main structural features are strike-slip faults. Dextral movements were measured along steep, W-E to NW-SE striking planes (Fig. 74). A few sinistral strike-slip faults were also observed with N-S to NNE-SSW strike. Locally, only normal faults or joints developed parallel to the maximal horizontal stress axis. These movements refer to a NE-SW extensional stress field. This phase was also detected by Zelenka et al. (2005) in the evaporite mining area more to the south (Alsótelekes), and by Fodor et al. (2005) during structural investigations along the Darnó Zone. The measured ~N-S directed sinistral strike-slip faults are subparallel to the Darnó Zone (Fig. 2). In fact, this phase could correspond to the often quoted sinistral slip of the Darnó Zone (Zelenka et al. 1983, Fodor et al. 2005). For the time span of this phase, late Ottnangian (~18.5 Ma) – middle Badeninan (~15 Ma) age was suggested (Fodor et al. 2005). For regional correlation, this stress field is coeval with the main rifting phase of the Pannonian basin (Fodor et al. 1999, Fodor 2010).

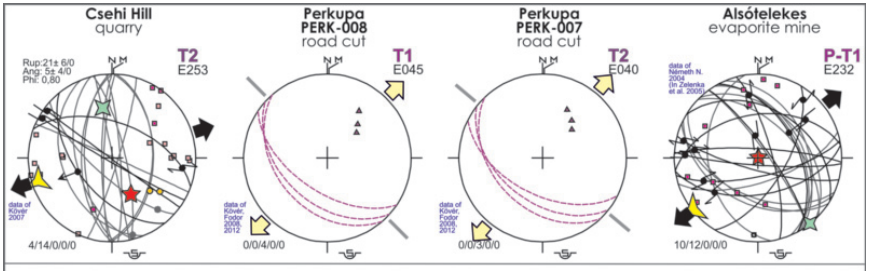

Figure 74. Stereograms of the D7 phase. Measurements were carried out in the outcrops of the Henc unit, Bódva series and the evaporite. The main structural elements are conjugate strike-slip faults. For legend, see Fig. 57.

7.9. D8 SE-NW extension

Several NE-SW trending normal faults were measured on the Akasztó Hill, in the dolomite quarry of Csipkés Hill W (Perk-12, -13) and on the Esztramos Hill (data of Fodor and Bergerat 1988) (Fig. 75). Outcrop-scale N-NNW dipping sinistral strike-slip faults occur locally. From these measurements, a SE-NW extensional stress field can be reconstructed. Normal or sinistral-normal oblique-slip faults can be supposed along the western margin of the Rudabánya Hills. The fault zone is particularly expressed near the Esztramos Hill. Similar phase was observed in the southern part of the Rudabánya Hills by Horváth et al. (2012), and Zelenka et al. (2005) and all along the Darnó Deformation Belt by Fodor (2005) (Fig. 75, Szőlősardó, Alsótelekes). They suggested late Badenian age for this deformation. Map-scale faults displacing late Miocene sediments (Horváth et al. 2012) demonstrate a continuation of extensional faulting up to the end of the Miocene or even into the Pliocene. This stress field marks the youngest deformation phase in the area.

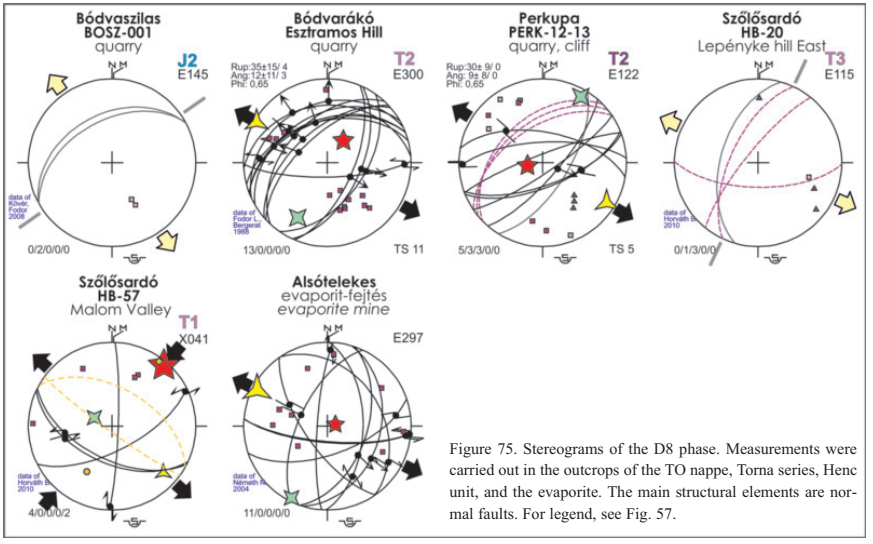

Figure 75. Stereograms of the D8 phase. Measurements were carried out in the outcrops of the TO nappe, Torna series, Henc unit, and the evaporite. The main structural elements are normal faults. For legend, see Fig. 57.

8. Pressure and temperature estimations of the nappe movements

Along the deformation zones characterized by major movements (nappe boundaries) the possibility of fluid migration is highly increased. Hydrostatically pressurized zone develops on the base of the nappes, where basal tectonic breccias (rauhwacke) were formed from the original rocks situated in the vicinity of the contact (Plašienka & Soták 1996). Meanwhile, newly formed, syn-kinematic minerals are growing from the overpressured fluids during the nappe emplacement. The pressure and temperature conditions during the deformation can be estimated by investigating the fluids trapped in primary fluid inclusions of these newly formed minerals.

Carbonate texture of the rauhwackes and their syn-deformational minerals were investigated by means of fluid inclusions (FI) microthermometry and microbarometry. Suitable basal rauhwackes were collected from the base of the Aggtelek nappe, Henc unit, Telekesoldal nappe and the Martonyi nappe (Appendix 1-3).

8.1. Petrography

8.1.2. Base of the Aggtelek nappe

The basal cataclastic breccias of the Aggtelek nappe were collected from several localities. From N to S the next outcrops were investigated: core Tornanádaska Tn-3, Akasztó Hill near Bódvaszilas village, Tilalmas Hill, from some roadcut outcrops between Perkupa and Szőlősardó villages. In borehole Tornanádaska Tn-3 just the evaporitic base of the Aggtelek nappe was reached, while on the Akasztó and Tilalmas Hills Aggtelek nappe juxtaposes the Akasztó unit, which is interpreted as part of the Telekesoldal nappe (Chapter 7.4.2). This lower structural unit contains Jurassic dark grey to brown slate and marl, whose biostratigraphical age was proven as Jurassic (Chapter 5.3.3) and metamorphic alteration as high-temperature anchi- to epizone (Chapter 6.4.1).

The sample from core Tn-3 (6-26m) is a matrix supported polimict breccia (Fig. 76.1). The carbonate matrix is light brown and fine grained. The clasts are few mm to cm in size. Dark grey dolomite or limestone, light grey limestone, red sandstone and yellow to grey marl are the most common clasts. The carbonates may derive from the Middle Triassic of the Aggtelek nappe (Gutenstein and Steinalm Fm.), while the marls can be either part of the Aggtelek or the underlying Telekesoldal nappe. The Lower Triassic Bódvaszilas Sandstone is most probably the surce of the red sandstone clasts.

The sample from the Akasztó Hill has similarly fine grained matrix, but containes a greater amount of clasts (Fig. 76.2). The clasts are just 1-5 mm in scale, and usually consist of light grey limestone supposingly from the Aggtelek nappe. Mm-scale cavities filled with red or brown calcite are present.

In case of the Tilalmas Hill the collected rauhwacke samples are characterized by reddish-brown colour (Fig. 76.3-4). The rocks are full of with cavities after dissolved or mechanically removed dolomite clasts. The clasts are bigger than in the previous samples, usually between 1 and 3 cm. They are mainly carbonates, but the original colour and texture cannot be observed due to alteration connected to the fluid migration. The clasts were most probably carbonates, and derived from the Aggtelek nappe. Different generations of crosscutting calcite veins can be observed, too.

The next locality group is more to the south, along the road leading from Perkupa to Szőlősardó

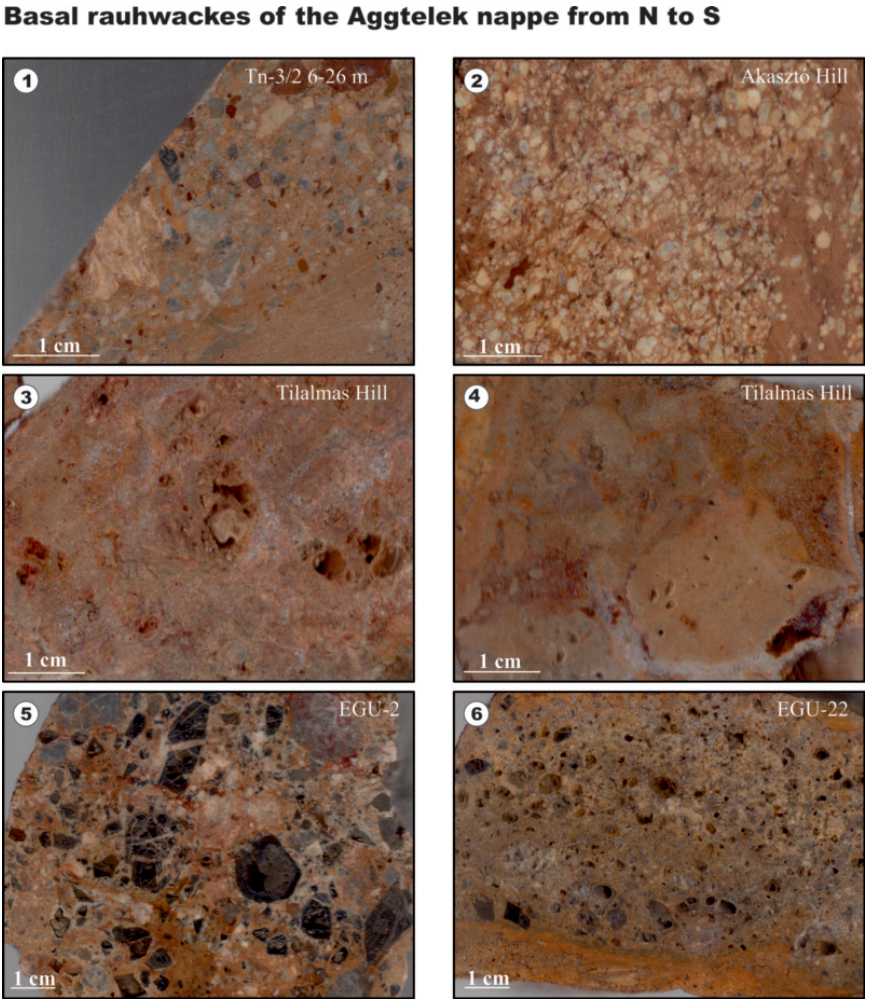

Figure 76. Different types of basal rauhwackes of the Aggtelek nappe. The main types are fine-grained, polymict breccia (1, 2), coarse-grained polymict breccia (4, 5) and matrix rich rauhwacke with cavities after dolomite clasts. There are clasts from the overriding Aggtelek nappe and maybe also form the Henc unit. The main components are black Gutenstein Dolomite (5, 6), light grey limestone (1, 2), T1 green shale and marl (1, 2). They often contains higly altered, pitted dolomite clasts (3).

village (Fig. 60). Structurally this tectonic breccia is situated between the Aggtelek nappe and the Henc unit (see chapter 7.4.1). The latter one is built up by Lower to Middle Triassic marl and ramp carbonates. From the several outcrops along the road two localities were investigated in more details: EGU-2 and -22 (Fig. 60).

The EGU-2 sample is a polymict breccia with brown matrix (Fig. 76.5). The clasts are mm to 3

cm in size. The main components are dark grey to black dolomites with white calcite veins, light grey limestone and brownish shale and marl (Fig. 76.5). The shale clasts are party missing due to the sample preparation processes. The cm sized carbonate grains usually have calcite rims. The clasts can derive both from the Aggtelek nappe and the Henc unit. The carbonate matrix is light brown, sometimes coloured to red by ferrous solutions.

Sample Egu-22 contains the same clast composition, but the average size of the grains is smaller, usually 3-4 mm (Fig. 76.6). Matrix rich, fine grained layers alternate with the corser-grained one.

8.1.2. Tectonic breccias from the Henc unit

Unfortunately, due to the poor outcropping conditions, it is not easy to define the exact structural position of these sample localities. These tectonic breccias are from the wide contact zone of Aggtelek nappe as the overthrusting structural unit, and the Telekesoldal nappe in footwall position. Between the two main nappes, lens-shaped, few 10 metres to few 100 m thick tectonic slices of Gutenstein Dolomite, Steinalm Limestone and various lithologies of the Lower Triassic of the Henc unit are situated within the main tectonic shear zone defined by the rauhwacke (for details see chapter 7.4.1.1). The samples from this contact zone were collected from the next localities from N to S: P-006, Csipkés Hill (P-122 and -129), and two samples from the range between the Henc and Telekes Valleys (P-172, -174).

P-006 defines the contact zone between a Lower Triassic slice of Henc unit and the Gutenstein Dolomite of the Bódva series (Appendix 2). The sample is built up by highly altered dolomite with very small amount of fine-grained matrix (Fig. 77.1). Several generations of veins penetrate the yellow to light brown carbonate breccia. On the western slope of Csipkés Hill rauhwackes located between the Henc unit and the Bódva series can be studied (for details see chapter 7.4.1.2). The overriding Gutenstein Dolomite becomes more and more altered in the vicinity of the basal contact zone. Relatively intact, cm sized dark dolomite clasts with white calcite veins swim in reddish brown, fine-grained, highly altered matrix (Fig. 77.2). In the direct contact zone polymict, matrix rich breccia is present, defining the nappe boundary. It contains cm sized clasts both from the dolomite of Henc unit and the Rhaetian to Jurassic marls of the TV series (Fig. 77.3).

Sample P-172 and P-174 (Fig. 77.4-7) are intra-Henc rauhwackes. They are between relatively intact tectonic slices of Lower Triassic red sandstone and Gutenstein Dolomite of the Henc unit (Fig. 60). All of the samples are matrix-rich polymict breccia. The matrix is light brown and fine-grained. The clasts are mm to cm in size, and the composition is red sandstone, green marl, brown marl and limestone. Light grey limestone and dolomite are also present among the clasts. To sume, it contains all the lithologies of the Henc unit.

8.1.3. Base of the Telekesoldal nappe

This nappe contact zone between the Bódva series and the overthrusting Telekesoldal nappe was investigated from two boreholes. **Rudabánya Rb-661** (for details see chapter 7.4.2, Fig. 23) penetrated the dark shales and rhyolite-bearing horizons of the upper structural unit, then reached the base of the nappe. This lower contact zone is characterised by an almost 100 m thick evaporitic breccia, containing tectonically incorporated rhyolite and slate fragments from the upper nappe (Fig. 78.1-4). At 180.3 m the sample is a chaotic, grain-supported tectonic breccia with green rhyolite and black slate clasts. The dark slate clasts are foliated often contains folded calcite veins (187 m, Fig. 78.1-2). The

Rauhwackes of the Henc unit from N to S

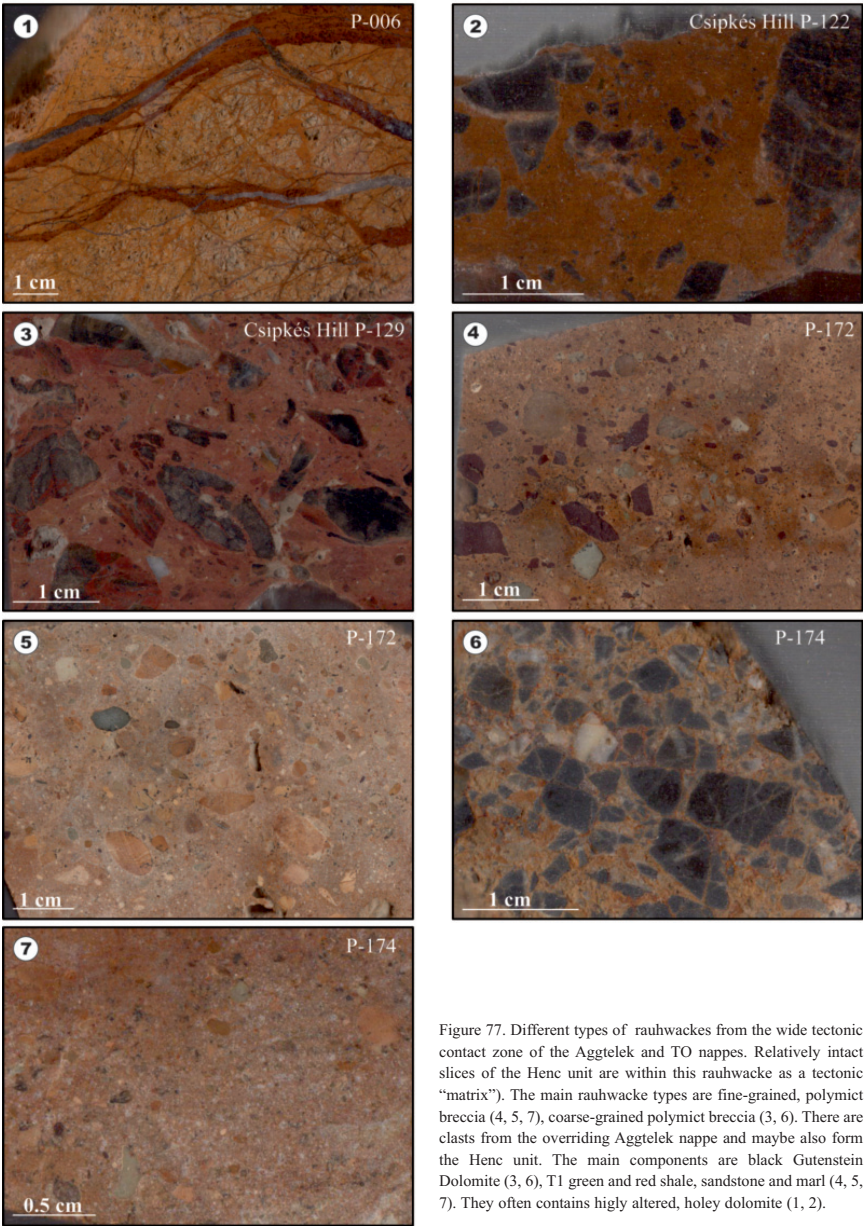

Figure 77. Different types of rauhwackes from the wide tectonic contact zone of the Aggtelek and TO nappes. Relatively intact slices of the Henc unit are within this rauhwacke as a tectonic "matrix"). The main rauhwacke types are fine-grained, polymict breccia (4, 5, 7), coarse-grained polymict breccia (3, 6). There are clasts from the overriding Aggtelek nappe and maybe also form the Henc unit. The main components are black Gutenstein Dolomite (3, 6), T1 green and red shale, sandstone and marl (4, 5, 7). They often contains higly altered, holey dolomite (1, 2).

Basal tectonic breccias of the Telekesoldal nappe

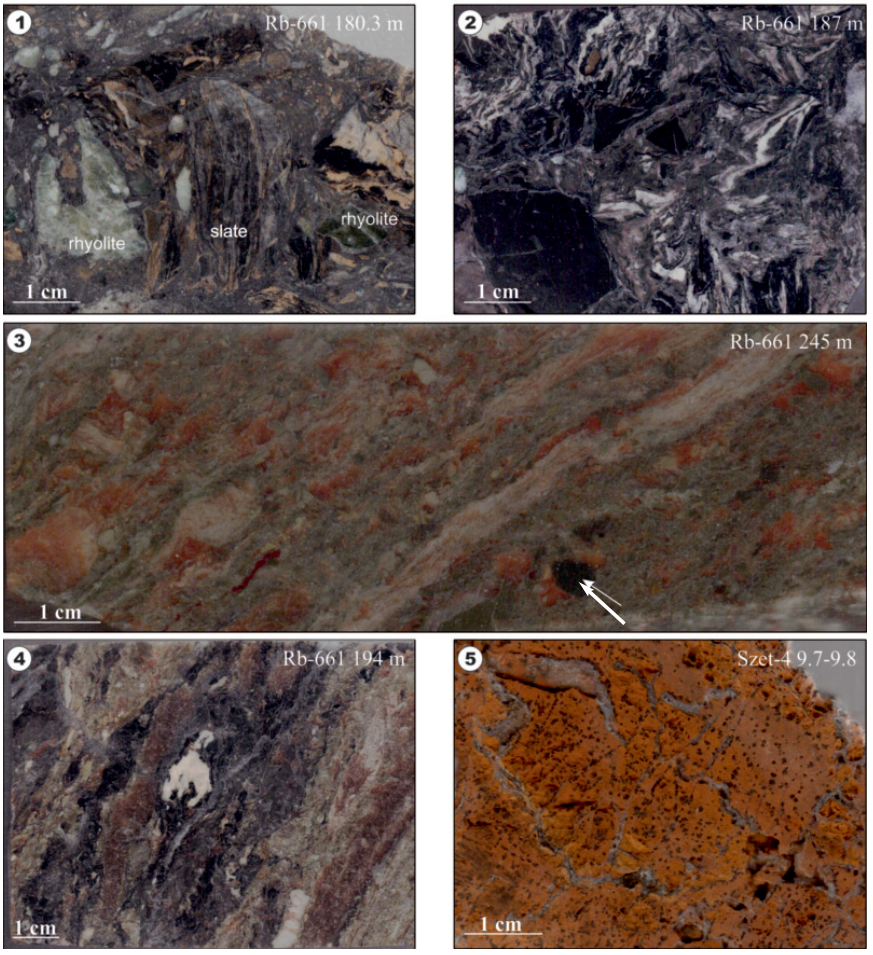

Figure 78. Different types of rauhwackes and tectonic breccias from the base of the TO nappe. In core Rb-661 TO nappe overlies an evaporitic mélange (1-4) with varying clast content. Close to the base of the TO nappe folded slate clasts are frequent along with rhyolite. The lower part of the evaporite mélange is built up by anhydrite as a matrix, gypsum, dolomite and sandstone. are the main components (3, 4). In the pressure shadow of the rigid black dolomite clasts orange gypsum crystals can grow (white arrow on 3). Borehole Szet-4 started from higly altered, pitted dolomite (5), which can be interpreted as part of the tectonic breccia zone between the TO nappe and the TV complex of the Bódva series.

folds are visible only in the slate clasts, and do not effect the matrix. It indicates that the slate had been already ductilely deformed before the formation of this basal tectonic breccia. The lower part of the contact zone is built up by sheard evaporite (mainly anhydrite), containing dolomite and gypsum clasts (Fig. 78.3-4). Dolomite clasts may derive from the lower Bódva series.

At the southeastern slope of the Csehi Hill (Appendix 3) borehole Szendrő Szet-4 (Fig. 17) started from an altered carbonate breccias, that was interpreted as the tectonic contact zone between the Telekesoldal nappe and the Bódva series (see chapter 7.4.2). This yellowish brown, alterd fault rock contains cavities after dolomite or limestone clasts, and some later cavities filled with calcite (Fig. 78.5). Several calcite veins penetrate the rauhwacke.

8.1.4. D5 contact of the Bódva series and the Telekesoldal nappe

Figure 79. Polymict rauhwacke from the D5 contact zone of Bódva series and TO nappe. It is a fine-grained, matrix rich polymict breccia with different clasts of the Bódva series.

On the southern slope of Dunnatető Hill the Bódva series thrust over the Telekesoldal nappe (Appendix 2, chapter 7.5.1). This contact zone was interpreted to be a late (D5) nappe contact. The main question of the rauhwacke studies was, if there is any difference in the fluid inclusions and the documented p and T conditions between the D4 and D5 thrust phases.

The collected P-22 sample is a matrix-rich, fine-grained, polymict breccia with 1-5 mm sized clasts (Figure 79). The matrix is reddish brown, and contains very small, mm to sub-mm sized cavities, often filled with newly formed minerals. The composition of the clasts is as follows: green shale or marl, grey marl, grey limestone, red limestone, yellow marl. Most of them may derive from the overriding Bódva series.

8.1.5. Contact of the Martonyi nappe and the Bódva series

Basal rauhwacke samples were collected east from the Bódvarákó window, where the Anisian Gutenstein Dolomite of the Martonyi nappe (Torna series) thrust over the Lower Triassic Bódvaszilas Sandstone of the Bódva series (Fig. 59e, chapter 7.4.3). The dark grey Gutenstein Dolomite of the upper nappe becomes more and more brecciated in the vicinity of the tectonic contact zone, and gradually progresses into cataclasite, then to microcataclasite and finally into matrix-rich rauhwacke (Fig. 80.1-4). Sample No 1 (Bódvarákó-1) has a reddish-brown matrix-rich texture with mm to cm sized dolomite fragments (Fig. 80.1). These fragments are usually highly altered. There are mm to cm sized cavities replacing the dolomite fragments (Fig. 80.1-2). These cavities are sometimes filled with calcite. Sample No 2 has similar texture, but there are some mm to cm sized marl or shale clasts besides the dolomites (Fig. 80.2). These clasts may derive from the lower Bódva series. TO-FL-151/a is a grain-supported dolomite breccia with reddish-brown matrix (Fig. 80.3). Greenish grey, cm sized marl clasts are also present, representing clasts from the lower nappe. The dark grey dolomite clasts most probably came from the overriding Martonyi nappe. Sample TO-FL-151/b is a finer-grained breccia with grain-supported texture (Fig. 80.4). The clasts are just mm sized, altered, brown to grey fragments. Some bigger clasts of relatively intact dark grey dolomite are also present among the smaller grains.

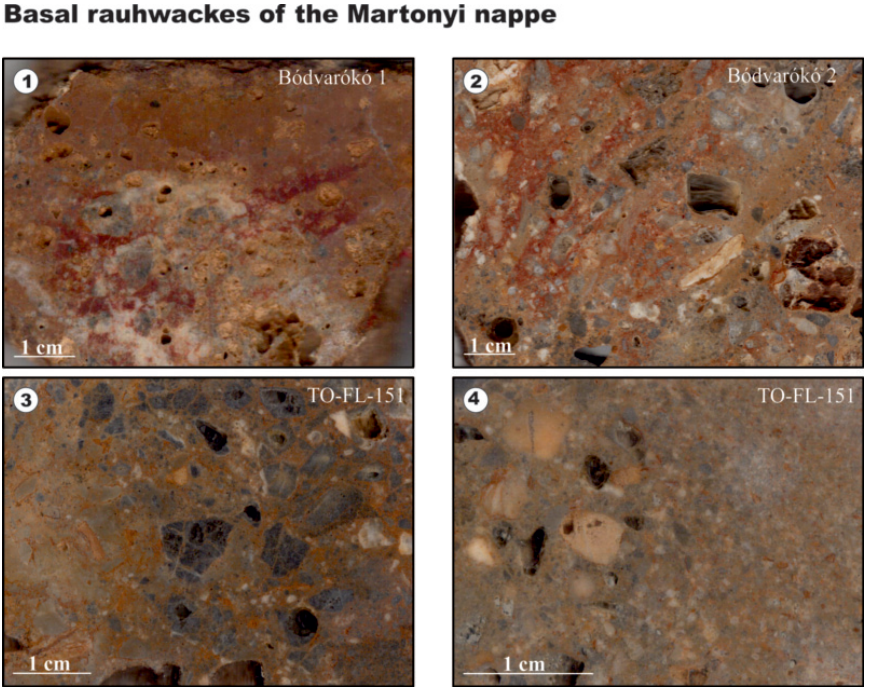

Figure 80. Rauhwackes from D4 tectonic contact zone of the Maronyi nappe (Torna series) and the Bódva series. The main rauhwacke types are poorly-sorted, polymict breccia (2, 3), and matrix-rich breccia. The main components are black Gutenstein Dolomite (3), and light grey limextone. They often contains higly altered, holey dolomite (1, 2).

8.2. FI studies

FI in authigenic quartz grains contain samples of synkinematic fluids that lubricated the thrust planes during the nappe emplacement. Samples Bódvarákó, Tilalmas Hill, Dunnatető Hill (P-22) and EGU-2 contained suitable synkinematic quartz grains for FI measurements. 72 inclusions of the Bódvarákó sample were measured, from which 50 p-T data were estimated. From the Tilalmas Hill sample group 32 inclusions were investigated, that resulted in 25 p-T datapair. 52 inclusions of EGU-2 provided 10 reliable estimates, while the 26 inclusions of Dunnatető Hill gave 16 results.

The trapped inclusions are three- to four-phase fluid inclusions containing liquid (saturated brine), vapour and halite or additional sylvite (Fig. 81.1-4). Respectively, they are either primary – trapped during crystal growth – or secondary – trapped along fracture planes. These trapped fluids are hypersaline brines of the system H_2O-NaCl-KCl-$CaCl_2$-$MgCl_2$-CO_2, with salinity of 28-42 wt.% NaCl eq. and KCl contents up to 14 wt.% (Table 2). Overall fluid salinity is calculated from the halite dissolution temperatures (Table 2), and does not reflect presence of other cations, therefore expressed as NaCl ekvivalents.

sample	FI measured	pT estimates
Bódvarákó	72	50
Tilalmas Hill	32	25
Dunnatető Hill	26	16
EGU-2	52	10

Eutectic temperatures

sample	Te
Bódvarákó-1-1-2	-50
Bódvarákó-1-2-1	-54
Bódvarákó-1-2-2	-54..-67
Bódvarákó-1-3-1	-53
Bódvarákó-1-3-13	-4
EGU-2-7-1-1	-45..-50
EGU-2-7-2-1	-45..-52
EGU-2-7-2-2	-47
EGU-2-7-4-1	-40
EGU-2-7-5-5	-50?
EGU-2-7-5-6	-43
EGU-2-7-5-8	-41
EGU-2-7-7-1	-49
EGU-2-7-7-6	-46
EGU-2-7-10-1	-46
Tilalmas-2-1-1	-32
Tilalmas-2-4-1	-44

Fluid salinity estimates

sample	min	max	n
Bódvarákó-1-1	31.6	32	3
Bódvarákó-1-2	28.1	37.7	28
Bódvarákó-1-3	33.1	35.5	25
Dunnatető-3-1	33.7	35.1	19
EGU-2-7-1	33.4	33.4	1
EGU-2-7-2	32.9	33.8	2
EGU-2-7-4	35.9	35.9	1
EGU-2-7-7	32.1	35.1	6
EGU-2-7-8	32.7	33.5	2
EGU-2-7-9	32.3	32.3	1
Tilalmas-2-2	41.9	41.9	1
Tilalmas-2-3	37.6	39.1	3
Tilalmas-2-4	36.5	39.2	21

Table 2. Measured fluid inclusion data from different rauhwackes of the Aggtelek-Rudabánya Hills. For tectonic classification of the localities see chapter 8.1)

In one sample from the base of Aggtelek nappe (EGU-7), native sulfur inclusions coexist with brine FI in heterogenous population, involving pure sulfur inclusions, pure brine FI and mixed composition FI with brine and accidentally trapped sulphur (Fig. 81.3-4). They imply existence of heterogenous mixture of two immiscible liquids on the nappe base, with molten sulfur "bubbles" intermixed with brine. Most likely mechanism to involve sulfur into circulating brine is thermochemical reduction of sulphates of the evaporites at the base of the Aggtelek Nappe (Deák-Kövér et al. 2011).

Homogenization temperatures (dissolution of halite crystal) and corresponding pressures are considered as lowest limit rather than true trapping conditions, and they vary depending on the nappe contacts. The lowest values derive from the D5 contact of Bódva (in upper position) and Telekesoldal (in lover position) nappes: 220-260 °C (Fig. 82) and 0.3-1.0 kbar (Fig. 83) (Deák-Kövér et al. 2011). These relatively low pressure values are in good correlation with the structural interpretations, considering this contact as a late, D5 nappe contact (Chapter 7.5.1, Appendix 2, Fig. 62, 67).

The supposed D4 nappe contacts (Aggtelek nappe on Telekesoldal nappe, Martonyi nappe on Bódva series) resulted in higher pressure values and much larger spans in both the temperature and pressure: 200-320 °C (Fig. 82) and 2.0-3.6 kbar (Fig. 83).

The source of the high temperature fluids is possibly the Martonyi and the Telekesoldal nappes themselves, where the peak temperature of the metamorphism (300–350 °C) correlates well with the "peak" temperature of these fluids (320 °C).

The low pressure values in case of the Bódva on Telekesoldal D5 contact strengthen our previous structural interpretation being a younger contact. However, part of the pressure data is quite enigmatic. FI from

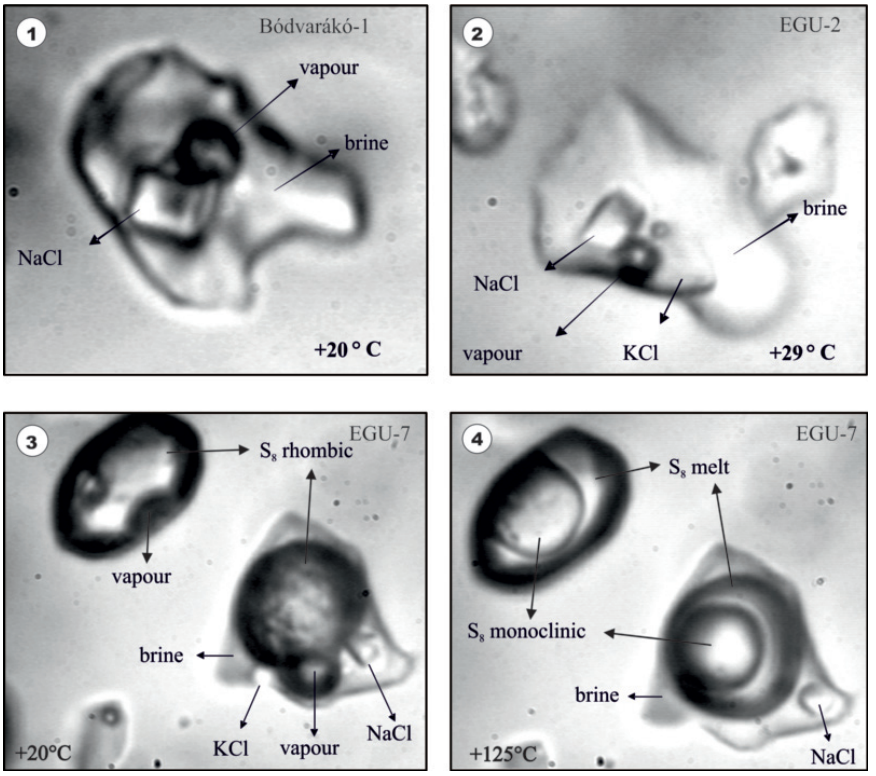

Figure 81. Samples for different kind of fluid inclusions in syndeformationally grown quartz crystals from rauhwackes.

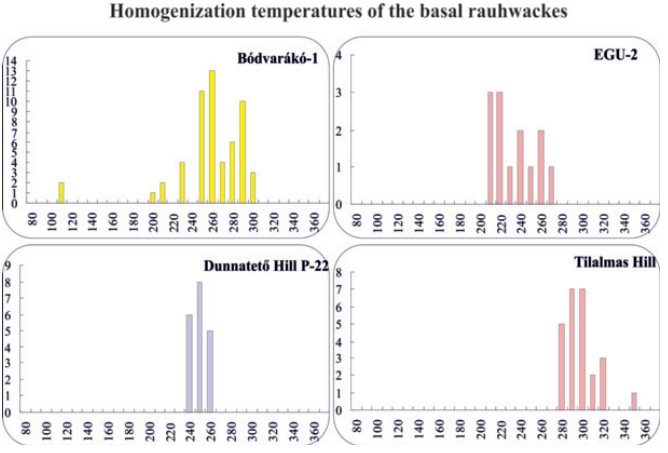

Figure 82. Homogenization temperatures from synkinematic quartz-hosted fluid inclusions. Sample P-22 is from D5 nappe contact, the others are from D4. The highest homogenization temperatures were measured, in case of D4 contacts, where low-grade rocks were involved in nappe movements (Bódvarákó, Tilalmas Hill).

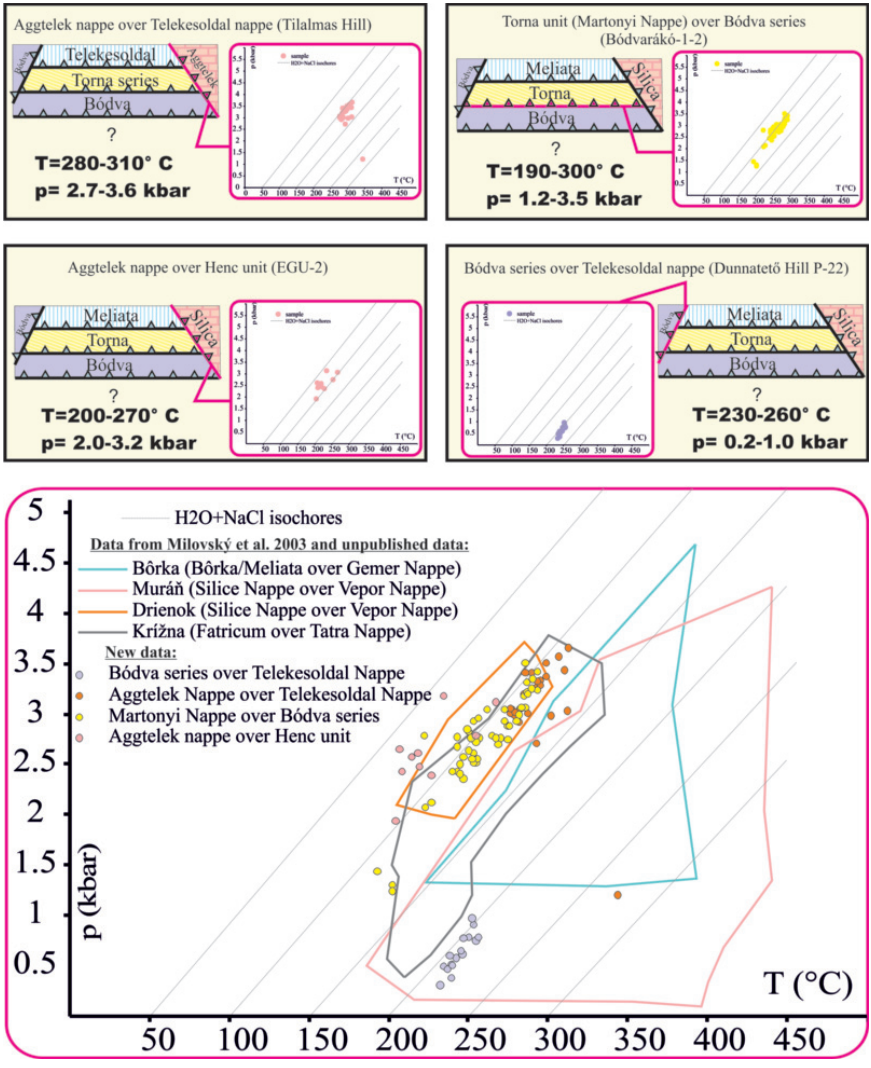

Figure 83. p-T conditions of the nappe movements estimated from fluid inclusions. D4 nappe contacts show similar values, while the p-T conditions of D5 movements were somewhat lower (purple dots). Physical conditions of D4 nappe stacking (yellow, orange and pink dots) were very similar to those measuerd in similar contatcs of the Western Carpathians (areas surrounded with colour lines).

basal Aggtelek rauhwackes refers to peak pressure of 3-3.5 kbar, while the supposed overall thickness of this nappe does not exceed 2-3 km (Szentpétery & Less 2006), referring to maximal lithostatic pressure of 1 kbar. Metamorphic petrologic data from Aggtelek nappe show no higher than diagenetic alteration even in the lower levels of the nappe (Árkai & Kovács 1986), suggesting that it always occupied an upper position in the nappestack, thus excluding its deeper burial by an even higher, now eroded tectonic unit.

This seemingly too high pressure can be caused by the enlarged stress driven by nappe emplacements. It is proven, that in convergent tectonic settings, fluid pressure may considerably exceed the lithostatic pressure, due to contribution of horizontal compressional stresses to the rock strength (Petrini & Podladchikov 2000). In the upper crust, where rocks are deformed in brittle way, the maximum sustainable fluid gradient may be as much as twice the lithostatic gradient. But in the case of the Aggtelek nappe, it is still just 2 kbar, in contrast with the estimated 3-3.5 kbar.

In summary, it is suggested, that the lowest p-T data represent "ambient" diagenetic conditions of pore fluids in basal formations. The "peak" p-T values roughly correlate with metamorphic grade of Telekesoldal and Martonyi nappes, which presumably fed the over- or underlying nappe base with their metamorphic fluids. Mixing of these hot overpressured fluids (rich in silica, alumina and alkalies) with cool formation fluids (in equilibrium with carbonates and evaporites) caused coeval precipitation of silicates (with prograde solubility) and calcite and anhydrite (retrograde solubility). Thermal overpressuring of basal fluid likely assisted thrust detachments by exceeding the shear strength of basal rocks.

8.3. Regional correlation of the obtained p-T data

Trends and patterns in p-T data for particular samples/localities strongly resemble those observed in Krížna nappe (Milovský et al., 2011) and in previously studied Murán nappe (Milovský et al. 2003). The p-T data-fields are strongly elongated roughly along isochore of H_2O-NaCl system with similar salt concentration as in the studied Rudabánya Hill brines (Fig. 83). This similarity strengthens the conclusion that the studied nappe contacts in Rudabánya Hills occupied a similar, high position in nappe pile than the Murán nappe. On the other hand, the base of the Bôrka nappe shows different values, which logically reflects its deeper structural position than the Rudabánya nappes. Finally, the p-T data of the youngest D5 thrust emplacement (Dunnatető Hill P-22) are in the low-pressure part of the data field of the Murán nappe, close to the Krížna nappe: it may mean that those Carpathian nappes could participate late-stage nappe emplacement, in addition to their higher-pressure movement.

9. Discussion

Metamorphic petrological, micro-tectonical, geochronological, sedimentological and micropaleontological data permitted the reinterpretation of the structural geometry, stratigraphical content, and stacking order of structural units in the central part of Rudabánya Hills, NE Hungary. As a result of my work the following structural units are defined in the study area.

9.1. New definition of the investigated structural units

Aggtelek nappe

The Aggtelek nappe is built up by the formations of the Silice facies unit (Fig. 8) in sense of Kovács (1989). This nappe occupies the uppermost structural position in the Aggtelek Hills. The nappe is part of the Silice nappe system (defined first by Kozur & Mock 1973) but I restrict the use of the term to a tectonic nappe found in the Aggtelek Karst area.

Henc unit

This structural unit is built up by different Triassic lithologies. At present it forms relative intact tectonic slices within the tectonic contact zone of the Aggtelek and Telekesoldal nappes. Rocks of this unit were already shown separately on the map of Less (1998) at the base of the Aggtelek nappe, what were interpreted as strike-slip lenses.

Telekesoldal nappe

The Telekesoldal complex, the Akasztó unit, the Nyúlkertlápa beds and the Hidvégardó series show very similar early deformation history (D1-D3) and well-pronounced high-temperature anchizonal to epizonal metamorphism. Their lithological characteristics are also similar (black slates, silicified or marly slates, sandstone turbidites, olistostromes). I suggest that these units were derived from the same sedimentary complex, the now enlarged TO complex.

The Telekesoldal complex represents a subduction-related complex, composed of black shales, sandstone turbidites and olistostrome horizons, deposited by gravity mass flows. Previous conception about separating the shale, sandstone olistolith, limestone olistolith and rhyolite lithofacies units in stratigraphic level and time (Grill 1988) is completely modified. The rhyolite forms not coeval subvolcanic bodies, but olistoliths. The Late Triassic volcanic age of the rhyolite is proved by new U-Pb radiometric data. The sandstone forms layers within the shale. Present-day lense-shaped occurrence of the sandstone is the result of extensional shear zones and formation of boudins in D4 or D5b deformation phase. Sandstone, micro-olistostrome and coarse-grained olistostrome layers are present in every stratigraphic level, and they do not show any kind of age distribution. Bajocian—Callovian age was proved by revising the radiolarian fauna and finding the first marine palynomorphs in the Aggtelek- Rudabánya Hills.

At present, the TO complex forms different nappe outliers of the same Telekesoldal nappe.

Torna series

New observations strengthen the conclusion of Less et al. (1988), Less (2000) and Fodor & Koroknai (2000) that the Torna series incorporates diverse Triassic successions, which were formed

on different paleogeographic position on the attenuated continental crust. In the early phase of its structural evolution (D1 in this work) it was thrust over by a nappe stack, most probably due to the ongoing subduction of the Neotethys Ocean. During this early phase the Telekesoldal complex directly juxtaposed the formations of Torna series (Chapter 7.1.2). From this time they participated in the low-grade metamorphic processes together. During this episode the Torna series suffered metamorphism under ~300-350°C and 3-4.5 kbar (Chapter 6.4, 6.5). Its deformational history can be characterized by S0-1 layer-parallel foliation, F2 tight folding and F3 kink-like folding (Fodor & Koroknai 2000) which is similar to the early deformational history of the TO complex (Chapter 7.1-7.3). This metamorphic and ductilely deformed tectonic unit thrust over the non-metamorphosed Bódva series during the D4 east to southeast verging nappe stacking phase. It resulted in the formation of the Martonyi-nappe, built up by formations of the Torna series. The later, D5 south-vergent thrust phase reorganized the nappe contacts, transporting non-metamorphic units (Bódva) again into higher structural position (e.g. Bódvarákó window). Small nappe outliers of the Martonyi nappe preserved on top of the southward moving Bódva series (e.g. Dunnatető Hill).

Bódva series

Structural units built up by the formations of this series are present in the Rudabánya Hills in two structural positions due to multiple nappe stacking events. It represents the lowermost known structural unit S to the Bódva River, where it was thrust over by the Telekesoldal nappe, the Henc unit and the Aggtelek nappe during D4 nappe stacking event. Juxtaposition of the metamorphosed TO nappe and the Bódva nappe surely postdates the very-low to low-grade metamorphic event, while the latter unit is proved to be suffered only diagenetic alteration (Chapter 6.4). This metamorphic on non-metamorphic nappe pile was reorganised by southward-verging thrusts in D5 phase, resulted in thrust of Bódva series over the TO complex.

Lithologically, the Bódva series is built up by formations of the Triassic Bódva facies unit in the sense of Kovács (1989). However, new observations and reinterpretation of several borehole data let expand the sedimentary age of the Bódva series into the Jurassic. According to this new interpretation, the Norian Hallstatt Limestone of the Bódva series gets more argillaceous upward and gradually progresses into red to green and then grey marl. Its Norian-Rhaetian age was proven by foraminifers. This variegated marl builds up the lowermost part of the TV complex. It progresses into grey marl and calcareous marl, containing significant amounts of redeposited crinoid fragments. The uppermost lithofacies unit of the TV is black shale, rich in radiolarians and sponge spicules. It is a typical deep pelagic basin facies, Bajocian to Early Bathonian in age, according to the revised radiolarian fauna.

In summary, it is suggested, that the TV complex is the original sedimentary cover of the Lower Triassic–Norian Bódva series.

9.2. Milestones of the deformation

In the next chapter I will give a short summary on the major steps in the deformation history revealed from structural, metamorphic petrographical and geochronological data.

Post-sedimentary deformation of the enlarged TO complex (including the NL beds, Jurassic rocks of the Akasztó unit, and probably the Hidvégardó series) and the Torna series started with a tectonic burial due to nappe stacking. Estimated p-T conditions are 1.5-4.5 kbar and 300-350°C, corre-

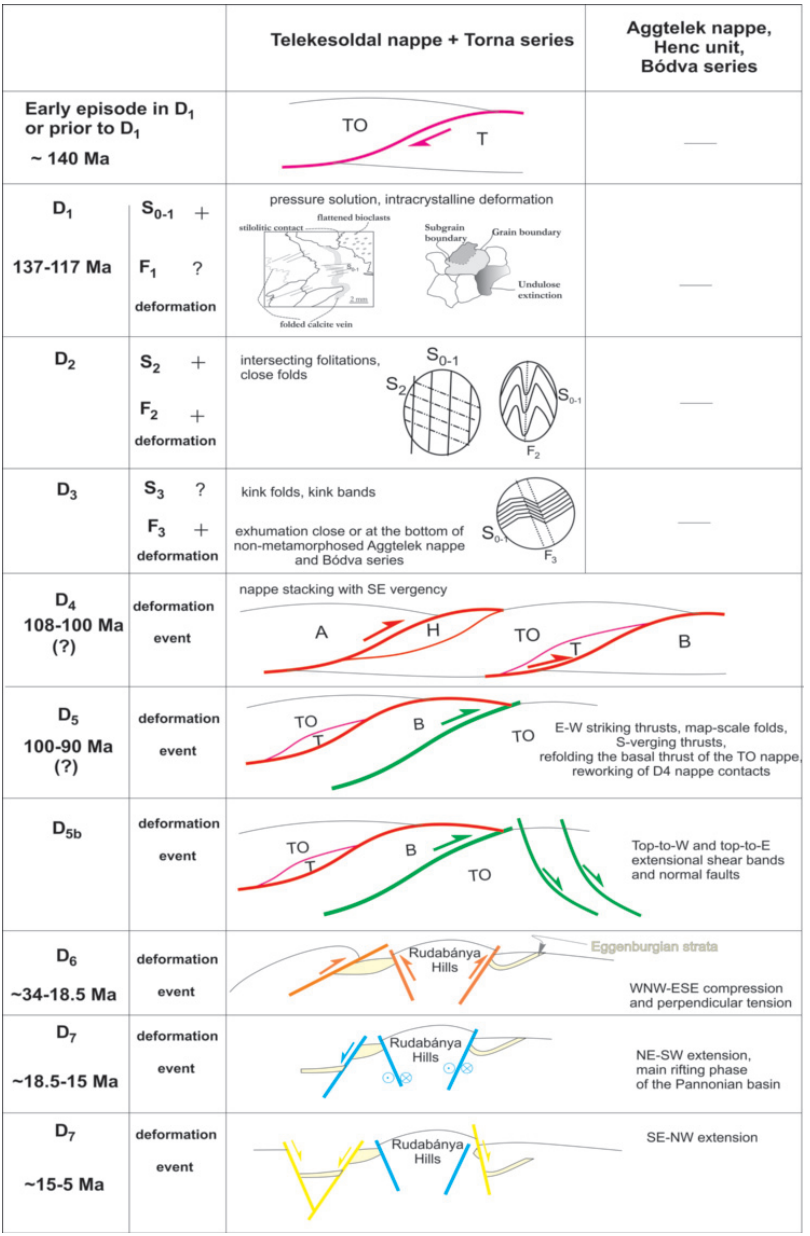

Figure 84. Milestones of the deformation observed in the central part of the Aggtelek-Rudabánya Hills. TO-Telekesoldal nappe, T-Torna series, H-Henc unit, B-Bódva series. For details see chapter 9.2.

sponding to 5–15 km burial. This tectonic burial resulted in foliation, folds, boudinage, lineation of stretched lithoclasts of the olistostromes, which represent the D1 and D2 phases (Fig. 84) in the TO nappe and in the rocks of the Torna series.

During the early part of the D1 phase or just preceeding this, the Torna series and TO nappe got in tectonic contact. This contact is preserved more or less intact in the Bódvarákó window, between the thin Bódvarákó series (Torna) and the tectonically overlying NL beds. Possibly during D2 phase the metamorphosed Torna series was localy overturned and formed large recumbent folds as proved biostratigraphyically and structurally in few places in the NE Rudabánya Hills (near Ha-3 borehole and Hidvégardó, Kovács & Árkai 1989, Fodor & Koroknai 2003).

The interpretation of K-Ar ages would put a time constraint of ca. **142 – 113 Ma** (earliest Cretaceous) for this process. The beginning of this time range indicate the oldest possible time for the low-grade metamorphic alteration, while the younger end of the time period may reflect partial resetting of the K-Ar system due to low-temperatue fluid movements connected to a later nappe stacking phase. The TO and Torna rocks were later exhumed to very shallow depth, close or at the bottom of non-metamorphosed Bódva series and its evaporitic sole. The exhumation was probably associated with kink-style folding at the transition of ductile and brittle deformation fields (D3 phase in the TO nappe and Torna series) (Fig. 84). Measured kink axes and pre-tilt reverse and thrust faults indicate NE-SW shortening for this D3 event.

The metamorphosed, deformed and exhumed TO and Torna rocks were emplaced onto the non-metamorphic Bódva series (**D_4 phase**) (Fig. 84). Outcrop- and map-scale structures refer to NW-SE compressional stress field (shortening) and southeast-vergent nappe enplacement, although the earlier model of Less (Less 2000) envisaged northwest-ward displacement of the Martonyi nappe over the Bódva series. The evaporitic sole was already involved in this movement, because it is under the TO nappe (Szö-4 and Rb-661 boreholes, respectively). The other metamorphic unit, the Torna series also participated in this phase, and formed a tectonically truncated nappe on the base of the TO nappe. On the northern part of the investigated area, it emplaced onto the non-metamorphosed Bódva unit. This is the case for Martonyi nappe, which is over the Bódva series, as mapped already by Less et al. (1988), published by Less (1998, 2000) and modified by Fodor & Koroknai (2000). A small klippe of Torna unit is also present in the same tectonic position on the Dunnatető Hill (Kövér 2005). More to the south, in the Telekes valley, only smaller-scale, tectonically truncated slices are preserved between the overriding TO nappe and the Bódva series.

Southeastward thrusting of the Aggtelek nappe also took place in this D4 phase. Several tectonic slices of different units were involved in the basal tectonic zone; this is marked mainly by evaporitic mélange in the north, and thick rauhwacke in the south. The evaporitic mélange incorporates lenses of basic and ultrabasic rocks of the Triassic oceanic crust. Lower to Upper Triassic slices of the **Henc unit** are present as relatively intact tectonic lenses within the basal rauhwacke.

Finally, the metamorphosed over non-metamorphosed tectonic couplet was thrust again onto the metamorphic TO nappe along an E-W striking thrust in the Bódva gorge (**D_5 phase**, Szalonna thrust of Szentpétery & Less 2006). Thrusting associated with reworking of the previous nappe contacts and map-scale F5 folding. This folding bended the basal D_4 thrust of the TO and the Martonyi nappe, and also the overthrusting Bódva series. Fold vergency of this deformation phase indicates southward tectonic transport. This was recognised by earlier workers and correctly figured on maps (Less et al. 1988, Less & Mello 2004, Péró et al. 2003). However, they tempted to relate this late event to the early nappe stacking, which is not the case on the basis of the recent structural analyses (Kövér

2005, Kövér et al. 2008).

Similar south-vergent thrusts were recognised SW from the study area, near Szőlősardó (Horváth 2010, Horváth et al. 2012). However, no metamorphic units were involved in the deformation, but thrusting and duplex-formation involved rocks similar to the Bódva series. Late-stage thrusting was recognised by the tectonic contacts of younger on older formations (tectonic omissions) and rauhwackes.

Grill et al. (1984) and Less (2000) considered the D_4 phase overthrusting of the Martonyi nappe as Miocene in age. However, the structures of the D_4 and D_5 phases are cut by the mid-Oligocene to Miocene-age Darnó Fault and covered by late Palaeogene sediments on both sides of the Rudabánya Hills, as shown on the pre-Cenozoic basement map of Haas et al. (2010). This geometry contradicts to the very young age of thrusting and put it back into the early Palaeogene or to the Cretaceous. In fact, the two K-Ar ages around 90-91 Ma (**87–94 Ma** within error bars) can tentatively be connected to any of the **D_4-D_5 phases**, which we consider as early Late Cretaceous in age (Fig. 84). The D_4 –D_5 phases obliterated the relative order of the primary D1 or earlier nappe stack. It is probably these deformation events which led to confusions and controversial views on the position of the different structural units. Tectonic units built up by the metamorphosed Triassic Torna series and Jurassic TO nappe can be located either above or below the different suites of the Bódva series and these suggested positions are probably not due to misunderstanding the structural geometry but to real complications of the D_4 and D_5 phases.

A notable extensional deformation, D5b was probably connected to the D5 phase: it appears in the now underthrusting TO unit, and may reflect the vertical loading of the overthrusting Bódva unit. Th resulted extension is perpendicular to the inferred south-vergent thrust motion.

The D1-D5 phases were followed by the widespread **denudation phases** which are characteristic in considerable part of the Pannonian-Carpathian area. The Cenozoic sedimentation started only in the mid-Oligocene near the Rudabánya Hills (Szentpétery & Less 2006). The formation of a compressional basin can be placed in the late Early Oligocene, documented by remnants of Kiscellian Formation. The origin of the basin was connected to shortening and crustal loading (Sztanó & Tari 1993) and the corresponding stress field was equally compressional (Fodor et al. 2005). This is probably this regional basin-forming deformation, to which the **D6** phase can be connected. In the Rudabánya Hills only small-scale faults appear. Further to the S (Alsótelekes Barbara quarry) Mesozoic rocks thrust over Early Miocene (Eggenburgian) (Fig. 84). The age of this phase can be **30-18.5 Ma**.

The following **D7** phase includes extensional and strike-slip faults, which dissects the established nappe pile. This phase can be correlated with the rifting of the Pannonian basin system (Fodor et al. 1999). Locally the rifting could have trastensional character and may involve sinsitral displacement along the Darnó zone. However, this slip could be just a reactivation of earlier faults, mostly strike-slip faults, and large-scale displacement was not demonstrated within the Rudabánya and Aggtelek Hills (Fig. 84). More important displacement could be located at the eastern margin of the Rudabánya Hills, where disturbed Miocene rocks are exposed (Szentpétery 1997). The last **D8** phase resulted in activation of normal faults. They can bound the Rudabánya Hills on the west, and other moderate displacement occur SW from the study area, near Szőlősardó (Horváth et al. 2012). NNE-SSW directed normal fault displaced all previous contacts at the eastern Rudabánya margin, as suggested by Fodor & Koroknai (2000). This deformation lasted from late Badenian to the Pliocene. No particular evidence was found for neotectonic deformation within the investigated area.

9.3. Regional correlation

9.3.1. Aggtelek nappe – part of the Silice nappe system

In the next chapter I will give a short overview about the correlation possibilities between the investigated nappes and the nappes of the Inner Western Carpathians (Fig. 85).

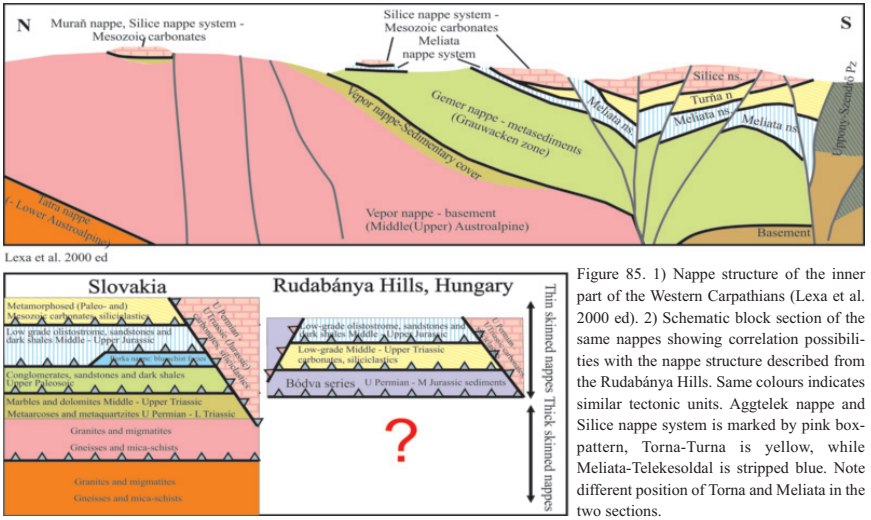

Figure 85. 1) Nappe structure of the inner part of the Western Carpathians (Lexa et al. 2000 ed). 2) Schematic block section of the same nappes showing correlation possibilities with the nappe structure described from the Rudabánya Hills. Same colours indicates similar tectonic units. Aggtelek nappe and Silice nappe system is marked by pink box-pattern, Torna-Turna is yellow, while Meliata-Telekesoldal is stripped blue. Note different position of Torna and Meliata in the two sections.

The Aggtelek nappe occupies the uppermost postiton in the nappe pile of the Aggtelek-Rudabánya Hills. Its lithological content, non-metamorphic nature and structural position strengthen its classification into the Silice nappe system, which was suggested by several authors (Kovács 1989, Less 2000, Szentpétery & Less 2006). On basis of my structural and metamorphic petrographical investigations, I agree with this classification (Fig. 85); while no signs of metamorphism or ductile deformation were found.

However, there is no such agreement about the original paleogeographic position of the Silice nappe system. Kovács (1984, 1989), and Less (2000) suggested the northern margin of the Neotethys Ocean as the original paleogeographic position. The main reason was the polarity of the facies units in the Middle and Late Triassic. The carbonate platform of the Aggtelek facies unit was facing to the south, where the Szőlősardó facies unit represented its slope more to the south. According to this classical model, the formations of the Bódva facies unit deposited in the basin, even more to the south from the Szőlősardó facies unit (Fig. 3., Kovács 1984, 1989). In contrast with this concept, Csontos (2000) and Csontos & Vörös (2004) interpreted the Silice nappe system as an exotic unit, a microcontinent, which detached from its original basement during the opening of the Neotethys Ocean. Even in this scenario, the nappe system would have originated from the northern margin of the ocean, but displaced prior to the onset of subduction. On the other hand, Hók et al. (1995), Rakús (1996) and Rakús et al. (1998) interpreted this unit as having been originated from the southern margin of the Meliata ocean.

9.3.2. Telekesoldal nappe – part of the Meliata nappe system

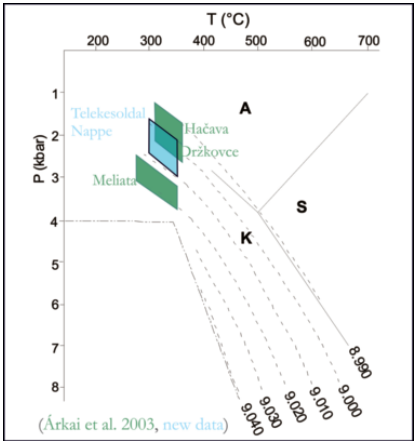

Figure 86. p-T data of the Early Cretaceous low-grade metamorphism in different nappes of the Meliata nappe system. This event post-dates the HP metamorphism of the Borka nappe slices. Green fields indicate data of Árkai et al. (2003).

Temperature, pressure and K-Ar isotopic age data obtained on the Jurassic metamorphic complex of Rudabánya Hills (TO, NL, Akasztó unit, and probably the Hidvégardó series) can now be compared with the values published by Árkai et al. (2003) from the Meliata nappe system, which represents an accretionary wedge. This unit is considered to be remnant of the subducted margin of the Meliata–Hallstatt branch of the Neotethys. The oldest tectonometamorphic event could be the subduction-related blueschist facies metamorphism (160–155 Ma; Faryad & Henjes-Kunst 1997, Maluski et al. 1993, Dallmeyer et al. 1996) which was only preserved in the blueschist facies tectonic units. The retrogression of the blueschist facies blocks and the coeval, prograde, high-T anchizonal metamorphism of the slaty "matrix" occurred between ca. 120 and 150 Ma, culminating probably at ca. 145–140 Ma, indicated by K-Ar age data determined on <2 μm size illite–K-white mica-rich fraction samples (Árkai 2003). The now-enlarged TO nappe show similar p–T conditions as the Meliata, Hacava and Držkovce localities of Meliata nappe system (Fig. 86), with which they share common lithological characteristics (Chapter 5.6.1). The temperature conditions of the Early Cretaceous very low to low-grade metamorphic event were similarly ca. 270-350°C at the Meliata type locality and TO (300-350°C), and slightly higher (ca. 340-350°C) at Hacava and Držkovce. Comparing the pressure data – on basis of the K-white mica b parameters – Držkovce, Hačava localities and the TO complex might represent lower pressure segments (min. 1.5–2.5 kbar), while Jurassic slates of the Meliata locality may be considered as a relatively higher pressure one (ca. 3.5 kbar). The age of metamorphism, deduced from the K-Ar data are very similar in the Meliata slates (ca. 150-120 Ma) and in the TO nappe (142-113 Ma). In summary, all of these similarities make possible to interpret the TO nappe as part of the Meliata nappe system of the widest sense (Fig. 85). This corroborates with conclusions suggested earlier by other authors (e.g. Csontos 1988, 1999).

9.3.3. Torna series – part of the Turna structural unit

The correlation of the low-grade metamorphosed Torna series of the Rudabánya Hills and the Turna nappe in Slovakia is a widespread idea, supported by most of the previous authors (Mello & Mock 1977, Less 1981, Less et al. 1988, Kovács et al. 1989, Árkai & Kovács 1986, Less 2000). In Slovakia, the anchi- to epimetamorphosed Turna series is classified into two nappes (Turna nappe and Slovenská skala nappe), and thought to thrust over the Meliata nappe (Plašienka et al. 1997). However, this relation is the opposite, seen from Hungary (Chapter 7.1.2, Fig. 85). As we expressed earlier (Kövér et al. 2009a), this controversy can be apparent, and the position of Torna/ Turna was reorganised several times with respect to first nappe stacking: during the D4 or D5 thrusting. These

late complications hinder the possibility to use the present-day position in the nappe stack for inferring the original nappe order.

The sequence of nappes was thought to reflect their paleogeographic position: the Turna nappe was placed by most authors on the southern side of the Neotethys Ocen (Plašienka 2000), although most recently Schmid et al. (2008) put it on the northern continental margin.

Lower structural units of the Western Carpathians are not exposed on the investigated area. However, the Bódva series, which occupies the lowest known structural position (Fig. 59, Appendix 3) has no equivalent unit further to the north (Fig. 85).

9.3.4 Geodynamic implication

In this chapter, I will present a wider geodynamic frame in which my research results can be incorporated. Of course, mainly ideas and models are suggested here, with the extensive use of former models, which were based on much wider experience than may detailed, but geographically limited works.

Concerning the Triassic paleogeography, my work did not resulted in major contribution, thus I accepted former models which count the existence of the Meliata Ocean and its attenuated continental margins. The only remark I can made that the Aggtelek–Szőlősardó–Bódva margin and the Torna/Turna and Bôrka should not necessarily placed on the same margin (as did Schmid et al. 2008). It is possible that the different sequences were derived from different positions, even from the same side of the margin. This is why I indicated two possible margin scenarios on Fig. 87.1.

Following my interpretations in chapter 5.3.5, a subduction-related basin can be supposed for the depositional area of the shales, sandstones and olistostromes of the Telekesoldal nappe, as part of the Meliata nappe system (Fig. 87.2). We have evidence for Bajocian-Callovian sedimentary age (~160-170 Ma) (Kövér et al. 2009b). Basalt clasts of the Meliata and TO units, which derived from the oceanic crust of the Neotethys Ocean can be explained by two separate ways. The first option suggests partial obduction of the oceanic crust onto the West Carpathian margin. This model was supposed by Schmid et al (2008). The obducting ophiolite thrust onto the pre-Permian basement. To keep the Silice nappe system in an upper, non-metamorphosed position, they suggested a crocodile structure for the northern margin: the obduction of the ophiolite and related accretionary wedge was bounded by a roof thrust. Presumably the Permian evaporite worked as a roof-thrust separating the underplating oceanic-derived nappe from the higher Mesozoic cover nappes (Silice nappe system). This model has several advantages e.g. explains the ophiolite clasts in the basal tectonic mélange of the Silice nappe system without placing the whole nappe system into a more southerly position than the oceanic crust. There is no need for deriving the Silice nappes either from the southern margin of the Neotethys Ocean (Hók et al. 1995, Lexa et al. 2003), or interpreting them as microcontinents or extensional allochtons (Rakús 1996, Rakús et al. 1998, Csontos 1999, Csontos & Vörös 2004). The case is the same for the Meliata-Silice nappe order, what can be explained easily with this model. However, there are some unexplained points, too. One of them is the deep subduction, HP metamorphism of the attenuated margin crust (Bôrka) and its exhumation onto the foot of the Silice nappe system.

Looking from the Eastern Alps, Jurassic obduction of the oceanic crust was suggested by other authors on basis of sedimentological observations. Tectonic shortening resulted in N-verging nappe movements started from the early Callovian was suggested by Gawlick et al. (1999) and slightly modified by Missoni & Gawlick (2011). The oceanic crust and the Mesozoic cover units of the atten-

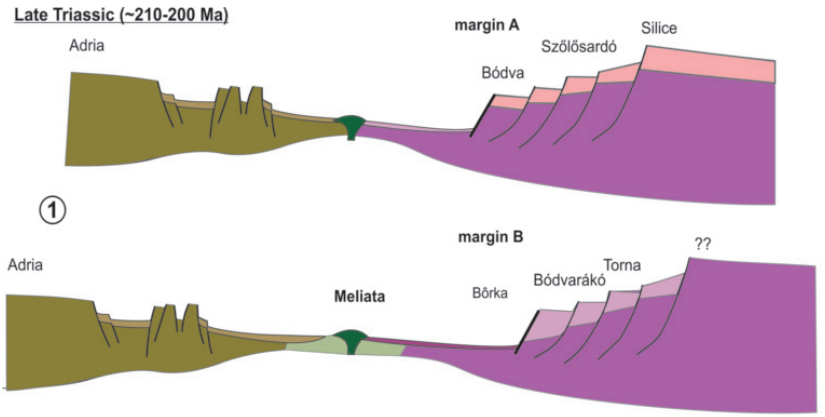

Figure 87. Suggested reconstruction of the Late Triassic - mid-Cretaceous geodynamic evolution. **1) Late Triassic**: supposed paleogeographic connections of the investigated units. They may derive from the same margin of the Meliata Ocean, but probably represents different segments of the Carpathian margin.

uated continental crust (Zlambach, Hallstatt, Dachstein facies zones) were involved in this nappe thrusting. At the front of the nappes sedimentary basins were formed supplied by clasts from the overriding structural units (for details, see chapter 5.6.2). This model does not depict the West Carpathian situation, where not the obducted oceanic crust occupies the highest tectonic position.

In my model I accept another concept, that the basalt clasts of the Meliata (including the TO complex) could derive from the upper oceanic plate of the ongoing intra-oceanic subduction (Figure 87.2). The Triassic pelagic limestone, marl and shale clasts might have originated from the cover of the attenuated continental crust, from which thin slices were detached, thrust onto the West Carpathian continental margin, and formed an imbricate wedge with slightly elevated topography. This thrusting concerned only the uppermost, Mesozoic part of the crust indicated by the clast composition. Such small imbricate structures could be the source to the southerly (and not northerly) located TO complex and Meliata accretionary wedge.

Southward subduction of the deeper part of crust was continuous during the subduction-related basin formation. During this time, some of the thinned continental and also oceanic crustal fragments, grouped in the Borka nappe were under way in the subduction channel. These slices, with both oceanic and continental crust protolith (Faryad 1995, Faryad & Henjes-Kunst 1997) suffered subduction-related HP metamorphism (Faryad & Henjes-Kunst 1997, Maluski et al. 1993, Dallmeyer et al. 1996). Although the 160–155 Ma metamorphism is a little bit younger event than the formation of the sedimentary basins (170-160 Ma) located on top of the subducting plate (Fig. 87.2), the two processes were roughly coeval.

Opening of the Penninic Ocean far to the west in Jurassic time lead to sinistral strike slip movements, and reorganisation of the westernmost part of the Neotethyan oceanic realm (Schmid et al. 2004, 2008, Stüwe & Schuster 2010). These Jurassic strike-slip movements were suggested in the Eastern Alps (Schuster & Frank 1999, Frank & Schlager 2006). According to Stüwe & Schuster (2010) the strike-slip motion has to be later than the obduction of the Dinaric ophiolite nappes

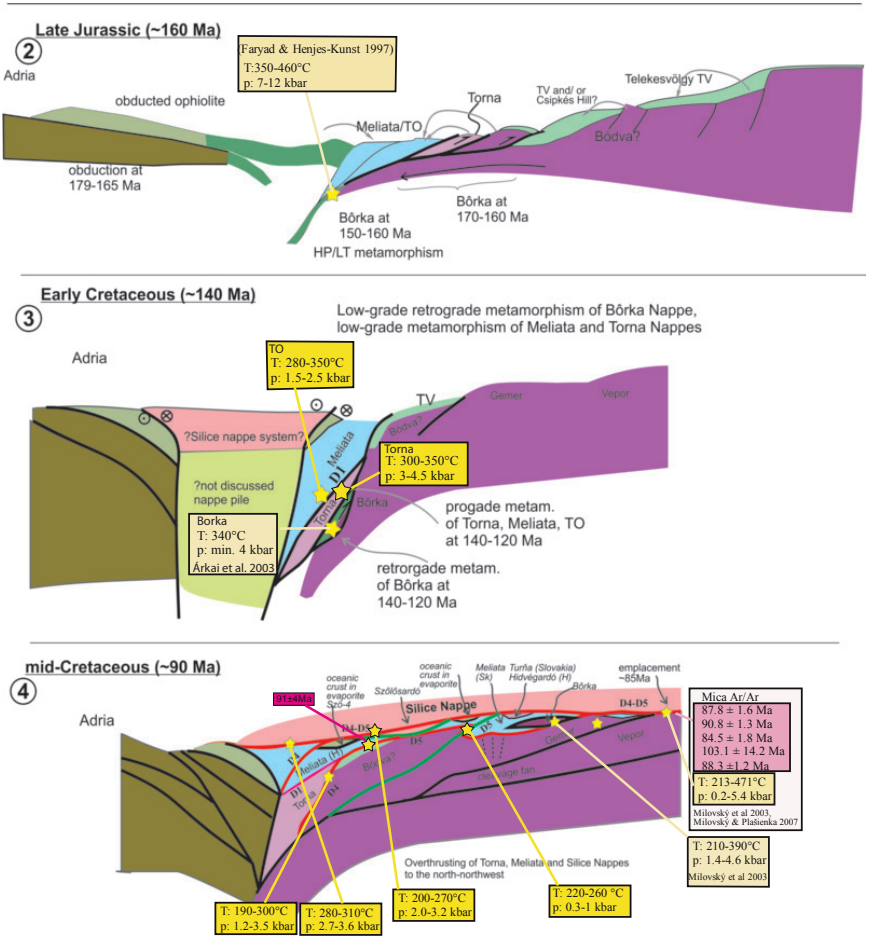

Figure 87. **2) Late Jurassic** depositional environment of the Meliata/TO units in a subduction-related basin. Basalt clasts may derive from the upper plate of the intra-oceanic subduction. Triassic pelagic limestone clasts are originated from detached slices of the uppermost part of the attenuated continental crust, which thtust onto the Carpathian margin. The ocean-continent transition zone represented by the Borka nappe enters the subduction zone, then suffer subduction related HP metamorphism at 160-155 Ma (Faryad & Henjes-Kunst 1997). **3) Early Cretaceous**: as a result of the Jurassic sinistral strike-slip movements the Silice nappe system has been transported into the investigated section. It can partly overrides ophiolitic units. The ongoing subductiun of the Carpathian margin drags the Torna and Meliata units into greater crustal depth, causing low-grade metamorphism. The HP metamorphosed Borka nappe is exhuming onto the foot of the Meliata-Torna units, and suffer retrograde low-grade metamorphism (120-140 Ma). **4) mid-Cretaceous**: major post-metamorphic nappe-stacking event (D4-D5) resulted in the described structural order of the tectonic units.

(170–160 Ma) and earlier than the onset of the Eoalpine compression in the Early Cretaceous (135 Ma). Frank & Schlager (2006) argued that Late Jurassic tectonics leading to the mentioned basin formations described by Gawlick et al. (1999) are related to this sinistral strike-slip event. Possible con-

tinuation of this sinistral strike-slip system further to the E, towards the area of the Western Carpathians was suggested by Frank & Schlager (2006).

My suggestion is that these movements may transport thinned continental fragments deriving from the NW margin of the Neotethys system far to the E, to the investigated area (Fig. 87.3). This would be the event which brings the Silice nappe system in the model section. The Silice nappe system could be in contact with the Meliata accretionary wedge, at least partly overthrusting it. This is the explanation why the basal evaporitic sole of the Silice nappes contains blocks from the obducted ophiolite pile.

Coeval and slightly post-dating this strike-slip event, in the early Cretaceous, subduction of the deeper continental crust of the West Carpathian margin continued. The uppermost, Mesozoic part of the thinned and already imbricated crust also entered the subduction zone, indicated by the medium-pressure metamorphism of the Torna structural unit (Fig. 87.3). Part of the Jurassic Meliata/TO sediments submerged into the subduction zone, too. This is the time (D1 phase of present work) when the Torna structural unit underplates the tectonically buried Meliata sedimentary mélange. Meanwhile, part of the already HP metamorphosed oceanic and continental crustal fragments (Borka nappe) completed their ascent in the subduction channel. This exhumation took place up to the foot of the buried Meliata sedimentary mélange.

Ongoing compression pushed tectonic slices of the HP unit into the Meliata unit as a tectonic matrix. From this point, it is not only a sedimentary, but also a tectonic mélange, containing slices of the exhumed HP Borka nappe. Shear direction from blueschists indicates northward transport (Faryad & Henjes-Kunst, 1997). In summary, the Torna–Meliata–Bôrka structural units get in contact in this relatively early time (~140 Ma). Low-grade prograde metamorphism of the Torna and Meliata tectonic units and retrograde metamorphism of the Bôrka HP nappe were coeval, indicated by K-Ar data (140-120 Ma; Árkai et al. 2003, and the present study). Position of the Bôrka HP nappe in the Meliata mélange as a tectonic "matrix" can explain its controversial tectonic position, situating either below or within the lower-grade Meliata nappe sensu strict. The juxtaposition and retrograde metamorphism largely post-dated the obduction, and slightly the presumed strike-slip displacement. On the other hand, the load of the Silice nappe system was probably not enough for the metamorphism of the coupled Torna and Meliata units, as one can infer from the model of Schmid et al. (2008). This is why I suggest deep tectonic burial of the combined Meliata-Torna units related to ongoing (renewed) subduction process (Fig. 87.3).

This low-grade metamorphism of the Meliata nappe system pre-dates the Cretaceous (110–90 Ma) metamorphism of the Gemer and Vepor nappes (Cambel & Král 1989, Plašienka 1991, Putiš 1991, Maluski et al. 1993, Kováč et al. 1994, Dallmeyer et al., 1996, Plašienka et al. 1997, Lexa et al. 2003) which underlie the Meliata nappe system in Slovakia. During this time span, the subduction shifted to the north, to the Vahic Ocean, which is the eastward continuation of the South Penninic Ocean (Plašienka 1999). The medium-grade metamorphism of the Vepor nappe (structurally equivalent with the Silvretta-Seckau nappe system in the Eastern Alps; Schmid et al. 2008) was connected to this event (Plašienka et al. 1997, Plašienka 1998).

However, more recent works of Janák et al. (2004) and Stüwe & Schuster (2010) connect this 90-100 Ma Eoalpine metamorphic event of the Upper Austroalpine nappes to the south-verging intracontinental subduction initiated within the continental (Austroalpine) plate. So maybe the metamorphism of the Vepor nappe is connected to this intracontinental subduction event.

This mid-Cretaceous Eoalpine phase resulted in both thick-skinned and thin-skinned nappe

movements in the Western Carpathians, too. Nappe emplacement is younging towards the NNW, as also indicated by propagation of foreland basins (Plašienka 1997, 1998, 2000). Measured tectonic transport directions are also to the N–NNW (Hók et al. 1993, 1994, 1995; Plašienka 1991; Putiš 1991) in several Western Carpathian units.

In the Silice – Meliata –Torna domain, the time period from ca. 115 up to 90 Ma correspond to major post-metamorphic nappe emplacements, which is testified by D4 and D5 phases in the Rudabánya Hills (Fig. 87.4). First, following the metamorphism and prior to the next major events, the coupled Meliata–Torna units should be exhumed close to the surface, probably close to the base of the Silice nappes. In the investigated area, during the D4 phase, the Silice nappe system definitely covered both the Meliata-TO and Torna units. On the other hand, the metamorphosed, ductilely deformed and exhumed units were thrust onto non-metamorphosed Bódva unit.

These nappe movements reached considerable distances, like demonstrated by the far-travelled slices of blueschist facies metamorphic rocks over the Gemer unit (Mello et al. 1997). Thin-skinned nappes of the Silice nappe system were also thrust over large distances along layers of fluid-overpressured cataclastic mush (rauhwacke). Among them, one of the final events could be the juxtaposition of the Muráň nappe (Silice nappe system) with the Vepor nappe, whose basal rauhwacke were dated as ~85 Ma (Milovský & Plašienka 2007). The Permian evaporitic sole of Silice nappe (similarly to the Juvavic nappes in the Northern Calcareous Alps; Gawlick et al. 1999), comprises tectonically incorporated Mesozoic ophiolitic fragments. This implies that during its emplacement, the nappe tore off some parts of the Meliata nappe and transported them above other units.

This is possibly also the time span when a cleavage fan formed in the Gemer unit (Lexa et al. 2003). They attributed this deformation to ~N-S shortening, which is also observed in the Rudabánya Hills, thus the events could be coeval and result from the same late-stage shortening of the complex nappe pile (Fig. 87.4).

Part of the D1 nappe contacts of Meliata–Bôrka–Torna were kept during this phase, like it could be the case for the Bódvarákó window. In the Rudabánya Hills, the Torna tectonic unit is preserved as lenses on the base of the Meliata nappe. However, reorganisation of the slices of the exhumed Meliata, Torna/Turňa and Bôrka nappes took place during these D4 and particularly D5 phases. These are the phases during which the Torna unit thrust over the Meliata sensu lato (formerly Hidvégardó series) in the northern Rudabánya Hills (Fig. 6., 7., 87.4.). This is why the Turňa nappe in Slovakia frequently positioned just below the Silice nappe. These late-stage nappe emplacement dominate the present tectonic structure of the Inner Western Carpathians. They are largely responsible for the contradictory views on the structure of the Aggtelek–Gemer–Rudabánya area. Hopefully, my work contributed in dissolving some of these controversies clarifying some points in the structure and structural evolution of this area.

10. Final conclusions

In my PhD work I established a new model on the Mesozoic tectonic evolution of the central part of the Rudabánya Hills. I combined structural, metamorphic petrological, geochronological and sedimentological investigations. As a result of this complex study, I defined the following structural units: Aggtelek nappe, Henc unit, Telekesodal nappe, Torna series, and Bódva series.

The Aggtelek nappe is part of the Silice nappe system and it is built up by a non-metamorphosed Upper Permian – Upper Triassic series. It is the uppermost nappe of the nappe-pile.

The Henc unit is built up by tectonic slices of Lower to Upper Triassic rocks. These slices are tectonically sheared into the wide nappe contact zone of the Aggtelek and Telekesoldal nappe marked by rauhwacke.

The Telekesoldal nappe is part of the Meliata nappe system, and its sedimentary age extends from Bajocian to Callovian evidenced by revision of the radiolarian fauna and new findings of dynoflagellata cysts. It is a subduction-related complex formed mainly by gravitational mass movements. Within the whole complex grain size alternates from clay (slate) to 100 m-sized olistolith blocks. Olistoliths and sandstone layers are present in each stratigraphic level. The main components are grey pelagic limestones, rhyolite and basalt. The different sized rhyolite clasts and bodies present in TO complex are proved to be olistoliths. 200–220 Ma formation age was evidenced by U/Pb method applied on zircon grains. Basalt clasts most probably derived from the uppermost part of the Mesozoic oceanic crust, referring to at least a close position of the oceanic upper crust and the depositional area.

The TO nappe together with the Torna series suffered very-low to low-grade metamorphism at ca. 140 Ma proved by metamorphic petrological and K/Ar geochronological data. The contact of these two tectonic units pre-dates the metamorphism. During this deep tectonic burial they were deformed in 3 phases by ductile deformation, probably between ca. 140 and 120 Ma. They participated in the post-metamorphic nappe movements together, preserving D1 nappe contacts in some localities e.g. in the Bódvarákó window and in the Telekes Valley Tributary Valley 8.

Concerning the Lower to Upper Triassic Bódva series the main result was finding evidences for its Jurassic sedimentary cover. It is most probable, that the Norian Hallstatt Limestone continuously develops into the variegated then grey marl of the Telekesvölgy complex. Age of the grey marl was determined Norian-Rhaetian by right of its foraminifera fauna. Sedimentary age of the upper part of the complex was refined to Bajocian-Bathonian by revising its radiolarian fauna.

The previously described structural units thrust onto each other in the Eoalpine phase (90-100 Ma) indicated by reset K/Ar ages. This D4 phase resulted in juxtaposition of the metamorphosed and the non-metamorphosed structural units. The vergency of the nappe movements was top-to-southeast in the central part of the Rudabánya Hills. Overthrusting of the Aggtelek nappe may indicates the last event of this phase. S-verging thrusts crosscut the previous nappe contacts in the next D5 phase. This deformation phase characterised by N-S compression resulted in large-scale folding, causing bended D4 nappe-contacts and locally overturning of the Bódva series. Finally, Cenozoic movements along reverse, strike-slip and normal faults complicated the present day structural geometry during D6, D7 and D8 phases. These deformations lasted from late Palaeogene up to the Pliocene.

Relative chronology of D4 and D5 thrust contacts were supplied by p-T data from basal cataclastic breccias of the overthrusting units. These contact zones are characterized by tectonic rauhwack-

es, which preserve newly-formed minerals grown from the circulating fluids during nappe emplacement. Trapped fluids in synkinematic minerals indicated temperature up to 200-320°C and pressure up to 3.6 kbar during the D4 nappe movements. Hot fluids most probably derived from the metamorphic units. Fluid inclusions from the D5 contact resulted in significantly lower p-T values, indicating thrusts in shallower crustal level.

These new results could be obtained only by the integration of tectonic, sedimentological, micropaleontological, metamorphic petrological and geochronological methods. Joint application of metamorphic petrologic data and observation of ductile deformation features lead to reliable classification of the structural units characterised by relatively small differences in lithology and burial depth. Along with the great number of KI and AI measurements the investigation of deformation mechanisms can be a great help approaching the transition zone of deep diagenesis and low-grade metamorphism. Classical micro- and meso-scale tectonic observations and stress field analysis are equally important in structural reconstruction. All these methods can be effectively supported by the studies of rauhwackes. These rocks provide essential information about the physical conditions of the structural movements, and makes easier to set up relative chronological orders. Ar-Ar or K-Ar age determination of the synkinematic micas can provide indispensable radiometric age, as was demonstrated for the Western Carpathians (Milovský et al. 2003), and hoped in the future for the study area as well.

As a summary, in an area built up by a diagenetic to low-grade metamorphosed thin-skinned nappe pile reliable model on the structural evolution can be set up only by the synchronous usage of a wide spectrum of methods.

11. Summary

During the PhD research a complex thin-skinned nappe pile of the Inner Western Carpathians was studied in the central part of the Rudabánya Hills. I suggested a new structural model and evolution on the basis of structural, metamorphic petrological, geochronological and paleontological data. The main directions of my work were (I) sedimentary features and age of the Jurassic subduction-related formations (II) new definition or redefinition of the tectonic units, (III) polydeformational tectonic evolution of the different nappes, (IV) p-T conditions of the metamorphic event in different tectonic units, (V) dating of the deformation phases (VI) p-T conditions of the nappe movements.

I redefined the lithological content, sedimentary age, metamorphic degree and structural position of five structural units (Aggtelek, Henc, Telekesoldal, Torna, Bódva). On the basis of new sedimentological, biostratigraphical and radiometric data Jurassic sedimentary age of the Telekesoldal and Telekesvölgy complexes and subduction-related depositional environment of the former were refined.

A new model of the structural evolution of the area consists of 8 deformation phases from earliest Cretaceous to present. The first 3 deformation events took place under ductile conditions, and affected only the metamorphosed structural units. The first nappe-stacking event pre-dated the metamorphism. Temperature and pressure conditions of the metamorphism were 300–350 °C and 1.5–3.5 kbar reaching low-grade metamorphism. K-Ar method suggested that the age of metamorphism and ductile deformation was about 143–116 Ma, while the post-metamorphic nappe stacking event happened around 90 Ma.

South-eastern and southern vergency of the nappe stacking phases were estimated from structural maps and using paleostress reconstructions from the measured fault-slip data. Physical conditions of these movements were estimated from basal tectonic breccias (rauhwacke), occurring along thrust planes of thin-skinned nappes. Their textures and syn-deformational minerals were studied by means of fluid inclusions microthermometry and microbarometry. On bases of these measurements the D4 nappe-stacking event was characterized by 200-320 °C and 2.0-3.6 kbar, while the younger D5 thrusting by 220-260 °C and 0.3-1.0 kbar. These data had a great importance during tectonic reconstructions and interpretation of the metamorphic petrological data.

This wide spectrum of new data set suggested notable revisions of the lithostratigraphic content, boundaries, and mutual relationships of formerly defined tectonic units of the Rudabánya Hills and contributed to the knowledge on deformation history of the Eastern Alpine–Western Carpathian orogenic belt.

12. Összefoglalás

Doktori kutatómunkám során a Belső Nyugati Kárpátok komplex takarórendszerének egy szeletét vizsgáltam a Rudabányai-hegység középső részén. Az elvégzett szerkezeti, metamorf kőzettani, geokronolóiai és őslénytani vizsgálatok alapján új modellt állítottam fel a terület szerkezeti fejlődésére. Munkám fő irányvonalai a következőek voltak: (I) a szubdukciós eseményekhez kapcsolódó jura képződmények szedimentológiai vizsgálata, korának pontosítása, (II) az egyes szerkezeti egységek definiálása, tartalmának, illetve szerkezeti helyzetének meghatározása, (III) a takarórendszer komplex deformációtörténetének vizsgálata, (IV) a különböző szerkezeti egységek metamorf fokának megállapítása, (V) a szerkezeti fázisok relatív és abszolút korának meghatározása, (VI) a takarós áttolódások nyomás és hőmérséklet viszonyainak becslése.

Kutatásom során újra definiáltam számos szerkezeti egység (Aggteleki takaró, Henc egység, Telekesoldali takaró, Tornai sorozat, Bódvai sorozat) kőzettani tartalmát, pontosítottam üledékes korát, metamorf fokát, illetve megállapítottam szerkezeti helyzetét. Szedimentológiai, őslénytani és új radiometrikus koradatok alapján pontosítottam a Telekesvölgyi és Telekesoldali jura sorozatok korát, valamint javaslatot tettem az üledékképződési környezetükre. A Telekesoldali sorozat lerakódása egy szubdukcióhoz köthető medencében történhetett.

A terület új szerkezetfejlődési modellje 8 deformációs fázisra osztható a kora-krétától napjainkig tartó időszakban. Az első három deformáció képlékeny körülmények között zajlott, és csak a metamorf szerkezeti egységeket érintette. Az első takaróképződési fázis még a metamorf esemény előtt történt. A metamorfózis 300–350 °C hőmérsékleten és 1,5–3,5 kbar nyomás mellett ment végbe. Ez a tartomány a magas hőmérsékletű anchizóna és az epizóna határán található. Az új K-Ar adatok alapján a metamorfózis és a vele egyidős képlékeny deformáció kora 143-116 Mév. Az ezt követő többfázisú takaróképződés nagyjából 90 Mév körül mehetett végbe.

Az elkészített szerkezeti térképek és feszültségtér-rekonstrukciók alapján délkeleti illetve déli irányú takarós áttolódásokat lehet valószínűsíteni. Ezen mozgások fizikai paramétereinek becslése céljából megvizsgáltam a takarók talpán elhelyezkedő tektonikus breccsákat (rauhwacke). Ezen tektonitok a deformációval egyidős ásványokat tartalmaznak, melyek a takarós áttolódásokat segítő fluidumokból cseppeket csapdáztak. Az elvégzett folyadékzárvány vizsgálatok alapján megállapítható, hogy a D4 deformációs fázis áttolódásai 200-320 °C-os hőmérséklet és 2,0-3,6 kbar-os nyomás viszonyok alatt mentek végbe. A későbbi, D5 fázisú mozgások paraméterei ennél egyértelműen alacsonyabbak: 220-260 °C és 0,3-1,0 kbar. Az így nyert nyomás és hőmérséklet adatok nagyban hozzájárultak a deformációs fázisok relatív sorrendjének meghatározásához, illetve a metamorf kőzettani adatok értelmezéséhez.

A számos különböző módszer együttes alkalmazása számos új eredményhez vezetett a szerkezeti egységek kőzettani tartalmára, határaira és deformáció történetére vonatkozóan, melyek hozzájárulnak a Keleti-Alpok és a Nyugati-Kárpátok szerkezetfejlődésének megértéséhez.

Acknowledgements

My PhD work was originally initiated and partly supervised by the late Sándor Kovács who, sadly, did not live to see this work completed. I would like to thank László Fodor for taking over all the hard work of supervising this project. He helped and encouraged me from my first steps in the field of geology. He often accompanied me on my trips to the field and to the not too friendly core depository. But above all I am glad that I have been able to profit from his experience in the "traditional" work of a geologist. Among many other things, my skills regarding field-work, the reading of maps and profiles were vastly improved. He helped to interpret the structural data and encouraged the development of new ideas and models. He also carefully reviewed the manuscript and gave constructive feedback.

My colleges at the Geological, Geophysical and Space Science Research Group provided friendly atmosphere and important moral support during my work. János Haas helpd a lot in the field of sedimentology, and provided financial and technical background for me. I am indebted to Kinga Hips for helping me at tricky thin sections and dolomites. Csaba Péró had valuable information on field work technics and had a wide knowledge on the whole area. Discussions with Zsófia Poros let me some introduction into the world of fluid inclusions and fluid migration. She was also a great help with interpreting the fluid inclusion data. Gábor Molnár is highly acknowledged for teaching me how to work with different coordinate systems. Barbara Beke and Attila Petrik was a great help with dobble-checking the references. I especially thank Éva Pacsirszky for solving all the administrative problems. Whith her special skills to talk to people and solve problems, she always found a way out from the labirinth of bureaucracy. Lunch-club with Orsolya Sztanó, Kinga Hips, László Fodor and Máron Palotai always let me have some fresh air, and flung me up.

Katalin Judik was my main contact person for all questions concerning low grade metamorphism, even after she changed position within the Geochemical Institute. I am indebted to her for many discussions concerning the metamorphic evolution of the study area and also for critical reviews of our common papers. I would like to thank Professor Péter Árkai for giving free run of his previous data and improving the common manuscripts with useful comments. Helps from other colleges (Tibor Németh, Mária Tóth) at the Geochemical Institute are highly acknowledged.

I am really greatful to Rastislav Milovský for making me fall in love with rauhwackes. His investigations on the field of basal tectonic breccias largely improved and supplied my tectonic interpretations. Field trips and connected discussions with him were really enjoyable part of my work. I am greatful for the field assistance of György Less and Norbert Németh, too. These trips improved my knowledge on the local geology and on field interpretation of deformation structures. Comments of Stefan Schmid, Bernhard Fügenschuh and Dušan Plašienka increased my knowledge on the wider Alpine-Carpathian-Dinaridic orogene.

I have benefited from the discussions with the participants of the CETEG, HUNTEK and Alpine Workshop conferences.

Kadosa Balogh is especially thanked for providing essencial K/Ar data, and introducing me into the basics of this very complicated isotope system. Sándor Józsa and Balázs Koroknai for their essential help in thin sections of magmatic and deformed rocks.

I would like to thank Ágnes Görög, Anette Götz and Péter Ozsvárt for providing me essential micropaleontologic data. Péter is especially acknowledged for the long-time online help support in different fields of smartness.

I am grateful to Urs Klötzli and Norbert Zajzon for helping me with their experience, but letting me discover the hidden traps of U/Pb dating.

I will definitely not finish this work without the continuous encouragement and edging from my friends: M. Deák, A. Bezzeg, D. Novák and T. Kovács. They always helped me coming out from desperation and carrying on with work. desperation and carrying on with work.

Last, and most definitely not least the most important support during my PhD-studies: I thank my family for their love and support in all parts of my life – be it private or scientific. Naturally, I thank my parents for their support, and making my studies possible in the first place.

The research was supported by the Hungarian Scientific Research Found OTKA No. 48824, 60965, and 61872.

References

Abu El-Ella R. 1991. Relationship between clay mineralogy and thermal maturity of Neogene-Quaternary shales in Ras El-Barr well, offshore Nile Delta, Egypt. – Marine and Petroleum Geology 8/3 296–301.

Anderson E. M. 1951. The dynamics of faulting and dyke formation with application to Britain. – Oliver & Boyd, Edinborough, 2nd edition, 206 p.

Angelier J. 1984. Tectonic analysis of fault slip data sets. – J. Geophysical Research 89, B7, 5835–5848.

Angelier J. 1990: Inversion of field data in fault tectonics to obtain the regional stress - III. A new rapid direct inversion method by analytical means. – Geophysical J. International 103, 363–373.

Árkai P. 1981. Report on the metamorphic petrological investigations of the Bükk and Aggtelek-Rudabánya Mts. (in Hungarian). – Manuscript, Geological Institute of Hungary.

Árkai P. 1985. Metamorphic petrologic investigations of the tectofacies units in NE Hungary (in Hungarian). – Manuscript, Institute for Geochemical Research, Hungarian Academy of Sciences, Geological Institute of Hungary.

Árkai P. 1989. Report on the evolution of low temperature metamorphic rocks (in Hungarian). – Manuscript, Geological Institute of Hungary.

Árkai P. 1991. Chlorite crystallinity: an empirical approach and correlation with illite crystallinity, coal rank and mineral facies as exemplified by Paleozoic and Mesozoic rocks of northeast Hungary. – J. Metamorphic Geology 9, 723–734.

Árkai P. & Kovács S. 1986. Diagenesis and regional metamorphism of the Mesozoic of Aggtelek–Rudabánya Mountains (Northeast Hungary). – Acta Geologica Hungarica 29/3–4, 349–373.

Árkai P., Balogh K. & Dunkl I. 1995a. Timing of low-temperature metamorphism and cooling of the Paleozoic and Mesozoic formations of the Bükkium, innermost Western Carpathians, Hungary. – Geologische Rundschau 84, 334–344.

Árkai P., Sassi F. P. & Sassi R. 1995b. Simultaneous measurements of chlorite and illite crystallinity: a more reliable tool for monitoring low- to very low-grade metamorphism in metapelites. A case study from the Southern Alps (NE Italy). – European Journal of Mineralogy 7, 1115–1128.

Árkai P., Merriman R.J., Roberts B., Peacor D.R. & Tóth M. 1996. Crystallinity, crystallite size and lattice strain of illite-muscovite and chlorite: comparison of XRD and TEM data for diagenetic to epizonal pelites. – European Journal of Mineralogy 8, 1119–1137.

Árkai P., Faryad S.W., Vidal O. & Balogh K. 2003. Very low-grade metamorphism of sedimentary rocks of the Meliata unit, Western Carpathians, Slovakia: implications of phyllosilicate characteristics. – International Journal of Earth Sciences 92, 68-85.

Árva-Sós E., Balogh K., Ravasz-Baranyai L. & Ravasz Cs. 1987. Mezozóos magmás kőzetek K-Ar kora Magyarország egyes területein. (K-Ar dates of Mesozoic igneous rocks in some areas of Hungary). – Annual Report of the Geological Institute of Hungary from 1987, 295–307.

Balla Z. 1983. A szarvaskői szinform rétegsora és tektonikája. – A Magyar Állami Eötvös Loránd Geofizikai Intézet 1982. Évi Jelentése, 42–65.

Balogh K. & Pantó G. 1949. A Rudabányai-hegység földtani térképe 1:25 000. – Magyar Állami Földtani Intézet kiadványa.

Balogh K. & Pantó G. 1952: A Rudabányai-hegység földtana. — *A Magyar Állami Földtani Intézet Évi Jelentése az 1949. évről, pp.* 135-154.

Balogh K. & Kovács S. 1977. Preliminary report on the examination of the Triassic of Rudabánya Hills (in Hungarian). – Manuscript, József Attila University, Szeged, Hungary.

Balogh K., Árváné Soós E. & Pécskay Z. 1984. Jelentés a Magyar Állami Földtani Intézet és az MTA Atommag Kutató Intézete között létrejött 4020/84 sz. kutatási szerződés keretében végzett vizsgálatokról. – Manuscript, Geological, Geophysical, Mining Archive of Hungary, Budapest.

Barker C.E. 1988. Geothermics of petroleum systems. Implications for stabilization of kerogen maturation after a geologically brief heating duration at peak temperature. In: Magoon L. (Ed.): Petroleum Systems of the United States. US Geol. Survey Bulletin, 26–29.

Bassoullet J.P. 1997. Foraminiferes. Les grands foraminiferes. In: Cariou E. & Hantzpergue P. (Eds.): Groupe français d'étude du Jurassique. Biostratigraphie du Jurassique ouest-européen et méditerranéen: zonations paralleles et distribution des invertébrés et microfossiles. – Bull. Centre Rech. Elf. Explor. Prod. Mém. 17, 293–304.

Baumgartner P.O., O'Dogherty L., Goričan S., Urquhart E., Pillevuit A. & De Wever P. 1995. Middle Jurassic to Lower Cretaceous Radiolaria of Tethys: Occurrences, systematics, biochronology. – Mém. Géol. Lausanne 23, 1-1162.

Bernoulli D., Weissert H. & Blome C.D. 1990. Evolution of the Triassic Hawasina Basin, Central Oman Mountains. In: Robertson A.H.F., Searle M.P. & Ries A.C. (Eds.): The Geology and Tectonics of the Oman Region. Blackwells, Oxford, 189–203.

Bousquet R. 2008. Metamorphic heterogeneities within a single HP unit: Overprint effect or metamorphic mix? – Lithos 103, 46–69.

Bystrický J. 1964. Slovenský kras. Stratigrafia a Dasycladaceae nezozoika Slovenského krasu. – Ústr. ÚStav Geo., Bratislava, 1–204.

Cambel B. & Král' J. 1989. Isotopic geochronology of the Western Carpathian crystalline complex: the present state. – Geol. Carpath. 40/4, 387– 410.

Channel J. & Kozur H. 1997. How many oceans? Meliata, Vardar, and Pindos oceans in Mesozoic Alpine paleogeography. – Geology 25, 183–186.

Crouzet C., Dunkl I., Paudel L., Árkai P., Rainer T.M., Balogh K. & Appel E. 2007. Temperature and age constraints on the metamorphism of the Tethyan Himalaya in Central Nepal: A multidisciplinary approach. – Journal of Asian Earth Sciences 30, 113–130.

Csontos L. 1988. Étude géologique d'une portion des Carpathes internes, le massif du Bükk (Nord-est de la Hongrie), (stratigraphie, structures, métamorphisme et géodinamique). – Ph.D. thesis, University Lille Flandres-Artois, 250, 327p.

Csontos L. 1999. Structural outline of the bükk Mts. (N Hungary). – Földtani Közlöny 129/4, 611–652.

Csontos L. 2000. Stratigraphic reevaluation of the Bükk Mts. (N. Hungary). – Földtani Közlöny 130/1, 95–132.

Csontos L. & Vörös A. 2004. Mesozoic plate tectonic reconstruction of the Carpathian region. – Palaeogeography, Palaeoclimatology, Palaeoecology 210, 1–56.

Dallmeyer R.D., Neubauer F., Handler R., Fritz H., Müller, H., Pana D. & Putiš M. 1996. Tectonothermal evolution of the internal Alps and Carpathians: evidence from 40Ar/39Ar mineral and whole-rock data. – Eclogae Geologicae Helvetiae 89, 203–227.

Deák-Kövér Sz., Milovský R. & Fodor L. 2011. Cretaceous nappe stacking in the Inner Western Carpathians – p-T conditions from basal rauhwacke studies. – Abstract, 10th Workshop on Alpine Geological Studies, CorseAlp 2011, 10-16 April 2011, Saint-Florent (Corsica), p. 26.

Dimitrijević M. N., Dimitrijević M. D., Karamata S., Sudar M., Gerzina N., Kovács S., Dosztály L., Gulácsi Z., Pelikán P. & Less Gy. 2003. Olistostrome/mélanges – an overview of the problems and preliminary comparison of such formations in Yugoslavia and Hungary. – Slovak Geol. Mag. 9/1, 3-21.

Dosztály L. 1994: Mesosoic radiolaria investigations in NE Hungary (in Hungarian). – Manuscript, Budapest, 1–108.

Dosztály L. & Józsa S. 1992. Geochronological evaluation of Mesozoic formations of Darnó Hill at Recsk on basis of radiolarians and K-Ar age data. – Acta Geologica Hungarica 35/4 371–393.

Dosztály L., Gulácsi Z. & Kovács S. 1998. Lithostratigraphy of the Jurassic formations of North Hungary (in Hungarian). In: Bérczi I. & Jámbor Á. (Eds.): Stratigraphy of the geological formations in Hungary. MOL – Geol. Inst. Hung., Budapest, 309–318.

Dosztály L., Józsa S., Kovács S., Less Gy., Pelikán P. & Péró Cs. 2002. North-East Hungary, post congress excursion guide. in: Vozár J., Vojtko R., Sliva L. (Eds.): Guide to geological excursions, XVIIth Congress of Carpathian – Balkan Geological Association, Bratislava, 104–117.

Faryad W. 1995. Phase petrology and P-T conditions of mafic blueschists from the Meliata unit, Western Carpathians, Slovakia. – Journal of Metamorphic Geology 13, 701–714.

Faryad W. & Henjes-Kunst F. 1997. Petrologic and geochronologic constraints on the tectonometamorphic evolution of the Meliata unit blueschists, Western Carpathians. In: Grecula P., Hovorka D. & Putiš M. (Eds.), Geological evolution of the Western Carpathians. Bratislava, 145–155.

Fodor L. 2010. Mezozoos-kainozoos feszültségmezők és törésrendszerek a Pannon-medence ÉNy-i részén – módszertan és szerkezeti elemzés. — Doctoral thesis, Hungarian Academy of Sciences, 129 pp.

Fodor L. & Koroknai B. 2000: Ductile deformation and revised stratigraphy of the Martonyi Subunit (Torna Unit, Rudabánya Mts.), Northeastern Hungary. – Geologica Carpathica 51/6, 355–369.

Fodor L. & Koroknai B. 2003. Multiphase folding on the Nagy-kő, Hídvégardó (Torna Unit, NE Hungary) (in Hungarian with English abstract). – Ann. Rep. Geol. Inst. Hungary from 2000–2001, 133–141.

Fodor L., Csontos L., Bada G., Györfi I. & Benkovics L. 1999. Tertiary tectonic evolution of the Pannonian basin system and neighbouring orogens: a new synthesis of paleostress data. In: Durand, B., Jolivet, L., Horváth, F. & Séranne, M. (eds): The Mediterranean Basins: Tertiary extension within the Alpine Orogen. Geological Society, London, Special Publications 156, 295–334.

Fodor L., Radócz Gy., Sztanó O., Koroknai B., Csontos L. & Harangi Sz. 2005. Tectonics, sedimentation and magmatism along the Darnó Zone. Post-Conference Excursion Guide for

3rd Meeting of the Central European Tectonic Studies Group, Felsőtárkány, Hungary. – Geolines 19, 142–162.

Foetterle F. 1869. Vorlage der geologischen Detailkarte des Umgebung von Torna und Szendrő. – Verh. Geol. Reichsanst. 7, 147–148.

Foscolos A.E, Powell T.G. & Gunther P.R. 1976. The use of clay minerals and inorganic and organic geochemical indicators for evaluating the degree of diagenesis and oil generating potential of shales. – Geochimica et Cosmochimica Acta 40/8, 953–966.

Frey M. 1987. Very low grade metamorphism of clastic sedimentary rocks. In: Frey M. (Ed.), Low Temperature Metamorphism. Blackie, Glasgow, 9–58.

Frisch W. & Gawlick H.-J. 2003. The nappe structure of the central Northern Calcareous Alps and its disintegration during Miocene tectonic extrusion – a contribution to understanding the orogenic evolution of the Eastern Alps. – Int. J. Earth. Sci. (Geol. Rundsch.) 92, 712–727.

Gawlick H.-J. 1996. Die früh-oberjurassischen Brekzien der Stubbergschichten im Lammertal – Analyse und tektonische Bedeutung (Nördliche Kalkalpen, Österreich). – Mitt. Gesell. Geol. Bergbaustud. Österr. 39/40, 119–186.

Gawlick H.-J. 2000. Sedimentologie, Fazies und Stratigraphie der obertriassischen Hallstätter Kalke des Holzwehralm-Schollenkomplexes (Nördliche Kalkalpen, Salzburger Land). – Jb. Geol. B.-A. Wien 142, 11–31.

Gawlick H.-J. & Frisch W. 2003. The Middle to Late Jurassic carbonate clastic radiolaritic flysch sediments in the Northern Calcareous Alps: sedimentology, basin evolution and tectonics – an overview. – Neu. Jb. Geol. Paläont. Abh. 230, 163–213.

Gawlick H.-J. & Suzuki H. 1999. Zur stratigraphischen Stellung der Strubbergschichten in den Nördlichen Kalkalpen (Callovium– Oxfordium). – Neu. Jb. Geol. Paläont. Abh. 211, 233–262.

Gawlick H.-J., Frisch W., Vecsei A., Steiger T. & Böhm F. 1999: The change from rifting to thrusting in the Northern Calcareous Alps as recorded in Jurassic sediments. Geol. Rdsch. 87, 644–657.

Gawlick H.-J., Frisch W., Missoni S. & Suzuki H. 2002. Middle to Late Jurassic radiolarite basins in the central part of the Northern Calcareous Alps as a key for the reconstruction of their early tectonic history – an overview. – Mem. Soc. Geol. Ital. 57, 123–132.

Grill J. 1988. Jurassic formations of the Rudabánya Mts. (in Hungarian with English abstract). – Annual Report Geol. Inst. Hungary from 1986, 69–103.

Grill J. 1989. Structural evolution of the Aggtelek-Rudabánya Mts., NE Hungary (in Hungarian with English abstract). – Annual Report of the Geological Institute of Hungary from 1987, 411–432.

Grill J. & Kozur H. 1986. The first evidence of the Unuma echinatus radiolarian zone in the Rudabánya Mts (Northern Hungary). – Geologische und Paleontologische Mitteilungen des Universität Innsbruck 13, 239–275.

Grill J., Kovács S., Less Gy., Réti Zs., Róth L. & Szentpétery I. 1984. Geology and evolutionary history of the Aggtelek-Rudabánya Mountains (in Hungarian). – Földtani Kutatás 27, 49–56.

Guggenheim S., Bain D.C., Bergaya F., Brigatti M.F., Drits V.A., Eberl D.D., Formoso M.L.L., Galán E., Merriman R.J., Peacor D.R., Stanjek H. & Watanabe T. 2002. Report of the Association Internationale Pour L'E´ tude Des Argiles (AIPEA) Nomenclature Committee

For 2001: Order, Disorder and Crystallinity in Phyllosilicates and the use of the ‘‘Crystallinity Index’’. – Clays and Clay Minerals 50, 406–409.

Guidotti C.V. Micas in metamorphic rocks. In: Bailey S.W. (Ed.): Micas, Reviews in Mineralogy, Mineralogical Society of America, Washington, 13, 1984, 357–467.

Guidotti C.V. & Sassi F.P. 1976. Muscovite as a petrogenetic indicator mineral in politic schists. – Neues Jahrbuch für Mineralogie Abhandlungen 127, 97-142.

Guidotti C.V. & Sassi F.P. 1986. Classification and correlation of metamorphic facies series by means of muscovite b0 data from low-grade metapelites. – Neues Jahrbuch für Mineralogie Abhandlungen 153/3, 363–380.

Guidotti C.V., Sassi F.P. & Blencoe J.G. 1989. Compositional controls on the a and b cell dimensions of 2M1 muscovite. – European Journal of Mineralogy 1, 71-84.

Haas J. & Kovács S. 2001. The Dinaridic–Alpine connection – as seen from Hungary. – Acta Geol. Hung. 44, 2–3, 345–362.

Haas J., Görög Á., Kovács S., Ozsvárt P., Matyók I., Pelikán P. 2006. Displaced Jurassic foreslope and basin deposits of Dinaridic origin in Northeast Hungary. – Acta Geologica Hungarica 49, 125–163.

Haas J., Budai T., Csontos L., Fodor L. & Konrád Gy. 2010. Pre-Cenozoic geological map of Hungary 1:500 000. – Geological Institute of Hungary, Budapest.

Haas J., Kovács S., Gawlick H.J., Grădinaru E., Karamata S., Sudar M., Péró Cs., Mello J., Polák M., Ogorelec B. & Buser S. 2011. Jurassic Evolution of the Tectonostratigraphic Units of the Circum-Pannonian Region. – Jahrbuch der Geologischen Bundesanstalt 151/3-4, 281–354.

Hagdorn H. & Velledits F. 2006. Middle Triassic crinoid remains from the Aggtelek platform (NE Hungary). – Neues Jahrbuch für Geologie und Paläontologie - Abhandlungen 240/3, 373–404.

Hips K. 2001. The structural setting of the Lower Triassic formations in the Aggtelek-Rudabánya Mountains (Northeastern Hungary) as revealed by geologic mapping. – Geologica Carpathica 52/5, 287–299.

Hók J., Kováč P. & Madaráš J. 1993. Extensional tectonics of the western part of the contact area between Veporicum and Gemericum (Western Carpathians). Miner. Slov. 27, 231–235.

Hók J., Ivanička J. & Kováčik M. 1994. Geological structure of the Rádziel part of the Tribec Mts.: new knowledge and discussion (Western Carpathians). – Miner. Slov. 26, 192–196.

Hók J., Kováč P. & Rakús M. 1995. Results of the structural investigations of the Inner Carpathians and their interpretation. – Mineralia Slovaca 25, 172–176.

Horváth B. 2010: A szőlősardói Henc-völgy földtani szerkezete. — MSc. thesis, Eötvös University, Department of Regional Geology, 77 p.

Horváth B., Fodor L. & Kövér Sz. 2012. Komplex rátolódások és szerkezetalakulás a szőlősardói Henc-völgy környezetében. – Földtani Közlöny, 142/3, in press.

Horváth P. 1997. High-pressure metamorphism and P-T path of the metabasic rocks in the borehole Komjáti-11, Bódva Valley area, NE Hungary. – Acta Mineralogica-Petrographica Szeged 37, 151–163.

Horváth P. 2000. Metamorphic evolution of gabbroic rocks of the Bódva Valley Ophiolite complex, NE Hungary. – Geologica Carpathica 51, 121–129.

Hunziker J.C. 1987. Radiogenic isotopes in very low-grade metamorphism. In: Frey, M. (Ed.): Low Temperature Metamorphism, Blackie and Son Ltd., Glasgow and London, 201–226.

Janák M., Froitzheim N., Lupták B., Vrabec M. & Ravna E.J.K. 2004. First evidence for ultrahigh-pressure metamorphism of eclogites in Pohorje, Slovenia: Tracing deep continental subduction in the Eastern Alps. – Tectonics 23/5, DOI: 10.1029/2004TC001641.

Józsa S., Horváth P. & Árkai P. 1996. Blue amphiboles from Meliata ophiolites in Northern Hungary. – Acta Mineralogica-Petrographica Szeged 37 Suppl. 58.

Judik K., Árkai P., Horváth P., Dobosi G., Tomljenović B., Tibljaš D., Balen D. & Pamić J. 2004. Diagenesis and low-temperature metamorphism of Mt. Medvednica, Croatia: Mineral assemblages and phyllosilicate characteristics. – Acta Geologica Hungarica 47/2-3, 151–176.

Kaminski M. A. 2004. The Year 2000 Classification of the Agglutinated Foraminifera. Proceedings of the Sixth International Workshop on Agglutinated Foraminifera. – Grzybowski Foundation Spec. Publ. 8, 237–255.

Karamata S. 2006. The geological development of the Balkan Peninsula related to the approach, collision and compression of Gondwanan and Eurasian units. In: Robertson A.H.F. & Mountrakis D. (Eds.): Tectonic development of the Eastern Mediterranean Region. – Geol. Soc. London, Spec. Publ. 260, 155–178.

Karamata S., Dimitrijević M.D., Dimitrijević M.N. & Milovanović D. 2000. A correlation of Ophiolitic belts and Oceanic realms of the Vardar Zone and the Dinarides. In: Karamata S. & Janković S. (Eds.): Geology and metallogeny of the Dinarides and the Vardar Zone. – Acad. Sci. Arts Rep. Srpska, Collect. Monogr. I., 191–194.

Kisch H.-J. 1983. Mineralogy and petrology of burial diagenesis (burial metamorphism) and incipient metamorphism in clastic rocks. In: Larsen G. & Chilingar G.V. (Eds.): Diagenesis in Sediments and Sedimentary Rocks. – Elsevier, Amsterdam, 289–493.

Klötzli U.S., Koller F., Scharbert S. & Höck V. 2001. Cadomian lower-crustal contributions to Variscan granite petrogenesis (South Bohemian Pluton, Austria): constraints from zircon typology and geochronology, whole-rock, and feldspar Rb–Sr isotope systematics. – Journal of Petrology 42, 1621–1642.

Koroknai B. 2004. Tectonometamorphic evolution of the Uppony and Szendrő Paleozoic units. – PhD thesis, Eötvös University, 239 p. (in Hungarian with English abstract).

Kováč M., Král J., Márton E., Plašienka D. & Uher P. 1994. Alpine uplift history of the Central Western Carpathians: geochronological, paleomagnetic, sedimentary and structural data. – Geologica Carpathica 45, 83–96.

Kovács S. 1984: Tisia-probléma és lemeztektonika – kritikai elemzés a koramezozoós fécieszónák eloszlása alapján. — Földtani Kutatás 27, 55-72.

Kovács S. 1986: Conodont-biostratigraphical and microfacies investigations in the Hungarian part of the Northeastern Rudabánya Mts (in Hungarian). — Annual Report of the Geological Institute of Hungary from 1984, 193–244.

Kovács S. 1988. Olistostromes and other deposits connected to subaqueous mass-gravity transport in the North Hungarian Paleo–Mesozoic. – Acta Geologica Hungarica 31/3–4, 265–287.

Kovács S. 1989. Geology of North Hungary, Paleozoic and Mesozoic terraines. – XXIst European Micropalaeontological Colloquium, Guidebook, Hungarian Geological Society, Hungary, Budapest, 1989, 15–37.

Kovács S. 1991. Rudabányai-hegység, Varbóc, Telekes-oldal, Telekesoldali Formációcsoport. – Magyarország geológiai alapszelvényei 149, a Magyar Állami Földtani Intézet kiadványa, Budapest.

Kovács S. 1992. Tethys "western ends" during the Late Paleozoic and Triassic and their possible genetic relationships. – Acta Geologica Hungarica 35, 329–369.

Kovács S. & Árkai P. 1989. A conodonta és mészkő-szöveti elváltozások jelentősége a diagenezis és a regionális dinamotermális metamorfózis határának felismerésével, Aggtelek – Rudabányai-hegységi példák alapján. – Manuscript, Archive Geol. Inst. Hungary, Budapest.

Kovács S., Less Gy., Piros O., Réti Zs. & Róth L. 1989. Triassic formations of the Aggtelek-Rudabánya Mts. (Northeastern Hungary). – Acta Geologica Hungarica 32, 31–63.

Kovács S., Szederkényi T., Árkai P., Buda Gy., Lelkes-Felvári Gy. & Nagymarosy A. 1997. Explanation of the terrane map of Hungary. – Annales Géologiques des Pays helléniques 37, 271–330.

Kovács S., Józsa S., Gulácsi Z., Dosztály L., B. Árgyelán G., Forián-Szabó M. & Ozsvárt P. 2005. Permo–Mesozoic formations of the Darnó Hill area, NE Hungary – a displaced fragment of the Inner Hellenidic – Inner Dinaridic accretionary complexes. In: Tomljenovič B., Balen D. & Vlahovic I. (Eds.): Abstracts book 7th Workshop on Alpine Geological Studies, Opatija, Croatian Geological Society, Zagreb, 51–52.

Kovács S., Haas J., Szebényi G., Gulácsi Z., Józsa S., Pelikán P., Bagoly Árgyelán G., Görög Á., Ozsvárt P., Gecse Zs. & Szabó I. 2008. Permo-Mesozoic formations of the Recsk-Darnó Hill area: stratigraphy and structure of the Pre-Tertiary basement of the Paleogene Recsk Ore Field. In: Földessy J. & Hartai É. (Eds.): Recsk and Lahóca Geology of the Paleogene Ore complex. – Geosciences, Publications of the University of Miskolc Series A, Mining, 73, Miskolc University Press, 33-57.

Kovács S., Sudar M., Grădinaru E., Karamata S., Gawlick H-J., Haas J., Péró Cs., Gaetani M., Mello J., Polák M., Aljinicic D., Ogorelec B., Kollar-Jurkovsek T., Jurkovsek B. & Buser S. 2011. Triassic evolution of the tectonostratigraphic units in the Circum-Pannonian region. – Jahrbuch Der Geologischen Bundesanstalt 151/3-4, 199-280.

Kozur H. 1991. The evolution of the Meliata-Hallstatt ocean and its significance for the early evolution of the Eastern Alps and Western Carpathians. – Paleogeography, Palaeoclimatology, Palaeoecology 87, 109–135.

Kozur H. & Mock R. 1973. Die Bedetung der Trias-Conodonten für die Stratigraphie und Tektonik der Trias in den Westkarpaten. – Geologische und Paleontologische Mitteilungen des Universität Innsbruck 3/2, 1–14.

Kozur H. & Mock R. 1985. Erste nachweis von Jura in der Meliata- Einheit der Sudlichen Westkarpaten. – Geol. Paläont. Mitt. Innsbruck 13/10, 223–238.

Kozur H. & Mock R. 1995. First evidence of Jurassic in the Folkmár Suture Zone of the Meliaticum in Slovakia and its tectonic implications. – Mineralia Slovaca 27/5, 301–307.

Kozur H. & Mostler H. 1992. Erster paläontologischer Nachweis von Meliaticum und Süd-Rudabányaicum in den Nördlichen Kalkalpen (Österreich) und ihre Beziehungen zu den Abfolgen in den Westkarpaten. – Geol. Paläont. Mitt. Innsbruck 18, 87–129.

Kozur H., Mock R. & Ožvoldová L. 1996. New biostratigraphic results in the Meliaticum in its type area around Meliata village (Slovakia) and their tectonic and paleogeographic significance. – Geologische und Paleontologische Mitteilungen des Universität Innsbruck 21, 89–121.

Kövér Sz. 2005. Deformation of metamorphic and non-metamorphic sequences in the central part of Rudabánya Hills, NE Hungary (in Hungarian with English abstract). – Manuscript, Master Thesis, Geol. Res. Group Hung. Acad. Sci., Eötvös Univ., Budapest, 1–130.

Kövér Sz., Fodor L., Kovács S., Csontos L. & Péró Cs. 2005. Deformation of metamorphic (Torna?) and non-metamorphic (Bódva) Mesozoic sequences in the central part of Rudabánya Hills, NE Hungary. – Geolines 19, 73–74.

Kövér, Sz., Fodor, L. & Kovács S. 2008: A Rudabányai-hegység jura képződményeinek szerkezeti helyzete és üledékes kapcsolata — régi koncepciók áttekintése és új munkahipotézis. — Annual Report of the Geological Institute of Hungary, 2006, 97–120.

Kövér, Sz., Fodor, L., Judik, K., Németh, T., Balogh, K. & Kovács, S. 2009a. Deformation history and nappe stacking in Rudabánya Hills (Inner Western Carpathians) unravelled by structural geological, metamorphic petrological and geochronological studies. – Geodinamica Acta 22, 3–29.

Kövér Sz., Haas J., Ozsvárt P., Görög Á., Götz A.E., & Józsa S. 2009: Lithofacies and age data of Jurassic foreslope and basin sediments of Rudabánya Hills (NE Hungary) and their tectonic interpretation. – Geologica Carpathica 60/5, 351-379

Kristan-Tollmann E. 1962. Stratigraphisch wertvolle Foraminiferen aus Obertrias-und Liaskalken der voralpinen Fazies bei Wien. – Erdöl-Zeitschrift 78, 228–233.

Kristan-Tollmann E. 1964. Beitrage zur Mikrofaunen das Rhät. II. Zwei charakterische Foraminiferengemeinschaften aus Rhätkalken. – Mitt. Gesell. Geol. Bergbaustud Wien 14, 135–147.

Kübler B. 1966. La cristallinité de l'illite et les zones tout à fait supérieures du métamorphisme. In: Etages tectoniques. – Univ. Neuchâtel, Inst. Geol., 105–122.

Kübler B. 1968. Evaluation quantitative du métamorphisme par la cristallinité de l'illite. – Bulletin Centre Recherche Pau SNPA 2, 385–397.

Less Gy. 1981. Explanation to the geological map 1:25000 of the Aggtelek-Rudabánya Mts., sheet Hidvégardó (in Hungarian). – Manuscript, Archive of the Geological Institute of Hungary.

Less Gy. 1987. Aggtelek–Rudabányai-hegység, Aggtelek, Haragistya, kutatóárok, Hallstatti Mészkő Formáció és Zlambachi Formáció. – Magyarország geológiai alapszelvényei 75, a Magyar Állami Földtani Intézet kiadványa, Budapest.

Less Gy. 1998. Földtani felépítés. In: Baross G. (szerk.): Az Aggteleki Nemzeti Park. – Mezőgazda Kiadó, 26–66.

Less Gy. 2000. Polyphase evolution of the structure of the Aggtelek–Rudabánya Mountains (NE Hungary), the southernmost element of the Inner Western Carpathians – a review. – Slovak Geological Magazine 6/2-3, 260–268.

Less Gy., Grill J., Róth L., Szentpétery I. & Gyuricza Gy. 1988. Geologic map of the Aggtelek–Rudabánya Hills 1:25.000. – Geological Institute of Hungary, Budapest.

Less Gy., Kovács S., Fodor L., Péró Cs. & Hips K. 1998. Geological cross sections through the Aggtelek-Rudabánya Mts., NE-Hungary. – XVIth CBGA Congress, Vienna, Austria, p. 337, Geol. Survey of Austria.

Less Gy. & Mello J. (Eds.) 2004. Geological map of the Gemer-Bükk area 1:100000 Geological Institute of Hungary, Budapest.

Lexa O., Schulmann K. & Ježek J. 2003. Cretaceous collision and indentation in the western Carpathians: View based on structural analysis and numerical modelling. – Tectonics 22/6, 1–16.

Liu X., Jahn B., Dong S., Lou Y. & Cui J. 2008. High-pressure metamorphic rocks from Tongbaishan, central China: U–Pb and 40Ar/39Ar age constraints on the provenance of protoliths and timing of metamorphism. – Lithos 105, 301–318.

MacCulloh T.H. & Naeser N.D. 1989. Thermal history of sedimentary basins; introduction and overview. In: Naeser N.D. & McCulloh T.H. (Eds.): Thermal History of Sedimentary Basins; Methods and Case Histories. – Springer Verlag, New York, 1–11.

Majoros P. 2008. Az Aggtelek–Rudabányai- és Bükk–hegység jura koru vulkanitjainak cirkonmorfológiai vizsgálata. – Diplomawork, Department of Mineralogy and Petrology, University of Miskolc. In Hungarian.

Maluski H., Rajlich P. & Matte Ph. 1993. $^{40}Ar/^{39}Ar$ dating of the Inner Carpathian Variscan Basement and Alpine mylonitic overprinting. – Tectonophysics 223, 313–337.

Mandl G.W. & Ondrejičková A. 1991. Über eine triadische Tiefwasserfazies (Radiolarite, Tonschiefer) in den Nördlichen Kalkalpen – ein Vorbericht. – Jb. Geol. B.-A., Wien 134, 309–318.

Mandl G.W. & Ondrejičková A. 1993. Radiolarien und Conodonten aus dem Meliatikum im Ostabschnitt der Nördlichen Kalkalpen (Österreich). – Jb. Geol. B.-A., Wien 136, 841–871.

Máthé Z. & Szakmány Gy. 1990. The genetics (formation) of rhyolite occurring in the Rudabánya Mts. (Northeastern Hungary). – Acta Mineralogica-Petrographica, Szeged 30, 81–92.

Mello J. 1974. Facial development and facial relations of the Slovak Karst Middle and Upper Triassic (West Carpathians, Southern part of Gemerids). – Schrift. Erdwiss. Komm. Österr. Akad. Wiss., 2, 147–155, Vienna.

Mello J. 1975. Pelagic and reef sediment relations of the Middle Triassic in the Silica nappe and transitional strata nature (the Slovak karst, West Carpathians). – Geol. Zborn. Geol. Carpathica, 26, 237–252, Bratislava.

Mello J. 1979. Meliata sequence in the Turna tectonic window. – Geologické Práce 72, 61–76.

Mello J. & Mock R. 1977. Nové poznatky o triase čs. časti Rudabanského pohoria. – Geologické Práce 68, 7–20.

Mello J., Elečko M., Pristaš J., Reichwalder P., Snopko D., Vass D. & Vozárová A. 1996. Geological map of the Slovensky Kras Mts., 1:50000. – Geological Survey of the Slovak Republic, Bratislava.

Mello J., Elečko M., Pristaš J., Reichwalder P., Snopko D., Vass D., Vozárová A., Gaál L., Hanzel V., Hók J. & Kováč P. 1997. Explanation notes to the geological map of the Slovak Karst, 1:50000. – Geological Institute of the Slovak Republic, Bratislava, 255 p.

Merriman R.J. & Frey M. 1999. Patterns of very low-grade metamorphism in metapelitic rocks. In: Frey M. & Robinson D. (Eds.): Low-Grade Metamorphism. – Blackwell Science, Oxford, 61–107.

Milovský, R. & Plašienka, D. 1998: Emplacement Mechanisms of the West Carpathian Cover Nappes. — Geolines 6, 45–46.

Milovský R. & Plašienka D. 2007. P-T-conditions and age of thrusting of some West-Carpathian thin-skinned nappes. In: Alpine Workshop Davos. – Abstract Volume, Swiss Academy of Sciences, p. 46–47.

Milovský R., Hurai V. Plašienka D. & Biroň A. 2003. Hydrotectonic regime at soles of overthrust sheets: textural and fluid inclusion evidence from basal cataclasites of the Murdan nappe (Western Carpathians, Slovakia). – Geodinamica Acta 16/1, 1–20.

Milovský R., van den Kerkhof A., Hoefs J., Hurai V. & Prochaska W. 2012. Cathodoluminescence, fluid inclusion and stable C–O isotope study of tectonic breccias from thrusting plane of a thin-skinned calcareous nappe. – Internationl Journal of Earth Sciences 101, 535–554.

Missoni S. & Gawlick H.J. 2011. Jurassic mountain building and Mesozoic-Cenozoic geodynamic evolution of the Northern Calcareous Alps as proven in the Berchtesgaden Alps (Germany). – Facies 57/1, 137-186.

Mock R., Sykora M., Aubrecht R., Ozvoldová L., Kronome B., Reichwalder P. & Jablonsky J. 1998. Petrology and stratigraphy of the Meliaticum near the Meliata and Jaklovce Villages, Slovakia. – Slovak Geological Magazine 4, 223–260.

Nádor A. 1988. A Dél-Gömörikum triász-jura határképződményei. – Annual Report of the Hungarian Geological Institute 35–59.

Odin, G. S., Adams C. J., Armstrong R. L., Bagdasaryan G. P., Baksi A. K. Balogh K., Barnes I. L., Boelrijk N. A. L. M., Bonadonna F. P.,Bonhomme M. G.,Cassignol C., Chanin L., Gillot P. Y., Gledhill A., Govindaraju A., Harakal R., Harre W., Hebeda E. H., Hunziker J. C., Ingamells C. O., Kawashita K., Kiss E., Kreutzer H., Long L. E., McDougall I., McDowell, F., Mehnert H., Montigny R., Pasteels P., Radicati F., Rex D.C.,Rundle C., Savelli C., Sonet J., Welin E. & Zimmermann J.L. 1982.: Interlaboratory standards for dating purposes. In: Odin G. S. (ed.) Numerical Dating in Stratigraphy, 123-149, Wiley & Sons, Chichester, New York, Brisbane.

Oravecz-Scheffer A. 1987. Triassic foraminifers of the Transdanubian central range. – Geologica Hungarica Series Paleontologica 50, 1–331.

Padan A., Kisch HJ. & Shagam R. 1982. Use of the lattice parameter b0 of the dioctahedral illite/muscovite for the characterization of P/T gradients of incipient metamorphism. – Contributions to Mineralogy and Petrology 79, 85–95.

Pálfy M. 1924. A Rudabányai hegység geológiai viszonyai és vasérctelepei. – A Magyar Állami Földtani Intézet Évi Jelentése 1924-ről 26/2, 1–27.

Pamić J., Kovács S. & Vozár J. 2002. The Internal Dinaridic fragments into the collage of the South Pannonian Basin. – Geol. Carpathica 53, 9–11.

Pantó G. 1956: A rudabányai vasércvonulat földtani felépítése. — MÁFI Évkönyv 44/2, 329–637.

Pantó G. & Földvári-Vogl M. 1950. Natrongabbro in the Bódva Valley. – Annual Report of the Geological Institute of Hungary 1939/3, 1–16 (in Hungarian).

Pelikán P. & Dosztály L. 2000. A bükkzsérci fúrások (D-Bükk) jura képződményei és szerkezetföldtani jelentőségük. – Földtani Közlöny 130/1, 25–46.

Péró Cs., Kovács S., Less Gy. & Fodor L. 2003. Geological setting of the Triassic „Hallstatt" (s.l.) facies in NE Hungary. – Annales Universitatis Scientiarum Budapestiensis de Rolando Eötvös Nominatae Sectio Geologica 35, 58–59.

Pessagno E.A. Jr. & Whalen P.A. 1982. Lower and Middle Jurassic Radiolaria (multicyrtid Nassellariina) from California, Eastcentral Oregon and the Queen Charlotte Islands, B.C. – Micropaleontology 28/2, 111–169.

Petrini K. & Podladchikov Y. 2000. Lithospheric pressure-depth relationship in compressive regions of thickened crust. – J. Metamorphic Geology 18/1, 67-77.

Piros O. 2002. Anisian to Carnian carbonate platform facies and dasycladacean biostratigraphy of the Aggtelek Mts, Northeastern Hungary. – Acta Geologica Hungarica 45/2, 119–151.

Piuz A. 2004. Microplaéontologie d'une plate-forme bioclastique échinodermique: Les calcaires a entroques du Bajocien du Jura méridional et de Bourgogne. – Terre & Environement, Section des Sciences de la Terre, Université de Geneve, 49, XIV, 1–267.

Plašienka D. 1991. Mesozoic tectonic evolution of the epi-Variscan continental crust of the Central Western Carpathians – a tentative model. – Miner. Slov. 23, 447–457.

Plašienka D. 1997. Cretaceous tectonochronology of the Central Western Carpathians, Slovakia. – Geologica Carpathica 48/2, 99–111.

Plašienka D. 1998. Paleotectonic evolution of the Central Western Carpathians during the Jurassic and Cretaceous. In: Rakús M. (Ed.): Geodynamic development of the Western Carpathians. – Geological Survey of Slovak Republic, Bratislava, 107–130.

Plašienka D. 1999. Definition and correlation of tectonic units with special references to some Central Westen Carpathian examples. – Mineralia slovaca 31, 3–16.

Plašienka D. 2000. Paleotectonic controls and tentative palinspastic restoration of the Carpathian realm during the Mesozoic. – Slovak Geological Magazine 6/2-3, 200–204.

Plašienka D. & Soták J. 1996. Rauhwackized carbonate tectonic breccias int eh Western Carpathian nappe edifice: introductory remarks and preliminary results. – Slovak Geological Magazine 1996/3-4, 287–291.

Plašienka D., Grecula P., Putiš M., Hovorka D. & Kováč M. 1997. Evolution and structure of the Western Carpathians: an overview. In: Grecula P., Hovorka D. & Putiš M. (Eds.): Geological Evolution of the Western Carpathians. – Mineralica Slovaca Monograph, Bratislava, 1–24.

Putiš M. 1991. Geology and paleotectonics of some shear zones in the West Carpathian crystalline complexes. – Miner. Slov. 23, 459– 473.

Rakús M. 1996. Jurassic of the innermost Western Carpathian zones – its importance and influence on the geodynamic evolution of the area. – Slovak Geological Magazine 1996/3-4, 311–318.

Rakús M., Potfaj M. & Vozárová A. 1998. Basic paleogeographic and paleotectonic units of the Western Carpathians. In: Rakús M. (Ed.): Geodynamic development of the Western Carpathians. – Geological Survey of Slovak Republic, Bratislava, 15–27.

Réti Zs. 1985. Triassic ophiolite fragments in an Evapritic Melange, Northern Hungary. – Ofioliti 10/2-3, 411–422.

Robertson H.E. & Lahann R.W. 1981. Smectite to illite conversion rates: effects of solution chemistry. – Clays and Clay Minerals 29, 129–135.

Salaj J., Borza K. & Samuel O. 1983. Triassic foraminifers of the West Carpathians. – Geologický ústav Dionýza Štúra, Bratislava, 1–213.

Salaj J., Trifonova E. & Gheorghian D. 1988. A biostratigraphic zonation based on benthic foraminifera in the Triassic deposits of the Carpatho-Balkans. – Rev. Paléobiologie, Vol. Spéc. Benthos 86/2, 153–159.

Schlagintweit F. & Ebli O. 1999. New results on microfacies, biostratigraphy and sedimentology of Late Jurassic–Early Cretaceous platform carbonates of the Northern Calcareous Alps. Part I: Tressenstein Limestone, Plassen Formation. – Abh. Geol. Bundesanst. 56/2, 379–418.

Schlagintweit F., Gawlik H.-J., Missoni S., Hoxha L., Lein R. & Frisch W. 2008. The eroded Late Jurassic Kurbnesh carbonate platform in the Mirdita Ophiolite Zone of Albania and its bearing on the Jurassic orogeny of the Neotethys realm. – Swiss J. Geosci. 101, 125–138.

Schmid S. M., Fügenschuh B., Kissling E. & Schuster R. 2004: Tectonic map and overall architecture of the Alpine orogen. — Swiss Journal of Geosciences 97/l, 93–117.

Schmid S.M., Bernoulli D., Fügenschuh B., Matenco L., Schefer S., Schuster R., Tischler M. & Ustaszewski K. 2008. The Alpine- Carpathian-Dinaridic orogenic system: correlation and evolution of tectonic units. – Swiss Journal of Geosciences 101/1, 139–183.

Schuster, R. & Frank, W. 2000. Metamorphic evolution of the Austroalpine units east of the Tauern Window: indications for Jurassic strike slip tectonics. – Mitt. Geol. Bergbau Stud. Österr., 42, 37-58.

Seresné Hartai É. 1980. Report on the structural geological investigation of Northeast Hungary. – Manuscript, Geological and Geophisical database of Hungary, Budapest, 169 p.

Stampfli G. M. & Borel G. D. 2002. A plate tectonic model for the Paleozoic and Mesozoic constrained by dynamic plate boundaries and restored synthetic oceanic isochrones. – Earth and Planetary Sciene Letters 196/1-2 17-33.

Steiger R.H.E. 1977. Jäger, Subcommission on geochronology: convention on the use of decay constants in geo- and cosmochronology. – Earth and Planetary Sciene Letters 12, 359–362.

Stüwe K. & Schuster R. 2010. Initiation of subduction in the Alps: Continent or ocean? – Geology 38/2, 175-178.

Suchý V., Sýkorová I., Stejskal M., Safanda J., Machovic V. & Novotná M. 2002. Dispersed organic matter from Silurian shales of the Barrandian Basin, Czech Republic: optical properties, chemical composition and thermal maturity. – International Journal of Coal Geology 53/1, 1–25.

Szakmány Gy., Máthé Z. & Réti Zs. 1989. The position and petrochemistry of the rhyolite in the Rudabánya Mts. (NE Hungary). – Acta Mineralogica-Petrographica Szeged 30, 81–92.

Szentpétery I. 1997. Sinistral lateral displacement in the Aggtelek- Rudabánya Mts. (North Hungary) based on the facies distribution of Oligocene and Lower Miocene formations. – Acta Geol. Hung. 40, 265–272.

Szentpétery I. & Less Gy. (Eds.) 2006. Geology of the Aggtelek-Rudabánya Hills – Explanation for the Geologic map of the Aggtelek–Rudabánya Hills 1:25.000 (1988) (in Hungarian). – Geological Institute of Hungary, Budapest, 2006, 92 p.

Sztanó O. & Tari G. 1993. Early Miocene basin evolution in Northern Hungary: Tectonics and Eustacy. — Tectonophysics 226, 485–502.

Tišljar J., Vlahović I., Velić I. & Sokač B. 2002. Carbonate platform megafacies of the Jurassic and Cretaceous deposits of the Karst Dinarides. – Geol. Croatica 55/2, 139–170. Trifonova E. 1993. Taxonomy of Bulgarian Triassic foraminifera. II. Families Endothyriidae to Ophthalmidiidae. – Geol. Balcanica 23/2, 19–66.

Tollmann A. 1976. Analyse des klassischen nordalpinen Mesozoikums. Stratigraphie, Fauna und Fazies der Nördlichen Kalkalpen. – Franz Deuticke, Wien, 602 p.

Vitális I. 1909. A Bódva–Tornaköz környékének földtani viszonyai. – A Magyar Állami Földtani Intézet Jelentése 1907-ről, 45–58.

Vlahović I., Tišljar J., Velić I. & Matičec D. 2005. Evolution of the Adriatic Carbonate Platform: Palaeogeography, main events and depositional dynamics. – Palaeogeogr. Palaeoclimatol. Palaeoecol. 220/3–4, 333–360.

Vojtko R., 2000. Are there tectonic units derived from the Meliata- Hallstatt trough incorporated into the tectonic structure of the Tisovec Karst? (Murán kartic plateau, Slovakia). – Slovak Geological Magazine 6/4, 335-346.

Wernli R. & Metzger J. 1990. Callorbis minor, n.g., n.sp., un nouveau foraminiferes des calcaires échinodermiques du Bajocien du Jura (France). – Eclogae. Geol. Helv. 83/1, 163–175.

Willner A.P., Glodny J., Geryaa T.V., Godoy E. & Massonn H.-J. 2004. A counterclockwise PTt path of high-pressure/low-temperature rocks from the Coastal Cordillera accretionary complex of south-central Chile: constraints for the earliest stage of subduction mass flow. – Lithos 75, 283–310.

Zaninetti L. 1976. Les Foraminiferes du Trias. – Riv. Ital. Paleont. 82/1, 1–258.

Zelenka, T., Baksa, Cs., Balla, Z., Földessy, J. & Földessy-Járányi, K. 1983: The role of the Darnó Line in the basement structure of Northeast Hungary. — Geologický Zborník Geologica Carpathica 34, 53–69.

Zelenka T., Kaló J. & Németh N. 2005: Az alsótelekesi gipsz-anhidrit dóm szerkezete. – Földtani Közlöny 135/4, 493–511.

Appendix Table 1: determined radiolarian fauna from the TV and To complexes

UAZ	Taxa	Varbóc-2 (Va-2) borehole (m)															Szet-3		Telekes Valley - Tributary valley 8						
		3.4	9.7	13.1	30.2	34.1	45.4	48.5	49.3	51.5	58.5	64.1	69.7	73	73.9	77.6	79.1	80.9	gr9	gr11	8-43	8-43a	8-47	8-47A	8-51	8-52	8-53	8-55a
	Acaeniotylopsis (?) sp.																			+					+			
	Acanthocircus (?) sp.																		+	+							+	
3–10	*Angulobracchia digitata* Baumgartner																		+									
	Angulobracchia sp.												+							+									
	Archaeodictyomitra cellulata O'Dogherty, Goričan and Dumitrica						+		+																			
	Archaeodictyomitra exigua Blome										+								+		+	+						
	Archaeodictyomitra patricki Kocher	+																										
	Archaeodictyomitra prisca Kozur and Mostler							+																				
	Archaeodictyomitra rigida Pessagno											+				+												
	Archaeodictyomitra sp. 1							+																+				
	Archaeodictyomitra sp. 2											+																
	Archaeodictyomitra sp. 3				+																							
	Archicapsa sp. 1	+									+	+											+					
	Archicapsa sp. 2													+														
	Archicapsa sp. 3																								+			
	Bagotum sp.														+													
1–9	*Bernoullius rectispinus* Kito et al.							+																				
	Bernoullius sp.																									+		
	Canoptum hungaricum Grill and Kozur							+			+	+	+				+							+	+			
	Canoptum sp. cf. *C. hungaricum* Grill and Kozur																	+										
	Canoptum rudabanyaense Grill and Kozur							+																				
	Canoptum sp.																+											
	Canoptum (?) sp.																			+								
1–4	*Cenosphaera* sp. X Yao																			+								
	Cyrtocapsa sp.						+																					
3–7	*Dictyomitrella* (?) *kamoensis* Mizutani and Kido	+						+																				
1–4	*Emiluvia lombardensis* Baumgartner																			+								
1–4	*Emiluvia* sp. cf. *E. lombardensis* Baumgartner																			+								
	Emiluvia sp.																			+								
	Emiluvia (?) sp.														+					+	+							
3–10	*Eucyrtidiellum nodosum* Wakita										+	+									+							
	Eucyrtidiellum (?) *quinatum* Takemura																								+		+	
	Eucyrtidiellum sp. cf. *E. unumaense* (Yao)											+																
	Eucyrtidiellum sp. 1	+		+						+	+																	
	Eucyrtidiellum sp. 2																	+										
5–8	*Eucyrtidiellum* sp. cf. *E. unumaense pustulatum* Baumgartner														+													
	Gorgansium sp.																		+									
4–11	*Homoeoparonaella argolidensis* Baumgartner																		+	+								
4–10	*Homoeoparonaella elegans* (Pessgno)																		+									
	Homoeoparonaella ? sp.																		+		+							
	Hsuum baloghi Grill and Kozur							+																				
	Hsuum belliatulum Pessagno and Whalen																+											
	Hsuum sp. cf. *H. belliatulum* Pessagno and Whalen																+											
5–8	*Hsuum matsuokai* Isozaki and Matsuda								+			+		+	+													
5–8	*Hsuum* sp. cf. *H. matsuokai* Isozaki and Matsuda														+													
3–6	*Hsuum mirabundum* Pessagno and Whalen	+			+			+			+						+											
	Hsuum sp. cf. *H. mirabundum* Pessagno and Whalen										+																	
	Hsuum rosebudense Pessagno and Whalen								+																			
	Hsuum sp. E in Hull										+																	
	Hsuum sp. cf. *H.* sp. 1 in O'Dogherty et al.																				+	+						
	Hsuum sp. cf. *H. cuestaense* Pessagno																								+			
	Hsuum sp. cf. *H. robustum* Pessagno and Whalen															+												
	Hsuum sp. 1													+		+	+											
	Hsuum sp. 2		+																									
	Hsuum (?) sp.				+																							
1–4	*Laxtorum* (?) *hichisoense* Isozaki and Matsuda													+	+							+				+		
	Laxtorum (?) sp. cf. *L.* (?) *hichisoense* Isozaki and Matsuda														+		+	+										
2–3	*Laxtorum* (?) *jurassicum* Isozaki and Matsuda																	+		+								
	Laxtorum (?) sp.														+	+												
1–6	*Orbiculiforma* sp. X sensu Baumgartner																		+	+								
	Orbiculiforma sp.																			+								
	Pantanellium sp. 1																		+									
	Pantanellium sp. 2																		+									
	Paronaella sp. B sensu Hull												+															
	Parahsuum carpathicum Widz and De Wever				+																							
	Parahsuum indomitum (Pessagno and Whalen)																											+
1–3	*Parahsuum izeense* (Pessagno and Whalen)																						+					

UAZ	Taxa	Varbóc-2 (Va-2) borehole (m)																Szet-3		Telekes Valley - Tributary valley 8							
		3.4	9.7	13.1	30.2	34.1	45.4	48.5	49.3	51.5	58.5	64.1	69.7	73	73.9	77.6	79.1	80.9	gr9	gr11	8-43	8-43a	8-47	8-47A	8-51	8-52	8-53	8-55a
1–7	*Parahsuum officerense* (Pessagno and Whalen)																+											
	Parahsuum sp. cf. *P. officerense* (Pessagno and Whalen)																	+										
	Parahsuum snowshoense (Pessagno and Whalen)											+	+															
3–8	*Parahsuum stanleyense* (Pessagno)	+																										
	Parahsuum sp.																						+					
	Paronaella mulleri Pessagno												+															
1–2	*Paronaella* sp. cf. *P. corpulenta* De Wever												+						+									
	Paronaella sp.																			+								
	Paronaella (?) sp.											+																
	Parvicingula sp. cf. *P. elegans* Pessagno and Whalen								+																			
	Parvicingula sp.	+									+																	
	Praeconocaryomma sp.												+															
1–11	*Praewilliriedellum convexum* (Yao)				+										+									+				
	Praewilliriedellum sp.										+																	
	Protunuma costata (Heitzer)						+																					
4–7	*Protunuma turbo* Matsuoka	+								+	+	+				+												
	Protunuma sp.											+				+												
	Protunuma (?) sp.														+													
	Pseudocrucella (?) sp.																		+									
	Pseudoeucyrtis buekkensis Grill and Kozur										+																	
	Pseudoeucyrtis elongata Grill and Kozur				+																							
	Pseudoeucyrtis sp.												+						+	+								
	Pseudodictyomitrella hexagonata (Heitzer)											+																
	Pseudodictyomitrella spinosa Grill and Kozur									+					+	+			+					+				
	Pseudodictyomitrella sp. cf. *P. spinosa* Grill and Kozur										+	+																
	Pseudodictyomitrella wallacheri Grill and Kozur										+					+												
	Semishuum fuchsi (Grill and Kozur)				+														+									
	Semishuum inexploratum (Blome)	+															+											
	Semishuum sp. cf. *S. inexploratum* (Blome)	+																										
	Semishuum sp. cf. *S. brokencotense* Pessagno, Blome and Hull				+																							
	Semishuum sp.			+	+																							
	Semishsuum (?) sp.	+																										
6–13	*Spongocapsula palmerae* Pessagno										+																	
5–7	*Stichocapsa robusta* Matsuoka	+		+	+		+	+		+		+																
5–5	*Stichocapsa* sp. E sensu Baumgartner	+																										
	Stichocapsa sp.					+																				+		
	Stichomitra sp.								+																			
	Striatojaponocapsa synconexa O'Dogherty, Goričan and Dumitrica	+		+																								
4–13	*Tetratrabs zealis* (Ožvoldová)														+													
3–11	*Transhsuum brevicostatum* (Ožvoldová)											+												+				
	Transhsuum sp. cf. *T. brevicostatum* (Ožvoldová)												+															
2–7	*Transhsuum hisuikyoense* (Isozaki and Matsuda)	+										+	+								+							
3–10	*Transhsuum maxwelli* (Pessagno)	+			+						+	+	+	+											+			
	Transhsuum sp. cf. *T. maxwelli* (Pessagno)										+								+									
	Tricalocapsa sp. cf. *T. fusiformis*								+																			
	Transhsuum sp. 1								+																			
	Transhsuum sp. 2							+																				
	Transhsuum sp. 3							+			+			+	+	+	+											
	Triactoma sp. cf. *T. jakobse* Carter																		+	+								
	Triactoma sp. cf. *T. jonesi* (Pessagno)											+																
	Triactoma sp. 1										+	+																
	Triactoma sp. 2																			+	+							
	Triactoma (?) sp.																		+	+								
4–5	*Tricolocapsa plicarum* (Yao)				+																							
	Tricolocapsa sp. cf. *T. plicarum* (Yao)								+																			
	Tricolocapsa sp.									+							+											
	Trillus sp. 1											+																
	Trillus sp. 2											+																
	Trillus (?) sp.													+														
1–6	*Tritrabs simplex* Kito and De Wever																		+									
	Tritrabs sp. cf. *T. ewingi* (Pessagno)																		+									
3–4	*Unuma typicus* Yao											+												+				
	Unuma sp.cf. *U. typicus* Yao																			+	+							
	Unuma ochiensis (Matsuoka)	+																										
	Unuma sp. F sensu Yao																		+									
	Unuma sp. cf. *U. echinatus* Ichikawa and Yao				+								+															
	Unuma sp.					+			+			+																
	Williriedellum sp.			+																								

Appendix Table 2: mineral composition of the studied samples

Metamorphic (and detrital) mineral phases+weathering products													
Structural unit	**Locality**	**Sample number**	**Lithology**	**Qtz**	**Pl**	**Rt**	**10 Å**	**Chl**	**SP**	**Hem**	**Py**	**Cal**	**Dol-Ank**
Bódva series (uppermost Triassic-Jurassic Telekesvölgy complex)	Core	SZET-4, 24,8 m	limestone, calcareous	***	*		**	*	min.	*		***	*
	Core	SZET-4, 47,7 m	limestone	***	*	*	*	*				***	*
	Core	SZET-4, 78,3 m	limestone	***	*		*	*				***	*
	Core	SZET-4, 151 m	limestone	***			*	*		*		***	
	Core	SZET-4, 162 m	limestone	***	min.		**	*		*		**	*
	Core	SZA-5/2	calcareous marl	***	*	min.	*	*			min.	***	*
	Core	SZA-5/3	dolomarl, shale	***	min.	min.	*	*		min.		*	*
	Core	SZA-5/5	calcareous marl	**	*	min.	min.	*			min.	***	*
	Core	VA-2, 10,6 m	siltstone	***	min.		*	*			*		*
	Core	VA-2, 71,3 m	silty claystone	***	min.		**	*			*		*
	Core	VA-2, 79,3 m	siltstone	***	min.		**	*			*		*
	Szár Hill	TV-2008/1	marl	***	min.		**		min.			*	
	TV 7	TV-2008/2	claymarl	***			*	*					
	TV 7	TV-2008/3	claystone	***	min.		**	min.	*	*		**	
	TV 8	TV-2008/4	marl	***	*		**	***					
	TV 7	TV-2008/5	claystone	***	*		*	min.	min.			***	
	TV 8	TV-2008/6	claystone	***	min.		**	min.	min.				
	Esztramos	To-153	marl	**	min.		**	min.	min.	min.		***	
Bódva series (Lower to Upper Triassic)	Core	RB-658 118.7 m	marl	***	*	min.	*	*	min.		min.	***	
	Core	RB-658 129 m (g)	calcareous shale	***	min.	min.	*	*			min.	**	**
	Core	RB-658 129 m (p)	calcareous shale	***		min.	*	*			min.	**	*
	Core	HA-4 23.4 m	dolomarl	***		min.	*	*			min.	*	**
	Core	P-74 195.9-196 m	claystone	***	min.	min.	*	*				*	*
	Core	SZA-4 518.5 m	dolomite	*			*			min.		**	***
	Core	SZA-4 532.2 m	dolomite	*			*			min.		**	***
	Core	VA-3, 56,8 m	calcareous marl	***	*	*	**	**		*		***	
	Core	VA-3, 77,6 m	calcareous siltstone	***	*	*	**	*		*		***	*
	TV 7	TV-7 Mn	Mn-bearing claystone	***	min.		**	min.	min				
	Bl	BL-2008/1	claystone, marl	***	min.		***			*			
	Core	BL-2 62-68 m	claystone, marl	**	min.		**			*		***	
	Core	BL-2 132.2 m	claystone, marl	***	min.		**	*				min.	*
	Core	BL-2 139.7 m	claystone, marl	***	min.		*	min.				*	*
	Esztramos	E-6	siltstone, claystone	***	*		***	min.	min.	min.			
	Esztramos	E-2008/1	siltstone, claystone	***	*		*		min.			**	
	Esztramos	E-7	siltstone, claystone	***	*		***	*	min.	min.			
	Bódvarákó	E-12	siltstone, claystone	***	min.		***	min.	min.				
	Esztramos	E-10	siltstone, claystone	***	*		**	min.	min.	min.			
	Dunnatető H.	27/A	limestone										
Telekesoldal nappe (Jurassic)	TV Hunter h.	TO-7/b	slate, metasiltstone	***	min.		***	*	min.			min.	
	Core	SZA-7 50.3 m	metasiltstone	***	*		**	*			*		*
	Core	SZA-7 141.2 m	slate	***	**	*	**	**				*	*
	Core	SZA-7 177.5 m	slate	***	*	*	**	**	min.	*		*	*
	Core	SZA-10 74 m	metaclaymarl	***	min.	*	**	**				**	*
	Core	SZA-10 91.4 m	metaclaymarl	***	*	*	**	**	min.			*	*
	Core	SZA-10 26. box	slate	***	*	*	**	**			*	*	*
	Core	SZA-12 12 m	slate	***		*	***+Pg	*					
	Core	SZA-12 31.4 m	slate	***	*	*	***	**		*			*
	Core	SZA-12 50.3 m	metasiltstone	***	**		***	**	*	*		**	**
	Core	SZA-12 71 m	marl	***	**		***	**			*	***	**
	Core	SZET-3 21-22 m	claymarl	***	*	min.	*	*			min.	**	*
	Core	SZET-3 33.8-34 m	claymarl	***	*	*	*	*			min.	**	*
	Core	SZET-3 63.9-64.2 m	silicified claystone	***	*	min.	*	*					
	Core	SZET-3 88.3-88.6 m	shale	***	*	min.	*	*			min.		
	Core	RB-658 4.5-5 m	silty claystone	***			min.	*				**	*
	Core	RB-661 21.3-21.7 m	marl	***	**	min.	*	*			min.	*	**
	Core	RB-661 86 m	claymarl	***		min.	*	*			min.	**	*
	Core	RB-661 148.5 m	marl	***		min.	*	*			min.	**	**
	Core	RB-661/ 216 m	dolomarl	***	*	min.	*	*			min.	*	**
Szö-3 borehole	Core	SZÖ-3 32 m	slate	***	min		**+Pg	**	min			min.	*
	Core	SZÖ-3 42.8-43 m	slate	***	min		**+Pg	***					
	Core	SZÖ-3 76.1 m	slate	***	min.	min.	**+Pg	**	*			*	*
	Core	SZÖ-3 86.2-87.4 m	slate	***	min		***+Pg	**					

Metamorphic (and detrital) mineral phases+weathering products														
Structural unit	**Sample number**	**Lithology**	**Qtz**	**Pl**	**Rt**	**10 Å**	**Chl**	**SP**	**Hem**	**Py**	**Cal**	**Dol-Ank**	**Kln**	**Gp**
Bódva series (uppermost Triassic-Jurassic Telekesvölgy Complex)	P-74/1	claystone	***	min.	min.	***	**				**	*		
	RB-658 118.7 m	marl	*	*	min.	***	***	*						
	RB-658 129 m (g)	calcareous shale	**	min.	min.	***	**			*				
	RB-658 129 m (p)	calcareous shale	*			**	***							
	SZA-5 11.6 m	calcareous marl	*	*	min.	**	***			min.				
	SZA-5 28.8 m	dolomarl, shale	**			***	***	min.					*	
	SZA-5 41.3 m	calcareous marl	*	*	*	**	***			min.				
	SZET-4 24.8 m	limestone, calcareous marl	**	*	*	***	**	*			min.			
	SZET-4 47.7 m	limestone	***	*	*	***	***	*			*			
	SZET-4 78.3 m	limestone	***	*		***	***	*						
	TV-2008/1	marl	*			***		min.					*	
	TV-2008/2	claymarl	***			**	**							
	TV-2008/3	claystone	*			***		**	min.					
	TV-2008/4	marl	min.			**	***							
	TV-2008/5	claystone	***	min.		*	*	*					*	
	TV-2008/6	claystone	**			***	*	*					*	
	VA-2, 10,6 m	siltstone	***	*		*	*				*			
	VA-2, 71,3 m	silty claystone	***	*		**	*			min.	*			
	VA-2, 79,3 m	siltstone	***			**	*			*	**			**
Bódva series (Lower to Upper Triassic)	27/A	limestone												
	BL-2 62-68 m	claystone, marl	*			***			*				*	
	BL-2 132.2 m	claystone, marl	*			***	**	min.						
	BL-2 139.7 m	claystone, marl	**			***	**	min.			*	*		
	BL-2008/1	claystone, marl	*			***			*					
	E-10	siltstone, claystone	min.	min.		***	*	min.	*				min.	
	E-12	siltstone, claystone	min.	min.		***	*	*	min.					
	E-2008/1	siltstone, claystone	min.	*		***		**					min.	
	E-6	siltstone, claystone	min.	min.		***	*	*	*				min.	
	E-7	siltstone, claystone	min.	min.		***	**	min.	min.					
	HA-4/1 EOM	dolomarl	***			**	**	*		*	*		min.	
	SZA-4 518.5 m	dolomite	*			***	*		min.				min.	
	SZA-4 532.2 m	dolomite	*	min.	min.	***	*	*	*				*	
	SZET-4, 151 m	limestone	***			***	***	*	**					
	SZET-4, 162 m	limestone	**			***	***	*	min.					
	TV-7 Mn	Mn-bearing claystone	**			***	**	min.					min.	
	VA-3, 77,6 m	calcareous siltstone, marl	*	min.		***	***	*	*					

Appendix Table 3: mineral composition of the studied samples (d<2μm)

Metamorphic (and detrital) mineral phases+weathering products														
Structural unit	**Sample number**	**Lithology**	**Qtz**	**Pl**	**Rt**	**10 Å**	**Chl**	**SP**	**Hem**	**Py**	**Cal**	**Dol-Ank**	**Kln**	**Gp**
Bódva series (uppermost Triassic-Jurassic Telekesvölgy Complex)	P-74/1	claystone	***	min.	min.	***	**				**	*		
	RB-658 118.7 m	marl	*	*	min.	***	***	*						
	RB-658 129 m (g)	calcareous shale	**	min.	min.	***	**			*				
	RB-658 129 m (p)	calcareous shale	*			**	***							
	SZA-5 11.6 m	calcareous marl	*	*	min.	**	***			min.				
	SZA-5 28.8 m	dolomarl, shale	**			***	***	min.					*	
	SZA-5 41.3 m	calcareous marl	*	*	*	**	***			min.				
	SZET-4 24.8 m	limestone, calcareous marl	**	*	*	***	**	*			min.			
	SZET-4 47.7 m	limestone	***	*	*	***	***	*			*			
	SZET-4 78.3 m	limestone	***	*		***	***	*						
	TV-2008/1	marl	*			***		min.					*	
	TV-2008/2	claymarl	***			**	**							
	TV-2008/3	claystone	*			***		**	min.					
	TV-2008/4	marl	min.			**	***							
	TV-2008/5	claystone	***	min.		*	*	*					*	
	TV-2008/6	claystone	**			***	*	*					*	
	VA-2, 10,6 m	siltstone	***	*		*	*				*			
	VA-2, 71,3 m	silty claystone	***	*		**	*			min.	*			
	VA-2, 79,3 m	siltstone	***			**	*			*	**			**
Bódva series (Lower to Upper Triassic)	27/A	limestone												
	BL-2 62-68 m	claystone, marl	*			***			*				*	
	BL-2 132.2 m	claystone, marl	*			***	**	min.						
	BL-2 139.7 m	claystone, marl	**			***	**	min.			*	*		
	BL-2008/1	claystone, marl	*			***			*					
	E-10	siltstone, claystone	min.	min.		***	*	min.	*				min.	
	E-12	siltstone, claystone	min.	min.		***	*	*	min.					
	E-2008/1	siltstone, claystone	min.	*		***		**					min.	
	E-6	siltstone, claystone	min.	min.		***	*	*	*				min.	
	E-7	siltstone, claystone	min.	min.		***	**	min.	min.					
	HA-4/1 EOM	dolomarl	***			**	**	*		*	*		min.	
	SZA-4 518.5 m	dolomite	*			***	*		min.				min.	
	SZA-4 532.2 m	dolomite	*	min.	min.	***	*	*	*				*	
	SZET-4, 151 m	limestone	***			***	***	*	**					
	SZET-4, 162 m	limestone	**			***	***	*	min.					
	TV-7 Mn	Mn-bearing claystone	**			***	**	min.					min.	
	VA-3, 77,6 m	calcareous siltstone, marl	*	min.		***	***	*	*					

Appendix Table 4: KI and AI values of the investigated samples

Structural unit	Locality	Sample number	KI (Δ °2Θ)	ChC(002) (Δ °2Θ)	Prev. Str. Poz.	New Str. Poz.
Bódva series (uppermost Triassic-Jurassic Telekesvölgy Complex)	TV 7	*A-RB-6*	*0.410*		TV	B/TV
	Core	*P-74 183.8-184 m*	*0.227*			B/TV
	Core	*P-74 190.9-191 m*	*0.335*			B/TV
	Core	P-74 195.9-196 m	0.357	0.255		B/TV
	Core	RB-658 118.7 m	0.297	0.282	TV	B/TV
	Core	RB-658 129 m (g)	0.328	0.246	TV	B/TV
	Core	RB-658 129 m (p)	0.283	0.307	TV	B/TV
	Core	SZET-4 24.8 m	0.331	0.241	TO	B/TV
	Core	SZET-4 47.7 m	0.348	0.243	TO	B/TV
	Core	SZET-4 78.3 m	0.397	0.240	B	B/TV
	Core	SZA-5 11.6 m	0.358		TO&B	B/TV
	Core	SZA-5 28.8 m	0.702		TO&B	B/TV
	Core	SZA-5 41.3 m	0.344	0.283	TO&B	B/TV
	Szár Hill	*RB-20*	*0.484*		TO&B	B/TV
	Szár Hill	TV-2008/1	0.521		TO&B	B/TV
	TV 7	TV-2008/2	0.467	0.421	TV	B/TV
	TV 7	TV-2008/3	0.442		TV	B/TV
	TV 8	TV-2008/4	0.309	0.326	TV	B/TV
	TV 7	TV-2008/5	0.384		TV	B/TV
	TV 8	TV-2008/6	0.470		TV	B/TV
	Core	VA-2, 10,6 m	0.421	0.295	TV	B/TV
	Core	VA-2, 71,3 m	0.454	0.315	TV	B/TV
	Core	VA-2, 79,3 m	0.457		TV	B/TV
Bódva series (Lower to Upper Triassic)	Dunnatető Hill	27/a	0.414		B	B/T
	Core	BL-2 62-68 m	0.487		B	B/T
	Core	BL-2 132.2 m	0.497	0.350	B	B/T
	Core	BL-2 139.7 m	0.456	0.362	B	B/T
	BI	BL-2008/1	0.637		B	B/T
	Esztramos	E-10	0.513		B	B/T
	Bódvarákó	E-12	0.524		B	B/T
	Esztramos	E-2008/1	0.509		B	B/T
	Esztramos	6 - E	0 7 4 . 0		B	T / B
	Esztramos	7 - E			B	T / B 3 . 0 1 0 5 . 0
	Hidvégardó	HA-4/1	0.509		B	B/T
	Core	*P-73 97.8-98 m*	*0.357*		B	B/T
	Core	*P-74 156.7-156.9 m*	*0.245*		B	B/T
	BI	*Rb-42*	*0.435*		B	B/T
	Core	SZA-4 518.5 m	0.323		B	B/T
	Core	SZA-4 532.2 m	0.309		B	B/T
	Core	SZET-4 151 m	0.323	0.334	B	B/T
	Core	SZET-4 162 m	0.298	0.274	B	B/T
	TV 7	TV-7 Mn	0.500		B	B/T
	Core	VA-3, 77,6 m	0.385	0.293	B	B/T

On Appendix Table 4-6 grey italics indicate data of Árkai (1981, 1985, 1989).

Structural unit	Locality	Sample number	KI (Δ °2Θ)	ChC(002) (Δ °2Θ)	Prev. Str. Poz.	New Str. Poz.
Telekesoldal complex (Jurassic)	Core	RB-658 4.5-5 m	0.284	0.256	TO	TO
	Core	RB-661 21.3-21.7 m	0.251	0.222	TO	TO
	Core	RB-661 86 m	0.306	0.257	TO	TO
	Core	RB-661 148.5 m	0.361	0.251	TO	TO
	Core	RB-661 212 m	0.313		TO	TO
	Core	*SZA-10 68.6 m*	*0.190*		TO	TO
	Core	SZA-10 74 m	0.288	0.234	TO	TO
	Core	SZA-10 91.4 m	0.275	0.232	TO	TO
	Core	*SZA-10 98.3 m*	*0.227*		TO	TO
	Core	*SZA-10 112.7 m*	*0.146*		TO	TO
	Core	*SZA-10 122.8 m*	*0.130*		TO	TO
	Core	*SZA-10 141.4 m*	*0.232*		TO	TO
	Core	SZA-10 26. box	0.304	0.242	TO	TO
	Core	SZA-12, 12 m	0.483		TO	TO
	Core	SZA-12 31.4 m	0.361	0.238	TO	TO
	Core	SZA-12 50.3 m	0.269	0.235	TO	TO
	Core	*SZA-12 59.8 m*	*0.191*		TO	TO
	Core	SZA-12 71 m	0.246	0.235	TO	TO
	Core	*SZA-12 88m*	*0.228*		TO	TO
	Core	SZA-7 50.3 m	0.278	0.276	TO	TO
	Core	*SZA-7 88.7 m*	*0.221*		TO	TO
	Core	SZA-7 141.2 m	0.287	0.232	TO	TO
	Core	*SZA-7 190.6 m*	*0.223*		TO	TO
	Core	*SZA-7 209 m*	*0.190*		TO	TO
	Core	*SZA-7 201.6 m*	*0.270*		TO	TO
	Core	SZET-3 21-22 m	0.377	0.245	TO	TO
	Core	SZET-3 33.8-34 m	0.417	0.258	TO	TO
	Core	SZET-3 63.9-64.2 m	0.320	0.285	TO	TO
	Core	SZET-3 88.3-88.6 m	0.363	0.273	TO	TO
	TV Hunter H.	To-7/b	0.398	0.316	TO	TO
Borehole Sző-3 (Jurassic)	Core	SZÖ-3 32 m	0.278	0.223	S (T1)	TO
	Core	SZÖ-3 42.8-43 m	n.m.		S (T1)	TO
	Core	SZÖ-3 76.1 m	0.283	0.237	S (T1)	TO
	Core	SZÖ-3 86.2-87.4 m	0.284	0.229	S (T1)	TO
	Core	SZÖ-3 152 m	0.297	0.240	S (T1)	TO
Nyúlkertlápa beds (?Jurassic)	Esztramos	*RB-70*	*0.163*		Me	TO
	Esztramos	T-26	0.211	0.265	Me	TO
	Esztramos	*BRK-5 59.8-59.9 m*	*0.176*		Me	TO
	Esztramos	T-26a	0.225	0.225	Me	TO
	Esztramos	*RB-72*	*0.221*		Me	TO
	Esztramos	*Á-26-70*	*0.275*		Me	TO
	Esztramos	*Á-26-72*	*0.256*		Me	TO
	Esztramos	*Á-26-73*	*0.224*		Me	TO

Structural unit	Locality	Sample number	KI (Δ °2Θ)	ChC(002) (Δ °2Θ)	Prev. Str. Poz.	New Str. Poz.
Torna series	Martonyi nappe	*Rb-62*	*0.166*		Tor	Tor
	Martonyi nappe	*Rb-31*	*0.178*		Tor	Tor
	Hidvégardó	Ha-3 84.7 m	0.199		Tor	Tor
	Martonyi nappe	*Rb-5*	*0.202*		Tor	Tor
	Bódvarákó	*Brk-5 130 m*	*0.218*		Tor	Tor
	Martonyi nappe	Tsza-1	0.224		Tor	Tor
	Hidvégardó	Ha-3 86 m	0.229		Tor	Tor
	Martonyi nappe	*Rb-82*	*0.231*		Tor	Tor
	Esztramos	E-1	0.234		Tor	Tor
	Martonyi nappe	NK-1	0.241	0.221	Tor	Tor
	Hidvégardó	Ha-3 72.5 m	0.259		Tor	Tor
	Bódvarákó	*Brk-5 94 m*	*0.277*		Tor	Tor
	Hidvégardó	Ha-3 129.5 m	0.281	0.227	Tor	Tor
	Hidvégardó	Ha-3 132 m	0.285	0.234	Tor	Tor
	Martonyi nappe	DT-V	0.289		Tor	Tor
	Martonyi nappe	*Mart-9 104 m*	*0.298*		Tor	Tor
	Martonyi nappe	Mart-10 5.4 m	0.331		Tor	Tor
	Bódvarákó	*Brk-6 103 m*	*0.341*		Tor	Tor
	Bódvarákó	*Brk-6 118.4 m*	*0.343*		Tor	Tor
	Martonyi nappe	Mart-10 8.2 m	0.368		Tor	Tor
	Martonyi nappe	*Rb-3*	*0.382*		Tor	Tor

Appendix Table 5: b0 parameters of the samples

Structural unit	Locality	Sample number	*b0*
Telekesoldal complex (Jurassic)	Core	RB-661 21.3-21.7 m	9.018
	Core	*SZA-10 68.6 m*	*8.995*
	Core	SZA-10 74 m	9.006
	Core	SZA-10 91.4 m	8.990
	Core	*SZA-10 98.3 m*	*8.994*
	Core	*SZA-10 112.7 m*	*8.993*
	Core	*SZA-10 122.8 m*	*8.987*
	Core	*SZA-10 141.4 m*	*8.989*
	Core	SZA-10 26. box	8.990
	Core	SZA-12 50.3 m	8.994
	Core	*SZA-12 59.8 m*	*8.994*
	Core	SZA-12 71 m	9.002
	Core	SZA-12 88m	8.993
	Core	SZA-7 50.3 m	9.001
	Core	*SZA-7 88.7 m*	*9.004*
	Core	SZA-7 141.2 m	8.992
	Core	*SZA-7 190.6 m*	*8.991*
	Core	*SZA-7 201.6 m*	8.992
	Telekes Val. Hunter H.	To-7/b	9.014
Nyúlkertlápa beds (?Jurassic)	Esztramos	RB-70	9.009
	Esztramos	T-26	9.001
	Esztramos	BRK-5 59.8-59.9 m	8.999
	Esztramos	T-26a	9.015
	Esztramos	RB-72	9.012
	Esztramos	Á-26-70	9.008
	Esztramos	Á-26-72	9.012
Torna series	Hidvégardó	Ha-3 84.7 m	9.018
	Bódvarákó window	*Brk-5 130 m*	*9.017*
	Hidvégardó	Ha-3 86 m	9.031
	Martonyi nappe	*Rb-82*	*9.010*
	Esztramos	E-1	9.031
	Hidvégardó	Ha-3 72.5 m	9.028
	Bódvarákó window	*Brk-5 94 m*	*9.013*
	Hidvégardó	Ha-3 129.5 m	9.002
	Martonyi nappe	*Mart-9 104 m*	*9.015*
	Martonyi nappe	Mart-10 5.4 m	9.016
	Bódvarákó window	*Brk-6 103 m*	*9.014*
	Bódvarákó window	*Brk-6 118.4 m*	*9.017*
	Martonyi nappe	Mart-10 8.2 m	9.012
	Martonyi nappe	*Rb-1*	*9.006*
	Hidvégardó	Ha-3 129.5 m	9.0018